

**On-trip Behavior of Truck Drivers on Freeways  
New mathematical models and control methods**

Sharma, Salil

**DOI**

[10.4233/uuid:a3d42b01-b207-4524-94c6-1c8cf642f687](https://doi.org/10.4233/uuid:a3d42b01-b207-4524-94c6-1c8cf642f687)

**Publication date**

2023

**Document Version**

Final published version

**Citation (APA)**

Sharma, S. (2023). *On-trip Behavior of Truck Drivers on Freeways: New mathematical models and control methods*. [Dissertation (TU Delft), Delft University of Technology]. <https://doi.org/10.4233/uuid:a3d42b01-b207-4524-94c6-1c8cf642f687>

**Important note**

To cite this publication, please use the final published version (if applicable).  
Please check the document version above.

**Copyright**

Other than for strictly personal use, it is not permitted to download, forward or distribute the text or part of it, without the consent of the author(s) and/or copyright holder(s), unless the work is under an open content license such as Creative Commons.

**Takedown policy**

Please contact us and provide details if you believe this document breaches copyrights.  
We will remove access to the work immediately and investigate your claim.

# **On-trip Behavior of Truck Drivers on Freeways: New mathematical models and control methods**

**Salil Sharma**

**Delft University of Technology**

This doctoral dissertation was funded by the Dutch Research Council (NWO), TKI Dinalog, Commit2Data, Port of Rotterdam, SmartPort, Portbase, TLN, Deltalinqs, Rijkswaterstaat, and TNO under project 'ToGRIP-Grip on Freight Trips' with grant number 628.009.001.



Cover illustration: Getty Images, rudzhan Nagiev, bestbrk

# **On-trip Behavior of Truck Drivers on Freeways: New mathematical models and control methods**

## **Dissertation**

For the purpose of obtaining the degree of doctor  
at Delft University of Technology,  
by the authority of the Rector Magnificus Prof.dr.ir. T.H.J.J. van der Hagen,  
chair of the Board for Doctorates,  
to be defended publicly on  
Tuesday 31 October 2023 at 15:00 o'clock

by

**Salil SHARMA**

Master of Science in Transportation Systems  
Technical University of Munich (TUM), Germany  
born in Jalaun, Uttar Pradesh, India

This dissertation has been approved by the promotor:  
Prof. dr. ir. J.W.C van Lint, Prof. dr. ir. L.A. Tavasszy, Dr. M. Snelder

Composition of the doctoral committee:

Rector Magnificus	chairperson
Prof. dr. ir. J.W.C van Lint	Delft University of Technology, promotor
Prof. dr. ir. L.A. Tavasszy	Delft University of Technology, promotor
Dr. M. Snelder	Delft University of Technology, promotor

Independent members:

Prof. R.L. Bertini	Oregon State University, USA
Prof. I. Papamichail	Technical University of Crete, Greece
Prof. dr. ir. B. De Schutter	Delft University of Technology
Dr. S. Moridpour	RMIT University, Australia
Prof.dr.ir. S.P. Hoogendoorn	Delft University of Technology, reserve member

**TRAIL Thesis Series no. T2023/18, the Netherlands Research School TRAIL**

TRAIL  
P.O. Box 5017  
2600 GA Delft  
The Netherlands  
E-mail: [info@rsTRAIL.nl](mailto:info@rsTRAIL.nl)

ISBN: 978-90-5584-337-4

Copyright © 2023 by Salil Sharma

All rights reserved. No part of the material protected by this copyright notice may be reproduced or utilized in any form or by any means, electronic or mechanical, including photocopying, recording or by any information storage and retrieval system, without written permission from the author.

Printed in the Netherlands

*Whatever happened, happened for the good.  
Whatever is happening, is happening for the good.  
Whatever will happen, will also happen for the good.  
(Bhagavad Gita)*



# Preface

I owe my deepest gratitude to Prof. Hans van Lint, Prof. Lóránt Tavasszy and Dr. Maaïke Snelder who accepted me as a doctoral student. I have benefited immensely from their vast knowledge and expertise in the interdisciplinary domain of transportation and logistics. I learned many valuable skills through continuous support and guidance, for which I am very thankful. I am very privileged to pursue this journey under your mentorship and to be a part of our wonderful research community.

I am very much indebted to Prof. Ioannis Papamichail who provided me with an opportunity to collaborate on a significant part of this dissertation. I thank you for your valuable and insightful advice on the fascinating topic of multi-class traffic control. I thank my doctoral committee members, Prof. Bart De Schutter, Prof. Robert Bertini, and Dr. Sara Moridpour, for reviewing my dissertation and providing me with constructive feedback that improved the quality of my dissertation.

I thank Dr. Wouter Schakel for inspiring discussions on lane-changing and traffic simulation. I greatly acknowledge his much appreciated help on the microscopic traffic simulator OpenTrafficSim. I thank Prof. Alexander Verbraeck, Dr. Ehab Al-Khannaq, Dr. Raphael Riebl and Peter Knoppers for the collaboration on truck platooning research.

I thank Dr. Ali Nadi for being a great collaborator on the ToGRIP project. It has been a pleasure working with you and I appreciate your kind help and exciting discussions.

I thank all the consortium partners of ToGRIP project for their generous support with data and constructive feedback throughout the project. I thank Dr. Taoufik Bakri for his kind help with Bluetooth and traffic data and thoughtful discussions.

I enjoyed my time with the Transport and Planning group. I thank my awesome colleagues and great scientific minds at DiTTLab and Freight & Logistics Lab – Panchamy, Tin, Raed, Michiel, Xiao, Simeon, Sanmay, Zahra, Guopeng, Muriel, Bobin, Ding, Ioanna and Rodrigo.



Special thanks to Dehlaila, Priscilla, Moreen, and Marije for their administrative support, which greatly facilitated my stay.

I would like to thank TRAIL research school for the support during PhD. Special thanks to Conchita for her help during the final phase of PhD.

Last but not least, my heartfelt gratitude goes to my beloved family for their unwavering encouragement. My wife, Richa, and our son Rishi, thank you for all the love.

Salil Sharma  
Den Haag, October 2023

# Content

- 1 Introduction ..... 1**
- 1.1 Motivation..... 1
- 1.2 Research gaps ..... 2
  - 1.2.1 Strategic driving behavior ..... 2
  - 1.2.2 Tactical driving behavior..... 2
  - 1.2.3 Operational driving behavior..... 3
- 1.3 Research aim and questions ..... 4
- 1.4 Research scope..... 4
- 1.5 Research context ..... 4
- 1.6 Scientific contributions ..... 5
  - 1.6.1 New insights ..... 5
  - 1.6.2 Novel methodologies..... 5
  - 1.6.3 Emerging scientific applications ..... 6
- 1.7 Practical contributions ..... 7
- 1.8 Dissertation organization ..... 7
- I: Strategic driving behavior on a freeway network ..... 9**
- 2 On-trip route choice behavior of truck drivers ..... 11**
- 2.1 Introduction..... 12
- 2.2 Data ..... 14
  - 2.2.1 Bluetooth dataset for trucks..... 14
  - 2.2.2 Attributes of route alternatives ..... 17
- 2.3 Methods ..... 18

2.3.1 Bi-objective optimization approach to simultaneously infer actual route choices and estimate the parameters of a route choice model .....	19
2.3.2 Decision rules .....	20
2.3.3 Choice set generation .....	21
2.4 Results.....	22
2.4.1 Simultaneous inference of actual route choices and estimation of parameters of route choice models.....	22
2.4.2 Latent class choice models .....	23
2.5 Discussion.....	24
2.6 Conclusions.....	26
<b>II: Tactical driving behavior around freeway bottlenecks.....</b>	<b>27</b>
<b>3 Merging and diverging strategies of truck drivers .....</b>	<b>29</b>
3.1 Introduction.....	30
3.2 Literature review.....	31
3.2.1 Drivers' heterogeneity with respect to their lane change maneuvers.....	31
3.2.2 Inefficiencies owing to lane-changing.....	31
3.3 Data and methods.....	31
3.3.1 Trajectory dataset .....	32
3.3.2 Identifying truck driver's merging and diverging maneuvers from trajectory data .....	33
3.3.3 Finite mixture modeling .....	33
3.3.4 Data preparation for finite mixture modeling.....	34
3.3.5 Indicator variables .....	34
3.3.6 Descriptive statistics of merging maneuvers.....	35
3.3.7 Descriptive statistics of diverging maneuvers.....	36
3.4 Results.....	37
3.4.1 Merging strategies of truck drivers.....	37
3.4.2 Diverging strategies of truck drivers .....	38
3.4.3 Contribution of truck driver's lane-changing behavior to turbulence .....	41
3.5 Discussion.....	44
3.5.1 Discussion of findings .....	44
3.5.2 Limitations.....	44
3.6 Conclusions.....	44
<b>4 Gap selection process during discretionary lane changing .....</b>	<b>47</b>
4.1 Introduction.....	48
4.2 Related background .....	49
4.2.1 Gated recurrent unit neural networks .....	49
4.2.2 Relevance of class imbalance to understanding lane-changing behavior .....	50

4.2.3	Interpreting a trained GRU neural network model.....	51
4.3	Data preparation to model gap selection using GRU neural network models.....	52
4.3.1	Trajectory data.....	52
4.3.2	Feature selection.....	54
4.3.3	Constructing data for training and testing .....	55
4.4	Experimental setup .....	56
4.4.1	Evaluation metric.....	56
4.4.2	Model specification .....	57
4.4.3	Selection of model parameters .....	58
4.5	Results.....	59
4.5.1	Passenger cars.....	59
4.5.2	Delivery vans.....	61
4.5.3	Trucks.....	63
4.6	Discussion.....	64
4.7	Conclusions.....	66
<b>5</b>	<b>A multi-class lane changing advisory system .....</b>	<b>67</b>
5.1	Introduction.....	68
5.2	Formulating a multi-class lane-changing LQR controller .....	69
5.2.1	Traffic system dynamics using a multi-class multi-lane traffic flow model .....	69
5.2.2	Optimal control problem formulation .....	73
5.2.3	Transferring the optimal LQR control to a real-world C-ITS based multi-class lane-changing advisory system.....	74
5.3	Implementation of the multi-class lane-changing advisory system in a microscopic traffic simulator .....	75
5.3.1	Lane-changing model .....	76
5.3.2	Implementing the lane-changing advisory system .....	76
5.4	Experimental setup .....	77
5.4.1	Study area .....	77
5.4.2	Demand profile.....	77
5.4.3	Simulation model parameters .....	78
5.4.4	Scenarios.....	78
5.4.5	Performance indicator .....	78
5.5	Selection of LQR controller's parameters .....	80
5.5.1	Reference values of set-points and weights associated with Q and R matrices .....	80
5.5.2	Selection of set-points .....	80
5.5.3	Selection of weighting matrices (Q and R) .....	81
5.6	Results and discussion .....	82

5.6.1	Quantitative evaluation of the performance of the LQR controller .....	83
5.6.2	Qualitative evaluation of the performance of the LQR controller .....	83
5.7	Conclusions.....	87
<b>III: Operational driving behavior around freeway bottlenecks .....</b>		<b>89</b>
<b>6</b>	<b>Impacts of a truck platooning application.....</b>	<b>91</b>
6.1	Introduction.....	92
6.2	Literature review.....	93
6.2.1	Modeling of truck platoons .....	93
6.2.2	Impact of truck platoons on traffic efficiency and safety.....	93
6.3	Longitudinal controller for truck platoons.....	94
6.3.1	Preliminaries.....	94
6.3.2	Cooperative adaptive cruise control .....	95
6.3.3	Adaptive cruise control.....	95
6.3.4	Cruise control .....	95
6.3.5	Verification tests for cooperative adaptive cruise control.....	96
6.4	Lateral controller for truck platoons.....	97
6.4.1	Lane-changing desire.....	98
6.4.2	Lane-changing sequence .....	99
6.4.3	Gap-creation ability of truck platoons.....	100
6.5	Experimental design .....	101
6.5.1	Network modeling and demand data.....	101
6.5.2	Truck platoon configuration.....	101
6.5.3	Scenarios.....	102
6.5.4	Performance indicators.....	104
6.6	Impact of a reference platoon configuration.....	105
6.6.1	Traffic scenario 1: Truck platoons on mainline carriageway.....	105
6.6.2	Traffic scenario 2: Truck platoons merging from an on-ramp.....	106
6.7	Impact of truck platoon's characteristics .....	107
6.7.1	Traffic scenario 1: Truck platoons on mainline carriageway.....	107
6.7.2	Traffic scenario 2: Truck platoons merging from an on-ramp.....	110
6.8	Global sensitivity analysis .....	114
6.8.1	Traffic scenario 1: Truck platoons on mainline carriageway.....	114
6.8.2	Traffic scenario 2: Truck platoons merging from an on-ramp.....	115
6.9	Discussion.....	115
6.10	Conclusions.....	117
<b>7</b>	<b>Conclusions.....</b>	<b>119</b>
7.1	Main findings.....	119

7.2 Overall conclusions.....	121
7.3 Recommendations for further research.....	122
7.3.1 Strategic driving behavior .....	122
7.3.2 Tactical driving behavior.....	122
7.3.3 Operational driving behavior.....	123
7.3.4 Integrated traffic models.....	124
7.4 Recommendations for practical use .....	124
<b>Bibliography .....</b>	<b>127</b>
<b>Summary .....</b>	<b>139</b>
<b>Samenvattig.....</b>	<b>141</b>
<b>About the author .....</b>	<b>143</b>
<b>TRAIL Thesis Series .....</b>	<b>147</b>



# 1 Introduction

## 1.1 Motivation

Congestion is a frequent problem on freeways. Congestion occurs when demand exceeds prevailing roadway capacity, or when—e.g. due to incidents or roadworks—the roadway capacity is reduced below prevailing demand (Cassidy and Bertini, 1999, Cassidy and Rudjanakanoknad, 2005, Daganzo, 2011, Murray-Tuite, 2008). Congestion is often considered a major challenge for the operations of road freight transport (ATRI, 2021). Because of congestion, trucking companies have been losing billions of dollars worldwide because trucks either have to take a detour or come to a standstill (TLN, 2020, Hooper, 2018). Trucks not only suffer from congestion but they also contribute to it and in turn affect traffic operations (Schreiter, 2013, Sarvi and Kuwahara, 2008, Moridpour et al., 2015). As a result, degradable freight and traffic operations on freeways inhibit economic growth and prosperity.

Understanding driving behavior and on-trip decision-making of truck drivers are critically important to design measures that mitigate the impacts of congestion on truck traffic, and vice versa, to design measures that mitigate the impacts of truck traffic on congestion. In this respect, the on-trip behavior of truck drivers can be decomposed—like driving behavior in general (Michon, 1985)—into strategical, tactical, and operational behavior (see Figure 1.1).

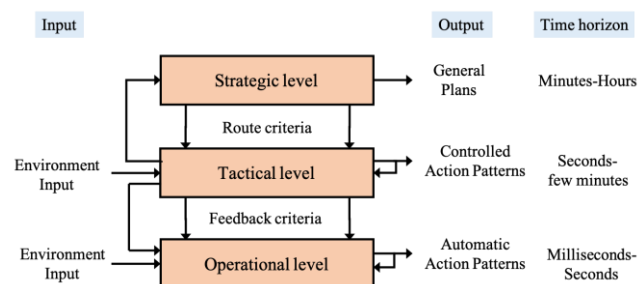


**Figure 1.1. The hierarchical structure of the on-trip driving behavior (adapted from Michon (1985)).**



The strategic level behavior involves routing decisions and may run over periods ranging from a few minutes to hours. The tactical level is determined by both the driver's general goals set at the strategic level and the current driving situation. This level depicts short-term path-planning (e.g. merging, diverging, or lane changing) and is typically executed across an interval of seconds. The finest scale of driver behavior is the operational level, which involves automatic action patterns (e.g. steering & accelerating of the vehicle) that are executed at a time scale ranging from milliseconds to seconds. Research on all three levels will equip us with improved knowledge about the complex on-trip behavior of truck drivers and tools to improve both freight and traffic operations on freeways.

## 1.2 Research gaps

Despite the growing importance of road freight transport and the challenges it faces, there are larger gaps in our knowledge when it comes to strategic, tactical, and operational behavior of drivers of trucks, in comparison to passenger cars. The modeling and control of these three levels for truck drivers is still developing around the use of new datasets, novel traffic management and control strategies, and requires significant new research. We introduce these needs below.

### 1.2.1 Strategic driving behavior

The earlier literature on route choice has used stated preference (SP) surveys and revealed preference (RP) GPS data to study how truck drivers select their routes during their trips (Arentze et al., 2012, Feng et al., 2013, Hess et al., 2015, Kamali et al., 2016, Knorrning et al., 2005, Oka et al., 2019, Sun et al., 2013, Toledo et al., 2020). Although valuable insights regarding route-specific characteristics have been obtained, the studies based on SP datasets might have validity issues since they solicit choice behavior in hypothetical situations. Although GPS datasets might alleviate the aforementioned limitations, they are often not publicly available and expensive to buy from service providers. In contrast to GPS data, there are other low-cost alternatives such as Automated Vehicle Identification (AVI) data such as camera, Bluetooth, and (freight) travel diaries. The AVI sensors can capture passing vehicles' movements to produce a large sample that is (more) representative of the population. Furthermore, these sensors can continuously record vehicles' movements over several periods of the day. However, these datasets are sparse (or unlabeled) as they lack actual route choices of drivers and only comprise origin, destination, and experienced travel time for a given trip. The lack of appropriate methods that can deal with the sparsity of AVI datasets further inhibits us to develop advanced route choice models for road freight, which are fundamental to our understanding of how road freight moves and can support the development of appropriate traffic and logistics interventions.

### 1.2.2 Tactical driving behavior

Tactical driving behavior, necessitated by lane changing, is shown to exert significant influence on road capacity (Cassidy and Rudjanakanoknad, 2005) and safety (Li et al., 2014) around freeway bottlenecks such as ramps and weaving sections. Whereas modeling of lane change behavior for drivers of passenger cars has been extensively studied, (Balal et al., 2016, Moridpour, 2017, Toledo et al., 2003, Toledo and Katz, 2009, Ahmed, 1999, Moridpour et al., 2012), research for drivers of trucks is limited due to the scarcity of empirical trajectory datasets (Moridpour et al., 2012). Lane changing is complex driving behavior that comprises several elements related to mandatory (merge/diverge) and discretionary (assessing gaps; deciding for or against one) lane changes. Although Moridpur et al. (2012) have studied motivations for

truck drivers to change lanes within their discretionary activities using limited data of only 39 trajectories of truck drivers, they do not explore other elements such as merge/diverge (mandatory) and gap selection (discretionary). Concerning merging and diverging behavior, the previous research shows that inter-driver differences exist within drivers that cannot be captured alone by adjusting driver behavior parameters in existing models (Keyvan-Ekbatani et al., 2016, Sun and Elefteriadou, 2012, Li, 2018, Li and Sun, 2018). Clearly, with such heterogeneity in the merging and diverging behavior of passenger car drivers, there is also large heterogeneity within truck drivers that remains to be explored. Moving on to the gap selection process, an important stage of the discretionary lane-changing process where drivers explicitly look for a suitable and safe opportunity to initiate their desired lane-changing maneuver, long-term temporal interdependencies (or the historical driving experience) and the impact of (external) topological factors have not yet been considered (Balal et al., 2016, Toledo and Katz, 2009, Punzo et al., 2011, Pang et al., 2020). Further, no comparison among gap selection process of multiple vehicle classes (passenger cars, delivery vans and truck drivers) is available due to the lack of research on datasets comprising the sufficient number of trajectories of those vehicle classes. Therefore, new and diverse datasets (van Beinum et al., 2018, van Beinum, 2018) are needed to be investigated to improve existing lane changing models in order to realistically capture traffic phenomena and accurately conduct traffic and safety assessments.

Turning now to controlling tactical behavior, research on lane change advisory systems shows that traffic efficiency around freeway bottlenecks can be improved (Roncoli et al., 2017, Tajdari et al., 2020, Markantonakis et al., 2019). The advisory system intends to balance traffic flow distribution on available lanes of a freeway around bottleneck areas. However, it has operated on traffic as a whole and not considered vehicle class-specific properties. The previous research notes that heterogeneity induced from vehicle class-specific properties can affect traffic efficiency (van Lint et al., 2008a, Schreiter, 2013); therefore, it is important to embed multiple vehicle classes in the lane-changing advisory framework to develop a generalized control scheme where the behavior of each vehicle class can individually be influenced. The generalized control schemes can be particularly useful for freeways with a high share of trucks.

### 1.2.3 Operational driving behavior

In contrast to the tactical level, control applications for the operational behavior of truck drivers has been researched extensively in the form of a truck platooning application (Calvert et al., 2019, Saeednia and Menendez, 2017, Ramezani et al., 2018, Tsugawa et al., 2016, Wang et al., 2019, Milanés and Shladover, 2014, Shladover et al., 2006). Although these studies evaluate the impact of truck platooning on traffic efficiency using real-world trials and traffic simulation, they do not fully capture the uncertainty associated with the traffic and safety impacts caused by different truck platooning characteristics (e.g., market penetration, length of the platoon, intra-platoon gap spacing, and desired speed) around freeway bottlenecks. These bottleneck sites are important to consider from the point of view of the (possible) driving conflict between a truck platoon and a vehicle either entering into or exiting the mainline carriageway. This calls for detailed sensitivity analysis to comprehensively examine individual and interaction effects of truck platooning characteristics on traffic efficiency and safety. Furthermore, situations involving truck platoons merging onto mainline carriageway have not yet been considered in the impact analysis framework. This would be an important step to support the deployment of truck platoons on significant freight corridors.

Thus far, it has been shown that there is a need to obtain new knowledge and insights about the on-trip behavior of truck drivers by developing new methods that can harness the potential of sparse travel datasets for route choice and investigating newly available trajectory datasets for lane changing. Furthermore, traffic management and control strategies need to be generalized

by embedding vehicle-class specific properties. Before truck platoons can be deployed in the real world, a comprehensive understanding of the uncertainty of their possible impacts on traffic operations is required.

### 1.3 Research aim and questions

The main aim of this dissertation is:

*To develop new mathematical models and control methods for the on-trip behavior of truck drivers and thereby improve both freight and traffic operations in terms of safety and efficiency.*

Below we detail this overall aim into research questions that pertain to strategical, tactical, and operational truck driving behavior, respectively.

#### I: Strategic driving behavior on a freeway network

Chapter 2: *How can characteristics of on-trip route choice behavior of trucks be estimated from sparse datasets?*

#### II: Tactical driving behavior around freeway bottlenecks

Chapter 3: *How can merging and diverging strategies of truck drivers be identified?*

Chapter 4: *What attributes affect the gap selection process of truck drivers within their discretionary lane changing, in comparison with other vehicle classes?*

Chapter 5: *To what extent can a lane changing advisory system for multiple vehicle classes improve traffic efficiency?*

#### III: Operational driving behavior around freeway bottlenecks

Chapter 6: *What is the impact of truck platoons with different characteristics on traffic efficiency and safety around a freeway bottleneck?*

### 1.4 Research scope

This dissertation deals with freeway traffic with or without freeway bottlenecks (e.g., on-ramps, off-ramps, weaving sections). Multi-lane freeways are considered in this dissertation. The studies are restricted to isolated freeway bottlenecks and multiple interacting bottlenecks are beyond the scope of this dissertation. This dissertation considers trucks, passenger cars and delivery vans. Other vehicle classes such as two-wheelers and buses are not considered. Furthermore, this dissertation concentrates on investigating and managing the on-trip decisions of drivers and does not address pre-trip or demand management. Finally, the focus is on exploring the effect of control strategies; topics like implementation and enforcement (of such strategies) are beyond the scope of this dissertation.

### 1.5 Research context

This doctoral research is part of the “ToGRIP-Grip on Freight Trips” project. The project is funded by the Dutch Research Council (Nederlandse Organisatie voor Wetenschappelijk Onderzoek or NWO) under the grant number 628.009.001 and involves TKI Dinalog,

Commit2data, Port of Rotterdam, SmartPort, Portbase, TLN, Deltalinqs, Rijkswaterstaat, and TNO as consortium members. The project has focused on a setting geographically located around the Port of Rotterdam in the Netherlands. The project has provided two PhD positions which were all based at the Delft University of Technology (TU Delft). The overall objective of ToGRIP is:

*“To develop a data-driven integrated traffic and logistics model that can be used to design interventions (executed by the Port, Road and other authorities) to combat travel time unreliability and to improve logistics operations.”- Snelder (2016).*

Within ToGRIP, two pillars have been identified: pre-trip and on-trip decisions of truck drivers. These two pillars are spread over four work packages: empirical analysis; integrated traffic and logistics model; interventions and knowledge utilization; and project management. This research fits in the second pillar and concerns the on-trip behavior of truck drivers. The first pillar is studied by Ali Nadi as a part of his doctoral research (Nadi, 2022).

## 1.6 Scientific contributions

This dissertation provides new insights, novel methodologies, and emerging scientific applications, which are described as follows.

### 1.6.1 New insights

- We show that the on-trip route choice characteristics of drivers can be estimated from sparse datasets that lack observations of route choices (Chapter 2).
- The findings in this dissertation suggest that the on-trip route choice characteristics of truck drivers can be best captured by segmenting them into four latent subgroups (Chapter 2).
- There exists a significant inter-driver heterogeneity in the merging and diverging behavior of truck drivers. The findings in this dissertation indicate that these truck merging and diverging behaviors can be clustered into two and three main strategies, respectively (Chapter 3).
- Systematic differences also exist between drivers of passenger cars, delivery vans, and trucks in the gap selection process within their discretionary lane changing activities (Chapter 4).
- A multi-class lane changing advisory system reduces travel times for both mainline and ramp vehicles around a merging section by delaying the breakdown of traffic flow and suppressing shock waves (Chapter 5).
- We identify and rank important characteristics of truck platoons concerning their impacts on traffic efficiency and safety (Chapter 6).
- The findings in this dissertation suggest a significance presence of interactions among characteristics of truck platoons that causes uncertainty in the traffic and safety impacts greater than that of varying each of the characteristics alone (Chapter 6).

### 1.6.2 Novel methodologies

To arrive at new insights, this dissertation develops the following:

*Novel mathematical models*

- We develop a novel method that combines data fusion and bi-objective optimization to estimate route choice models from a sparse dataset that lacks actual route choices of drivers. The data fusion step of our method leverages the timestamps of a trip contained in a sparse dataset (Chapter 2).
- We apply the finite mixture modeling technique (Little, 2013) to cluster merging and diverging patterns of truck drivers using a feature set that comprises their spatial, temporal, kinematic and gap-acceptance attributes (Chapter 3).
- We apply gated recurrent unit neural networks (Cho et al., 2014) based models to investigate the gap selection process of passenger cars, trucks, and delivery vans by accounting for long term temporal interdependencies (Chapter 4).
- We use an explainable artificial intelligence (AI) technique such as gradient-based measure (van Lint, 2004, Simonyan et al., 2014) to explain what gated recurrent unit neural networks (or so-called black-box models) have learned and whether this learning makes sense behaviorally (Chapter 4).
- We utilize a global level sensitivity analysis technique, Borgonovo importance measure (Borgonovo, 2007), to capture the uncertainty associated with the traffic and safety impacts of truck platoons (Chapter 6).

*Novel control methods*

- We design a cooperative intelligent transportation system (ITS) based multi-class lane changing advisory system that utilizes an optimal linear quadratic regulator (Chapter 5).
- We develop linear feedback controllers that govern the behavior of truck platoons in cooperative adaptive cruise, adaptive cruise, and cruise modes (Chapter 6).

*Novel modules for a microscopic simulation model*

- We develop a module for a multi-class lane changing advisory system and implement it in a microscopic simulation model. The extended simulator is used to assess the performance of the proposed advisory system to mitigate congestion around a merging section (Chapter 5).
- We extend a microscopic simulation model with new implementations of controllers that govern the behavior of truck platoons in order to evaluate their impacts on traffic efficiency and safety (Chapter 6).

**1.6.3 Emerging scientific applications**

The main scientific application of this dissertation lies in the development of a simulation-based dynamic multi-class traffic assignment model with the following unique features.

- Vehicle class-specific on-trip route choice models (Chapter 2)
- Vehicle class-specific lane changing models (merging/diverging and gap selection studies from Chapter 3 and 4)
- Traffic management and control modules (e.g., a multi-class lane changing advisory system developed in Chapter 5)
- Modules to simulate the operations of truck platoons (Chapter 6)

This dynamic multi-class traffic assignment model can be used for traffic and safety assessments as well as ex-ante evaluations of ITS applications. Moreover, this model can also be a good choice to develop an integrated traffic and logistics model that can be used to study the impact of port and terminal activities on the traffic system, and vice-versa, to analyze the impact of traffic operations on port and terminals.

## 1.7 Practical contributions

This dissertation contributes to practice by presenting:

- *A method to estimate route choice characteristics from readily available datasets*: This tool can be used to estimate route choice models from sparse AVI datasets (e.g., Bluetooth, camera) which can be obtained readily from traffic management agencies but lack actual route choices of drivers (Chapter 2).
- *Insights to improve freeway design guidelines for ramps and weaving sections*: Insights about the merging and diverging behavior of truck drivers and their contribution to turbulence can be used to evaluate and improve freeway design guidelines for ramps and weaving sections (Chapter 3).
- *Automated gap selection systems for multiple vehicle classes*: A data-driven (or automated) gap selection system can be used to inform drivers of multiple vehicle classes (passenger cars, delivery vans, trucks) whether an available gap should be accepted or rejected. This tool can be integrated as an advanced driver assistance system application (ADAS) to improve safety during lane-changing and also holds vast potential for connected and autonomous vehicles (Chapter 4).
- *A cooperative ITS-based multi-class lane-changing advisory system to improve traffic efficiency around freeway bottlenecks*: This advisory system is generalized to distinguish vehicle classes and its positive impact on traffic efficiency is shown. This system can leverage the potential of cooperative ITS technology and advises drivers to change lanes in order to balance traffic flow over available lanes of a carriageway around freeway bottlenecks (Chapter 5).
- *Optimal truck platooning configurations around freeway bottlenecks*: The case study identifies optimal truck platooning configurations that can be deployed in different traffic conditions and would not deteriorate traffic operations in terms of efficiency and safety (Chapter 6).

## 1.8 Dissertation organization

The structure of the dissertation is presented in Figure 1.2. The research questions are addressed in six chapters that form the main body of this dissertation.

The main body is divided into three hierarchical levels of the on-trip behavior of truck drivers. First, Chapter 2 focuses on the strategic behavior of truck drivers by estimating their on-trip route choice characteristics. This chapter presents a novel two-step approach that combines data fusion and bi-objective optimization. With this approach, their route choice characteristics and inter-driver heterogeneity are investigated for a case study on port (of Rotterdam)-to-hinterland trips in the Netherlands.

The next three chapters are dedicated to their tactical driving behavior around freeway bottlenecks and focus on three elements: merging/diverging, gap selection process, and lane

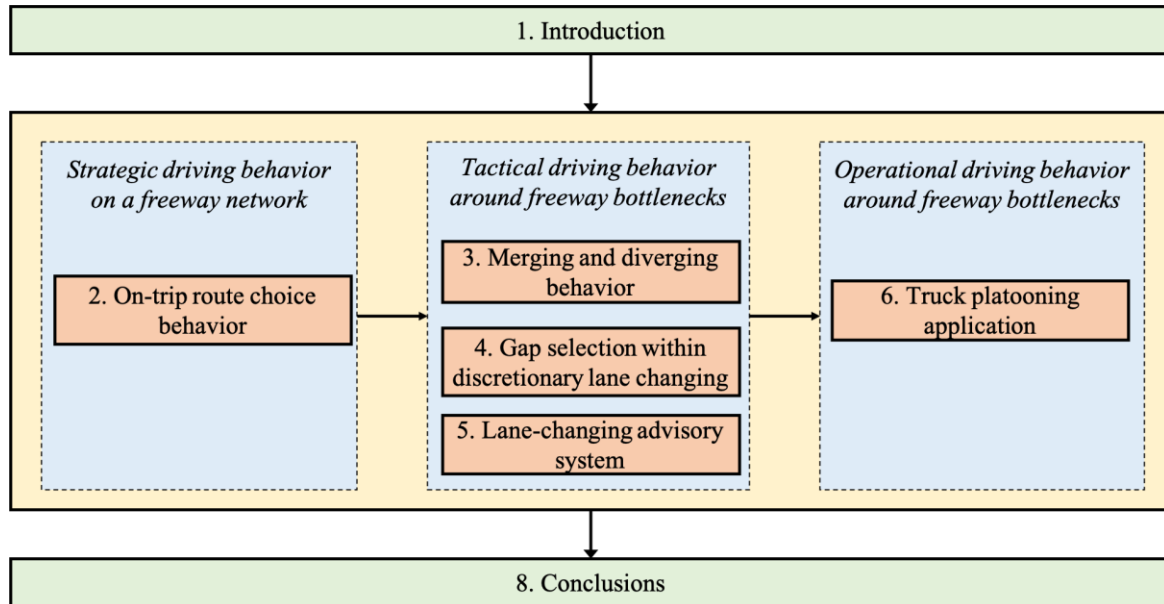


**Figure 1.2. Outline of the dissertation.**

changing advice. Chapter 3 presents the underlying heterogeneity in the merging and diverging behavior of truck drivers around freeway bottlenecks through the finite mixture model based clustering analysis. Chapter 4 presents how the gap selection process of truck drivers within their discretionary lane changing activities is influenced by three-dimensional feature space that includes their kinematic and physical characteristics, their interactions with surrounding vehicles, and their perceptions of the road topology by applying gated recurrent neural network models and explainable artificial intelligence techniques. Afterward, this process is compared with those of passenger car drivers and delivery van drivers to understand the differences in multiple vehicle classes. Chapter 5 presents a C-ITS based lane-changing advisory system to improve traffic operations and evaluates the performance of this system using a microscopic simulation tool.

Next, Chapter 6 focuses on the operational driving behavior of truck drivers and concentrates on the truck platooning application. This chapter presents how characteristics of a truck platooning configuration affect traffic operations around a freeway bottleneck using a microscopic simulation tool.

Finally, chapter 7 presents the conclusions of the dissertation. This chapter summarizes the main research findings, presents the overall conclusions, and discusses their scientific and practical implications. Directions for future research are also discussed in this chapter.

# **I: Strategic driving behavior on a freeway network**





## 2 On-trip route choice behavior of truck drivers

---

Chapter 1 showed the need for understanding the on-trip behavior of truck drivers. One of the hierarchical levels within on-trip behavior is the strategic one. The most important element within the strategic level to investigate is the on-trip route choices of truck drivers. State-of-the-art has not explored the usability of sparse automatic vehicle identification (AVI) data to estimate route choice characteristics. This chapter contributes to answering the first research question of this dissertation and fills this gap. This chapter proposes a novel method based on data fusion and bi-objective optimization to deal with the sparsity of AVI datasets. The usefulness of this method is demonstrated to estimate characteristics of on-trip route choices of truck drivers from fusing sparse Bluetooth data with loop-detector data.

This chapter is based on the following journal and conference papers:

Sharma, S., van Lint, H., Tavasszy, L. and Snelder, M. 2022. Estimating Route Choice Characteristics of Truck Drivers from Sparse AVI Data through Data Fusion and Bi-objective Optimization. *Transportation Research Record*, 2676(12), pp. 280–292.

Sharma, S., van Lint, H., Tavasszy, L. and Snelder, M. 2022. Estimating Route Choice Characteristics of Truck Drivers from Sparse Bluetooth Data through Data Fusion and Bi-objective Optimization. Paper presented in *101<sup>st</sup> Annual Meeting of the Transportation Research Board*.

---

## 2.1 Introduction

Road transport has been the main choice for inland freight transport within the European Union accounting for 76.30% of the modal share in 2019. Especially in the Netherlands where the port of Rotterdam generates most of the freight activity, the share of road freight is estimated at over 50% in 2019 (Eurostat, 2021). This reliance on road transport calls for robust and reliable traffic operations. On the one hand, freight transport contributes to congestion and on the other hand, trucking companies in the Netherlands have suffered economic damage due to road congestion. This economic damage is estimated to be 1.5 billion euros for 2019 and this cost has been increasing yearly (TLN, 2020). Therefore, a thorough investigation of on-trip route choices of truck drivers is fundamental to our understanding of how road freight moves which in turn can support the development of advanced traffic and logistics interventions.

The estimation of route choice models requires data that is typically collected using either stated-preference (SP) or revealed-preference (RP) surveys. The pros and cons of SP and RP-based approaches are widely known. SP studies solicit choice behavior in hypothetical scenarios where the actual choices might be different than the ones stated. RP studies rely on rich activity datasets and don't have these validity limitations, however, RP data cannot be collected under the same rigorously controlled circumstances as SP data (Hess et al., 2015). Nonetheless, there has been a recent shift to study route choices of truck drivers from SP-based studies (Arentze et al., 2012, Feng et al., 2013, Peeta et al., 2000, Rowell et al., 2014, Toledo et al., 2013) to RP-based studies due to the availability of trajectory (mostly GPS) datasets (Hess et al., 2015, Knorrning et al., 2005, Oka et al., 2019, Ben-Akiva et al., 2016, Sharma et al., 2019, Luong et al., 2018, Toledo et al., 2020). Although GPS data are appealing because of their spatial (i.e., location) and temporal (i.e., timestamps) richness to investigate route choices, few limitations are associated with collection and coverage. These data are often not publicly available and are expensive to buy from service providers. Furthermore, they might not capture a representative sample of the population over a limited period. In contrast to GPS data, there are other low-cost alternatives such as Automated Vehicle Identification (AVI) data. These data are collected from fixed-location sensors (e.g., Bluetooth sensors or traffic cameras), which can be installed by road authorities on many different strategically chosen locations. These fixed-location sensors can alleviate the limitations of GPS data in two ways. First, these sensors can capture passing vehicles' movements to produce a large sample that is (more) representative of the population. Second, these sensors can continuously record vehicles' movements over several periods of the day.

Fixed-location sensors have some advantages over mobile sensors (i.e. GPS); however, little research effort has been put to harness the potential of such data for route choice modeling (Cao et al., 2020). The key reason for that is that these sensors may not fully cover a road network sufficiently to make the underlying route choice observable (in the mathematical sense, e.g. Viti et al. (Viti et al., 2014)). The result typically is a sparse dataset that comprises origin, destination, and experienced travel time for a given trip. This sparse dataset is unlabeled in the sense that it lacks actual route choices of drivers, and as such cannot be used to estimate discrete choice models. To deal with the sparsity issue, extra information about estimated travel times of route alternatives is required to infer the most likely chosen route, i.e. the missing label. A possibility is to use another independent dataset (e.g., loop-detector data, floating car data) to derive this information. The estimation problem relies on the inference of the most likely chosen route, and this inference can be approached from the following two perspectives:

1. The most likely route chosen by a driver will maximize his perceived utility.

2. The most likely route chosen by a driver will minimize the deviation between experienced and estimated travel times.

Note that the deviation of travel times is computed from two independent datasets and might be associated with some uncertainty (van Lint et al., 2008b). Therefore, a naïve approach that assigns missing labels based on the lowest deviation value might produce erroneous estimates of model parameters. In contrast, (Cao et al., 2020) combine the aforementioned two perspectives into a single objective function, based on the so-called network-free model (Bierlaire and Frejinger, 2008), to model route choices using camera (also sparse data) and GPS data. Although their approach is promising, it strongly depends on the quality of the available GPS data, and how representative they are for the population. Moreover, their method incorporates the second perspective through a measurement equation to supply prior beliefs, which come from distributional assumptions, about a route present in the choice set.

Motivated by these issues, we propose an alternative approach that fuses a sparse Bluetooth dataset with path travel times derived from densely spaced loop detectors. To estimate how long a trip would take on alternative routes, we use a trajectory-based travel time estimation approach (Van Lint, 2010). In this way, our approach does not depend on GPS data and their variability. In addition, the estimation problem is investigated in a bi-objective optimization setting that allows capturing the interdependency between the conflicting perspectives: utility maximization and deviation minimization. Therefore, this approach can be used to simultaneously infer actual route choices (labels) and estimate the parameters of a route choice (discrete choice-based) model under minimal assumptions. As a result, this approach is applied to estimate route choice characteristics of truck drivers operating in the Netherlands.

Turning now to route choice phenomena of truck drivers, existing literature has studied time-of-day impacts and the latent class segmentation in SP-based contexts (Rowell et al., 2014, Feng et al., 2013, Arentze et al., 2012) where full experimental control is exerted by researchers and the data may suffer from hypothetical bias. The study of these two effects is particularly important for road freight because of two reasons. First, it can provide us with insights into the vulnerability of road freight operations, especially in peak hours. Second, latent class choice models, unlike mixed logit models (Toledo et al., 2020), do not require the knowledge of any mixing distribution, thus making them more useful for policy and decision-makers of logistic and traffic sectors. This indicates a need to study these effects using route choices of truck drivers observed in real-world situations. This chapter fills this research gap by using a Bluetooth dataset. Please note that this chapter does not use data collected from either SP or RP surveys.

This chapter aims to estimate route choices characteristics of truck drivers using a sparse AVI or Bluetooth dataset that lacks actual route choices. This chapter contributes to the existing literature by:

1. estimating the route choice characteristics of truck drivers from a sparse AVI dataset, where actual route choices are lacking, in combination with loop-detector data through bi-objective optimization; and
2. investigating time-of-day effects and latent segmentation within route choices of truck drivers from Bluetooth data that include their decisions in real-world situations.

This chapter is structured as follows. Section 2.2 will describe an approach to building a database of truck drivers and route-specific attributes using a sparse Bluetooth dataset and loop-detector data. Section 2.3 is concerned with the methodology where the bi-objective optimization approach and latent class modeling approach are described. Then, Section 2.4 presents the modeling results and Section 2.5 discusses key findings. Finally, Section 2.6 concludes this chapter. Note that route and path are used interchangeably in this chapter.

## 2.2 Data

This section first describes an approach to building a Bluetooth dataset for truck drivers that can be used for modeling their route choices. Afterward, this section presents attributes of route alternatives necessary to capture the route choice behavior of truck drivers.

### 2.2.1 Bluetooth dataset for trucks

Bluetooth stations record the time stamp and identity of the passing vehicle equipped with a Bluetooth sensor. The identity is captured in the form of a media access control address (or MAC address). The travel time between two Bluetooth stations can be retrieved by comparing the timestamps. For this chapter, the Bluetooth data are provided by the Bluetooth service from the port of Rotterdam. It is a query-based service that returns data in the JavaScript Object Notation (JSON) format. This service ensures privacy by masking the real MAC address. However, Bluetooth data, in general, does not provide information related to vehicle types. This chapter uses a three-step approach to prepare a Bluetooth dataset for trucks. First, we identify pairs of Bluetooth stations that can be used to identify vehicle types. Second, we prepare a database of truck drivers by storing their hashed MAC IDs. Finally, these MAC IDs are used to identify a truck trip from Bluetooth data. These trips provide key information (such as origin-destination (OD) pair, and trip duration) that is necessary to estimate their route choice characteristics.

#### Identification of Bluetooth stations that can cluster travel time

Clustering has been used in the past to infer vehicle types by analyzing travel times between two Bluetooth sensors (Sharma et al., 2019, Namaki Araghi et al., 2016). In our data, we have found 2 pairs of Bluetooth stations near the ring of Rotterdam (A15 and A4) where each pair comprised one main Bluetooth station and one ancillary Bluetooth station (Figure 2.1). These pairs can cluster travel time observations in both travel directions thus resulting in four sections for our analysis.



**Figure 2.1. Two pairs of Bluetooth stations that can cluster travel times in both traffic directions.**

### Identification of truck drivers in the Bluetooth dataset

The method to extract truck-specific data from the Bluetooth dataset is presented in Figure 2.2. For a given day and a pair of Bluetooth stations, congested periods from the dataset are removed since vehicles are observed to behave similarly as shown by travel time plots. Afterward, outliers are removed using a quartile-based method (Tukey, 1993) Then, we apply the Gaussian

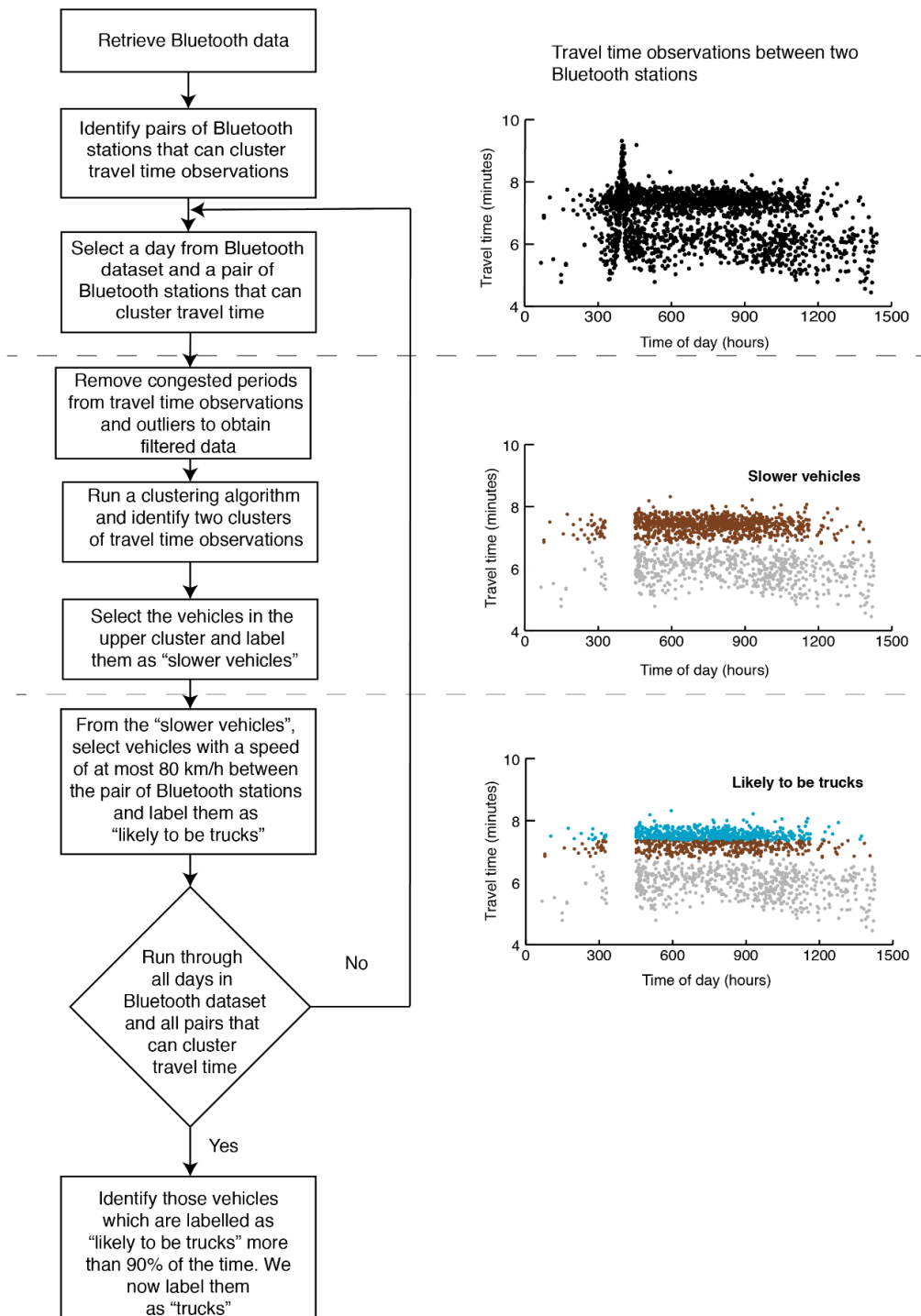


**Figure 2.2. Extracting trucks-specific observations from Bluetooth dataset.**

mixture model-based technique (Reynolds, 2009) to cluster travel time observations into one of the two groups: faster and slower vehicles. Note that the slower vehicle's group might contain some of the slower passenger cars. Therefore, we use the regulatory speed limit of trucks on motorways in the Netherlands, i.e., 80 km/h as a filter to remove undesired passenger cars and label the rest of the vehicles as “likely to be trucks”. We iterate over different days (October and November 2017) and one of the four sections that can cluster travel time observations. After this process, we label vehicles that are found in the “likely to be trucks” category more than 90% of the time and are detected at least three times by any pair of the Bluetooth stations as “trucks”. This process results in a database of hashed MAC IDs that represent truck drivers.

### Identification of truck trips

Having identified truck IDs, we can now turn to obtain truck trip data between an ID pair. In this chapter, we consider trips of truck drivers between a port node and a hinterland node (see Figure 2.3). Four hinterland nodes, which are strategic in terms of freight flows, are considered at shorter and longer distances from the port. A total of eight OD pairs by considering trips in both directions for a single OD pair. Since Bluetooth observations lack information about the route chosen by a truck driver between an origin-destination pair, we use anchor points to alleviate some of the limitations of the Bluetooth dataset. An anchor point is defined as a Bluetooth station that lies between an origin and a destination node. Thus, the trips made by truck drivers in our data represent journeys over an origin node, an anchor point, and a destination node.

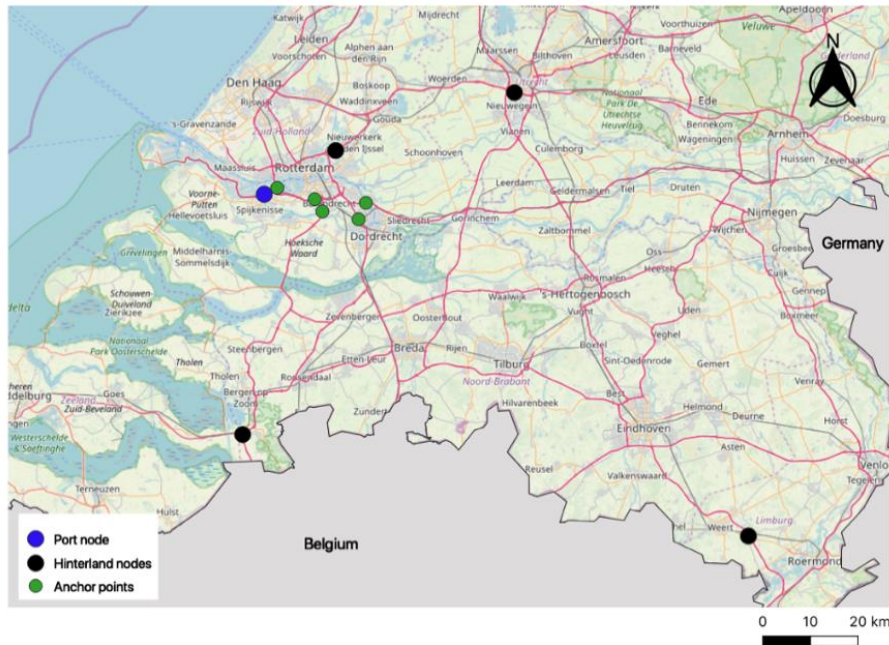


**Figure 2.3. Locations of the port node, hinterlands nodes, and anchor points in the Netherlands.**

In addition, we also filter out anomalies (e.g., long breaks) occurring in the trip data using a rule-based approach. Let  $TT_{obs,n}$  be the journey time incurred by a truck driver  $n$  while making a trip over an origin node, an anchor point ( $a_n$ ), and a destination node. This travel time is retrieved from the Bluetooth dataset. An anchor point allows us to reduce the choice set for a

truck driver  $n$ , i.e.,  $C_n$  to a viable subset  $A_n$ . All those route alternatives for a truck driver  $n$  that pass through the anchor point  $a_n$  are present in  $A_n$ .  $TT_{in}$  refers to the expected travel time over a route alternative  $i$  for a truck driver  $n$ . Then, the journey time ( $TT_{obs,n}$ ) of a truck driver  $n$  should lie between the minimum expected travel time and the maximum expected travel time among route alternatives present in the viable choice set  $A_n$ . A tolerance of 10% is added to the minimum and maximum expected travel time. We assume that any trip beyond this threshold would have incurred long breaks. Therefore, a continuous trip should satisfy the following Equation 2.1:

$$0.9 * \left( \min_{i \in A_n} TT_{in} \right) \leq TT_{obs,n} \leq 1.1 * \left( \max_{i \in A_n} TT_{in} \right) \quad (2.1)$$

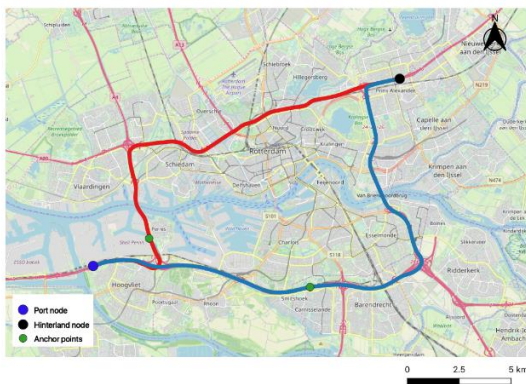
This step has produced a total of 14928 trips made by truck drivers during October and November 2017. Next, we present key attributes that characterize a truck trip.

## 2.2.2 Attributes of route alternatives

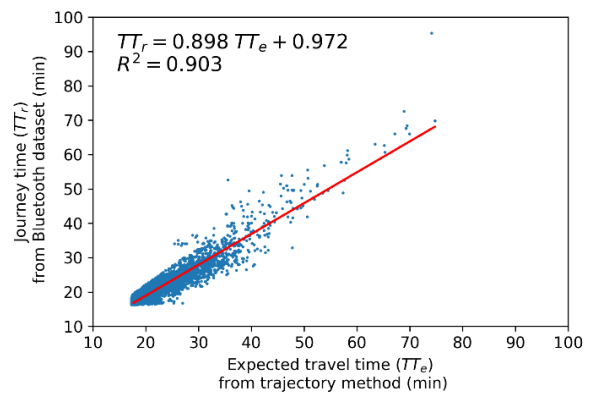
We consider three attributes: expected travel time, travel distance, and travel time unreliability at the time of departure.

### Expected travel time

We use expected travel time at the time of departure as one of the attributes of route alternatives. We use loop-detector data (Regiolab-Delft) and apply the filtered speed-based (FSB) trajectory method (Van Lint, 2010) to compute the expected travel time for a truck driver over a path between an origin-destination pair. In the Netherlands, loop-detectors are roughly located at every 500 m and can densely cover the road network. Between the origin-destination pair shown in Figure 2.4, for which route choices are known beforehand, we compared the expected travel time with the journey time obtained from Bluetooth data. The t-test shows that journey time obtained from the Bluetooth dataset ( $TT_r$ ) and expected travel time computed from the trajectory method ( $TT_e$ ) are equal (t-statistic = 11.37, p-value=8.08e-30). The unit of expected travel time is in minutes.



(a) Origin destination pair with two known routes



(b) Travel time comparison

**Figure 2.4. Travel time comparison between journey time obtained from Bluetooth data and expected travel time derived from the FSB trajectory method.**



### Travel distance

The travel distance of a route alternative between two Bluetooth stations is measured using Google Maps API. The unit for travel distance is in kilometers.

### Travel time unreliability at the time of departure

We use a skewness-based travel-time unreliability indicator (van Lint et al., 2008b). It can be interpreted as the likeliness of incurring a very bad travel time relative to median travel time, as defined in Equation 2.2:

$$\lambda_{skew} = \frac{TT_{90} - TT_{50}}{TT_{50} - TT_{10}}, \quad (2.2)$$

where  $\lambda_{skew}$  is the measure of travel time unreliability and  $TT_x$  refers to  $x$  percentile of travel time observations.  $\lambda_{skew}$  is computed for four time periods of a day: morning peak hours (06:30-09:30), day (09:30-16:00), evening peak hours (16:00-19:00), and night (19:00-06:30). Afterward, morning and evening peak hours were combined into peak hours. Day and night constituted off-peak hours. For the computation of travel time unreliability, we select the travel times incurred over a path in the previous 10 days. Having discussed the dataset and the attributes, the next section presents our methodology to estimate route choice models using sparse data.

## 2.3 Methods

This chapter proposes a new model estimation framework to estimate route choice characteristics from a sparse AVI or Bluetooth dataset. Figure 2.5 presents this framework that accepts truck-specific trip data, obtained through clustering, and travel times of alternative paths derived from loop-detectors as inputs. Subsequently, a bi-objective program is formulated to simultaneously infer actual route choices and parameters of a route choice model. Finally, a latent class choice analysis is conducted to identify segments with truck drivers' route choice behavior.

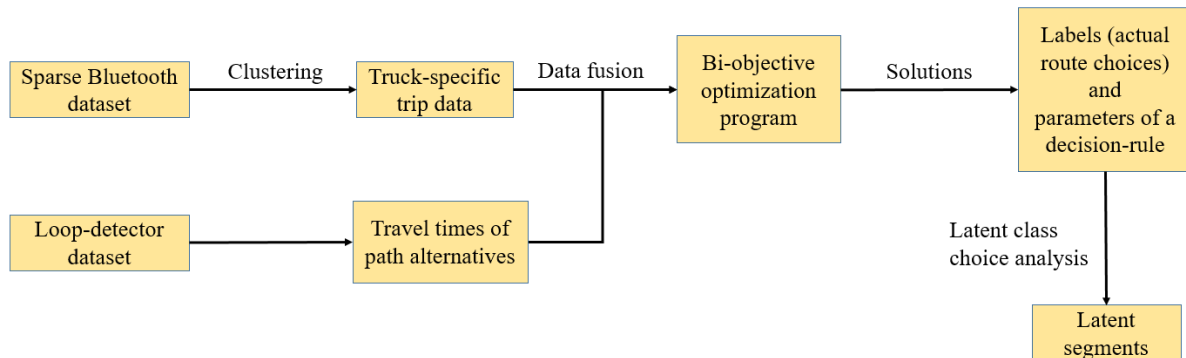


**Figure 2.5.** A framework to estimate route choice characteristics of truck drivers from sparse Bluetooth data.

The rest of the section is divided into three parts. The first part presents the problem formulation and solution approach. The second part discusses the decision rules that capture the behavior of decision-makers. Finally, the third part describes our approach to generate choice sets.

### 2.3.1 Bi-objective optimization approach to simultaneously infer actual route choices and estimate the parameters of a route choice model

#### Problem description

This chapter proposes a bi-objective model that simultaneously considers the two objectives. On one hand, the proposed model aims at maximizing the log-likelihood of an entire dataset of choice observations. Here, the likelihood of an entire dataset is simply the product of individual choice probabilities. On the other hand, the model aims at minimizing the total deviation between experienced and estimated travel times of a path. The main optimization decisions for the proposed model are as actual route choices (labels) and parameter estimates of a route choice model.

#### Notations

The mathematical notations used in the chapter are listed in Table 2.1.

**Table 2.1 Notations**

Notation	Description
<b>Indices</b>	
$i$	index of a route alternative
$n$	index of a truck driver
<b>Sets</b>	
$N$	set of truck drivers, $n \in N$ or $N = \{1, \dots, n\}$
$C_n$	set of route alternatives for a truck driver $n$
$A_n$	set of route alternatives for a truck driver $n$ passing through an anchor point $a_n$
$a_n$	anchor point for a truck driver $n$
<b>Parameters</b>	
$TT_{obs,n}$	experienced travel time for a truck driver $n$ retrieved from Bluetooth dataset
$TT_{in}$	estimated travel time for a truck driver $n$ over a route alternative $i$
$\beta_{min}$	the user-specified minimum value for parameters $\beta$
$\beta_{max}$	the user-specified maximum value for parameters $\beta$
<b>Decision variables</b>	
$y_{in}$	binary variable, 1 if a truck driver $n$ chooses a route $i$ , 0 otherwise
$\beta$	coefficients of the utility function

#### Mathematical model

$$\text{Max } F_1 = \sum_{n \in N} \sum_{i \in C_n} y_{in} (\ln P_{in}(\beta)) \quad (2.3)$$

$$\text{Min } F_2 = \sum_{n \in N} \sum_{i \in C_n} y_{in} (TT_{in} - TT_{obs,n})^2 \quad (2.4)$$

Subject to:

$$\sum_{i \in A_n} y_{in} = 1 \quad \forall n \in N \quad (2.5)$$

$$y_{in} \in \{0,1\} \quad \forall n \in N, \forall i \in C_n \quad (2.6)$$

$$\beta_{min} \leq \beta \leq \beta_{max} \quad (2.7)$$

The objective function (2.3) maximizes the log-likelihood of the sample. The probability for a truck driver  $n$  choosing a route  $i$  is expressed by  $P_{in}(\beta)$ , which depends on the type of decision

rule employed. The objective function (2.4) minimizes the squared deviation between the experienced travel time obtained from the Bluetooth data and the estimated travel time derived from loop-detector data. Constraint (2.5) ensures that truck drivers can be assigned to at most one route that is present in the choice set  $A_n \in C_n$ . Constraints (2.6) and (2.7) state the type of decision variables and their restrictions.

### Solution approach

In bi-objective optimization problems, there is no single optimal solution that can simultaneously optimize all the objective functions. In these cases, decision-makers look for the most preferred solution. For these problems, the efficient (or Pareto optimal) solution is the solution that cannot improve one objective function without deteriorating at least one of the rests. A well-known technique to solve bi-objective optimization problems is the  $\varepsilon$ -constraint method (Aghaei et al., 2011). This technique optimizes one main objective while other objectives act as constraints. In this chapter, our main objective ( $F_1$ ) is to maximize the log-likelihood of the sample considering  $F_2$  as a constraint (see Equation 2.8).

$$\text{Max } F_1$$

$$\text{subject to } F_2 \leq \varepsilon \tag{2.8}$$

We consider that  $F_2$  is upper bounded by  $\varepsilon$ , i.e., the total squared deviation between Bluetooth reported journey time and expected travel time computed using the trajectory method should not be more than  $\varepsilon$ . We vary the value of  $\varepsilon$  from  $F_{2, \min}$  to  $F_{2, \max}$  using a payoff table (Aghaei et al., 2011), which consists of all objective values, when each objective is optimized subject to constraints. The set of all obtained solutions for the entire range of  $\varepsilon$  are considered Pareto optimal front of the bi-objective optimization problem. Among the obtained Pareto optimal solution, the most preferred one is selected by the decision-maker according to the specific preference of the application. We use an optimization-specific algebraic modeling language AMPL (AMPL, 2019) to code our optimization formulation and use Bonmin solver (Bonmin, 2019).

### 2.3.2 Decision rules

Having formulated the optimization problem formulation, we will now discuss decision rules that describe the process used by the decision-maker to choose an alternative. We consider three decision rules: multinomial logit, path size logit, and latent class choice models.

#### Multinomial logit models

Random utility theory assumes that drivers are perfectly rational and they have perfect discrimination capabilities (Ben-Akiva and Bierlaire, 2003). It is assumed that the utility for a driver  $n$  associated with route alternative  $i$  in the choice set  $C_n$  is the sum of a deterministic part ( $V_{in}$ ) and a random part ( $\epsilon_{in}$ ). We consider a linear utility specification; therefore, we have  $V_{in} = \beta X$ . Here,  $\beta$  refers to parameters associated with route attributes  $X$ . If we assume that the error terms of the utility function are independent and identically Gumbel distributed, the choice probability of each alternative  $i$  can be described in Equation 2.9 as:

$$P_{in} = \frac{e^{\mu V_{in}}}{\sum_{j \in C_n} e^{\mu V_{jn}}}. \tag{2.9}$$

Thereby,  $\mu$  is a positive scale parameter and is related to the Gumble variable.

### Path size logit models

Typically, in route choice modeling, the alternatives are often correlated. Therefore, we use a correction factor (Ben-Akiva and Bierlaire, 1999). The path size correction factor quantifies the similarity of a route alternative with other route alternatives present in the choice set and its values range from zero to one. A distinct route, which is unique and does not overlap with other route alternatives in the choice set, has a path size of one. Path size correction for a route alternative  $i$  corresponding to a truck driver  $n$  is defined in Equation 2.10 as:

$$PS_{in} = \sum_{a \in \Gamma_i} \left( \frac{l_a}{L_i} \right) \frac{1}{\sum_{j \in C_n} \delta_{aj}}, \quad (2.10)$$

where  $a$  is a link in the route alternative  $i$ .  $\Gamma_i$  is the set of links present in the route alternative  $i$ .  $l_a$  refers to the length of link  $a$  and  $L_i$  is the length of route alternative  $i$ .  $\sum_{j \in C_n} \delta_{aj}$  indicates the total number of route alternatives, present in the choice set of a driver  $n$ , sharing link  $a$ . By including a path size ( $PS$ ) correction factor (Ben-Akiva and Bierlaire, 1999), we deal with the correlation among route alternatives. Thus, the choice probability for a driver  $n$  to choose a route alternative  $i$  is given by Equation 2.11:

$$P_{in} = \frac{e^{\mu(V_{in} + \ln PS_{in})}}{\sum_{j \in C_n} e^{\mu(V_{jn} + \ln PS_{jn})}}. \quad (2.11)$$

### Latent class choice models

Latent class models are used to capture unobserved heterogeneity in the behavior of truck drivers (Ben-Akiva and Bierlaire, 1999). The underlying assumption is that heterogeneity may be produced by taste variations. The latent class model is given by Equation 2.12:

$$P_{in} = \sum_{s=1}^S \pi_{ns} P_{in}(\beta_s), \quad (2.12)$$

where  $\beta_s$  are class-specific parameter estimates and  $\pi_{ns}$  is the probability that driver  $n$  belongs to a segment  $s$  and can be given by Equation 2.13:

$$\pi_{ns} = \frac{\exp(\delta_s \gamma_n)}{\sum_s \exp(\delta_s \gamma_n)}, \quad (2.13)$$

where  $\delta_s$  is a class-specific constant and to be estimated and  $\gamma_n$  refers to individual-specific socio-economic characteristics.

For model selection, we use the Bayesian information criterion (BIC) (Schwarz, 1978). The BIC value is defined mathematically in Equation 2.14:

$$BIC = -2 \ln(\mathcal{L}) + K \ln(n), \quad (2.14)$$

where  $\mathcal{L}$  is the log-likelihood of the model,  $K$  refers to the number of estimable parameters in the model, and  $n$  denotes the number of observations in the dataset. We compute the BIC value for each model under consideration and select the one with the smallest criterion value (Burnham and Anderson, 2004).

### 2.3.3 Choice set generation

Analyzing individual decision-making requires not only knowledge of what has been chosen, but also of what has not been chosen. Therefore, we require a set of available alternatives (also termed as a choice set) that an individual considers during a choice process. We use the Breadth-

First Search on Link Elimination (BFS-LE) method to find repeated least-cost paths between an origin-destination pair (Rieser-Schüssler et al., 2013). This algorithm is a link-elimination approach where links of the current least-cost path are removed one at a time to calculate subsequent least-cost paths. We check the commonality of generated least-cost paths and only store unique paths in the route choice set by using travel time as our cost function. A maximum number of 30 unique paths between an origin-destination pair served as the termination criteria. This value is set as a target choice set size considering the computational tractability of the bi-objective optimization program.

## 2.4 Results

This section first presents the results of an optimization model that is used to simultaneously estimate route choices and parameters of a route choice model. Then, this section presents segments of truck drivers using the latent class choice model.

### 2.4.1 Simultaneous inference of actual route choices and estimation of parameters of route choice models

The Pareto curve captures the trade-off between the two conflicting objectives considered in this chapter. Figure 2.6 illustrates the Pareto curves for the multinomial and path size logit models. The solution ‘a’ is obtained when the deviation is minimized, whereas the solution ‘b’ is obtained when the utilities of drivers are maximized. Among the obtained solutions that lie on the Pareto curve, we select the solution ‘c’ where the value of  $\varepsilon$  refers to a reasonable estimate of the total squared deviation for sample data. For the origin-destination (OD) pair shown in Figure 2.4, the mean squared deviation is computed as 5.43 square minutes over an average distance of 31.20 km between the same OD pair. This average distance is the mathematical average of the length of all route alternatives between an OD pair. Note that that the mean squared deviation is assumed to increase linearly over longer distances due to errors in loop-detector data or the inability of Bluetooth observations to detect vehicle activity in between. The value of  $\varepsilon$  for sample data is computed to be 196833.64 square minutes.

Table 2.2 shows the model fit of the multinomial logit and path size logit models. For both the models, all the parameters are significant, and they have expected signs except the travel time unreliability in off-peak hours. The path size logit model outperforms the multinomial logit

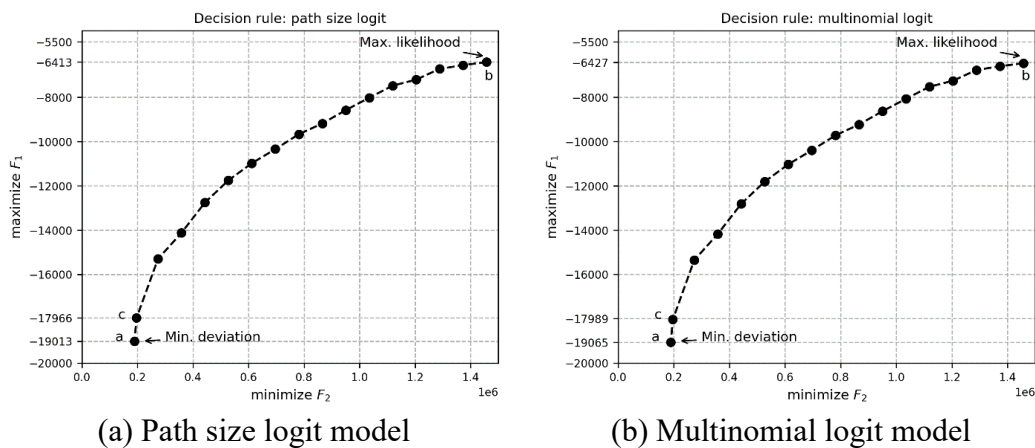


**Figure 2.6. Bi-objective optimal Pareto-curve for Likelihood and deviation objectives for two different decision rules. The preferred solution is ‘c’ where the deviation is 196833.64 square minutes.**

model based on the likelihood ratio test ( $p$ -value  $< 0.01$ ). The path size logit model not only improves the model fit but can also correct the correlation among route alternatives. The path size logit model shows that truck drivers negatively value the travel time, travel distance, and travel time unreliability in peak hours. The path-size parameter estimate's positive coefficient is consistent with the findings of (3). A positive estimate for path correction term denotes that truck drivers prefer unique routes (i.e., routes with less overlap). We test truck drivers' preferences concerning the travel time unreliability in peak and off-peak hours. During peak hours, truck drivers, in general, stay away from unreliable routes. However, during off-peak hours, they are more likely to make risky route choices. If we now turn to heterogeneity in the route choice behavior of truck drivers, we will present the results of latent class choice models.

**Table 2.2 Route choice models for truck drivers**

Parameters	Path size logit model			Multinomial logit model		
	<i>Value</i>	<i>Rob. std. error</i>	<i>Rob. t-test</i>	<i>Value</i>	<i>Rob. std. error</i>	<i>Rob. t-test</i>
Natural log of path size based on travel distance	0.492	0.067	7.31			
Travel distance (km)	-0.097	0.002	-47.70	-0.090	0.002	-44.00
Expected travel time (min)	-0.023	0.002	-13.30	-0.025	0.001	-13.90
Travel time unreliability if departing in off-peak hours	0.072	0.003	18.40	0.063	0.003	18.00
Travel time unreliability if departing in peak hours	-0.046	0.004	-11.30	-0.035	0.003	-9.72
Number of observations			14928			14928
Initial log-likelihood			-25655.720			-25655.272
Final log-likelihood			-17966.610			-17989.800
Adjusted Rho-square			0.299			0.298
Likelihood ratio (LR) test with respect to the multinomial logit model			46.38			
p-value of LR test			<0.01			

#### 2.4.2 Latent class choice models

We use the solutions of the optimization problem generated from the path size logit model as actual route choices of truck drivers to segment truck drivers. We estimate a latent class choice model using the PandasBiogeme (Bierlaire, 2020). Using the BIC criterion, we find that the model with 4-segments performs best as it has the least value for the BIC criterion (see Table 2.3). The proportions of truck drivers belonging to the 4-segment model are 15.41%, 37.05%, 39.82%, and 7.72%. The signs of parameter estimates for travel time are negative as expected. Similarly, the signs of parameter estimates for travel distance are negative except for segment 4. The parameters for the route choice model show that truck drivers value path overlap/correction factor and travel time unreliability differently.

**Table 2.3 Comparison of latent class models for different number of segments**

Parameters	Latent segments				
	1	2	3	4	5
Final log-likelihood	-17966.61	-17054.19	-17029.96	<b>-16756.74</b>	-16860.90
Adjusted Rho-squared	0.299	0.334	0.335	<b>0.346</b>	0.341
Segment proportions (%)	100.00	37.61	33.91	<b>15.41</b>	1.72
		62.39	3.61	<b>37.05</b>	24.55
			62.48	<b>39.82</b>	10.39
				<b>7.72</b>	43.84
					19.50
Estimated parameters	5	11	17	<b>23</b>	29
AIC	35943.22	34130.37	34093.92	<b>33559.48</b>	33779.80
BIC	35981.27	34214.09	34223.30	<b>33734.53</b>	34000.52

Table 2.4 shows that segments 2 and 3 constitute three-fourth of truck drivers. A majority of truck drivers belong to segment 3, and they seem to prefer the shortest distance and shortest time routes. Their preference to choose routes with high overlaps makes them more flexible in unexpected situations such as congestion. However, they show risky behavior during both peak and off-peak hours by having a likeliness for routes with unreliable travel times. Compared to segment 3, truck drivers belonging to segment 2 form a second majority and they are less sensitive to prefer the shortest distance and shortest time routes. Unlike segment 3, truck drivers in segment 2 show a preference for routes with less overlap. Their preference to select a unique route is in contrast to the behavior shown by a majority of truck drivers. However, they are concerned about the reliability of travel times during peak hours which prompts them to make informed routing decisions and decreases the possibility to incur longer travel times. Around one-fourth of truck drivers belong to segments 1 and 4. Truck drivers belonging to segment 1 behave more like segment 3 except for their sensitivities to the unreliability of travel times. Their sensitivities to travel time and distance are similar to other segments, i.e., they negatively value longer time or distance routes. However, they are prone to choose unreliable routes during peak hours. Truck drivers in segment 4 account for only 7.72%. They value shortest time routes but they have an unexpected affinity for longer distant routes. It can be explained by their preference to choose a route with high overlaps. In doing so, they travel longer distances between an OD pair. Also, they are more likely to choose an unreliable route since they are not significantly affected by the unreliability of travel times during peak hours.

## 2.5 Discussion

This section first begins with discussing the plausibility of route choice characteristics of truck drivers estimated from a sparse Bluetooth dataset. Then, this section elaborates on the advantage and limitations of our estimation approach from an application's perspective. Finally, we provide implications of our findings to designing policies.

This chapter found that truck drivers can be segmented into four groups based on their preferences to travel distance, expected travel time to destination, the unreliability of travel time on a route at the time of departure. The number of segments is more compared to the previous research (Rowell et al., 2014, Feng et al., 2013). A possible explanation for this might be that the previous research (Rowell et al., 2014, Feng et al., 2013) used data from SP surveys. Whereas, this chapter has used empirical data that include choices in real-world situations. Another possible explanation is that previous research focused on different business and demographic needs (urban logistics in the Netherlands (Feng et al., 2013) and regional logistics in Washington state, USA (Rowell et al., 2014)) compared to the port logistics.





Another significant aspect of our findings is that a majority of truck drivers prefer paths with a high degree of overlaps, which indicates that they value the availability of a large number of alternatives to minimize the risks during their trips. These results corroborate the findings of Anderson et al. (Anderson et al., 2017). In addition, truck drivers seem to prefer paths with unreliable travel times during peak hours. This outcome is contrary to a previous study that suggests that truck drivers value reliability (Bogers and Van Zuylen, 2004). Our results seem to be consistent with Luong et al. (Luong et al., 2018). These results are likely to be related to the behavior of short-haul truck drivers or the ones departing in the off-peak hours who may take a chance to reach their destination by choosing an unreliable path.

Let us now turn to our estimation approach, which is formulated as a bi-objective optimization program. Our study raises the possibility that passive data sources (Bluetooth data and loop-detector data) can be used to estimate route choice models. This approach might alleviate the need to perform expansive data collection from SP or RP surveys to understand driving behavior. Different types of fixed-location sensors other than Bluetooth such as cameras, Wi-Fi sensors, mobile phone towers can be used as input. This formulation can also be applied to freight-specific sparse datasets such as freight trip diaries, which also lack actual route choice observations – with these we could develop advanced commodity-specific route choice models. In this way, the estimation approach opens new possibilities to use sparse datasets in generating insights about route choice behavior of drivers. Limitations of the approach are the following. First, loop-detectors in other regions may not be densely located due to high costs of installation. We recommend considering the use of other data (e.g., floating car data) in such cases. Second, clustering of vehicles based on speed works well for the Netherlands but may not deliver promising results in countries with low speed limit compliance or different driving policies in place (e.g. keep-your-lane policy). Here, further research on mode identification from a sparse dataset would be recommended.

In terms of implications for practice, our model indicates that few truck drivers prefer less reliable routes during peak hours. There could be a benefit in including reliability of travel time in route planning or navigation systems, to support companies in making the trade-off between travel time, costs and reliability. Further research should be undertaken to investigate the objective of truck drivers behind choosing unreliable routes. Also, the model could inform the design of interventions by traffic management agencies, such as peak-hour congestion charging or segment-specific route guidance.

## 2.6 Conclusions

This chapter estimates route choice characteristics of truck drivers using sparse automatic vehicle identification (AVI) data. A novel method that uses data fusion and a bi-objective optimization program is proposed to deal with the sparsity of the AVI dataset, which lacks actual route choices (labels). This method can simultaneously estimate the actual route choices and the parameters of a route choice model. This method is successfully applied on a sparse Bluetooth dataset of truck drivers making trips from and to the port of Rotterdam in the Netherlands. The resulting models can identify four latent segments within the route choice behavior of truck drivers and capture the effects of time of day (peak and off-peak hours).

In future investigations, it might be possible to incorporate panel effects (or repeated choices made by a driver) within the current framework. Despite the usefulness of our estimation method in delivering behaviorally consistent findings, future work is required to establish the validity of this method. A possible approach is to conduct a driver survey that can supply the ground truth in addition to a sparse dataset. A further study on investigating route choice behavior of car drivers and its comparison with this study can provide useful insights towards managing significant freight corridors.

## **II: Tactical driving behavior around freeway bottlenecks**



### 3 Merging and diverging strategies of truck drivers

---

Previous chapter showed how truck drivers make decisions at the strategic level and choose a route during their trips. After deciding on a route, truck drivers often encounter congestion around freeway bottlenecks located on a particular route. Around these bottlenecks, it is worth investigating their lane changing behavior. One of the elements within lane changing is to understand how truck drivers merge or diverge around these locations. Previous literature lacks an understanding of which strategies truck drivers employ to merge or diverge around ramps and weaving sections. To address this gap, this chapter aims to identify key merging and diverging strategies of truck drivers and contributes to answering the second research question of this dissertation. This chapter applies a finite mixture modeling-based clustering approach on a large trajectory dataset that contains 298 merging and diverging maneuvers of truck drivers around ramps and weaving sections.

This chapter is based on the following published journal and conference papers:

Sharma, S., Snelder, M., Tavasszy, L. and van Lint, H. 2020. Categorizing merging and diverging strategies of truck drivers at motorway ramps and weaving sections using a trajectory dataset. *Transportation Research Record*, 2674(9), pp. 855-866.

Sharma, S., Snelder, M., Tavasszy, L. and van Lint, H. 2020. Categorizing merging and diverging strategies of truck drivers at motorway ramps and weaving sections using a trajectory dataset. Paper presented in 99<sup>th</sup> *Annual Meeting of the Transportation Research Board*.

---

### 3.1 Introduction

Driving behavior is generally captured using a combination of longitudinal and lateral behavior models. Whereas the longitudinal model is used to capture inter-vehicle interactions such as car following at a lane level, the lateral model governs switching between lanes and all the tasks associated with it (e.g., assessing gaps, deciding for or against one and executing this decision). Previous research has shown that significant differences exist between the lane changing characteristics of different classes of vehicles such as passenger cars and trucks (Aghabayk et al., 2011, Moridpour et al., 2012). However, driver behavior, especially for lane changing, for trucks is an overlooked research area compared to passenger cars (Moridpour et al., 2012, Rahman et al., 2013). Even within a single class of vehicles, Ossen et al. (2006) reported that inter-driver differences exist that cannot be captured alone by adjusting driver behavior parameters in existing models. The heterogeneity these authors found in car following encompasses the differences in driving styles that can best be described by a (dynamic) distribution of car-following models with a distribution of parameters. Clearly, with such heterogeneity in the car-following behavior, there is also large heterogeneity in the lane-changing behavior. A deeper understanding of this heterogeneity in the lane-changing behavior (of multiple road user-classes) is essential to better capture real-world phenomena.

Motorway bottlenecks such as ramps, weaving sections, or lane drops present significant obstacles to vehicles and are a major source of travel delays (Taale and Wilmink, 2016). For truck-dominated motorways, the bottlenecks can cause unreliable traffic operations, thus introducing uncertainty in the logistics system. As a result, freight tour planning and terminal operations can also be affected. In the vicinity of these bottlenecks, the lane-changing behavior is shown to affect traffic throughput, safety, and turbulence (van Beinum et al., 2018, Tilg et al., 2018, Cassidy and Rudjanakanoknad, 2005, Chen and Ahn, 2018, Laval and Daganzo, 2006, Golob et al., 2004, Kondyli and Elefteriadou, 2012). A limited body of research has shown that heterogeneity exists within the merging and diverging behaviors of drivers (Keyvan-Ekbatani et al., 2016, Li, 2018, Li and Sun, 2018). However, they do not take into account the behavior of truck drivers who are a significant part of traffic on truck-dominated motorways.

Consequently, the main objective of this chapter is to identify heterogeneity in the merging and diverging behavior of truck drivers. Using recent data collection efforts by van Beinum (2018), we have a detailed trajectory dataset for motorway ramps and weaving sections, located in the Netherlands, which we have used in this chapter to explore and cluster heterogeneity in the lane-changing behavior of trucks. The contributions of this chapter are two-fold. First, this chapter categorizes truck drivers in accordance with their merging and diverging behavior using the trajectory dataset. Second, this chapter analyzes and presents the contributions of truck drivers to the turbulence in the vicinity of motorway bottlenecks.

This chapter is structured as follows. First, Section 3.2 presents a literature review on the heterogeneity of drivers with respect to their lane-changing maneuvers and inefficiencies caused owing to lane-changing phenomena. Next, Section 3.3 describes the trajectory dataset, presents descriptive data statistics related to the merging and diverging maneuvers of truck drivers, and explains the finite mixture modeling technique to categorize these maneuvers. Afterward, Section 3.4 presents the merging and diverging strategies of truck drivers and shows the role of truck drivers' merging and diverging strategies in causing turbulence at motorway bottlenecks. Then Section 3.5 discusses the results and presents limitations. Lastly, Section 3.6 concludes this chapter.

## 3.2 Literature review

This section presents a literature review on identifying drivers' heterogeneity with respect to their lane-changing maneuvers and highlighting the role of lane-changing in causing inefficiencies around motorway bottlenecks.

### 3.2.1 Drivers' heterogeneity with respect to their lane change maneuvers

Sun and Elefteriadou conducted a focus group study with 21 participants to identify four types of drivers using clustering for urban streets and developed a utility-based lane change model (Sun and Elefteriadou, 2011). Later, Sun and Elefteriadou conducted a test-drive with an instrumented vehicle for 40 participants (Sun and Elefteriadou, 2012). Their results show that the drivers' lane change behavior can be classified into three to four clusters, and the clusters are consistent between drivers' background-based and driver's behavior-based analysis. Although the studies focus on an urban setting, the results emphasize drivers' heterogeneity in their lane changing decisions.

Keyvan-Ekbatani et al. looked at the lane-change decision process as an integrated task which also involves car-following or longitudinal actions (Keyvan-Ekbatani et al., 2016). They conducted both interviews and field tests on 10 participants. They reported that drivers use several strategies for merging and diverging maneuvers. However, the sample was too small to draw any statistical inferences. Li and Sun analyzed 370 merging maneuvers from the NGSIM dataset and reported four categories based on clustering: early merging drivers at high speed, early merging drivers at low speed, late merging drivers at low speed and late merging drivers at high speed (Li and Sun, 2018). However, they do not consider gap selection in the decision process. Li classified the merging maneuvers of 374 vehicles into two classes based on finite mixtures of logistic regression: risk-rejecting (who try to merge as soon as possible and will accept a larger gap) and risk-taking (who are less sensitive to the gap size and pay more attention to the surrounding traffic conditions to save travel time) drivers (Li, 2018).

The aforementioned studies have shown that motivations and reasoning for lane-changing vary between drivers. However, there exists a gap in our understanding of heterogeneity with respect to the lane change phenomena of truck drivers.

### 3.2.2 Inefficiencies owing to lane-changing

At motorway bottlenecks, local phenomena such as lane changes, speed, and headway variabilities affect traffic throughput and safety (Cassidy and Rudjanakanoknad, 2005, Chen and Ahn, 2018, Kondyli and Elefteriadou, 2012, Laval and Daganzo, 2006, Golob et al., 2004, Lee et al., 2003a, Lee et al., 2003b). van Beinum et al. showed that lane change maneuvers in the vicinity of motorway ramps and weaving sections are primary contributors to the turbulence (van Beinum et al., 2018). It has also been suggested that the concentration of lane changes at the beginning of a weaving section decreases the overall capacity of the bottleneck (Lee and Cassidy, 2008, Sulejic et al., 2017). The behavior of trucks might have serious effects on the surrounding traffic owing to their lane change maneuvers, especially under heavy traffic conditions (Pan et al., 2016). Although previous studies have identified inefficiencies owing to the lane-change process, these works have not explicitly examined the role of truck drivers' lane change characteristics in causing turbulence at motorway bottlenecks.

## 3.3 Data and methods

This section first describes the trajectory dataset. Then, we present a method to identify the lane change maneuvers of truck drivers from this dataset. Our hypothesis is that merging and diverging maneuvers relate to the behavioral characteristics of truck drivers, and these

behavioral characteristics can be grouped to capture the underlying heterogeneity among truck drivers. To this, we present a theoretical background of the finite mixture modeling approach to test our hypothesis. Lastly, we present descriptive statistics of the data collected for finite mixture modeling. The relevant MATLAB and R codes used in this chapter can be accessed at [https://github.com/salilrsharma/truck\\_trajectory](https://github.com/salilrsharma/truck_trajectory).

### 3.3.1 Trajectory dataset

This chapter utilizes trajectory datasets from four locations in the Netherlands as shown in Figure 3.1 (van Beinum, 2018). Overall, we consider one on-ramp, one off-ramp, and five weaving sections. Each location comprises two bottleneck sites on each side of a bi-directional motorway. We considered the following bottleneck sites to have a sufficient number of lane changes performed by truck drivers in this chapter. In parentheses, we denote the ramp or weaving segment length of each bottleneck site.

- Zonzeel-north: On-ramp (340 m)
- Zonzeel-south: Off-ramp (230 m)
- Klaverpolder-north: Weaving (610 m)
- Klaverpolder-south: Weaving (530 m)
- Ridderkerk-north: Weaving (740 m)
- Princeville-east: Weaving (1000 m)
- Princeville-west: Weaving (1130 m)

The above sites have a three-lane mainline carriageway and one auxiliary lane except for the Klaverpolder site which has a two-lane mainline carriageway and one auxiliary lane. This dataset was collected using a high-resolution camera attached to a hovering helicopter. The sites represent isolated discontinuities and their lengths are at most 1100 m meaning that the trajectories can be captured using the helicopter method.



**Figure 3.1. Locations of freeway ramps and weaving sections considered for collecting trajectory data in the Netherlands.**

For each site, 30 min of the video feed was collected at the onset of evening congestion, that is, between 14:00 and 17:00 h. For further information about the data collection, the reader may refer to van Beinum et al. (van Beinum et al., 2018). The processed empirical trajectory dataset, in the form of MATLAB files and video feed, is available online (van Beinum, 2018). This trajectory dataset contains the position of every vehicle at every time step. Every vehicle is tagged along with the length and width of the vehicle. To infer trucks from the empirical trajectory dataset, we used the vehicle length as the primary criterion. Vehicles longer than 12 m in length are labeled as trucks.

### 3.3.2 Identifying truck driver's merging and diverging maneuvers from trajectory data

The lane-changing process for a vehicle begins when it starts to drift laterally and ends when it stabilizes its lateral position after changing to a neighboring lane. The time instances are marked as lane change initiation and lane change completion, respectively. Figure 3.2 shows an example of a truck driver performing a merging maneuver in which a relative increase in the lateral position of a vehicle with respect to time is marked as the initiation and the time instant after which the lateral position stabilizes as completion. Lane change duration can be defined as the time difference between the lane change completion and lane change initiation process.

### 3.3.3 Finite mixture modeling

We assume that the overall population heterogeneity results from the underlying two or more distinct homogeneous subgroups or latent classes of individuals. The components in these models are not directly observed and lie latent for some or all of the individuals in the population. Therefore, the mixture models express the overall population distribution as a finite

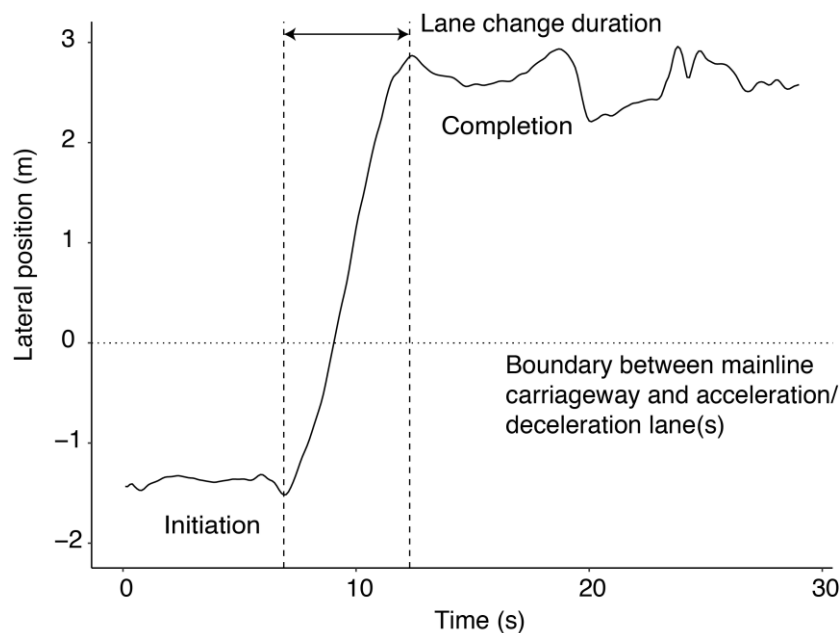


**Figure 3.2.** Lateral movement of a truck driver during the merging process.



mixture of some fixed number of components (Little, 2013). In these models, there are two main types of variables: latent variables (e.g., a latent class variable which is not directly observed) and manifest or indicator variables (e.g., observable response variables). The observed values of indicator variables refer to imperfect indications of an individual's true underlying latent class membership. For a finite mixture model, there are two parts: the measurement model and the structural model. The measurement model specifies the relationship between the underlying latent variable and the corresponding manifest or indicator variable. Whereas the structural model specifies the distribution of the latent variable in the population (Little, 2013).

For model selection, we used the Bayesian information criterion (BIC). The BIC value has been derived by Schwarz (1978), and mathematically it can be defined in Equation 3.1.

$$\text{BIC} = -2 \ln(\mathcal{L}) + K \ln(n) \quad (3.1)$$

where  $\mathcal{L}$  is the log-likelihood of the model,  $K$  refers to the number of estimable parameters in the model, and  $n$  denotes the number of observations in the dataset. We computed the BIC value for each model under consideration and selected the one with the smallest criterion value (Burnham and Anderson, 2004).

### 3.3.4 Data preparation for finite mixture modeling

We assumed that the topology or the type of bottleneck affects the mandatory lane-changing maneuvers of truck drivers; therefore, we grouped sites into three categories.

1. On/off-ramp
2. Short weaving section
3. Long weaving section

For weaving sections, 1000–1100 m long sections are classified as long weaving and 500–700 m long sections as short weaving. In one case (short weaving with merging maneuver), we grouped two similar sites so we could increase the data available for modeling. Next, we present indicator variables for categorizing merging and diverging maneuvers.

### 3.3.5 Indicator variables

We considered the spatio-temporal and gap-acceptance characteristics of the lane-changing process. Figure 3.3 illustrates the vehicles involved in the lane-changing process and presents the related indicator variables.

#### Spatio-temporal aspects of lane change

We consider location as where a truck driver initiates the lane change maneuver and duration to complete that maneuver. We fixed the origin at the beginning of a bottleneck section and the location variable increases in the driving direction. For merging maneuvers, a relative value is used with respect to the total length of the bottleneck so that we can combine similar sites. Whereas, for a diverging maneuver, an absolute value of longitudinal position is used.

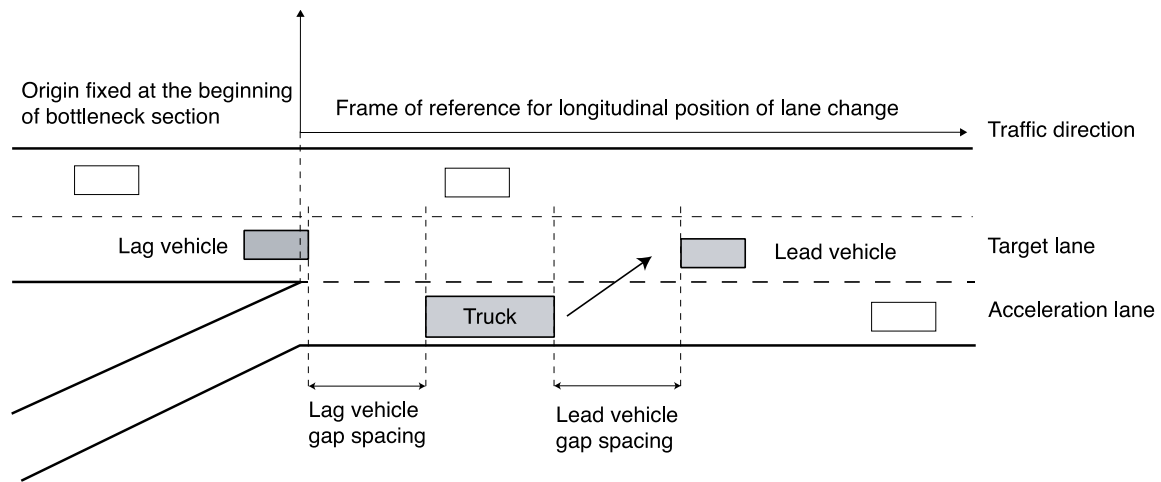


**Figure 3.3. Vehicles involved in a lane change process and related indicator variables.**

### Kinematic behavior during lane change

We consider the instantaneous speed of truck driver as the point he/she initiates the lane change maneuver as a representation of vehicle kinematics.

### Gap acceptance behavior

We consider the interactions of a lane-changing vehicle using the lead (predecessor) and lag (follower) vehicles in the target lane. Therefore, we use accepted lead and lag gap spacing as indicators. We use a default value of 250 m for the lag and lead gap spacing in case no vehicle (lag or lead vehicle) is in sight when a truck driver initiates a lane change maneuver. A higher value such as 250 m also suggests that a lane-changing vehicle is not affected by a leader or follower in the target lane. During the data collection, the camera captures more of the area than just the bottleneck section; therefore, 250 m is a justified assumption in this respect.

We consider categorical variables to indicate whether a truck driver has accepted largest available lead or lag gap spacing. We first store all the available lead/lag gaps for a truck driver in a list until the time of lane change initiation. We compare the chosen lead/lag gap with the maximum available lead/lag gap. For the comparison, we assume that truck drivers are indifferent toward small gains and choose a threshold of 10 m. If the chosen gap and maximum available gap differ more than the threshold, we say that a truck driver has intentionally chosen a smaller gap. We ensure that the categorical variable will take a value of 1 in this case and 0 in all other cases.

Next, we present descriptive statistics of data collected for merging and diverging maneuvers.

### 3.3.6 Descriptive statistics of merging maneuvers

In Table 3.1, we present descriptive statistics of the merging maneuvers of truck drivers. Aside from the categorical gap acceptance indicator, all other indicators are assumed to be a mixture of Gaussian distribution. Relative location of lane change initiation can be converted to a censored Gaussian distribution as lane changes will only initiate from the beginning of the bottleneck section.

**Table 3.1. Descriptive statistics of data collected for merging maneuvers**

Parameter	Type	Mean	SD	Min.	Max.
<b>On-ramp: Zonzeel-north (340 m)</b>					
Number of observations		50			
Relative location of lane change initiation	Gaussian	0.07	0.16	0.00	0.82
Lane change duration (s)	Gaussian	9.76	3.07	5.20	18.10
Speed at merge initiation (km/h)	Gaussian	81.94	4.98	72.21	97.32
Accepted lag gap spacing (m)	Gaussian	104.86	91.97	1.34	405.54
Accepted lead gap spacing (m)	Gaussian	113.63	124.69	2.03	555.59
Accepted largest lag gap	Binomial	0.06	0.23	0.00	1.00
Accepted largest lead gap	Binomial	0.04	0.19	0.00	1.00
<b>Short weaving: Ridderkerk-north (740 m) and Klaverpolder-north (610 m)</b>					
Number of observations		30			
Relative location of lane change initiation	Gaussian	0.09	0.18	0.00	0.59
Lane change duration (s)	Gaussian	8.86	3.97	4.40	23.20
Speed at merge initiation (km/h)	Gaussian	85.30	10.14	62.25	97.09
Accepted lag gap spacing (m)	Gaussian	122.95	79.785	16.09	250.00
Accepted lead gap spacing (m)	Gaussian	103.10	92.970	2.96	431.99
Accepted largest lag gap	Binomial	0.13	0.34	0.00	1.00
Accepted largest lead gap	Binomial	0.06	0.25	0.00	1.00
<b>Long weaving: Princeville-west (1130 m)</b>					
Number of observations		48			
Relative location of lane change initiation	Gaussian	0.03	0.07	0.00	0.32
Lane change duration (s)	Gaussian	8.86	2.79	4.60	16.80
Speed at merge initiation (km/h)	Gaussian	83.93	4.98	69.90	99.83
Accepted lag gap spacing (m)	Gaussian	176.23	94.84	10.75	250.00
Accepted lead gap spacing (m)	Gaussian	134.19	102.38	1.23	351.75
Accepted largest lag gap	Binomial	0.06	0.24	0.00	1.00
Accepted largest lead gap	Binomial	0.02	0.14	0.00	1.00

Note: SD = standard deviation; Min. = minimum; Max. = maximum.

### 3.3.7 Descriptive statistics of diverging maneuvers

In Table 3.2, we present descriptive statistics for the data related to the diverging maneuvers of truck drivers. We observe that the bottleneck sites do not feature a real conflict for diverging truck drivers as the mean value of the accepted lag/lead gap spacing is more than 190 m. It also signifies that the initiation of diverging maneuvers is unaffected by the presence of a lag/lead vehicle in the target lane. Therefore, we did not consider indicator variables related to gap acceptance behavior for finite mixture modeling to categorize diverging maneuvers. In the next section, we discuss the results of finite mixture modeling to categorize the lane-changing maneuvers of truck drivers.

**Table 3.2. Descriptive statistics of data collected for diverging maneuvers**

Parameter	Type	Mean	SD	Min.	Max.
<b>Off-ramp: Zonzeel-south (230 m)</b>					
Number of observations		47			
Location of lane change initiation (m)	Gaussian	-65.27	44.78	-230.34	17.46
Lane change duration (s)	Gaussian	9.93	2.52	5.00	18.80
Speed at diverge initiation (km/h)	Gaussian	80.49	4.80	66.13	94.77
Accepted lag gap spacing (m)	Gaussian	250.00	0.00	250.00	250.00
Accepted lead gap spacing (m)	Gaussian	245.27	32.39	27.93	250.00
<b>Short weaving: Klaverpolder-south (530 m)</b>					
Number of observations		80			
Location of lane change initiation (m)	Gaussian	13.12	48.51	-38.64	159.82
Lane change duration (s)	Gaussian	8.48	2.33	5.30	14.70
Speed at diverge initiation (km/h)	Gaussian	83.13	3.58	73.01	92.08
Accepted lag gap spacing (m)	Gaussian	230.52	63.59	1.93	250.00
Accepted lead gap spacing (m)	Gaussian	195.29	82.62	4.12	250.00
<b>Long weaving: Princeville-east (1000 m)</b>					
Number of observations		43			
Location of lane change initiation (m)	Gaussian	63.45	166.58	-23.57	756.76
Lane change duration (s)	Gaussian	8.64	2.52	4.00	16.00
Speed at diverge initiation (km/h)	Gaussian	82.57	5.70	72.43	97.49
Accepted lag gap spacing (m)	Gaussian	218.30	75.22	1.93	250.00
Accepted lead gap spacing (m)	Gaussian	216.47	69.41	0.78	250.00

Note: SD = standard deviation; Min. = minimum; Max. = maximum.

## 3.4 Results

The finite mixture models are estimated using the `depmixS4` package in R (Visser and Speekenbrink, 2010). To avoid locally optimal solutions, the models are estimated 500 times for each class and then the model with the lowest value of BIC is selected for that class. The proportion of truck drivers  $P$  accepting the largest available lead/lag gap is computed at the zero-value of covariate from the parameter estimate  $\delta$ , as shown in Equation 3.2.

$$P = \frac{\exp(0)}{\exp(0)+\exp(\delta)} = \frac{1}{1+\exp(\delta)} \quad (3.2)$$

Next, we present the categories of truck drivers with respect to their merging and diverging maneuvers.

### 3.4.1 Merging strategies of truck drivers

Figure 3.4 presents the fit of finite mixture models with respect to the BIC statistic. Based on the BIC statistic (being lowest in the 2-component finite mixture model), two latent classes of truck drivers are considered with respect to their merging maneuvers over different topologies.

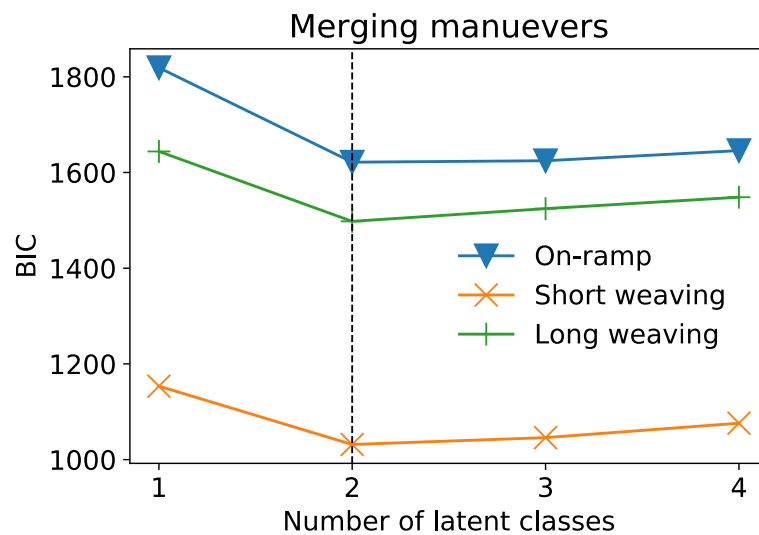


**Figure 3.4. Categorizing the merging maneuvers of truck drivers.**

Note: BIC = Bayesian information criterion.

Table 3.3 presents the profile of two-classes of truck drivers. Class I is the largest class and is characterized by a truck driver's affinity to initiate merging maneuvers as early as possible after reaching the acceleration lane. The proportion of truck drivers belonging to class I is 61.02%, 69.90%, and 65.21% for the on-ramp, short weaving, and long weaving section, respectively. Truck drivers initiate the merging process at a mean longitudinal position of 1.7 m, 2.8 m, and 2.26 m after the beginning of on-ramp, short weaving, and long weaving sections, respectively. Truck drivers belonging to this class show a tendency to accept a gap from a set of the initial few gaps available to them. The urge to merge at the earliest possible opportunity prompts a truck driver to accept the largest gap spacing from that initial set of available gaps.

Class II is the smallest class and comprises truck drivers who either could not find a suitable gap earlier, or intentionally accept a smaller gap later on. The proportion of truck drivers belonging to class II is 38.98%, 30.10%, and 34.79% for the on-ramp, short weaving, and long weaving section, respectively. Truck drivers in class II initiate the merging process within a mean longitudinal position of 75.82 m, 205.80 m, and 115.26 m after the beginning of the on-ramp, short weaving, and long weaving sections, respectively. The proportion of truck drivers belonging to class II who reject the largest available lag gap and accept a smaller one is 16%, 45%, and 18% for the on-ramp, short weaving and long weaving sections, respectively. Although 11% and 23% of truck drivers belonging to class II reject the largest available lead gap spacing for on-ramp and short weaving sections, respectively.

### 3.4.2 Diverging strategies of truck drivers

Figure 3.5 presents the fit of finite mixture models with respect to the BIC statistic. Based on the BIC statistic (being lowest in the 3-component finite mixture model), three latent classes of truck drivers are considered with respect to their diverging maneuvers over different topologies. Table 3.4 presents the profile of three-classes of truck drivers. The classes are characterized by the location of lane change initiation, instantaneous speed of a truck, and lane change duration. For an off-ramp, the proportion of truck drivers belonging to class I, II, and III is 19.30%, 46.85%, and 33.85%, respectively. Truck drivers belonging to class I start the diverging maneuver 136.09 m before the beginning of the bottleneck and some of them might utilize the

Table 3.3. Profile of two latent class model for truck drivers' merging maneuvers

Parameters	Class							
	I			II				
	Mean	SD	Est.	Prop.	Mean	SD	Est.	Prop.
<b>On-ramp</b>								
Proportion (%)	61.02				38.98			
Relative location of lane change initiation	0.005	0.002			0.183	0.223		
Lane change duration (s)	8.98	2.60			10.96	3.29		
Accepted lag gap spacing (m)	95.59	80.16			119.38	104.21		
Accepted lead gap spacing (m)	63.34	47.13			192.38	159.54		
Speed at initiation (km/h)	81.50	4.69			82.63	5.21		
Accepted largest lag gap			-12.61	1.00			-1.70	0.84
Accepted largest lead gap			-15.67	1.00			-2.16	0.89
<b>Short weaving</b>								
Proportion (%)	69.90				30.10			
Relative location of lane change initiation	0.004	0.003			0.294	0.212		
Lane change duration (s)	8.21	2.64			10.36	5.60		
Accepted lag gap spacing (m)	140.15	78.17			82.59	63.08		
Accepted lead gap spacing (m)	109.15	103.72			87.24	49.10		
Speed at initiation (km/h)	84.90	8.27			83.56	6.45		
Accepted largest lag gap			-12.20	1.00			-0.22	0.55
Accepted largest lead gap			-16.06	1.00			-1.25	0.77
<b>Long weaving</b>								
Proportion (%)	65.21				34.79			
Relative location of lane change initiation	0.002	0.001			0.102	0.103		
Lane change duration (s)	8.86	2.73			8.84	2.80		
Accepted lag gap spacing (m)	185.63	83.87			158.61	107.95		
Accepted lead gap spacing (m)	115.02	97.11			170.12	99.21		
Speed at initiation (km/h)	85.04	5.50			81.86	2.55		
Accepted largest lag gap			-11.81	1.00			-1.51	0.82
Accepted largest lead gap			-3.41	0.96			-18.79	1.00

Note: SD = standard deviation; Est. = estimate; Prop. = proportion.

Table 3.4. Profile of three latent class model for truck drivers' diverging maneuvers

Parameters	Class									
	I			II			III			
	Mean	SD		Mean	SD		Mean	SD		
<b>Off-ramp</b>										
Proportion (%)	19.30			46.85			33.85			
Location of lane change initiation (m)	-136.09	37.55		-64.79	9.73		-25.56	9.73		20.66
Lane change duration (s)	13.70	2.04		10.08	0.83		7.57	0.83		1.19
Speed at diverge initiation (km/h)	80.34	2.62		82.56	6.22		79.05	6.22		3.49
<b>Short weaving</b>										
Proportion (%)	75.00			7.50			17.50			
Location of lane change initiation (m)	-9.08	11.77		9.34	1.48		109.91	1.48		34.62
Lane change duration (s)	7.95	1.92		13.6	0.71		8.55	0.71		1.47
Speed at diverge initiation (km/h)	82.93	3.83		84.28	1.85		83.47	1.85		2.71
<b>Long weaving</b>										
Proportion (%)	52.89			32.56			14.55			
Location of lane change initiation (m)	-17.09	5.23		40.42	34.30		408.19	34.30		200.21
Lane change duration (s)	9.16	2.47		8.25	1.51		7.65	1.51		3.61
Speed at diverge initiation (km/h)	82.52	6.55		81.90	3.63		84.28	3.63		5.35

Note: SD = standard deviation.

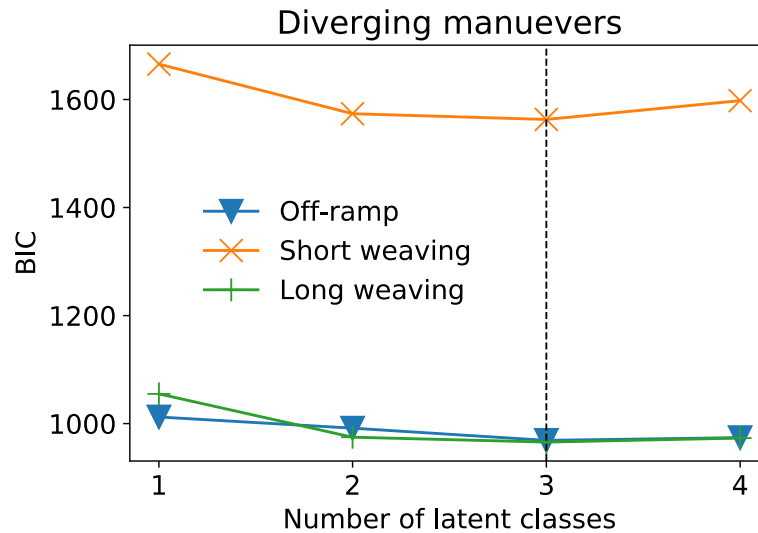


**Figure 3.5. Categorizing the diverging maneuvers of truck drivers.**

Note: BIC = Bayesian information criterion.

hard shoulder, which is also confirmed by the video feed (van Beinum, 2018). Whereas truck drivers belonging to class II and III start their diverging maneuvers 64.79 m and 25.56 m before the beginning of a bottleneck, respectively. The closer to the beginning of a bottleneck a truck driver starts diverging, the shorter will be the lane change duration; truck drivers belonging to class III have 7.57 s of mean lane change duration.

For a short weaving section, the proportion of truck drivers belonging to class I, II, and III is 75.00%, 7.50%, and 17.50%, respectively. Class I truck drivers, being the largest group, start the diverging maneuver 9.08 m before the beginning of a bottleneck. However, truck drivers belonging to class II and III start their diverging maneuvers 9.34 m and 109.91 m after the beginning of the bottleneck, respectively.

For a long weaving section, the proportion of truck drivers belonging to class I, II, and III is 52.89%, 32.56%, and 14.55%, respectively. Similar to the short-weaving section, class I truck drivers, being the largest group, start the diverging maneuver 17.09 m before the beginning of the bottleneck. Truck drivers belonging to class II and III start their diverging maneuvers 40.42 m and 408.91 m after the beginning of the bottleneck, respectively.

The mean speed of truck drivers at lane change initiation is around 80 km/h in all cases. In Table 3.2, descriptive data statistics show that the presence of a lead or lag vehicle in the target lane does not affect the diverging maneuver. Therefore, class III truck drivers over short and long weaving sections have a preference to diverge later than the majority of truck drivers belonging to class I and II. Next, we discuss the contribution of truck drivers' lane change behavior in the vicinity of a bottleneck to the turbulence.

### 3.4.3 Contribution of truck driver's lane-changing behavior to turbulence

Lane-change maneuvers in the vicinity of motorway ramps and weaving sections are primary contributors to turbulence (van Beinum et al., 2018). To identify the contributions of truck drivers to turbulence, we considered the following six sites with significant truck-related merging or diverging maneuvers. We excluded Ridderkerk-north from this analysis as only eight trucks merged onto the mainline motorway at this site.

- Zonzeel-north: On-ramp (merging)



- Klaverpolder-north: Short weaving section (merging)
- Princeville-west: Long weaving section (merging)
- Zonzeel-south: Off-ramp (diverging)
- Klaverpolder-south: Short weaving section (diverging)
- Princeville-east: Long weaving section (diverging)

In addition to trucks, we also considered other vehicles present in the traffic. The vehicles are further classified based on their lengths.

- Category 1: Vehicle's length smaller than 5.6 m (e.g., passenger cars)
- Category 2: Vehicle's length in between 5.6 and 12 m (e.g., busses, vans, etc.)
- Category 3: Vehicle's length longer than 12 m (e.g., trucks)

In Figures 3.6 and 3.7, we show a comparison of spatial distribution of lane changes performed by different categories of vehicles. For these figures, the longitudinal position of the lane-changing maneuver refers to the one in which a vehicle crosses the lane boundary. It can be observed that at least 50% of lane changes occur within the initial 25% of the ramp or weaving segment length.

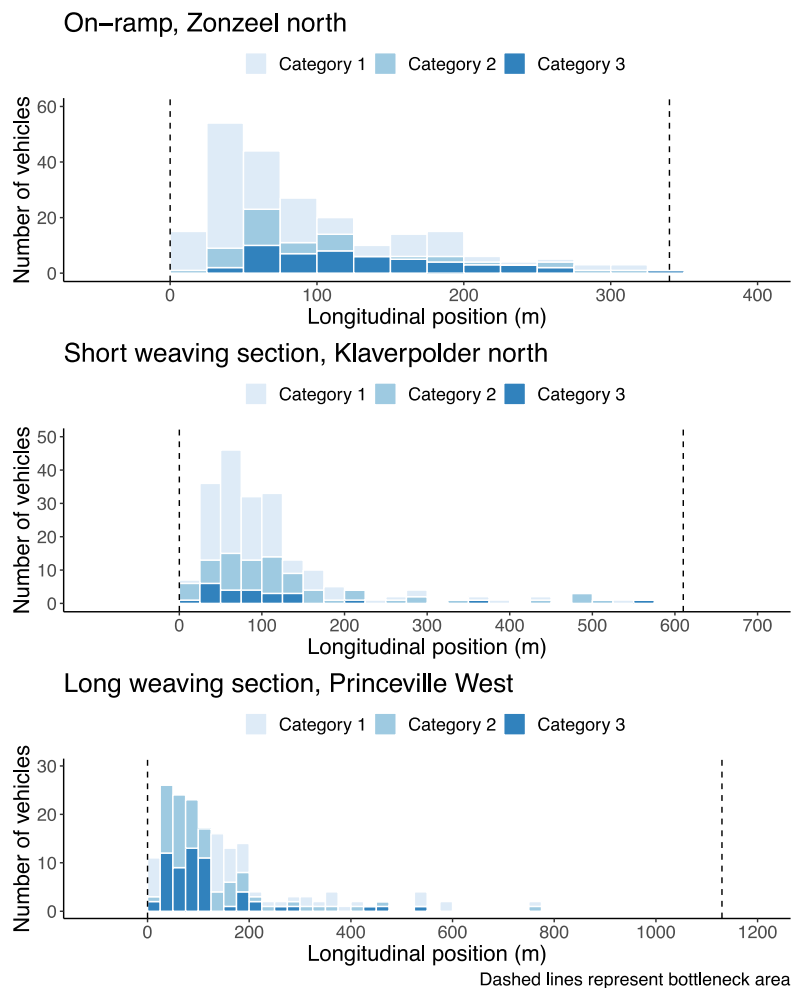


**Figure 3.6. Concentration of merging maneuvers at on-ramp, short weaving and long weaving sections.**

Within the initial 25% of the ramp or weaving segment length, the proportion of truck drivers performing merging maneuvers is 25.49%, 87.50%, and 94.91% for the on-ramp, short weaving and long weaving sections, respectively. Furthermore, 76.47% of truck drivers can merge at the on-ramp (Zonzeel-north site) within the initial 50% of the ramp length. It can be inferred that truckdrivers require a certain minimum distance on the acceleration lane (i.e., around 150 m) to change lanes.

Similarly, within the initial 25% of the ramp or weaving segment length, the proportion of truck drivers performing diverging maneuvers is 80.39%, 80.00%, and 78.43% for the on-ramp, short weaving and long weaving sections, respectively. The findings indicate that a high proportion of truck drivers change lanes within the initial 25% of the ramp or weaving segment length; these actions lead to turbulence at the beginning of a motorway bottleneck.

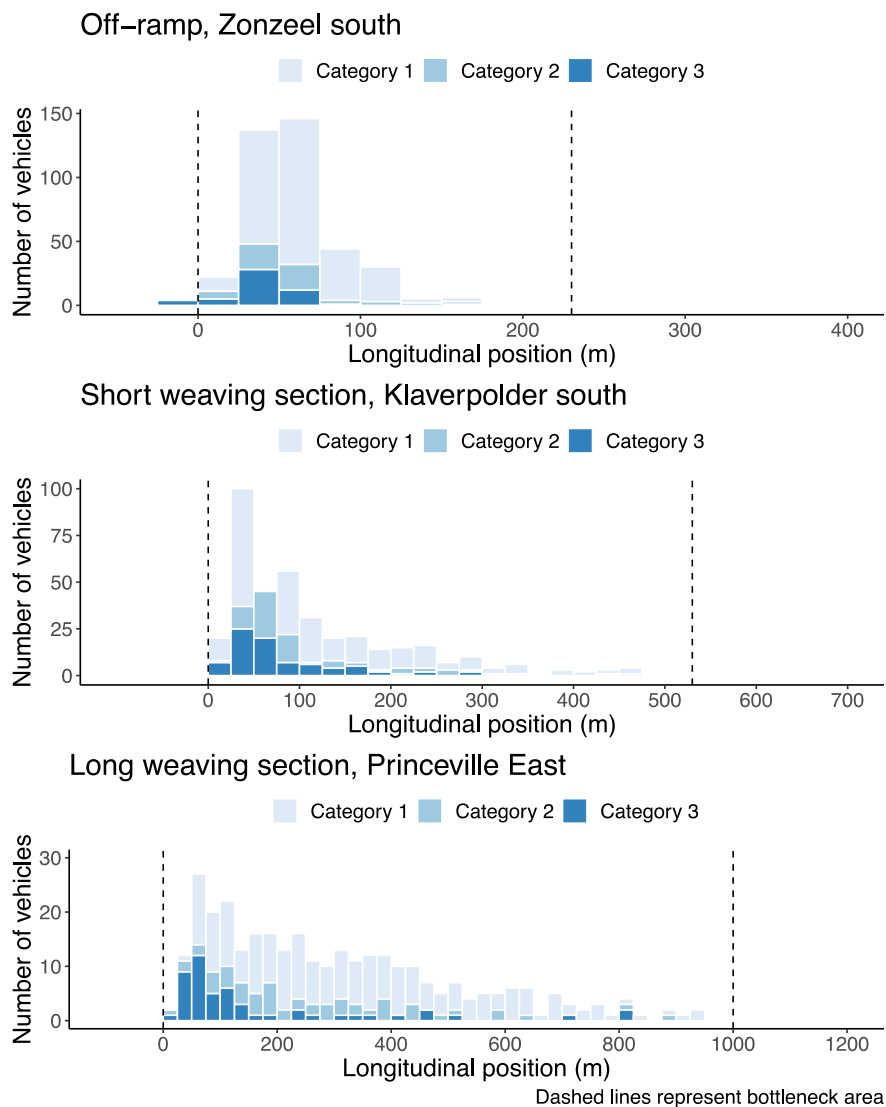


**Figure 3.7. Concentration of diverging maneuvers at off-ramp, short weaving and long weaving sections.**

## 3.5 Discussion

### 3.5.1 Discussion of findings

Our main finding is that truck drivers can be categorized with respect to their merging and diverging strategies into two and three categories, respectively. Previously, similar results have been reported for the driver population as a whole in previous research focused on lane-changing (Li, 2018, Li and Sun, 2018, Sun and Elefteriadou, 2011, Sun and Elefteriadou, 2012). The number of categories with respect to either merging/diverging is consistent over different topologies. We also found that the lane change locations of truck drivers are heavily right-skewed. Similar to our findings, a strongly right-skewed distribution of lane-changing positions has previously been reported for weaving sections by Menendez and He (2017). However, they have not considered individual vehicle categories. In that respect, our findings can be used in multi-class models in which distributions related to lane-changing characteristics of truck drivers (e.g., lane-change position, lane-change duration, etc.) can be supplied as exogenous inputs to such models.

The right-skewed distribution of lane-changing positions also explains the contribution of truck drivers to the turbulence we usually observe in the vicinity of freeway bottlenecks. Similar findings are reported in van Beinum et al., but they did not look at the spatial distribution of lane changes for different categories of vehicles (van Beinum et al., 2018). Truck drivers who make use of longer distances are the ones who either select a suitable gap or intentionally accept a smaller gap to merge onto the mainline carriageway. Whereas gap acceptance does not seem to be a primary factor in the diverging strategies of truck drivers, still, around 15% of truck drivers are observed to take an exit at a longer distance over weaving sections. The findings seem to suggest that truck drivers do not fully utilize the available ramp and weaving segment length. Near the beginning of these areas, a raised level of turbulence has serious implications for traffic efficiency and safety. Our findings indicate that motorway design guidelines should give due attention to the multi-class nature of traffic. For instance, motorways with a high percentage of trucks require longer acceleration and deceleration lanes.

### 3.5.2 Limitations

The internal preferences which truck drivers may have in their mind while performing their mandatory lane-changing maneuvers and their socio-economic characteristics cannot be observed from the trajectory dataset. Stated-preference surveys or driving simulator experiments can be used to gain insights into those internal mechanisms. The findings presented in this chapter are valid for truck drivers operating in the Netherlands. We expect that these findings may apply to other European countries with similar driving regulations. For other countries, similar studies should be performed so that findings related to merging and diverging strategies of international truck drivers can be compared. A comparison of this scale would allow us to design tools to not only improve current models, but also perform improved traffic and safety assessments.

## 3.6 Conclusions

This chapter uses a trajectory dataset, collected for ramps and weaving sections located in the Netherlands, to identify heterogeneity within truck drivers with respect to their merging and diverging strategies. We use finite mixture models to categorize truck drivers using their spatial, temporal, kinematic, and gap acceptance attributes of lane changing. The results indicate that we can classify truck drivers into two with respect to their merging strategies and into three with respect to their diverging strategies. The findings of this chapter can be implemented into microscopic simulation packages to better replicate the lane-changing behavior of truck drivers

at motorway ramps and weaving sections. The categorization helps us to infer the spatial distribution of lane changes performed by truck drivers. For both merging and diverging, the majority of truck drivers show an affinity to initiate the lane change process at the earliest opportunity which is characterized by a right-skewed distribution. This behavior leads to a higher number of lane changes being performed at the beginning of a motorway bottleneck section. In this respect, the effect on traffic efficiency and safety near these areas owing to different merging and diverging strategies adopted by truck drivers should be evaluated. For future work, control strategies can be designed to reduce the effect of lane changes in the vicinity of motorway bottlenecks. A promising direction could be to optimize the spatial distribution of mandatory lane changes for multiple user classes of motorway traffic.



## 4 Gap selection process during discretionary lane changing

---

The previous chapter showed inter-driver heterogeneity by identifying merging and diverging strategies of truck drivers. The second element within lane changing focuses on how truck drivers traveling on the mainline carriageway would select gaps around ramps and weaving sections. A lack of understanding of how truck drivers select available gaps to execute discretionary lane changes arises primarily due to the scarcity of truck-specific data. To fill this gap, this chapter aims at obtaining insights into the gap selection process of truck drivers and drivers of other vehicle classes (e.g., passenger cars and delivery vans) and contributes to answering the third research question of this dissertation. This chapter applies gated recurrent unit neural network models on a large trajectory dataset to unravel the gap selection process of multiple vehicle classes within their discretionary lane changes.

This chapter is based on the following journal and conference papers:

Sharma, S., van Lint, H., Tavasszy, L. and Snelder, M. 2022. Unraveling Gap Selection Process during Discretionary Lane Changing by Vehicle Class. *IEEE Access*, 10, pp. 30643-30654.

Sharma, S., van Lint, H., Tavasszy, L. and Snelder, M. 2022. Unraveling the Gap Selection Process of Truck Drivers within Their Discretionary Lane- changing through Gated Recurrent Unit Neural Networks. Paper presented in *101<sup>st</sup> Annual Meeting of the Transportation Research Board*.

---

## 4.1 Introduction

Lane-changing is an important aspect of driving behavior that has a significant influence on road capacity (Cassidy and Rudjanakanoknad, 2005), safety (Li et al., 2014), and emissions (Li and Sun, 2017). Two main categories of lane changing can be distinguished: mandatory and discretionary. Mandatory lane changes arise from either infrastructural or traffic control related constraints, or from the drivers' need to follow a path that leads to his or her—*for brevity, we will use male adjectives in the ensuing—destination*. Discretionary lane changes are associated with the driver's desire to improve his current driving conditions. Discretionary lane-changing (DLC) is typically structured as a hierarchical process (Moridpour et al., 2012, Balal et al., 2016) where a driver (1) makes a decision-in-principle (that driving conditions on the current lane are below some desired level and can be improved by shifting to another lane); assesses (2) the options for this lane change (which target lane to move to) and (3) the necessary conditions (the suitability of available gaps on potential target lane(s)); and then finally (4) takes action (initiates and executes the lane change) or not (rejects available gaps, or even abandons the entire lane change maneuver).

Gap selection is an important stage of the lane-changing process where drivers explicitly look for a suitable and safe opportunity in order to initiate their desired lane-changing maneuver. This stage has been extensively studied for passenger car drivers (Ahmed, 1999, Toledo et al., 2003, Balal et al., 2016, Pang et al., 2020, Xie et al., 2019) whereas other vehicle classes such as trucks or delivery vans have not received any attention. Although previous research (Saeednia and Menendez, 2017, Laval and Daganzo, 2006) shows that trucks seem to significantly affect traffic operations, only the first two steps of the hierarchical model for DLC decisions of truck drivers have been investigated (Moridpour et al., 2012). Inter-vehicle interactions during lane change have been shown to affect traffic operations; therefore, it is of vital importance to investigate and compare the lane change behavior of multiple vehicle classes to ensure reliable, efficient, and safe traffic operations. To the best of our knowledge, this chapter is the first that focuses particularly on the third step of this hierarchy, studies the gap selection process of delivery van and truck drivers within their DLC maneuvers, and compares it with that of passenger car drivers.

The gap selection behavior of vehicles can be formulated as a binary decision problem with two outcomes: lane-changing (accept) and lane-keeping (reject). This problem is solved using a wide range of techniques in the existing literature: rule-based (Gipps, 1986), statistical (Toledo et al., 2003, Ahmed, 1999), econometrical (Pang et al., 2020), and artificial intelligence (AI) models (Balal et al., 2016, Xie et al., 2019). Most of the earlier works assume instantaneous decision-making in the sense that only features or variables at a specific time instant affect the gap selection decision process. Typically, this time instant is taken just before a vehicle starts shifting laterally, which is an indication that a gap has been accepted (Balal et al., 2016, Punzo et al., 2011). Although some literature (Pang et al., 2020, Toledo and Katz, 2009, Tang et al., 2020) shows that historical data may also influence the gap selection process, such long-term interdependencies are typically not considered. In this chapter, we consider the long sequences (or trajectories) of up to 20 sec to fill this gap.

The objective of this chapter is to obtain insights into the gap selection process of multiple vehicle classes in their DLC maneuvers using AI. To this end, we frame the gap selection process of truck drivers as a many-to-one sequence classification problem and train a gated recurrent unit neural network (GRUNN) model to learn and model such temporal dependencies over longer periods. To assess what this neural network, in the end, has learned—and whether this makes sense behaviorally, we apply explainable AI techniques such as a gradient-based technique (Simonyan et al., 2014) and variable importance.

Most previous research works calibrate and validate their gap selection models using data from a specific type of topology (e.g., a weaving section (Toledo et al., 2003, Balal et al., 2016, Pang et al., 2020, Xie et al., 2019)). In this chapter, we use a larger trajectory dataset that covers many different topologies situated around 14 different bottlenecks in the Netherlands including on-ramps, off-ramps, and weaving sections (van Beinum, 2018, van Beinum et al., 2018). We incorporate these different topologies in the gap selection model as part of the feature set fed to the GRUNN model and consider for example type of topology, length of the freeway bottleneck, and the number of lanes on the mainline carriageway.

This chapter contributes to the existing literature by:

1. building gated recurrent unit neural network models to capture the gap selection process of multiple vehicle classes (passenger cars, delivery vans, and trucks) during their discretionary lane changing;
2. considering historical sequential data and external factors arising from topologies in the modeling framework of the gap selection process; and
3. comparing the gap selection process of multiple vehicle classes (passenger cars, delivery vans, and trucks) by unraveling their latent gap selection mechanisms and identifying key features that impact their gap selection through explainable AI techniques.

This chapter is organized in the following way. First, section 4.2 provides a theoretical background on GRU neural networks and related techniques to interpret their predictions. Subsequently, section 4.3 describes the data generation process. Next, section 4.4 presents an experimental setup to model the gap selection process of truck drivers. Subsequently, section 4.5 presents the model performance and its interpretability. Afterward, the findings and their implications are discussed in section 4.6. Finally, this chapter concludes in section 4.7.

## 4.2 Related background

A gated recurrent unit neural (GRU) network model is selected in this chapter to model the gap selection behavior of multiple vehicle classes (passenger cars, delivery vans, and trucks). A major advantage of this approach over other approaches (e.g., rule-based, econometrical, statistical, fuzzy-logic) is that it can learn long-term temporal interdependencies. The first part of this section discusses the inner workings of GRU neural networks. The second part presents strategies to handle class imbalance which is often a case in real-world trajectory datasets. To interpret predictions and learn more about the gap selection behavior, the third part of this section presents explainable AI techniques.

### 4.2.1 Gated recurrent unit neural networks

A recurrent neural network (RNN) is a widely used method that can handle time-series data for prediction purposes. However, an RNN suffers from well-known problems of vanishing and exploding gradients during backpropagation and is not very good at capturing very long-term dependencies. To overcome these obstacles, long short-term memory (LSTM) neural networks were proposed (Hochreiter and Schmidhuber, 1997). Cho et al. (Cho et al., 2014) proposed a GRU neural network or GRUNN, which is a variant of LSTM. Compared to LSTM, GRUNNs have simplified connections and a reduced number of parameters. While LSTM contains three gates (input gate, forget gate, and output gate), the GRU comprises two gates, namely the update gate and the reset gate. The update gate controls the extent to which the state information of the previous moment is passed to the current state. While the reset gate controls how much information of the previous state is stored in the current candidate state  $\tilde{h}_t$ . In this way, GRU can



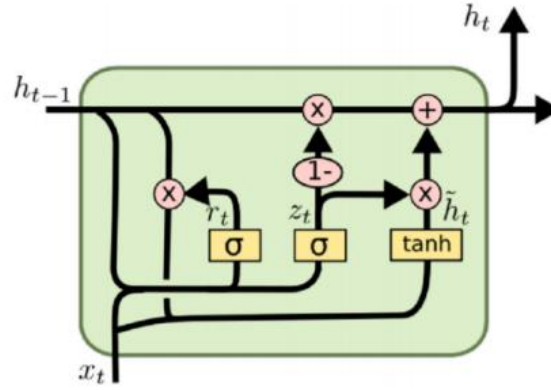


**Figure 4.1. Architecture of a GRU cell (adapted from (Cho et al. (2014))).**

improve upon the training efficiency by relying on the memory ability of neurons and fewer tensor operations. The architecture of a GRU cell is shown in Figure 4.1.

The forward propagation process of GRU is as follows (see Equations 4.1-4.4):

$$z_t = \sigma(W_z \cdot [h_{t-1}, x_t] + b_z) \quad (4.1)$$

$$r_t = \sigma(W_r \cdot [h_{t-1}, x_t] + b_r) \quad (4.2)$$

$$\tilde{h}_t = \tanh(W_h \cdot [r_t * h_{t-1}, x_t] + b_h) \quad (4.3)$$

$$h_t = (1 - z_t) * h_{t-1} + z_t * \tilde{h}_t \quad (4.4)$$

where  $x_t$  denotes the input vector at time  $t$ .  $h_t$  denotes the state of the system at time  $t$ .  $\tilde{h}_t$  denotes the current candidate state.  $z$  and  $r$  denote the update gate and reset gate, respectively.  $\sigma$  denotes the Sigmoid function.  $W_z$ ,  $W_r$ , and  $W_h$  refer to weight matrices.  $b_z$ ,  $b_r$ , and  $b_h$  refer to bias vectors.

#### 4.2.2 Relevance of class imbalance to understanding lane-changing behavior

Most of the current research on lane-changing does not address the problem of class imbalance. However, there seems to be a large gap between the number of lane-changing trajectories and lane-keeping trajectories in most of the collected datasets (Balal et al., 2016). This results in class imbalance because of an unequal distribution of instances belonging to target classes. The performance of traditional classifiers is likely to be affected if they are trained on imbalanced datasets. To handle this problem, previous research has used several techniques: data-level methods, algorithmic modifications, and ensemble methods (Choudhary and Shukla, 2021). In this chapter, we use cost-sensitive learning (an algorithmic approach) and an ensemble method which are particularly useful in imbalanced classification problems.

##### Cost-sensitive learning

It is an algorithmic method where we specify different misclassification costs for instances belonging to different classes. Class-specific weights are computed in Equation 4.5.

$$W_i = \frac{N}{C * n_i} \quad (4.5)$$

where  $W_i$  denotes the weight for class  $i$ ,  $N$  denotes the total number of instances,  $C$  denotes the total number of classes, and  $n_i$  denotes the number of instances belonging to the class  $i$ .

### Ensemble method

This approach incorporates the strengths of random under-sampling (RUS) and bagging (Choudhary and Shukla, 2021). RUS is a form of data sampling that randomly selects majority class instances and removes them from the dataset until the desired class distribution is achieved. In this way, several balanced training subsets are created by RUS of the majority class. Each subset contains all the minority class instances and an equal number of randomly selected majority class instances. The number of training subsets i.e.  $M$  can be chosen equal to the imbalance ratio (Choudhary and Shukla, 2021). In this way, we train  $M$  different models and aggregate their output using the majority voting approach to determine the final prediction.

### 4.2.3 Interpreting a trained GRU neural network model

The interpretability of AI models is a challenging problem that has been gaining increasing attention for the last few years. In this chapter, we consider a gradient-based technique (Simonyan et al., 2014, van Lint, 2004) to interpret the trained model. The advantages of this technique over other methods (e.g., Shapely values) are the ease of implementation and faster processing time. The backpropagation-based approach (Simonyan et al., 2014, van Lint, 2004) is used to compute the attributions for all input features in a single forward and backward pass through the network and adapted for our use. Given a single target output, the goal is to determine the contribution of each input to the output. Let's define  $N$  as the total number of instances in the test dataset, and the input has a shape of  $(T \times F)$ . Here,  $T$  denotes the total number of time steps and  $F$  denotes the total number of features. Equation 4.6 presents the contribution of input  $x_{tf}^n$  to the output  $S(x^n)$  for a single instance  $n$ .

$$g_{tf}^n = \left| \frac{\partial S(x^n)}{\partial x_{tf}^n} \right| \quad \forall n \in N, t \in T, f \in F \quad (4.6)$$

where  $g_{tf}^n$  denotes attributions (or contributions) that are of the same shape as that of input  $x_{tf}^n$ . Then, we run over all the instances present in the test dataset and compute the global-level attribution  $g_{tf}$  using Equation 4.7.

$$g_{tf} = \frac{1}{N} \sum_{n=1}^N g_{tf}^n \quad \forall t \in T, f \in F \quad (4.7)$$

The matrix  $G \in \mathbb{R}^{T \times F}$  is composed of  $g_{tf}$  elements that contain the average value of absolute gradient. A heat map or attribution map generated from the matrix  $G$  can reveal the dynamics behind the gap selection process of drivers. Higher values of the elements of the matrix  $G$  imply greater importance on the prediction output. Further, we can derive feature importance ( $G_f$ ) and time-step importance ( $G_t$ ) using Equations 4.8 and 4.9.

$$G_f = \frac{1}{T} \sum_{t=1}^T g_{tf} \quad \forall f \in F \quad (4.8)$$

$$G_t = \frac{1}{F} \sum_{f=1}^F g_{tf} \quad \forall t \in T \quad (4.9)$$

### 4.3 Data preparation to model gap selection using GRU neural network models

This section is composed of three parts. The first part presents the characteristics of the trajectory dataset. Afterward, the second section describes the feature set used to build gap selection models. Finally, the third section elaborates on creating datasets for training and testing the models.

#### 4.3.1 Trajectory data

In this chapter, a trajectory dataset is used to develop the gap selection decision models for multiple vehicle classes (van Beinum, 2018). This dataset is a freely available resource that has been used in research before to understand driving behavior (van Beinum et al., 2018, Sharma et al., 2020). The data comprise vehicle trajectories obtained through aerial imaging in the vicinity of 14 freeway bottlenecks located in the Netherlands, which include 3 on-ramps, 3 off-ramps, and 8 weaving sections (see Figure 4.2).

This dataset was collected using a high-resolution camera attached to a hovering helicopter. The sites represent isolated discontinuities and their lengths are at most 1100 m meaning that the trajectories can be captured using the helicopter method. For each site, 30 min of the video feed was collected at the onset of evening congestion, that is, between 14:00 and 17:00 h. These 14 bottleneck sites included in this dataset sites either have a three-lane or a two-lane mainline carriageway with one auxiliary lane. For further information about the data collection, the reader may refer to van Beinum et al. (van Beinum et al., 2018). Note that traffic operates under keep-right regulations in the Netherlands. Further, trucks are forbidden to drive on the left lane on carriageways with more than 2 lanes, except in the case of  $2 \times 2$  weaving sections (where they are allowed to drive on the left-most lane).

The trajectory dataset is processed as follows.

1. We label vehicles shorter than 5.6 m as cars and longer than 12 m as trucks. Vehicles that fall in between are labeled as delivery vans.
2. Vehicles traveling on mainline carriageways are considered; vehicles entering onto a mainline carriageway from an on-ramp or exiting a mainline carriageway through an off-ramp are not considered since these two maneuvers fall under mandatory lane changing.

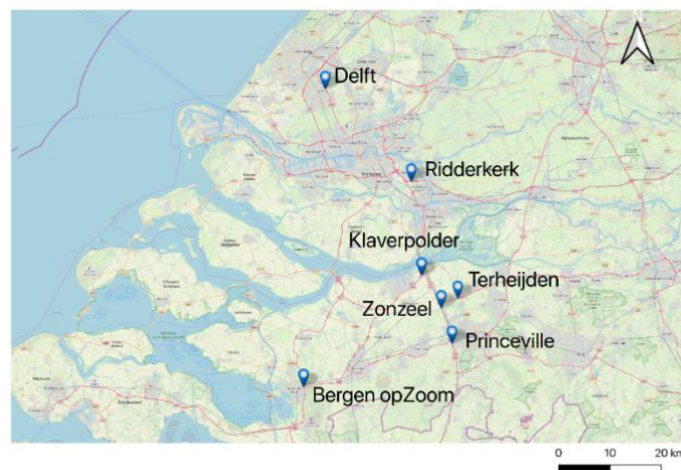


**Figure 4.2.** Locations where the trajectory dataset is collected (each location comprises two bottleneck sites on each side of a bi-directional motorway).

3. Vehicles making multiple lane changes on the mainline carriageway are excluded since these are more likely to be mandatory lane changes. Similar consideration is also made in a previous study (Balal et al., 2016).
4. Only vehicles changing lanes from right to left on mainline carriageways are considered. Vehicles changing lanes to the right side are excluded because traffic operates under keep-right regulations in the Netherlands.
5. In this way, two types of trajectories are considered: lane keeping (drivers do not change lanes) and lane changing (drivers change lanes to their left).
6. The trajectory data contain noisy speed and acceleration estimates. We use a Savitzky–Golay filter (Ahn et al., 2013) to improve these estimates.
7. Concerning lane keeping trajectories, only trajectories pertaining to drivers who show normal or relaxed car following behavior are included. Any aggressive car following behavior, if detected, is used to exclude that trajectory. Aggressiveness in the car-following behavior is assessed through a time-to-collision-based (TTC) indicator. The aggressiveness is assumed to be present if the TTC value is less than 4 s, which is also used in previous research (Horst, 1991, Faber et al., 2020).
8. To account for the effect of historical information, a maximum span of 20 s is considered to analyze the gap selection decision process since more than 95% of truck drivers are observed to change lanes within the first 20 s in the trajectory dataset.
9. For every vehicle in the trajectory dataset, we have position (lateral and longitudinal coordinates), length, dynamics (speed, acceleration), relative measurements with the surrounding vehicles (distance gap and relative speed) available at a resolution of 10 frames/second.
10. Relevant data are sampled at a frequency of 0.5 s which means we collect two data points per second. The average parameter values for a sampling instant  $t$  are computed by averaging data for the interval  $[t - 0.4, t]$  (Balal et al., 2016). The reasons for taking the average value over 0.5 s are (a) to maintain consistency with the previous research (Balal et al., 2016, Moridpour et al., 2012, Toledo et al., 2003, Siuhi and Kaseko, 2010); (b) to reduce the error caused by using instantaneous values in the trajectory data; and (c) to be in line with driver's perception time (Balal et al., 2016).
11. The lane-changing process for a vehicle begins when it starts to drift laterally and ends when it stabilizes its lateral position after changing to a neighboring lane. The time instances are marked as lane change initiation and lane change completion. For a lane changing vehicle, the lane change initiation point is termed as  $T$  which refers to a relative increase in the lateral position of a vehicle with respect to time. 40 data points within a span of  $[T - 19.5, T]$  are considered for a lane changing trajectory as shown in Figure 4.3.
12. For a lane keeping vehicle,  $T$  refers to the last point in its observed or recorded trajectory. As shown in Figure 4.3, 40 data points are considered within a span of  $[T-19.5, T]$ .

A total of 3,647 trajectories of passenger car drivers are obtained out of which 2,803 are lane-keeping and 844 are lane-changing trajectories. For delivery van drivers, a total of 1,080 trajectories are extracted out of which 898 are lane-keeping and 182 are lane-changing trajectories. A total of 2,226 trajectories of truck drivers are obtained out of which 2,103 are lane-keeping and 123 are lane-changing trajectories. Further, vehicle class-specific datasets suffer from class imbalance due to the presence of fewer lane-changing labels compared to the dominant lane-keeping labels.

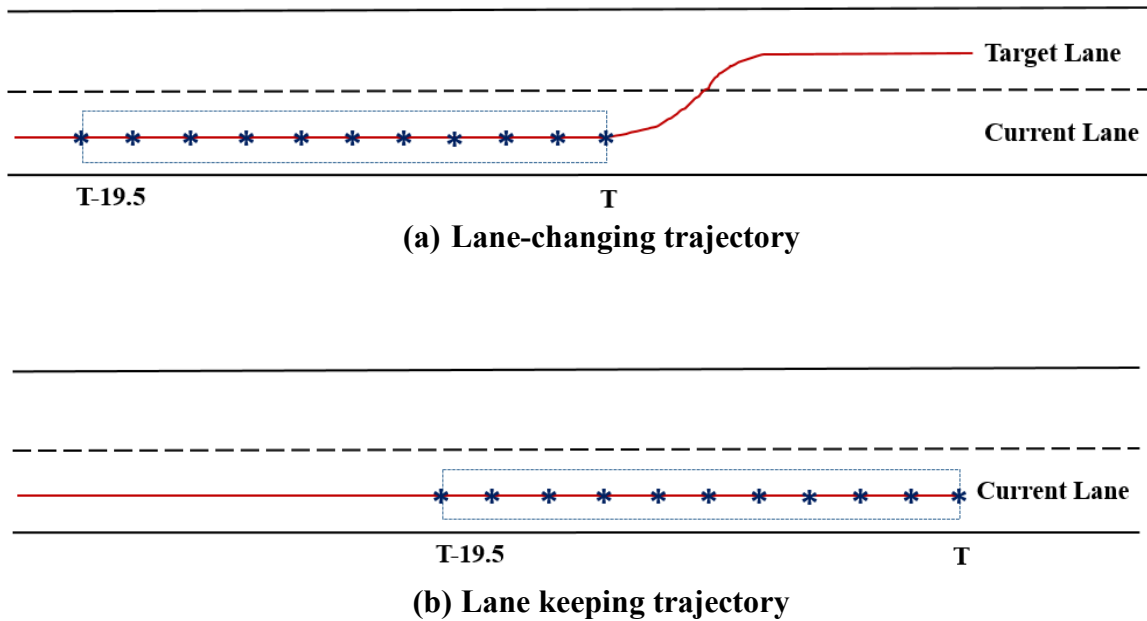


**Figure 4.3.** Figure showing span and data sampling for (a) lane-changing and (b) lane-keeping trajectories of drivers (Note: \* denotes a data sampling instant at a resolution of 0.5 s.).

### 4.3.2 Feature selection

Trajectories can be viewed as sequences of decisions (lane-changing/lane-keeping) taken by drivers over time. At each time step, drivers can consider different features to make a decision. A typical gap selection scenario at a specific instant of time is presented in Figure 4.4. Here, the subject vehicle (SV) is trying to move to the target lane from his current lane. During this process, the SV might be involved in interactions with up to four vehicles in its surroundings, as also considered by Balal et al. (Balal et al., 2016). In the current lane, the SV interacts with its current leader (CL) and current follower (CF). Whereas in the target lane, its interactions are with the future leader (FL) and future follower (FF).

In this chapter, we consider three dimensions that are hypothesized to affect this decision process. These capture the characteristics of the subject vehicle, its interaction with surrounding vehicles, and its perception of a topology (see Table 4.1). Typically, only the first two dimensions are considered in previous research works (Pang et al., 2020, Xie et al., 2019, Balal et al., 2016, Ahmed, 1999, Toledo et al., 2003).

Please note that it might not always be the case for the SV to be involved with four other vehicles during its lane changing process. For such situations where a surrounding vehicle is

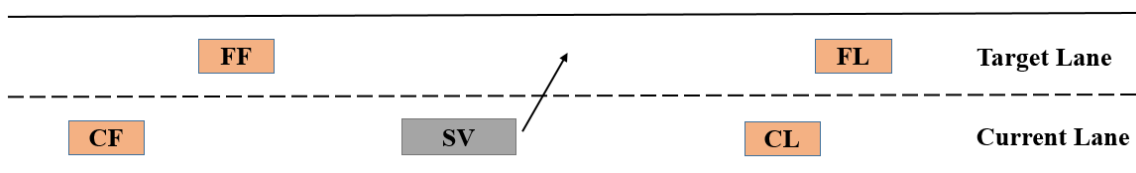


**Figure 4.4.** A driver during the gap-selection process. (Note: SV: subject vehicle; CL: current leader; CF: current follower; FL: future leader; and FF: future follower)

**Table 4.1. Features describing vehicle's interaction during lane-changing**

Features	Unit	Description
<i>Dimension 1: Characteristics of the subject vehicle</i>		
$v_{SV}$	m/s	Speed of the vehicle SV
$a_{SV}$	m/s <sup>2</sup>	Acceleration of the vehicle SV
$l_{SV}$	m	Length of the vehicle SV
<i>Dimension 2: Interaction of the subject vehicle with surrounding vehicles</i>		
$d_{CL}$	m	Distance gap between the vehicle SV and the vehicle CL
$d_{CF}$	m	Distance gap between the vehicle SV and the vehicle CF
$d_{FL}$	m	Distance gap between the vehicle SV and the vehicle FL
$d_{FF}$	m	Distance gap between the vehicle SV and the vehicle FF
$\Delta v_{CL}$	m/s	The speed difference between the vehicle SV and the vehicle CL, i.e. $v_{SV} - v_{CL}$
$\Delta v_{CF}$	m/s	The speed difference between the vehicle SV and the vehicle CF, i.e. $v_{SV} - v_{CF}$
$\Delta v_{FL}$	m/s	The speed difference between the vehicle SV and the vehicle FL, i.e. $v_{SV} - v_{FL}$
$\Delta v_{FF}$	m/s	The speed difference between the vehicle SV and the vehicle FF, i.e. $v_{SV} - v_{FF}$
$t_{CL}$	-	Type of the vehicle CL (truck or non-truck)
<i>Dimension 3: Subject vehicles' perception of a topology</i>		
$n_{lanes}$	-	Number of lanes on the mainline carriageway (2 or 3)
$l_{top}$	m	Length of the topology
$t_{top}$	-	Type of the topology (on-ramp, off-ramp, weaving section)

not observed or recorded in the trajectory dataset, we use a default value of 250 m for the distance gap spacing. A higher value such as 250 m also suggests that a vehicle is not affected by an unobserved surrounding vehicle. During the data collection, the camera captures more of the area than just the bottleneck section; therefore, 250 m seems to be a justified assumption in this respect. Similarly, for the speed of an unobserved surrounding vehicle, we assume its speed to be 0 m/s to compute the speed difference with the SV.

### 4.3.3 Constructing data for training and testing

Having identified key features, we will now prepare data for our GRUNN model.

#### Data split

We split the whole dataset into three parts: 80% training dataset, 10% validation dataset, and 10% test dataset. Table 4.2 shows the instances belonging to lane-keeping and lane-changing classes for every considered split and every vehicle class. The model is trained on the training dataset. Hyperparameters of the model are tuned using the validation dataset. Finally, the performance of the model is tested on a test dataset.

**Table 4.2. Data split for vehicle classes**

Vehicle class	Label	Training dataset (80%)	Validation dataset (10%)	Test dataset (10%)
Passenger cars	Lane-changing	675	84	85
	Lane-keeping	2242	280	281
Delivery vans	Lane-changing	158	20	20
	Lane-keeping	705	88	89
Trucks	Lane-changing	98	12	13
	Lane-keeping	1682	210	211

### Feature engineering

We consider 12 continuous and 3 categorical features (see Table 4.1). To support faster learning, the continuous features are standardized (Zheng and Casari, 2018) where the values of each feature vector component  $x_i$  are centered around the mean with a unit standard deviation (see Equation 4.10):

$$\tilde{x}_i = \frac{x_i - \mu_{x_i}}{s_{x_i}} \quad (4.10)$$

where  $\tilde{x}_i$  depicts the normalized feature vector component, and  $\mu_{x_i}$  and  $s_{x_i}$  the mean and standard deviation of  $x_i$ .

Categorical features are converted into numerical forms via one-hot encoding (Zheng and Casari, 2018), which represents categorical features in  $k$  possible categories as a binary feature vector of length  $k$ . The binary vector marks the class label with a value of 1 and all other positions with a value of 0. Consequently, a total of 19 features are considered in this chapter. The target is a binary variable that comprises two labels: lane-changing (LC) and lane-keeping (LK). These labels are encoded as integer variables where 1 and 0 refer to lane-changing and lane-keeping, respectively. First, we learn a standardization function on the training dataset. Then, we transform validation and test datasets using the already learned standardization function to ensure that the model is not peaking at these two datasets.

### Padding the trajectory data

When processing sequence data, it is common for individual samples to have different lengths. In our case, not all trajectories contain sufficient data for the desired span of 20 s. This is where padding is used to make all sequences in a batch of a given standard length (i.e., 40 time steps in our case) before one starts training the network. In this chapter, trajectories are pre-padded so that they all are of the same size, i.e., 40 time steps.

## 4.4 Experimental setup

This section begins by specifying the evaluation metric that is used to assess the model performance. Subsequently, the architecture of the proposed GRUNN model and its parameters that need to be optimized are presented.

### 4.4.1 Evaluation metric

The confusion matrix is widely used to evaluate the performance of a classifier as shown in Table 4.3. For the binary classification, a confusion matrix is represented as a  $2 \times 2$  matrix,

**Table 4.3. Confusion Matrix**

		Predicated class	
		Positive	Negative
Actual class	Positive	True positive (TP)	False negative (FN)
	Negative	False positive (FP)	True negative (TN)

which comprises four elements: TP (true positives), the number of correctly predicted positive instances; TN (true negatives), the number of correctly predicted negative instances; FP (false positives), the number of incorrectly predicted negative instances; and FN (false negatives), the number of incorrectly predicted positive instances.

These elements are used to derive traditional evaluation metrics such as accuracy ( $= \frac{TP+TN}{TP+TN+FP+FN}$ ). Having discussed previously that our dataset is an imbalanced dataset with more instances of lane-keeping (majority or negative class) than lane-changing (minority or positive class) ones, traditional evaluation metrics might provide biased results (Peng et al., 2020, Elamrani Abou Elassad et al., 2020). Therefore, we consider geometric mean accuracy or G-mean that integrates recalls of both classes and is used in previous research to classify imbalanced datasets. G-mean can be expressed by Equation 4.11:

$$\text{G-mean} = \sqrt{TPR \cdot TNR} \quad (4.11)$$

where  $TPR \left( = \frac{TP}{TP+FN} \right)$  denotes true positive rate or accuracy on the minority class and  $TNR \left( = \frac{TN}{TN+FP} \right)$  denotes true negative rate or accuracy on the majority class. G-mean tries to maximize the accuracy of each class while keeping these accuracy values balanced. Thus, a higher G-mean value indicates that the comprehensive performance of a classifier is better.

#### 4.4.2 Model specification

The model is specified using several layers which take an input, i.e., a trajectory, and outputs the target; i.e., a label denoting either a lane-changing or lane-keeping decision. The following layers are considered in this chapter.

1. Input layer: The input is of the shape (time steps, number of features). For this chapter, the input is of the shape (40, 19).
2. Masking layer: A masking layer is added on top of the input layer so that model knows that missing time steps of an input should be skipped when processing the data. These missing time steps can be identified using the padded values which we have described earlier during data processing.
3. A gated recurrent (GRU) layer: A GRU layer followed by a dropout layer is added on top of the masking layer. The dropout layer is used to avoid overfitting and can subsequently improve the model generalization. The GRU layer can memorize previous information and feed the same to next time-steps using the activation function. In the case of a multi-layered GRUNN, more GRU layers can be stacked here. Each of which is followed by a dropout layer.
4. Dense layer: The output of the (final) GRU layer is collected at the latest time-step  $T$  using a dense layer. We use the Sigmoid activation function here to output the probability of classifying a trajectory as a lane-changing one.



### 4.4.3 Selection of model parameters

In this section, we discuss the model parameters of our GRUNN model that include hyperparameters of the GRUNN model and a choice of strategy to deal with class imbalance. A selection of optimal hyperparameters is shown to improve the GRUNN model performance (Zhang et al., 2020). Therefore, the following hyperparameters are considered in this chapter.

1. The number of hidden layers: The multi-layer neural network architectures are shown to improve model performance and can achieve better realization than a single-layer architecture (Utgoff and Stracuzzi, 2002). Therefore, we investigate the model performance with more than one hidden layer.
2. The number of units: The number of hidden units is a very important parameter of our GRUNN model, as the different number of hidden units may greatly affect the prediction precision. To choose the best value, we experiment with different hidden units and select the optimal value by comparing the predictions.
3. Dropout rate: Dropout is a technique to reduce overfitting. Its central idea is to take a model that is overfitting and train sub-models derived from it by randomly removing units for each training batch. The number of units to retain is controlled by a hyperparameter known as the dropout rate.
4. Learning rate: Learning rate is a parameter related to the optimization algorithm used while training the neural network. It controls how quickly the algorithm updates the weights at each iteration. A larger learning rate makes the model learn faster.
5. Batch size: A neural network is trained in batches. A batch is defined as the number of samples used for each iteration during the training process. Therefore, it is important to find the optimal batch size to achieve a good model performance.

Two strategies are used to handle the class imbalance problem in our case where the majority class (LK) contains 17 times more instances than the minority class (LC). The first strategy deals with class imbalance by assigning different classes with different weights, which are in proportion to their corresponding misclassification costs. The second strategy deals with training a model on a balanced dataset that has equal distribution of both majority (or LK) and minority (or LC) classes. An ensemble classifier is developed which aggregates the results by training models on several balanced datasets. The number of balanced datasets is equal to the proportion of instances in the majority class to the minority class.

In this chapter, the grid-search method is used to search for the optimal values of parameters. As shown in Table IV, the tuning range is the range out of which the most appropriate value is selected. For each combination of hyperparameters and a choice of strategy to deal with class imbalance, we train the GRUNN on the training dataset. The proposed model uses the Adam algorithm (Kingma and Ba, 2015) as our optimizer. The maximum number of epochs is set as 100 and the early stopping criterion is adopted to prevent overfitting. In this process, the training is stopped if its performance does not improve over 10 consecutive epochs. All the experiments are coded with Keras 2.4.0, TensorFlow 2.3.0, scikit-learn 0.24.1, NumPy 1.19.2, and pandas 1.2.3 in python 3.8.5.

Three separate GRUNN models are built: GRUNN-PC (passenger cars), GRUNN-DV (delivery vans), and GRUNN-T (trucks). After comparing the model's performance (or G-mean) on the validation dataset under different parameter values, the optimal values of hyperparameters are selected. Table 4.4 shows the selected hyperparameters for these three models.

**Table 4.4. Parameter Selection for GRUNN Models**

Model parameters	Tuning range	Selected value		
		Passenger cars	Delivery vans	Trucks
		GRUNN-PC	GRUNN-DV	GRUNN-T
<i>Hyperparameters of the GRUNN model</i>				
Number of hidden layers	1, 2	2	2	2
Number of units	32, 64, 128	128	64	64
Dropout rate	0.1, 0.2, 0.3, 0.4, 0.5	0.1	0.1	0.3
Learning rate	0.01, 0.005, 0.001, 0.0005, 0.0001	0.001	0.01	0.0005
Batch size	32, 64, 128, 256, 512	256	128	64
<i>Handling class imbalance</i>				
Approach	Cost-sensitive learning, ensemble learning	Cost-sensitive learning (LC weight: 2.16, LK weight: 0.65)	Cost-sensitive learning (LC weight: 2.74, LK weight: 0.61)	Cost-sensitive learning (LC weight: 9.11, LK weight: 0.53)

## 4.5 Results

Having identified the best model parameters, this section will focus on applying these models to respective test datasets. The performance of the trained GRUNN models (GRUNN-PC, GRUNN-DV, and GRUNN-T) are evaluated on the respective test datasets that have been kept aside. This section is further divided with respect to the vehicle classes considered in this chapter. In each subsection, the prediction performance of models is discussed in the first part. After that, model interpretability (or explainable AI) techniques are used to explain what models have learned to gain insights into the gap selection process.

### 4.5.1 Passenger cars

Table 4.5 shows the performance of the trained GRUNN model for passenger cars, i.e., GRUNN-PC. It can be observed that this model achieves the G-mean of 88.35%. This model can accurately predict 87.05% of LC and 89.67% of LK trajectories.

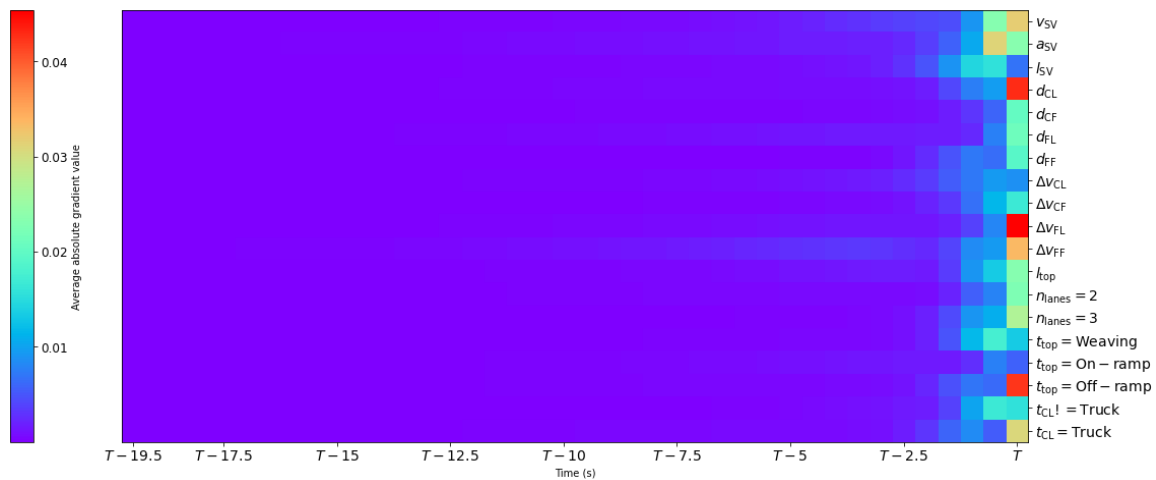
Now, we will use model interpretability (or explainable AI) techniques to discover new knowledge about the gap selection process of passenger cars. Figure 4.5 shows the dynamics behind the gap selection process of passenger cars by using a heat map. This heat map is a 2D representation, consisting of average absolute gradient values, that can be used to determine what parts of the input contribute to the classification, and how important are these parts to the result. It can be observed that passenger car drivers seem to dynamically vary their attention

**Table 4.5. Model Performance on the Test Dataset for Passenger Cars (GRUNN-PC)**

		Predicated class		Classification accuracy (%)
		LC	LK	
Actual class	LC	74	11	87.05
	LK	29	252	89.67

over the feature set. For instance, they seem to consider their characteristics (speed and acceleration) to be more important than other features at the time instant  $T - 0.5$  s. On the contrary, at the time instant  $T$ , which is closer to the instance of their decision-making, they seem to shift their attention to their interactions with surrounding vehicles (distance gap of the vehicle SV with the vehicle CL ( $d_{CL}$ ) and the speed difference between the vehicles SV and FL ( $\Delta v_{FL}$ )) and topological related features (the type of topology ( $t_{top} = \text{Off-ramp}$ )).

Let us now turn to the variable importance, which captures its contribution to the target activation using gradient values. The higher the value of the gradient, the higher will be the contribution of that variable on the target activation. We consider both feature importance and time importance, at a global level, to explain the gap selection process of passenger car drivers (see Figure 4.6). Looking at the feature importance, the three features that contribute most to the target activation are a passenger car driver's speed ( $v_{SV}$ ), his acceleration ( $a_{SV}$ ), and the speed difference with the vehicle FF ( $\Delta v_{FF}$ ). Their reliance on their interactions with their respective future followers might indicate that they consider safety during lane changing. The feature importance plot suggests that topological features might not play a significant role in the gap selection process of passenger car drivers since their characteristics and their interactions with surrounding vehicles seem to dominate their gap selection process. If we now consider the time importance, it is observed that around three-fourths of the contribution can be captured by the time interval  $[T - 1.5, T]$ . This suggests that passenger car drivers do not rely only on instantaneous information at  $T$  rather they also consider historical information when it comes to gap selection. Nevertheless, a large value of the average gradient at the time instance  $T$  indicates the passenger car drivers seem to place higher weights on the instantaneous information to decide whether to accept or reject gaps.

**Figure 4.5. Heat map showing the dynamic gap selection process of passenger cars.**

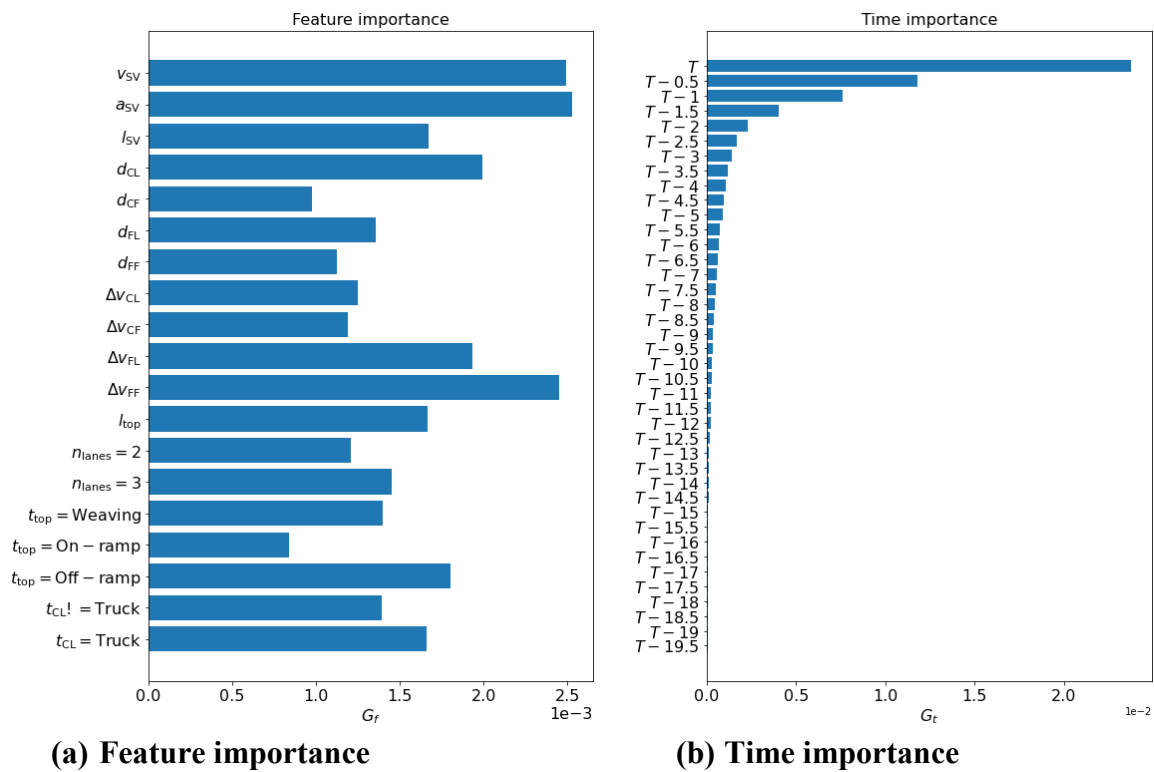


Figure 4.6. Variable importance for passenger cars.

#### 4.5.2 Delivery vans

Table 4.6 presents the model performance for delivery vans. The GRUNN-DV model is able to achieve the G-mean of 84.06%. The accuracies with which this model can predict LC and LK trajectories are balanced. The model can accurately predict 85% of LC and 83.14% of LK trajectories.

Table 4.6. Model Performance on the Test Dataset for Delivery Vans (GRUNN-DV)

		Predicated class		Classification accuracy (%)
		LC	LK	
Actual class	LC	17	3	85.00
	LK	15	74	83.14

Figure 4.7 shows the dynamics behind the gap selection process of delivery van drivers by using a heat map. It can be observed that delivery van drivers also seem to dynamically vary their attention over the feature set similar to passenger car drivers. However, noticeable gradients for delivery van drivers encompass more time instants than passenger car drivers. This suggests that delivery van drivers utilize more historical information than passenger car drivers towards selecting gaps.

Let us now turn to the variable importance, which captures its contribution to the target activation using gradient values. We consider both feature importance and time importance, at a global level, to explain the gap selection process of delivery van drivers (see Figure 4.8). Looking at the feature importance, the three features that contribute most to the target activation

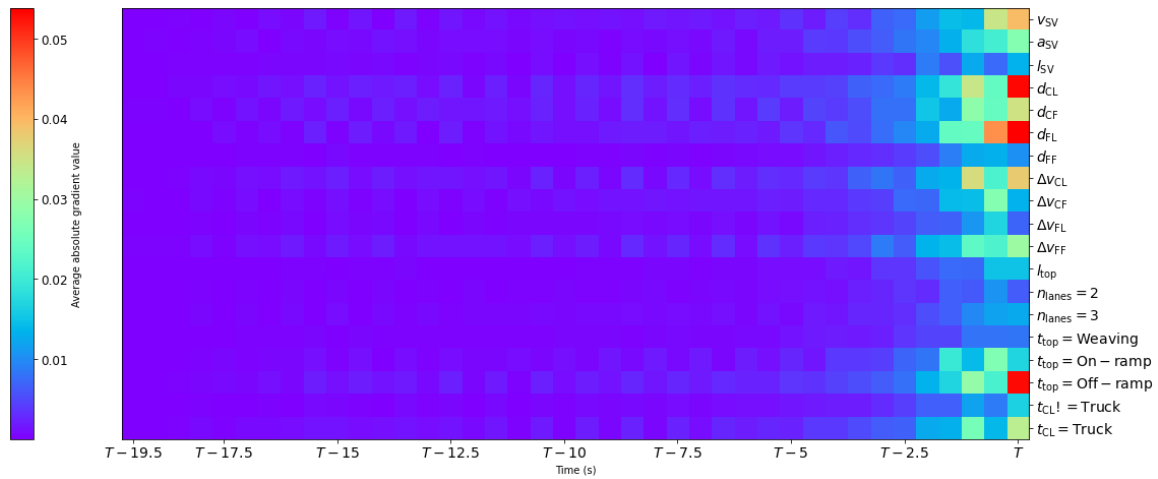


Figure 4.7. Heat map showing the dynamic gap selection process of delivery vans.

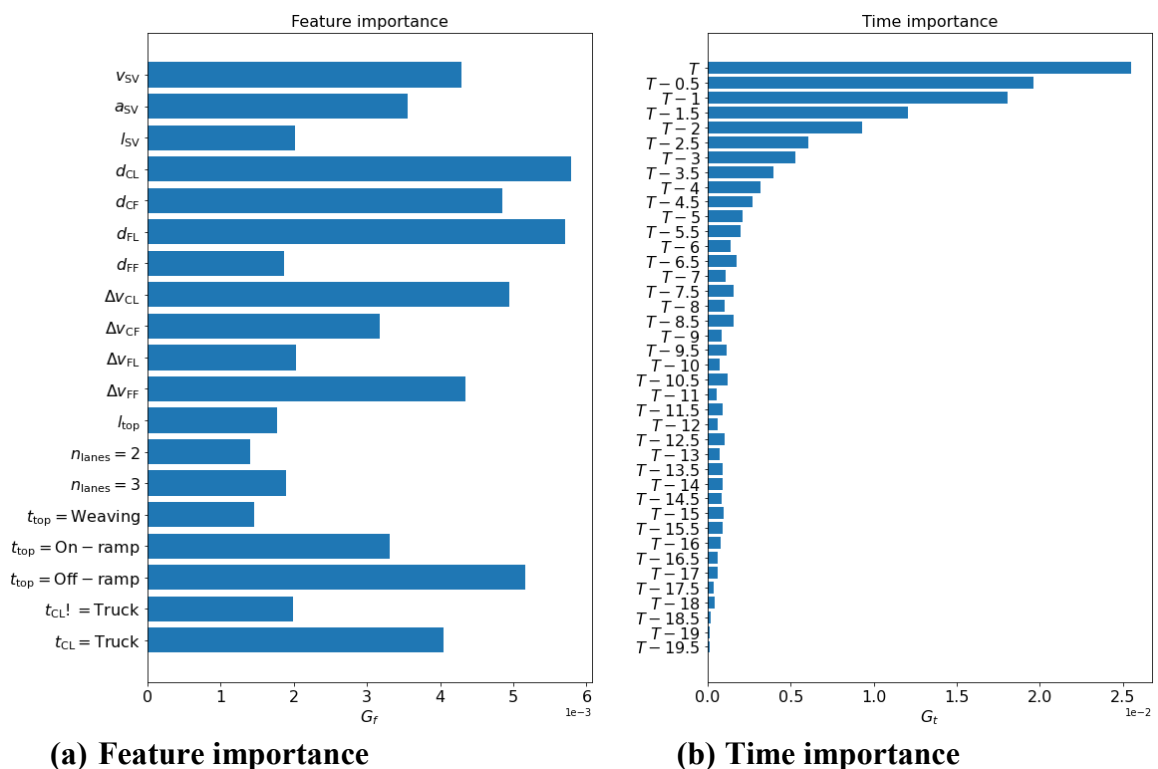


Figure 4.8. Variable importance for delivery vans.

are the interactions of delivery van drivers with surrounding vehicles, captured by the distance gap with the vehicle CL ( $d_{CL}$ ) and the vehicle FL ( $d_{FL}$ ), and type of topology ( $t_{top} = \text{Off-ramp}$ ). The feature importance suggests that delivery van drivers consider their interactions and their perception of a topology more salient than their characteristics. Further, their reliance on their interactions with the current leader and future leader might indicate they consider them as a trade-off to evaluate traffic conditions and maneuverability on both lanes. If we now consider the time importance, it is observed that around three-fourths of the contribution can be captured by the time interval  $[T - 3, T]$ . Interestingly, most of the effect is produced by the gradient values computed at the time instance  $T$  as also highlighted in the heat map. This suggests that

delivery van drivers not only consider historical information from previous time-steps but also rely on current information to decide on the gap selection.

### 4.5.3 Trucks

Third, the performance of the model for trucks (GRUNN-T) is discussed in Table 4.7. This model can achieve the G-mean of 87% on the respective test dataset of trucks. Further, the model can accurately predict 92.31% of LC and 82% of LK trajectories.

**Table 4.7. Model Performance on the Test Dataset for Trucks (GRUNN-T)**

		Predicated class		Classification accuracy (%)
		LC	LK	
Actual class	LC	12	1	92.31
	LK	38	173	82.00

Figure 4.9 shows the dynamics behind the gap selection process of truck drivers by using a heat map. Truck drivers, similar to passenger car and delivery van drivers, dynamically vary their attention on the considered feature set. Yet, truck drivers differ in the manner how salient they consider historical information. The heat map in Figure 4.9 indicates that they seem to be more anticipatory (Zheng, 2014) than passenger car or delivery van drivers as noticeable gradient values cover more time span than passenger car and delivery van drivers.

Moving to the variable importance (Figure 4.10), the three features that contribute most to the

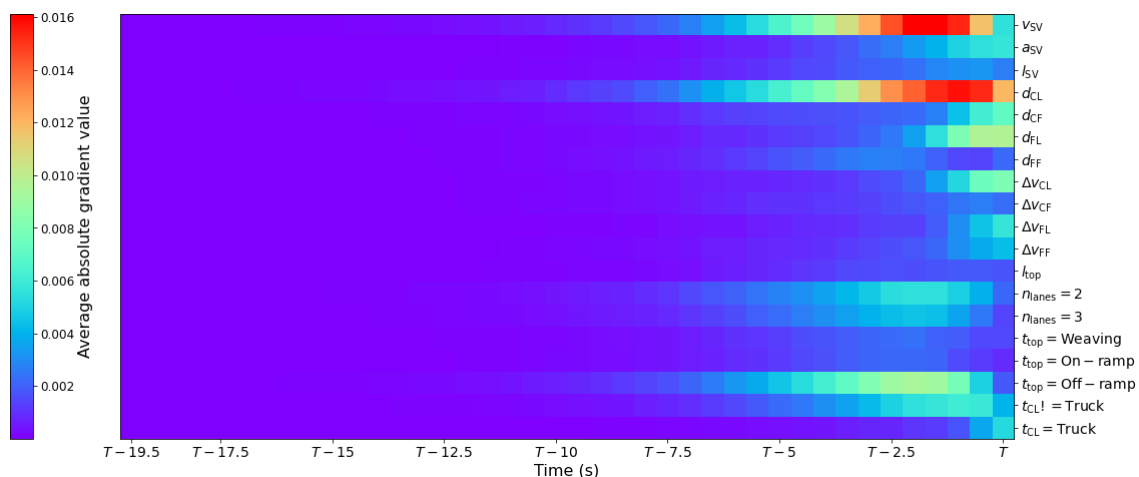


**Figure 4.9. Heat map showing the dynamic gap selection process of trucks.**

target activation are the truck driver's speed ( $v_{SV}$ ), the distance gap he maintains with the vehicle CL ( $d_{CL}$ ), and the type of topology he is driving on ( $t_{top} = \text{Off-ramp}$ ). These top three features also encompass all three dimensions (subject vehicle's characteristics, its interaction with surrounding vehicles, and its perception of the topology) considered while developing the feature set and thus showing entirely different behavior than both passenger car and delivery van drivers. Consequently, these features have much more impact on the classification score

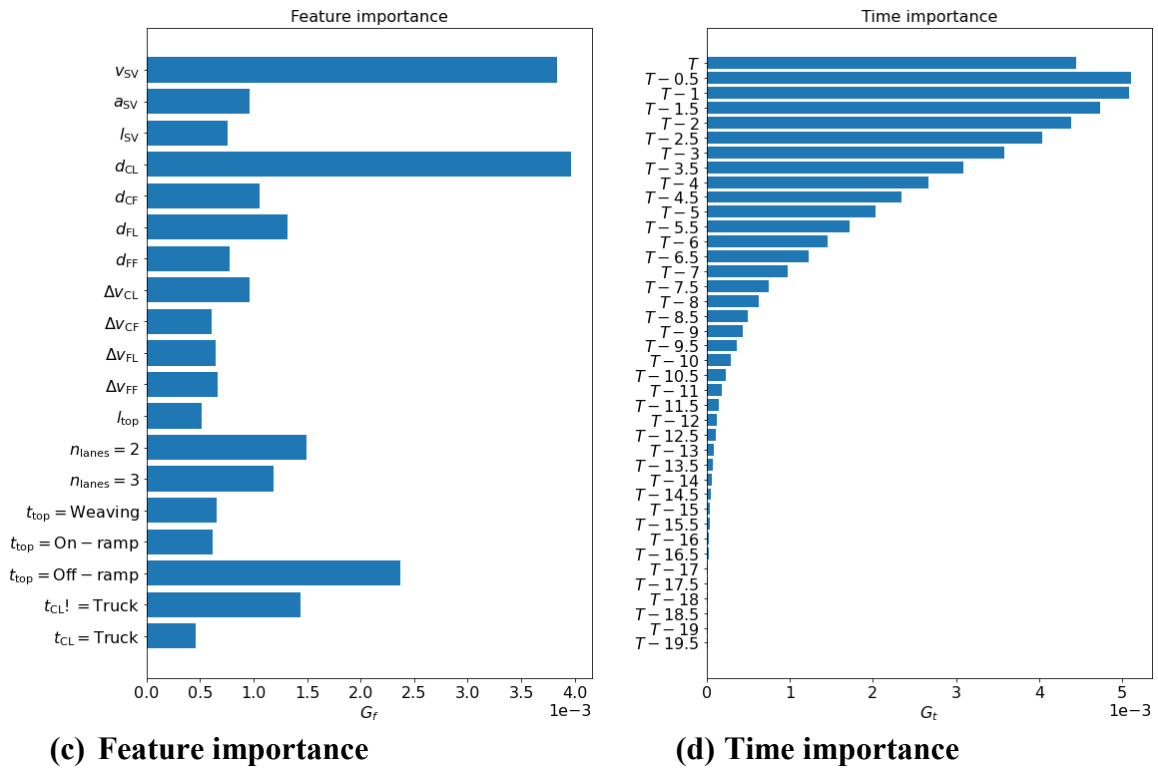


**Figure 4.10. Variable importance for trucks.**

than other features. If we now consider the time importance, it is observed that around three-fourths of the contribution can be captured by the time interval  $[T - 6, T]$ . This suggests that truck drivers do not rely only on instantaneous information at  $T$  rather they also consider previous time-steps or historical information when it comes to gap selection.

## 4.6 Discussion

The discussion section is composed of four parts. In the first part, the uniqueness of the trajectory dataset is described. Next, the gap selection behavior of multiple vehicle classes is compared. Then, the performance of our models (GRUNN-PC, GRUNN-DV, and GRUNN-T) is compared with the state-of-the-art. The last part discusses the implications and possible applications of our models.

This chapter has used a large trajectory dataset that contains multiple vehicle classes. 3,647 trajectories of passenger car drivers, 2,226 trajectories of truck drivers, and 1,080 trajectories of delivery van drivers are present in this dataset. Unlike the widely used NGSIM dataset (Coifman and Li, 2017), our dataset contains significant numbers of trucks and delivery vans. This has a significant advantage over the earlier study focused on modeling lane-changing motivations of trucks (Moridpour et al., 2012), which used limited data of only 39 trajectories of truck drivers. Moreover, this dataset is also unique in terms of analyzing the behavior of delivery van drivers as other available trajectory datasets (e.g., NGSIM (Coifman and Li, 2017) and highD (Krajewski et al., 2018)) may not contain delivery vans.

Three GRUNN models are proposed in this chapter: GRUNN-PC (passenger cars), GRUNN-DV (delivery vans), and GRUNN-T (trucks). These three models show that there exist significant differences with respect to the gap section process among these three vehicle classes (see Table 4.8). Passenger car drivers seem to be more concerned about their kinematic features

and the motion of the lag vehicle in the target lane during gap selection. Whereas delivery van drivers give more weight to the traffic conditions in the current and target lane by looking at their gap spacing with the respective leading vehicles along with their perception of the topology. Truck drivers, on the other hand, consider a three-dimensional view that includes their vehicle kinematics (speed), their interactions with the surroundings (gap spacing with the current leader), and their perception of topology. Our findings demonstrate that topological factors are important to consider while analyzing the lane-changing behavior especially of commercial vehicles such as delivery vans and trucks. This fills a gap in the literature, as highlighted by Rahman et al. (Rahman et al., 2013). An advantage of our models is that they can be used on a general road network consisting of multiple topologies (e.g., on-ramps, off-ramps, and weaving sections). If we compare the time importance for multiple vehicle classes, we observe that gap selection is not an instantaneous process but a sequential one. This finding is consistent with previous research (Balal et al., 2016, Punzo et al., 2011, Xie et al., 2019) which noted that passenger car drivers seem to consider lagged information for a specific time instant in their gap selection process. We show that the effect of memory or historical information is more salient for trucks than passenger cars or delivery vans. Especially, the last 6 seconds largely influence the gap selection process of truck drivers. Time importance plots also suggest that historical information generally has a fading effect on the gap selection process of vehicles which means that memory is not always constant. Previous research has also noted similar fading effects for the car following behavior (Huang et al., 2018).

This chapter used imbalanced datasets to analyze the gap selection behavior of multiple vehicle classes. A large body of research is concentrated on passenger cars where most of these works built balanced datasets retrieved from widely used NGSIM data. In lieu of any reference study on the gap selection behavior of delivery van and truck drivers, the performance of our three models is compared with previous research on passenger car drivers which uses imbalanced datasets (Balal et al., 2016, Ng et al., 2020, Zheng et al., 2014, Tang et al., 2020). These studies report G-mean in the range of 66.39-90.50% which is in accordance with the performances of our models. It is also encouraging to compare the performance of our models with other traffic-related studies (Elamrani Abou El Assad et al., 2020, Peng et al., 2020) on imbalanced classification which report G-mean in the range of 70.40-88.50%. It seems that the performance of our models (GRUNN-PC, GRUNN-DV, and GRUNN-T) is on par with these earlier studies. Due to the dataset used, the empirical findings presented in this chapter seem to be valid for drivers operating in the Netherlands. We expect that these findings may apply to all European countries with similar driving regulations. For other countries with different driving rules, further research is recommended so that the gap selection process of international drivers can be compared. This chapter is an important step in improving our understanding regarding the

**Table 4.8. Comparison of the gap selection process of multiple vehicle classes**

Vehicle class	Salient time span (s)	Salient dimensions (features)		
		SV characteristics	Interaction of SV with surrounding vehicles	Perception of topology
Passenger cars	[T-1.5, T]	++	+	o
Delivery vans	[T-3.0, T]	o	++	+
Trucks	[T-6.0, T]	+	++	+

Note: SV: Subject vehicle;

Feature importance scale: ++ very important; + important; o less important



microscopic phenomena of multiple vehicle classes that give rise to macroscopic or observable effects. Overall, these findings hold the potential to improve current models, to perform improved traffic and safety assessments, and eventually to support the design of advanced autonomous systems, for example aiming at guidance for the lane changing process. These advanced systems may use sensors instrumented in the subject vehicle or vehicle-to-vehicle (V2V) communication technology to feed inputs to the GRU neural network model. The variables related to the perception of a road topology may be transmitted via digital mapping services.

## 4.7 Conclusions

Gap selection is an important part of the discretionary lane changing activity. To understand and unravel the latent gap selection mechanisms of multiple vehicle classes, we use gated recurrent unit neural network (GRUNN) models on a large and unique trajectory dataset, collected for the Netherlands, that comprises lane changing trajectories of passenger cars, delivery vans, and trucks. The proposed vehicle class specific models are able to handle the class imbalance observed in the trajectory dataset. Moreover, these models can capture temporal interdependencies, by incorporating historical information, and the effect of external factors arising from the perception of a road topology.

The proposed models are interpreted using explainable AI techniques in order to obtain insights into the gap selection process of multiple vehicle classes. We show that gap selection is a sequential process governed by the impact of historical information or decisions and this impact fades over time. Passenger cars and delivery vans mostly utilize up to 3 seconds of recent driving experiences towards selecting gaps in contrast to trucks which rely on a longer duration of nearly up to 6 seconds. Using feature importance, we find that the most important factors associated with gap selection differ by vehicle classes. Passenger cars focus on their kinematic features (speed, acceleration) and their interactions with surrounding vehicles (the speed difference with the lag vehicle in the target lane). Whereas delivery vans utilize their interactions (gap spacing with current and future leading vehicles) and the type of topology. Trucks, on the other hand, consider a three-dimensional view that includes their kinematics (speed), their interactions with the surroundings (gap spacing with the current leading vehicle), and their perception of topology during their gap selection process.

The issue of lane-changing is an intriguing one that could be usefully explored in further research by using recent advances in AI and newly available trajectory datasets. Future research might explore the lane-changing execution of multiple vehicle classes. More broadly, a further study could also build integrated models, by also accounting for the inter-driver difference, to capture full lane-changing dynamics.

## 5 A multi-class lane changing advisory system

---

Previous chapters focusing on lane changing at the tactical level presented insights into several elements such as merging, diverging, and gap selection. This chapter investigates how lane changing behavior around freeway bottlenecks can be influenced to improve traffic efficiency. Current lane changing advisory systems operates on the traffic flow as a whole and disregard different vehicle classes of which it is composed. To address this gap, this chapter proposes a multi-class lane changing advisory system that embeds vehicle class-specific properties contributes to answering the fourth research question of this dissertation. This chapter further applies the proposed advisory system on a merging section to evaluate its performance.

This chapter is based on the following journal and conference papers:

Sharma, S., Papamichail, I., Nadi, A., van Lint, H., Tavasszy, L. and Snelder, M. 2022. A Multi-class Lane-changing Advisory System for Freeway Merging Sections Using Cooperative ITS. *IEEE Transactions on Intelligent Transportation Systems*, 23(9), pp. 15121-15132.

Sharma, S., Papamichail, I., Nadi, A., Van Lint, H., Tavasszy, L. and Snelder, M. 2021. A Multi-class Lane-changing Advisory System for Freeway Merging Sections. Paper presented in *16<sup>th</sup> IFAC Symposium on Control in Transportation Systems*. IFAC-PapersOnLine, 54(2), pp. 93-98.

---

## 5.1 Introduction

Traffic congestion on freeways causes large delays and therewith high societal costs. Freeway bottlenecks (e.g., merging sections, lane-drops, work zones, etc.) locally cause congestion that may spill back to other parts of the network. When traffic demand exceeds the capacity of a merging section, it becomes an active bottleneck which results in the formation of a queue on the near-side lane of a mainline carriageway. The queue then spreads laterally to other lanes and triggers a drop in the discharge flow or a phenomenon known as capacity drop (Cassidy and Bertini, 1999, Cassidy and Rudjanakanoknad, 2005). Data from several studies suggest that traffic flow is unevenly distributed over available lanes of a freeway (Knoop et al., 2010, Wu, 2006, Amin and Banks, 2005). Around a merging section, unbalanced flow distribution might also contribute to traffic breakdown on a heavily used lane (i.e. near-side lane) while there is spare capacity available on the other lanes.

In recent years, technological breakthroughs in communication and automation have enabled us to research and develop new cooperative intelligent transportation system (C-ITS) solutions to help tackle the problem of congestion. This system enables vehicles to exchange relevant information with other vehicles (V2V) or with the road infrastructure (V2I or I2V) using communication technology in order to create in-vehicle and cooperative systems (Sjoberg et al., 2017). Using C-ITS, this chapter presents an in-vehicle lane-changing advisory system that aims at improving traffic efficiency by balancing the distribution of traffic flow around merging sections.

Existing research has recognized that the traffic situation in the vicinity of freeway bottlenecks can be improved by efficiently assigning traffic flow to available lanes on freeways. Rule-based approaches are proposed in (Zhang and Ioannou, 2017, Schakel and van Arem, 2014) where vehicles are advised a suitable lane in the vicinity of bottlenecks. Although these approaches can be applied in real-time, they require enough knowledge about the traffic system to generate a set of instructions. In (Ramezani and Ye, 2019, Zhang et al., 2019, Subraveti et al., 2020), the lane assignment problem is treated as an optimization program. However, the inherent computational processing time associated with these approaches might hinder their real-time applicability. In contrast to the above approaches, several approaches based on the optimal control theory have been proposed in (Markantonakis et al., 2019, Roncoli et al., 2016, Roncoli et al., 2017, Tajdari et al., 2019, Tajdari et al., 2020). These approaches can be implemented in real-time and do not require a set of rules for operations, thus alleviating the limitations of rule-based and optimization-based approaches. However, previous studies solely focus on passenger cars and do not embed multiple vehicle classes in the lane-changing advisory framework. Heterogeneity induced from class-specific properties can affect traffic efficiency (van Lint et al., 2008a). This chapter addresses this research gap by incorporating multiple vehicle classes by means of passenger car equivalents within a multi-class multi-lane macroscopic traffic flow model. We use this traffic flow model to design a multi-class lane-changing advisory system based on a linear quadratic regulator (LQR).

Controllers can be designed in a way to guarantee stability in the sense that they often have tunable parameters that affect how the controlled system stabilizes. In this respect, an LQR controller contains two weighting matrices that regulate the penalties with respect to state variables and control actions. These weights are selected by a designer and affect the behavior of the LQR controller. In (Markantonakis et al., 2019, Roncoli et al., 2016, Roncoli et al., 2017, Tajdari et al., 2019, Tajdari et al., 2020), these weights are selected using trial-and-error-based approaches. Other classical approaches include Bryson's method (Johnson and Grimble, 1987) and pole placement (Saif, 1989). However, these approaches are often time-consuming and labor-intensive processes. Some studies have formulated the selection of weighting matrices for an LQR controller as an optimization problem and solved it using meta-heuristics (Habib et

al., 2017, Das et al., 2013, Hassani and Lee, 2016, Liang et al., 2018). These methods can explore the search space in an informed manner and converge to the optimal solutions. Compared to optimization-based approaches, the response surface method can reveal meaningful information from a small number of experiments. Approximation or meta-models can be developed to map the relationship between performance characteristics and design variables in order to determine the optimum design parameters (Myers et al., 1997, Ziegel, 1997). In this chapter, we adopt the response surface method to find these weighting matrices that ensure a robust performance for an LQR controller.

Further, we use microscopic simulation to evaluate the performance of the proposed controller around merging sections, in contrast to (Tajdari et al., 2019) and (Tajdari et al., 2020), since a microscopic traffic simulator provides a real-world testbed to test an in-vehicle lane-changing advisory system.

To this end, the objective of this study is to propose a multi-class lane-changing controller around a merging section to improve its traffic efficiency. To the best of our knowledge, this is the first multi-class LQR controller for lane-changing. This chapter contributes to the existing literature by:

1. developing a multi-class lane-changing advisory system based on a linear quadratic regulator (LQR);
2. performing a response surface-based approach to select the optimal weights of the LQR controller; and
3. evaluating the performance of the LQR controller around a merging section using a microscopic traffic simulator.

This chapter is structured as follows. Section 5.2 formulates a multi-class lane-changing LQR controller. Next, section 5.3 describes the approach to implement the proposed controller in microscopic simulation software. Then, section 5.4 describes the experimental setup to evaluate the proposed controller. In section 5.5, we describe the optimum selection of set points and the weights of the LQR controller. We present and discuss our results in section 5.6. Finally, we conclude this chapter in section 5.7.

## 5.2 Formulating a multi-class lane-changing LQR controller

This section first develops a linear time invariant system based on a multi-class multi-lane traffic flow model. Then, we formulate an LQR controller. Lastly, we discuss the possible implementation of this LQR controller as a C-ITS based application.

### 5.2.1 Traffic system dynamics using a multi-class multi-lane traffic flow model

Based on a linear multi-lane traffic flow model proposed in Roncoli et al. (2016), we consider a multilane freeway as shown in Figure 5.1. The freeway is divided into  $i = 0, \dots, N$  segments of length  $L_i$ . Each such segment is composed of  $j = m_i, \dots, M_i$  lanes, where  $m_i$  and  $M_i$  denote the minimum and maximum indices of lanes for segment  $i$ . It is assumed that  $j = 0$  corresponds to the segment(s) on the rightmost lane. In Fig. 1,  $m_0 = 0$  and  $M_0 = 2$ . Each element of the resulting grid is termed as a cell with index  $(i, j)$ . According to the definition, the total number of cells from the origin to segment  $i$  is  $H_i = \sum_{r=0}^i (M_r - m_r + 1)$ , and the total number of cells

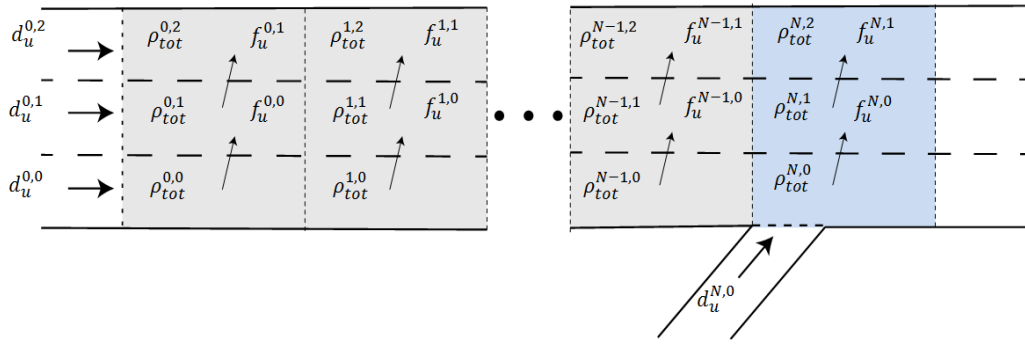


**Figure 5.1. A hypothetical freeway stretch with an on-ramp.**

for the whole stretch is  $\bar{H} = H_N$ . To formulate the model in discrete time, we consider the discrete-time step  $T$ , indexed by  $k = 0, 1, \dots$ , where the time is  $t = kT$ .

First of all, we will focus on defining the dynamics of a multi-class traffic system comprising  $U$  number of vehicle classes. For every vehicle class  $u$ , the conservation of vehicles can be defined as:

$$\frac{\partial \rho_u}{\partial t} + \frac{\partial q_u}{\partial x} = 0, \quad (5.1)$$

where  $\rho_u$  and  $q_u$  refer to the class-specific density and class-specific flow at time  $t$  and location  $x$ , respectively.

Under assumptions of homogeneous and stationary conditions, class-specific density and flow are related, according to the continuity equation, as

$$q_u = \rho_u v_u, \quad (5.2)$$

where  $v_u$  refers to the class-specific average speed and can be expressed as  $v_u = V_u^e(\rho_{tot})$ . Here,  $V_u^e$  denotes the class-specific equilibrium speed which is a function of the total effective density  $\rho_{tot}$  in pce/km.  $\rho_{tot}$  is described by a function of the class-specific densities ( $\rho_u$ ) and the dynamic pce values ( $\eta_u$ ) and reads  $\rho_{tot} = \sum_u \eta_u \rho_u$ . This dynamics shows in a simple way that controlling (effective) densities of user class  $u$  naturally affects the speed and in turn the (effective) densities of all other classes (van Lint et al., 2008a).

Now, the evolution of density for every vehicle class  $u$  in a cell  $(i, j)$ , proposed in (1), can be cast in discrete form as

$$\rho_u^{i,j}(k+1) = \rho_u^{i,j}(k) + \frac{T}{L_i} \left( q_u^{i-1,j}(k) - q_u^{i,j}(k) \right) + \frac{T}{L_i} \left( f_u^{i,j-1}(k) - f_u^{i,j}(k) \right) + \frac{T}{L_i} d_u^{i,j}(k), \quad (5.3)$$

where  $\rho_u^{i,j}(k)$  is the density of vehicle class  $u$  in a cell  $(i, j)$  at time instant  $kT$ ;  $q_u^{i,j}(k)$  is the longitudinal flow of vehicle class  $u$  leaving cell  $(i, j)$  and entering cell  $(i+1, j)$  during the time interval  $[kT, (k+1)T)$ ;  $f_u^{i,j}(k)$  is the net lateral flow of vehicle class  $u$  leaving cell  $(i, j)$  and entering cell  $(i, j+1)$  during time interval  $[kT, (k+1)T)$ ; and  $d_u^{i,j}(k)$  is the external flow of vehicle class  $u$  entering the network in cell  $(i, j)$  either from mainline or an on-ramp during the time interval  $[kT, (k+1)T)$ .

The discretization should also satisfy the following Courant–Friedrichs–Lewy CFL condition:

$$\frac{L_i}{T} \geq \max\{v_u^{i,j}\}_{u=1,\dots,U} \quad (5.4)$$

Since each cell has a mix of vehicle classes, the effective density of a cell  $(i, j)$  can be defined using passenger car-equivalents (pce) of vehicle classes:

$$\rho_{tot}^{i,j}(k) = \sum_u \eta_u^{i,j}(k) \rho_u^{i,j}(k), \quad (5.5)$$

where  $\rho_{tot}^{i,j}(k)$  is the effective density of a cell  $(i, j)$  at time instant  $kT$  [pce/km]; and  $\eta_u^{i,j}(k)$  is the passenger car equivalent for a vehicle class  $u$  in a cell  $(i, j)$  at time instant  $kT$ .

Similarly, total flow in passenger car-equivalents in a cell  $(i, j)$  can be defined as:

$$q_{tot}^{i,j}(k) = \sum_u \eta_u^{i,j}(k) q_u^{i,j}(k), \quad (5.6)$$

where  $q_{tot}^{i,j}(k)$  is the total longitudinal flow of vehicle class  $u$  leaving cell  $(i, j)$  and entering cell  $(i + 1, j)$  during time interval  $[kT, (k + 1)T)$  [pce/h]; and  $\eta_u^{i,j}(k)$  is the passenger car equivalent for a vehicle class  $u$  in a cell  $(i, j)$  at time instant  $kT$ .

By combining Equations 5.3, 5.5, and 5.6, the evolution of the effective density of a cell  $(i, j)$  can be expressed as

$$\begin{aligned} \rho_{tot}^{i,j}(k+1) = \sum_u \left\{ \eta_u^{i,j}(k) \rho_u^{i,j}(k) + \frac{T}{L_i} \left( \eta_u^{i-1,j}(k) q_u^{i-1,j}(k) - \eta_u^{i,j}(k) q_u^{i,j}(k) \right) + \right. \\ \left. \frac{T}{L_i} \left( \eta_u^{i,j-1}(k) f_u^{i,j-1}(k) - \eta_u^{i,j}(k) f_u^{i,j}(k) \right) + \frac{T}{L_i} \eta_u^{i,j}(k) d_u^{i,j}(k) \right\}. \end{aligned} \quad (5.7)$$

Depending on the network topology, some terms in the above equation may not be present. Lateral flows  $f_u^{i,j}$  only exist for  $m_i \leq j < M_i$ . Thus, the total number of lateral flows are computed as  $\bar{F} = U(\bar{H} - N)$ .

Recall the relationship between macroscopic traffic flow parameters:

$$q_u^{i,j}(k) = \rho_u^{i,j}(k) \cdot v_u^{i,j}(k). \quad (5.8)$$

Combining Equations 5.7 and 5.8, we get

$$\begin{aligned} \rho_{tot}^{i,j}(k+1) = \sum_u \left\{ \left( 1 - \frac{T}{L_i} v_u^{i,j}(k) \right) \eta_u^{i,j}(k) \rho_u^{i,j}(k) + \frac{T}{L_i} \left( \eta_u^{i-1,j}(k) v_u^{i-1,j}(k) \rho_u^{i-1,j}(k) \right) + \right. \\ \left. \frac{T}{L_i} \left( \eta_u^{i,j-1}(k) f_u^{i,j-1}(k) - \eta_u^{i,j}(k) f_u^{i,j}(k) \right) + \frac{T}{L_i} \eta_u^{i,j}(k) d_u^{i,j}(k) \right\}. \end{aligned} \quad (5.9)$$

The proposed control actions are intended for usage before the possible onset of congestion, aiming to delay or avoid it. In this case, we may assume that the overall traffic flow entering the controlled area is bounded as it does not exceed the bottleneck capacity (e.g., using a variable speed limit controller for mainline traffic) and the proposed controller itself can avoid the creation of congestion. We can put forward the following assumptions to simplify Equation 5.9.

1. Average speed in all cells remains at a constant value, i.e.  $v_u^{i,j}(k) = v_{crit} \forall i, j, u, k$ .  $v_{crit}$  also refers to the speed of the slower vehicle class. All vehicle classes travel with the same critical speed at the critical density (Schreiter, 2013). Please note that this assumption is only made to design a multi-class lane-changing controller. We will later see in a

simulation-based case study (Section 5.6) that this assumption does not limit the performance of the proposed controller. Due to its robust feedback-based mechanism, the controller is able to improve traffic efficiency around a merging section.

2. Since speed remains at a constant value, we can also assume fixed passenger car equivalents.

Under these assumptions, for two-vehicle classes, cars and trucks, Equation 5.9 can be reformulated as follows:

$$\begin{aligned} \rho_{tot}^{i,j}(k+1) = & \frac{T}{L_i}(v_{crit})\rho_{tot}^{i-1,j}(k) + \left(1 - \frac{T}{L_i}(v_{crit})\right)\rho_{tot}^{i,j}(k) + \frac{T}{L_i}\left(\eta_c^{i,j-1}f_c^{i,j-1}(k) - \right. \\ & \left. \eta_c^{i,j}f_c^{i,j}(k)\right) + \frac{T}{L_i}\left(\eta_t^{i,j-1}f_t^{i,j-1}(k) - \eta_t^{i,j}f_t^{i,j}(k)\right) + \frac{T}{L_i}\left(\eta_c^{i,j}(k)d_c^{i,j}(k) + \eta_t^{i,j}(k)d_t^{i,j}(k)\right), \end{aligned} \quad (5.10)$$

where subscripts  $c$  and  $t$  denote cars and trucks, respectively.

Now the above system in Equation 5.10 can be considered as an LTI system

$$\underline{x}(k+1) = A\underline{x}(k) + B\underline{u}(k) + \underline{d}(k) \quad (5.11)$$

where

$$\underline{x} = [\rho_{tot}^{0,m_0} \dots \rho_{tot}^{0,M_0} \quad \rho_{tot}^{1,m_1} \dots \rho_{tot}^{N,M_N}]^T \in \mathbb{R}^{\bar{H}}, \quad (5.12)$$

$$\underline{u} = \begin{bmatrix} f_c^{0,m_0} \dots f_c^{0,M_0-1} & f_c^{1,m_1} \dots f_c^{N,M_N-1} \\ f_t^{0,m_0} \dots f_t^{0,M_0-1} & f_t^{1,m_1} \dots f_t^{N,M_N-1} \end{bmatrix}^T \in \mathbb{R}^{\bar{F}}, \quad (5.13)$$

$$\underline{d} = \left[ \frac{T}{L_i}(\eta_c^{0,m_0}d_c^{0,m_0} + \eta_t^{0,m_0}d_t^{0,m_0}) \dots \frac{T}{L_i}(\eta_c^{0,M_0}d_c^{0,M_0} + \eta_t^{0,M_0}d_t^{0,M_0}) \quad \frac{T}{L_i}(\eta_c^{1,m_1}d_c^{1,m_1} + \eta_t^{1,m_1}d_t^{1,m_1}) \dots \frac{T}{L_i}(\eta_c^{N,M_N}d_c^{N,M_N} + \eta_t^{N,M_N}d_t^{N,M_N}) \right]^T \in \mathbb{R}^{\bar{H}}. \quad (5.14)$$

This LTI system in Equation 5.11 can be used to formulate an optimal control problem that is aimed at maximizing traffic efficiency by balancing flows among lanes on a freeway.  $A \in \mathbb{R}^{\bar{H} \times \bar{H}}$ , composed of  $a_{rs}$  elements, represents the connection between pairs of subsequent cells connected by a longitudinal flow and  $B \in \mathbb{R}^{\bar{H} \times \bar{F}}$ , composed of  $b_{rs}$  elements, reflects the connection of adjacent cells connected by lateral flows. These elements are given by:

$$a_{rs} = \begin{cases} 1 - \frac{T}{L_i}(v_{crit}), & \text{if } r = s \text{ and } (i = N \text{ or } m_{i+1} \leq j \leq M_{i+1}) \\ \frac{T}{L_i}(v_{crit}), & \text{if } r > H_0 \text{ and } s = r - M_{i-1} + m_i - 1 \\ 0, & \text{otherwise} \end{cases} \quad (5.15)$$

$$b_{rs} = \begin{cases} \eta_c^{i,j} \frac{T}{L_i}, & \text{if } j > m_i \text{ and } (s = r - i) \\ -\eta_c^{i,j} \frac{T}{L_i}, & \text{if } j < M_i \text{ and } (s = r - i + 1) \\ \eta_t^{i,j} \frac{T}{L_i}, & \text{if } j > m_i \text{ and } (s = r + \bar{H} - N - i) \\ -\eta_t^{i,j} \frac{T}{L_i}, & \text{if } j < M_i \text{ and } (s = r + \bar{H} - N - i + 1) \\ 0, & \text{otherwise} \end{cases} \quad (5.16)$$

where  $r = H_{i-1} + j - m_i$ .

## 5.2.2 Optimal control problem formulation

The optimal control minimizes a cost function to steer a system to the desired state. The following quadratic cost function, over an infinite time horizon, has been defined:

$$\min J = \sum_k^\infty \left\{ \sum_i \sum_j \alpha^{i,j} (\rho_{tot}^{i,j}(k) - \hat{\rho}_{crit}^{i,j})^2 + \sum_{i=0}^{N-1} \sum_{j=m_i}^{M_i-1} \sum_u \varphi_u^{i,j} f_u^{i,j}(k)^2 \right\}, \quad (5.17)$$

where  $(i, j)$  are the targeted cells;  $\hat{\rho}_{crit}^{i,j}$  is the desired set-point;  $\alpha^{i,j}$  is the weight associated with the targeted cell  $(i, j)$ ; and  $\varphi_u^{i,j}$  is the weight associated with the control actions for a vehicle class  $u$  at a cell  $(i, j)$ . The cost function aims to penalize the difference between selected cell densities and the corresponding pre-defined set points. In addition, it also penalizes excessive lane changes, thus maintaining small control inputs.

Equation 5.17 can be written in the matrix form as follows:

$$\min J = \sum_{k=0}^\infty \left\{ [C \underline{x}(k) - \hat{y}]^T Q [C \underline{x}(k) - \hat{y}] + \underline{u}(k)^T R \underline{u}(k) \right\}, \quad (5.18)$$

where  $Q = Q^T \geq 0$  and  $R = \begin{bmatrix} \phi_c I_{\bar{F}/2} & 0_{\bar{F}/2} \\ 0_{\bar{F}/2} & \phi_t I_{\bar{F}/2} \end{bmatrix}$  are the weights associated with tracking and control actions, respectively.  $\hat{y}$  refers to a vector of set-points and is of dimension  $\mathbb{R}^{\bar{Y}}$ .  $C$  reflects the cells that are tracked. The parameters  $\phi_c > 0$  and  $\phi_t > 0$  penalize fluctuations of car and truck-specific lateral flows, respectively.

The matrix  $C$  is of dimension  $\mathbb{R}^{\bar{Y} \times \bar{H}}$ . Each row of matrix  $C$  contains a single element that corresponds to the cell that is tracked with the value of one, while the rest of the elements are equal to zero. Since, in this chapter, we target only cells in section  $N$ , the matrix  $C$  can be written as follows:

$$C = [0_{\bar{Y} \times (\bar{H} - \bar{Y})} \ I_{\bar{Y} \times \bar{Y}}]. \quad (5.19)$$

The problem defined in Equation 5.18 is subject to the linear dynamics presented in Equation 5.11. Assuming the system is stabilizable and detectable, we can solve this type of problem using a linear quadratic regulator. Since the stabilizability and detectability for such systems have been established in (Roncoli et al., 2016) and (Roncoli et al., 2017), the solution to the proposed optimal control problem can be given by the following linear feedback-feedforward control law:

$$\underline{u}^*(k) = -K \underline{x}(k) + \underline{u}_{ff}, \quad (5.20)$$



where

$$K = (R + B^T P B)^{-1} B^T P A, \quad (5.21)$$

$$P = C^T Q C + A^T P A - A^T P B (R + B^T P B)^{-1} B^T P A, \quad (5.22)$$

$$\underline{u}_{ff} = (R + B^T P B)^{-1} B^T F (C^T Q \underline{\hat{y}} - P \underline{d}), \quad (5.23)$$

$$F = (I - (A - B K)^T)^{-1}. \quad (5.24)$$

The feedback gain matrix can be computed offline by solving the Riccati equation. Note that in the derivation of LQR, we have assumed that the external flows  $d$  are constant. For practical implementation, we may assume that external flows can be measured. In that case, the feedforward term becomes time-varying. Now, we can rewrite Equation 5.20 and 5.23 as follows:

$$\underline{u}^*(k) = -K \underline{x}(k) + \underline{u}_{ff}(k), \quad (5.25)$$

$$\underline{u}_{ff}(k) = \Phi - \psi \underline{d}(k), \quad (5.26)$$

where  $\Phi = (R + B^T P B)^{-1} B^T F (C^T Q \underline{\hat{y}})$  and  $\psi = (R + B^T P B)^{-1} B^T F P$  may be calculated offline.

### 5.2.3 Transferring the optimal LQR control to a real-world C-ITS based multi-class lane-changing advisory system

The proposed feedback-feedforward control law, given by (25), can effectively be used to design a real-world C-ITS based lane-changing advisory system since the computation of control inputs depend on the feedback gain matrix  $K$ , the feedforward term comprising matrices  $\Phi$  and  $\Psi$ , measurement of state variables and external flows arising from outside the boundary of the considered system. For practical applications, the computation of matrices  $K$ ,  $\Phi$ , and  $\Psi$  may be done once offline. Once we have these matrices, online computation is only limited to a few matrix-vector multiplications, as shown in (25) and (26). The measurement of state variables or density of each considered cell is required every time step in real-time. To produce these measurements, a traffic state estimator (Herrera and Bayen, 2010, Seo et al., 2015, Bekiaris-Liberis et al., 2017, Papadopoulou et al., 2018, Yuan et al., 2012, Yuan et al., 2014) can be embedded in the control loop.

The proposed lane-changing advisory system requires an exchange of information between the traffic control center and vehicles. Vehicles are required to have connectivity in order to facilitate this exchange. Before control inputs or lane-changing advice are sent to the vehicles, it is vital to know vehicles' position (i.e., lane and location) and type (e.g., cars or trucks). We might require roadside units (RSUs) to gather position and vehicle type data via V2I communications for a particular cell. These data would be processed at the traffic control center to know which vehicles are present in a specific cell. With this information, the traffic control center can then issue lane-changing advice to a selection of vehicles through I2V communications (e.g., via RSUs) to indicate whether they need to change lanes. In practice, the selection of vehicles may be based on their destinations known beforehand to improve the positive effects arising from the advisory system. This system only advises vehicles to change lanes as it does not force them to change lanes. However, any mismatch between the control inputs or advised lane changes and actual lane changes due to compliance rate may be balanced

by the feedback nature of the proposed controller. Spontaneous lane changes might also arise, but it may be reduced by issuing additional lane-keeping advices to drivers not selected earlier. Lane-changing advice may be communicated to vehicles using an in-vehicle interface (e.g., smartphone application or vehicle's touchscreen) in the form of text or sound. A number of C-ITS real-world applications also prefer these modes of issuing advice to drivers (Fukushima, 2011, Kanazawa et al., 2010). Figure 5.2 shows a C-ITS-based multi-class lane-changing advisory framework for a merging section.

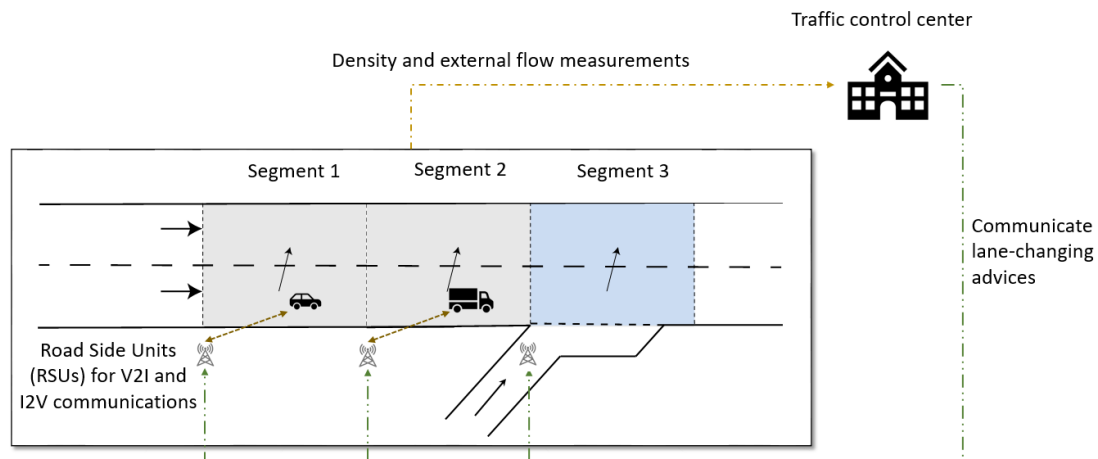


Figure 5.2. C-ITS based multi-class lane-changing advisory framework.

### 5.3 Implementation of the multi-class lane-changing advisory system in a microscopic traffic simulator

The proposed control strategy is tested using the microscopic traffic simulator OpenTrafficSim (van Lint et al., 2016), which is a Java-based open-source software package. It combines IDM+ as the car-following model (Schakel et al., 2010) and the lane-changing model with relaxation and synchronization (LMRS) as the lane-changing model (Schakel et al., 2012). We assume that there is no latency in V2I or I2V communication at the controller level. The proposed controller requires density measurements for all cells that are considered for the lane-changing advisory system and external demand that arise from outside the system boundaries. To realize the control actions, we keep individual lists of vehicles (cars and trucks) present in those cells. Note that we keep an individual list for every such cell which is of interest to the lane-change controller. Since this is a dynamic list, it gets updated every time a vehicle enters or exits that cell. Depending on the control action, we randomly select the desired number (requested by the controller) of cars and trucks from the list for a specific cell. These vehicles (cars and trucks) are instructed to follow the lane-change advisory using the lane-changing model (LMRS). Please note that some of the vehicles may not be able to perform lane changes due to the logic of the lane-changing model; however, this limited compliance is balanced by the feedback nature of the proposed controller. Next, we present the LMRS model.

### 5.3.1 Lane-changing model

We have selected the Lane change model with Relaxation and Synchronization (LMRS) as our base model (Schakel et al., 2012). The LMRS is based on the desire of a vehicle to change lanes that comes from several motivations. The base LMRS model aggregates considered motivations as follows:

$$d^{y,z} = d_r^{y,z} + \theta_v^{y,z}(d_s^{y,z} + d_b^{y,z}), \quad (5.27)$$

where  $d^{y,z}$  is the total/aggregated desire to change lanes.  $d_r^{y,z}$ ,  $d_s^{y,z}$ , and  $d_b^{y,z}$  refer to the desire for following a route, the desire to gain or maintain speed, and the desire to follow a keep-right policy, respectively. Here,  $\theta_v^{y,z}$  denotes the weights associated with voluntary motivations. The desire toward voluntary motivations ( $d_v^{y,z}$ ) comes from  $d_s^{y,z}$  and  $d_b^{y,z}$ .

The value of the desire to change from lane  $y$  to lane  $z$  is  $d^{y,z}$ , and it ranges between -1 and 1, where only positive values influence a lane-changing decision. The positive range is divided into four areas ( $0 < d_{\text{free}} < d_{\text{sync}} < d_{\text{coop}} < 1$ ) which determines the way a lane-change is performed. In the following, we discuss how a lane-changing is performed if the desire ( $d$ ) falls in one of the four areas.

1.  $d < d_{\text{free}}$ : the desire is too small for a vehicle to perform a lane change.
2.  $d_{\text{free}} \leq d < d_{\text{sync}}$ : a vehicle performs a lane change if it is possible.
3.  $d_{\text{sync}} \leq d < d_{\text{coop}}$ : if the adjacent gap in the target lane is not feasible, a vehicle aligns its speed to that of the leader in the target lane.
4.  $d_{\text{coop}} \leq d$ : the follower in the target lane adjusts its behavior to create a suitable gap to a lane-changing vehicle.

We extend this model to implement the LQR controller proposed in this chapter.

### 5.3.2 Implementing the lane-changing advisory system

The base LMRS model is essentially a linear-in-parameter formulation that can be extended to incorporate several other voluntary motivations. Consequently, we extend this base model to accommodate a lane change advisory framework in the following equation:

$$d^{y,z} = d_r^{y,z} + \theta_v^{y,z}(d_s^{y,z} + d_b^{y,z} + d_a^{y,z}), \quad (5.28)$$

where  $d_a^{y,z}$  refers to an additional incentive that is triggered if a vehicle receives lane change advice from the control center. This incentive is formulated as follows:

$$d_a^{y,y-1} = \begin{cases} d_{\text{free}}, & \text{if a vehicle receives the lane change advice} \\ 0, & \text{otherwise} \end{cases} \quad (5.29)$$

$$d_a^{y,y+1} = 0, \quad (5.30)$$

where  $y$ ,  $y - 1$ , and  $y + 1$  refer to the current lane, left lane, and right lane in the direction of driving.

Once a vehicle gets the lane change advice, it has an additional desire  $d_{\text{free}}$  to move to its left lane. If the adjacent gap on the left lane is not suitable, the subject vehicle will continue in the current lane. Since we assume European driving conditions in our simulations, we expect

vehicles to follow the keep-right policy. Therefore, we deactivate the subject vehicle's adherence to the keep-right policy ( $d_b^{y,z}$ ) until it passes the merging section so that vehicle complies with the advisory issued by the traffic control center.

## 5.4 Experimental setup

In this section, we describe the network, demand profile, and model parameters used for simulation, scenarios considered, and the performance indicators to assess the performance of the LQR control-based lane-changing advisory framework.

### 5.4.1 Study area

We consider a merging section for the evaluation of the proposed multi-class lane change controller. The merging section (i.e., Ter Heijde) with a 2-lane mainline carriageway is located on the A59 freeway in the Netherlands (see Figure 5.3). The acceleration lane is 320 m long. The upstream segment of the considered merging section is 2 km long. We consider three segments, numbered as 0, 1, and 2 in Figure 5.3, each 500 m long where vehicles will respond to lane change advisory issued by the control center. The nominal speed limit is 80 km/h for all those segments. This value is also the speed limit for trucks on freeways in the Netherlands.

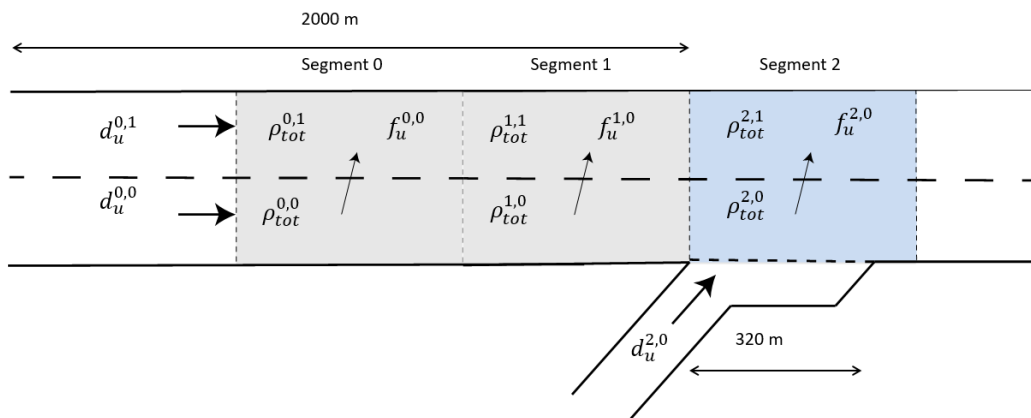
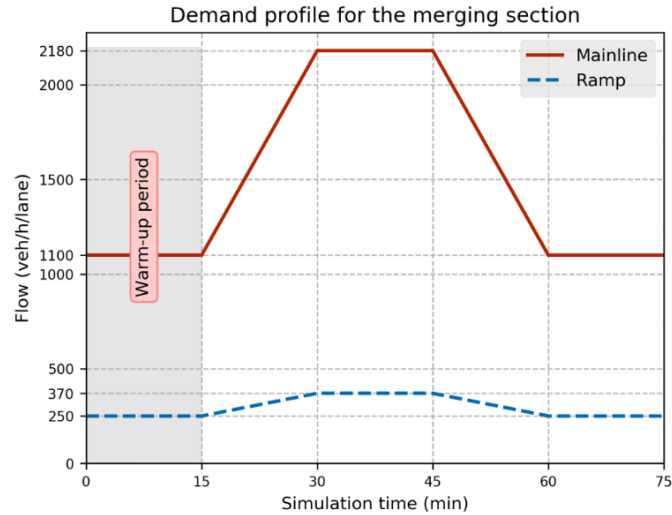


Figure 5.3. 2-lane mainline carriageway with an on-ramp

### 5.4.2 Demand profile

We consider a trapezoidal demand profile for mainline and ramp traffic (see Figure 5.4). This trapezoidal demand is used to generate vehicles in the network. The generation time of vehicles in the network depends on randomly distributed generation time-headways. In this chapter, we have assumed exponentially distributed headways. The share of trucks is 15% in the traffic mix. All simulations are conducted for 75 minutes of which the first 15 minutes are taken as the warm-up time. The purpose of warm-up time is to fill the network so that appropriate effects can be analyzed.



**Figure 5.4. Demand profile for the experimental setup**

### 5.4.3 Simulation model parameters

Most of the simulation model parameters are equal to the default values which are calibrated for a freeway network located in the Netherlands by (Schakel et al., 2012). For trucks, we use the desired speed distribution (km/h) obtained from a web-based survey, i.e.,  $v_{\text{des, truck}} = N(84.14, 3.92)$ . The lane-changing duration for truck drivers is obtained from a trajectory dataset (van Beinum, 2018, van Beinum et al., 2018). We use this dataset to obtain a normally distributed lane-changing duration (s) (i.e.,  $N(8.32, 2.19)$ ) for truck drivers. The simulation model parameters are tabulated in Table 5.1.

### 5.4.4 Scenarios

We consider two scenarios to evaluate the performance of the LQR control-based lane-changing advisory framework.

1. No-control: In this case, vehicles are not issued lane change advisory.
2. LQR control: In this case, mainline vehicles are issued lane change advisory every 20 s. We assume that 100% of vehicles present in the traffic mix are connected vehicles that are able to receive the advisory. For cars, we use a pce value of 1.0. For trucks, we use a pce value of 1.61 which is taken from (Schreiter, 2013) where pce values are calibrated using a trajectory dataset.

### 5.4.5 Performance indicator

We consider the Total Time Spent in the system (TTS in veh·h) as the performance indicator to evaluate the performance of the proposed controller. We do not take warm-up time into account to compute the TTS. TTS can be mathematically expressed as:

$$\text{TTS} = \sum_{i=1}^N (t_{\text{exit}}^i - t_{\text{enter}}^i), \quad (5.31)$$

where  $t_{\text{enter}}^i$  and  $t_{\text{exit}}^i$  refer to the time instant a vehicle  $i$  enters and exits the network, respectively.  $N$  denotes the total number of vehicles that have passed through the merging

**Table 5.1 Simulation model parameters**

Symbol	Value	Description
<b>Car-following parameters</b>		
$a_{car}$	1.25	Maximum (desired) car-following acceleration for cars ( $m/s^2$ )
$a_{truck}$	0.40	Maximum (desired) car-following acceleration for trucks ( $m/s^2$ )
$b$	2.09	Maximum comfortable car-following deceleration ( $m/s^2$ )
$b_0$	0.50	Maximum adjustment deceleration ( $m/s^2$ )
$b_{crit}$	3.50	Maximum critical deceleration ( $m/s^2$ )
$f_{speed}$	1.00	The speed limit adherence factor for cars and trucks
$s_0$	3.00	Car-following stopping distance (m)
$T_{max}$	1.20	Maximum car-following headway (s)
$T_r$	0.50	Reaction time (s)
$v_{des, car}$	$N(123.7,12)$	Desired (maximum) speed for cars (km/h)
$v_{des, truck}$	$N(84.14,3.92)$	Desired (maximum) speed for trucks (km/h)
$l_{car}$	4.00	Length of cars (m)
$l_{truck}$	15.00	Length of trucks (m)
<b>Lane-changing parameters</b>		
$d_{free}$	0.365	Free lane change desire threshold
$d_{sync}$	0.577	Synchronized lane change desire threshold
$d_{coop}$	0.788	Cooperative lane change desire threshold
$T_{min}$	0.56	Minimum car-following headway (s)
$\tau$	25	Headway relaxation time (s)
$v_{cong}$	60	Speed threshold below which traffic is considered congested (km/h)
$v_{gain}$	50	Anticipation speed difference at full lane change desired (km/h)
$x_0$	295	Look-ahead distance (m)
$t_0$	43	Look-ahead time for mandatory lane changes (s)
$t_{lc,car}$	3	Lane change duration for passenger cars (s)
$t_{lc,truck}$	$N(8.32,2.19)$	Lane change duration for trucks (s)

section in the simulation period. TTS can be further divided into the Total Travel Time for mainline vehicles (TTT) and the Total Waiting Time for ramp vehicles (TWT) to gain insight into how the proposed controller affects their efficiency to pass through a merging section.

## 5.5 Selection of LQR controller's parameters

This section focuses on the selection of the LQR controller's parameters. First, we present an analysis of the choice of set points. Lastly, we present a response-surface-based method to optimally select the weights of Q and R matrices.

### 5.5.1 Reference values of set-points and weights associated with Q and R matrices

For the sensitivity analysis presented in this section, we use reference values for the set-points, and weights of Q and R matrices. For the set points, we use the critical density of the lane as the reference value. To compute the critical density, we generate fundamental diagrams (see Figure 5.5) for the no-control case using data collected from 10 simulation runs. We use 40 pce/km/lane as the critical density for both the near-side and off-side lanes. With the given reference values of the set-points and desire threshold, we use a trial-and-error approach to select the reference weights for the Q and R matrices as:

$$Q = 10^2 I_2, \quad (5.32)$$

$$R = 10^1 I_6, \quad (5.33)$$

where  $\phi_c = \phi_t = 10^1$ .

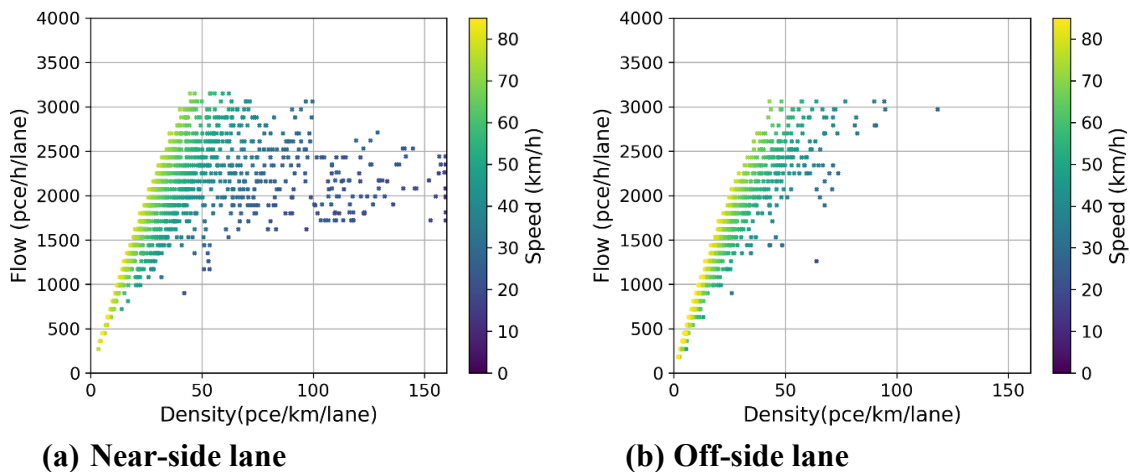


**Figure 5.5. Fundamental diagrams for (a) near-side; and (b) off-side lanes for 10 different simulation runs conducted for the no-control scenario.**

### 5.5.2 Selection of set-points

To assess the impact of set-points on the performance of the LQR controller, we select the reference values of the desire threshold and weights of the Q and R matrices. The critical density for each lane is computed as 40 pce/km/lane for which the system is able to maintain free-flow conditions. This value is taken as a starting point to define set points. We further increase this value in steps up to 45 pce/km/lane. Figure 5.6 shows the performance of the LQR controller for the considered values of set-points with fixed Q and R matrices for 10 simulation runs. It can be observed that the LQR controller results in the best performance in terms of TTS of the system for the value of 41 pce/km/lane. We use this value as set points for our experiments.

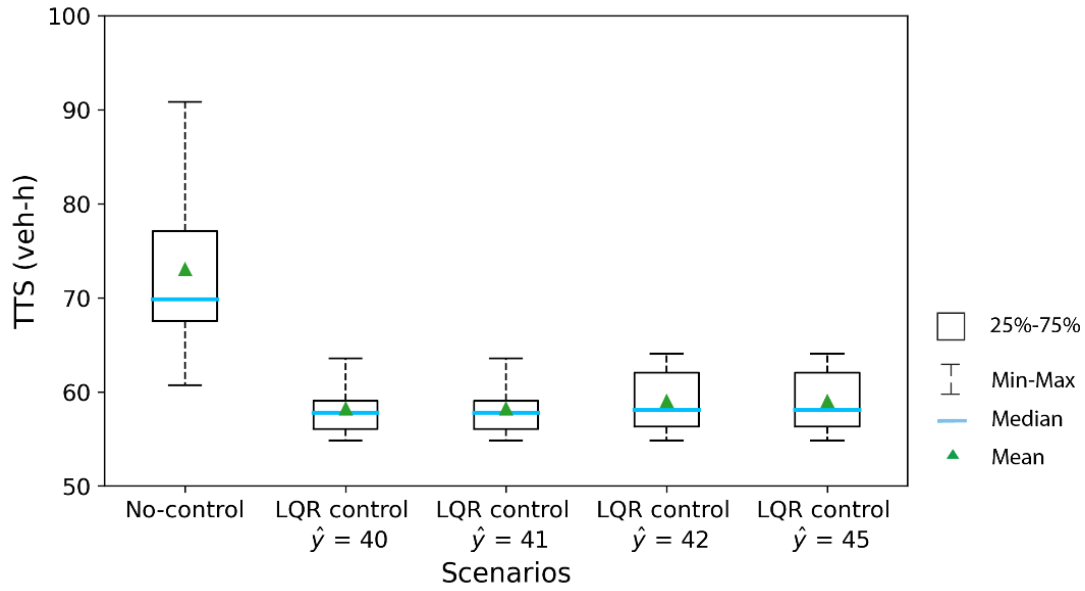


**Figure 5.6. Influence of set-points ( $\hat{y}$ ) on the performance of the LQR controller for 10 simulation runs.**

### 5.5.3 Selection of weighting matrices (Q and R)

Now, we analyze the impact of weighting matrices (Q and R) on the performance of the LQR controller. The tuning of Q and R matrices presents a trade-off between tracking precision and the system's stability. In this section, we present a response-surface-based approach to select optimal weighting matrices of the LQR controller. This technique maps the impact of design variables on the processes. The technique can be separated into the following three stages (Baş and Boyacı, 2007).

1. selection of design variables,
2. selection of experimental design and model fitting, and
3. visualization of response surface and determination of optimal design parameters.

Next, we describe these steps in the detail.

#### Selection of design variables

Our design variables are the weighting matrices of the LQR controller. We consider that Q and R matrices are diagonal in nature and they can be expressed as follows for our test case:

$$Q = 10^{\theta_1} I_2, \quad (5.34)$$

$$R = 10^{\theta_2} I_6. \quad (5.35)$$

where  $\theta_1$  and  $\theta_2$  refer to the parameters intending to change the weights of the Q and R matrices. Here, we assume that  $\phi_c = \phi_t = 10^{\theta_2}$ .

#### Selection of experimental design and model fitting

We use the Latin hypercube sampling method to generate a response surface with input variables of  $\theta_1$  and  $\theta_2$  (McKay et al., 1979). The design range of input variables is considered



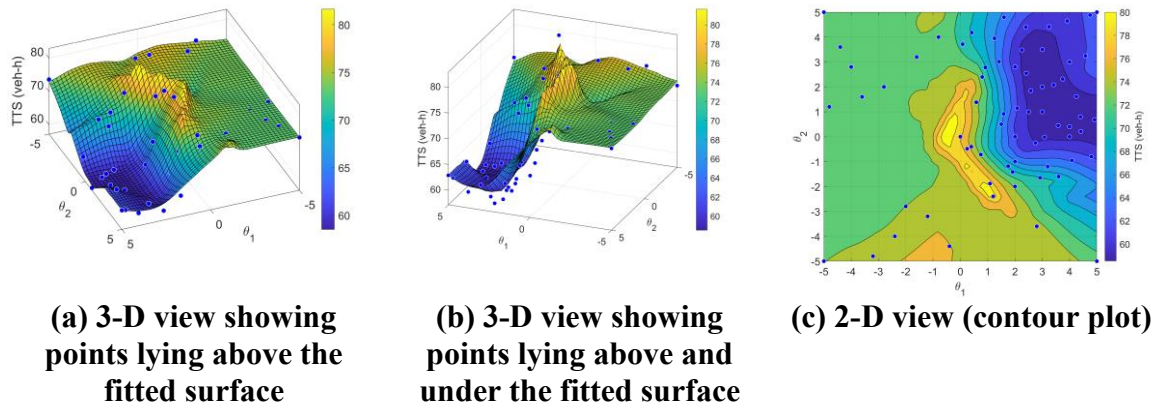


**Figure 5.7. Response surface generated by varying the weights of Q and R matrices (color bar shows TTS values where low TTS values are highlighted in blue)**

as  $-5 \leq \theta_1, \theta_2 \leq 5$ . We use a two-step approach to produce the response surface. First, we use 35 design points in the above design range of input variables. Then, we further focus on a smaller area ( $0 \leq \theta_1 \leq 5$  and  $-2 \leq \theta_2 \leq 5$ ) where there might be a higher possibility for a minimum to occur. In this area, we sample additional 30 design points. Overall, we use 65 design points to produce the response surface. The dependent variable is considered as TTS, which is obtained as the average TTS from 10 simulation runs. We use Lowess smoothing or locally weighted linear regression-based surface fitting procedure to convert the discrete design space to a continuous one (see Figure 5.7). Lowess smoothing is a non-parametric technique to fit surfaces (Cleveland and Devlin, 1988). The fitting process is estimated locally by using the weighted neighborhood points with their distance to the observed point. The proportion of neighborhood points in the estimation depends on the span size. After analyzing root mean square error (RMSE), we choose a span size of 0.25 (RMSE= 2.53). The produced fit has  $R^2 = 0.8990$  and adjusted  $R^2 = 0.8843$  which indicates that 89.90% of the total variation can be explained by the fitted model.

### Visualization of response surface and determination of optimal design parameters

The response surface and the contour plot show that multiple combinations of  $\theta_1$  and  $\theta_2$  yield similar performance. In the dark blue region (see Figure 5.7), the LQR controller is little sensitive to the changes in the values of  $\theta_1$  and  $\theta_2$ . In order to guarantee a stable LQR controller, the values of  $\theta_1$  and  $\theta_2$  should be selected from the dark blue region shown in the contour plot. Next, we present and discuss simulation results in order to discuss the performance of the LQR controller at a merging section.

## 5.6 Results and discussion

In the scope of this work, we target only cells in segment 2 of the merging section. We use fundamental diagrams to find the set points for the LQR controller. For both the near-side and off-side lanes at segment 2, we use 41 pce/km/lane as set-points that is closer to their critical density values. The weights of the LQR controller are obtained from the contour plot. Q and R matrices are selected as  $10^3 I_2$  and  $10^1 I_6$ , respectively. The LQR controller gains are computed offline and simulations are conducted using those values. In the following, we present a quantitative and qualitative evaluation of the performance of the LQR controller.

### 5.6.1 Quantitative evaluation of the performance of the LQR controller

The performance of the LQR controller, in terms of TTS, is evaluated over 10 simulation runs (see Figure 5.8 (a)). We obtain a TTS value of 73.04 veh·h for the no-control case. In comparison to the no-control case, we obtain an average TTS equal to 57.74 veh·h in the controlled case which is around 21% improvement (t-statistic = 4.63, p-value = 0.001). The variance is significantly reduced in the control scenario thus indicating the consistent performance of the proposed lane-changing advisory system. Next, we discuss how the LQR controller affects the travel times of mainline and ramp vehicles.

Figure 5.8 (b) presents the performance of the LQR controller in terms of TTT over 10 simulation runs. In the no-control case, an average TTT is computed to be 69.36 veh·h. When the LQR controller is applied, the average TTT is obtained as 55.59 veh·h which implies 19.85% improvement (t-statistic = 4.38, p-value = 0.001) than the no control case. The performance of the LQR controller in terms of TWT over 10 simulation runs is shown in Figure 5.8 (c). For ramp vehicles, an average TWT is computed to be 3.68 veh·h for the no-control case. The LQR controller is able to improve the average TWT by 41.55% (t-statistic=7.81, p-value=1.77e-5) as the average TWT gets reduced to 2.15 veh·h.

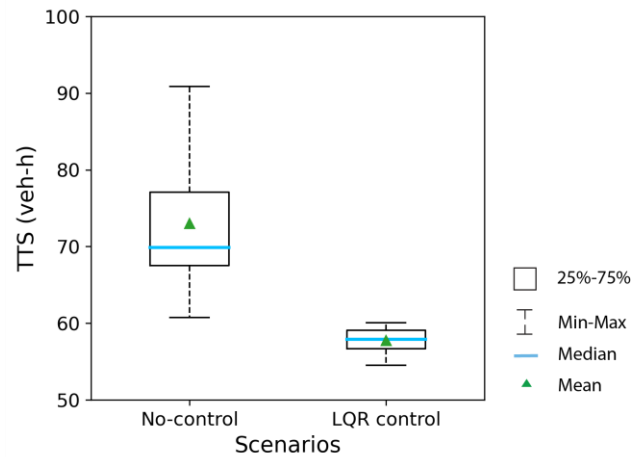
Overall, the LQR controller is able to improve traffic efficiency for both mainline and ramp vehicles thus showing significant improvement at the system level. Next, we present a qualitative evaluation concerning the performance of the LQR controller.

### 5.6.2 Qualitative evaluation of the performance of the LQR controller

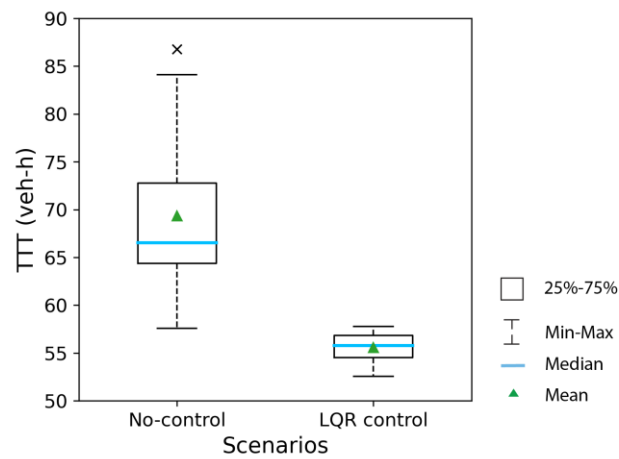
In Figure 5.9, we present an evaluation of the performance of the LQR controller for an average scenario in terms of speed-contour plots, density profile, and outflow profile. By looking at speed-contour plots, we can observe that the LQR controller is able to suppress shockwaves in the system. Furthermore, we can observe that density values for both near-side and off-side lanes lie around set-points chosen for the LQR-control case compared to the no-control case. In the LQR control case, we observe that the distribution of traffic is more balanced since we observe similar density profiles for both lanes at segment 2. Figure 5.9 (d) shows the observed outflow at the merging section. In the no-control scenario, the traffic flow on the nearside lane breaks down at around 2880 pce/h/lane before reaching its capacity.

This also triggers a breakdown in the offside lane, before reaching its capacity, where for some time windows we observe outflow even lower than 500 pce/h/lane. Whereas in the LQR control scenario, we observe that outflow is reaching higher values (i.e., 3060 pce/h/lane) for a longer period of time without incurring traffic breakdown.

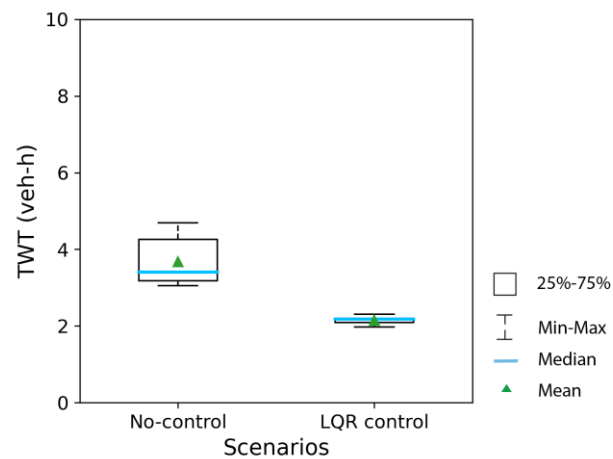
Interestingly, we observe a dip in density and outflow between 35-45 minutes in the LQR control scenario. This is We also analyze the performance of the LQR controller by comparing the lane-specific fundamental diagrams generated attributed to the demand profile presented in Figure 5.10. To generate this demand profile, we have placed loop-detectors at the entrance of the mainline and ramp. Figure 5.10 shows a similar dip in traffic demand between 35-45 minutes. The results suggest that the buildup of density on the near-side and off-side lane follows the traffic pattern under the LQR control scenario. The LQR controller recognizes the randomly distributed demand (or generation of vehicles in the network) and effectively balances the distribution of traffic on both lanes.



**(a) Total Time Spent in the system (TTS)**



**(b) Total Travel Time for mainline vehicles (TTT)**



**(c) Total Waiting Time for ramp vehicles (TWT)**

**Figure 5.8. Comparison between no-control and LQR control scenario for system (TTS), mainline (TTT) and ramp (TWT) vehicles.**

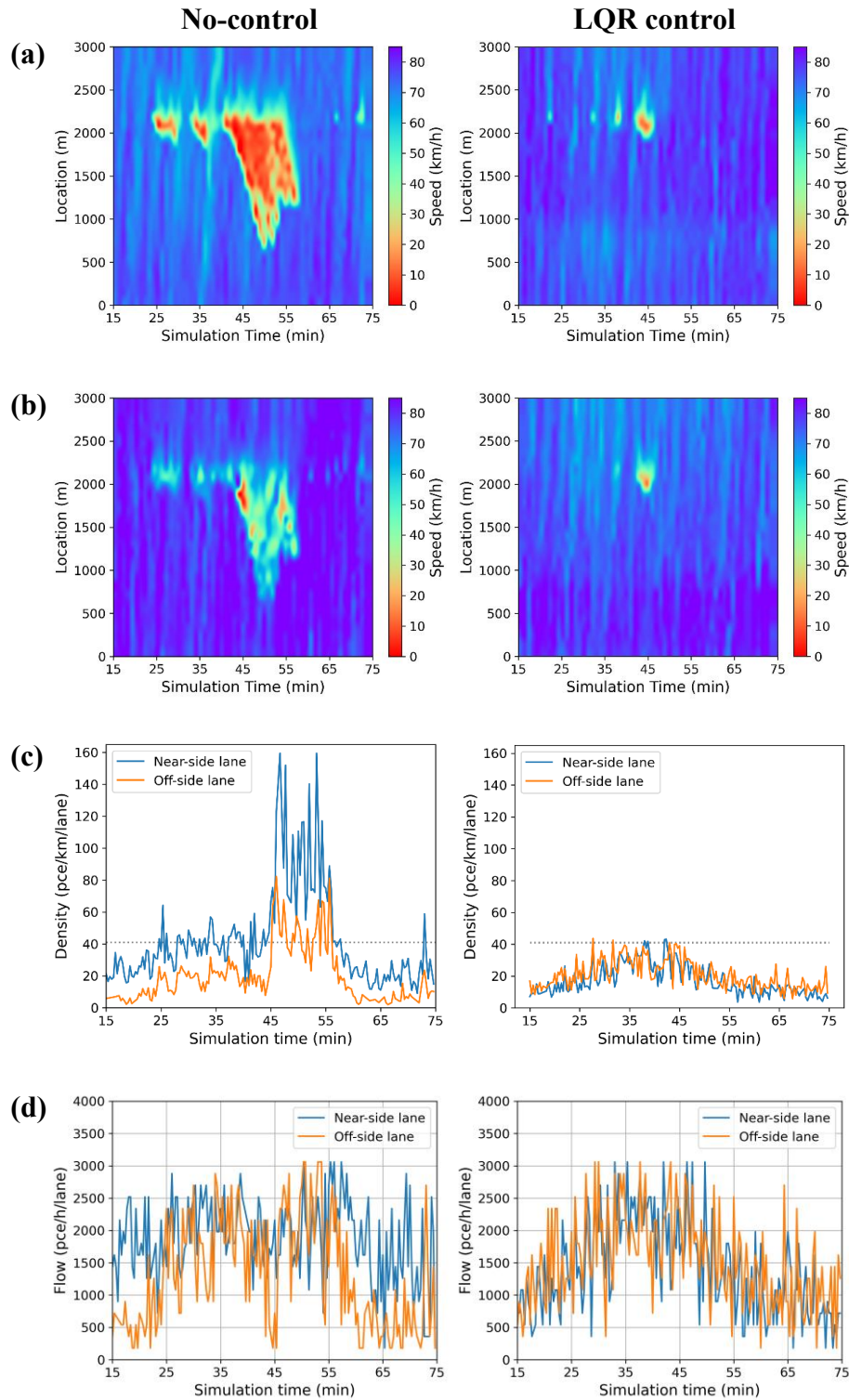


**Figure 5.9. Qualitative assessment of the LQR controller's performance for an average scenario (a) speed contour plots for the near-side lane (b) speed contour plots for the off-side lane, (c) density profile for near-side and off-side lanes at segment 2, and (d) outflow profile for near-side and off-side lanes at segment 2.**

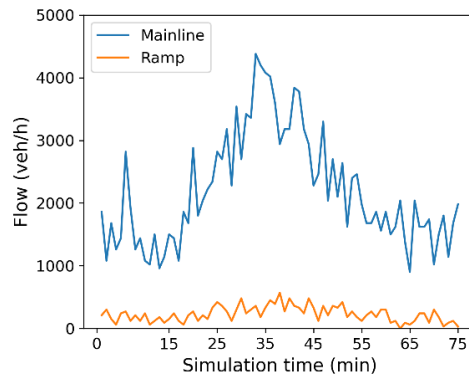


**Figure 5.10.** Demand profile generated for an average scenario under the LQR control case.

We also analyze the performance of the LQR controller by comparing the lane-specific fundamental diagrams generated for segment 2 from 10 simulation runs. Figure 5.11 shows that the LQR controller can improve the traffic efficiency around the merging section and successfully prevents the breakdown of traffic.

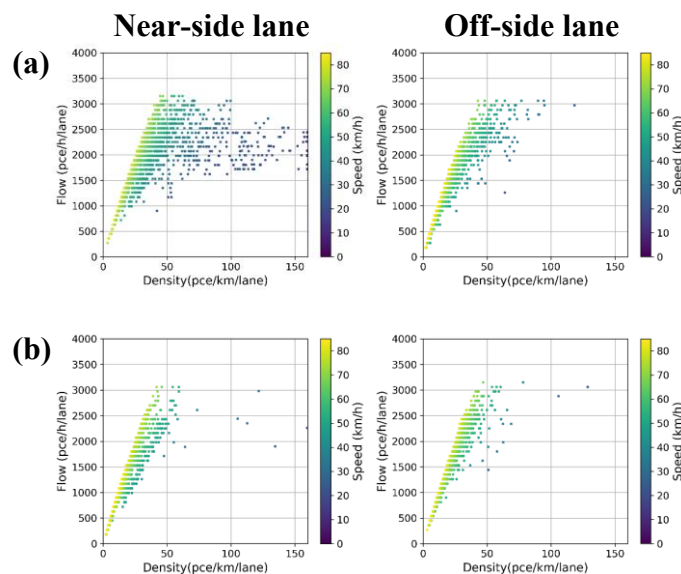
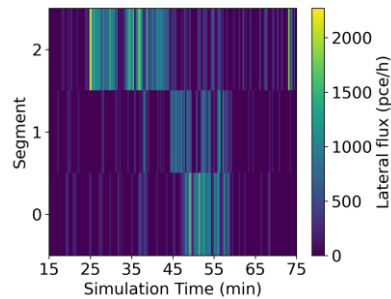


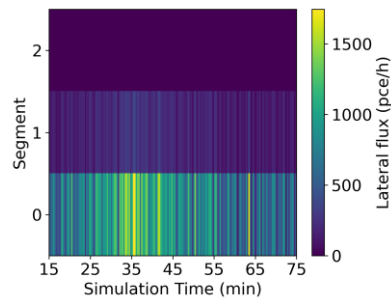
**Figure 5.11.** Lane-specific fundamental diagrams at segment 2 generated for (a) no-control and (b) LQR control scenario using data collected from 10 simulation runs.

Now we will look at the distribution of lateral flux, from left to right side, over considered three segments around the merging section. Figure 5.12 (a) shows that a high amount of lane-changing activity at segment 2, which is close to the merging section, for the no-control scenario. It appears that vehicles react to the congestion only if they can witness any impact within their visible range or look-ahead distance. Since the congestion starts to build up at the near-side lane after 35 minutes, the lane-changing activity starts to shift upstream to segments 0 and 1. Figure 5.12 (b) presents the lateral flux advised by the LQR controller. We observe that the LQR controller emphasizes proactive lane-changing and advises vehicles to consider lane-changing ahead of reaching close to the merging section. In Figure 5.12 (c), we present the realized lateral flux in the LQR control scenario. This realization depends on the gap-seeking behavior of vehicles governed by the LMRS model. Lateral flux is distributed in a way

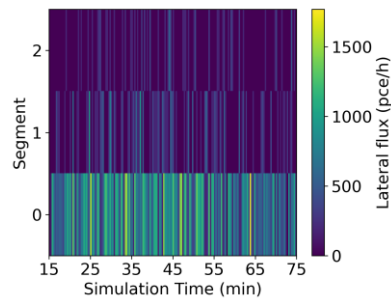
so that vehicles perform most of the lane-changing activity upstream at segment 0. We do note a few lane changes at segment 2 which can be attributed to the selection of vehicles and their ability to seek gaps.



(a) Lateral flux in the no-control scenario



(b) Lateral flux advised by the LQR controller



(c) Lateral flux realized in the LQR control scenario

**Figure 5.12. Contour plots of lateral flux in (a) the no-control scenario, (b) advised LQR control scenario, and (c) the realized LQR control scenario.**

## 5.7 Conclusions

This chapter develops a multi-class lane-changing advisory system based on a linear quadratic regulator. This system uses V2I and I2V communications and can be viewed as a cooperative intelligent transportation systems application. We evaluate the performance of this system using microscopic simulation. The results indicate that this system can improve traffic efficiency around a merging section. Moreover, it brings substantial travel time benefits for both mainline and ramp vehicles. The findings will be of interest to traffic management agencies and logistics companies which are especially concerned about the travel time reliability of freight corridors.

In the future, the effectiveness of the proposed framework can be evaluated for a scenario that includes truck platoons along with passenger cars and trucks. In addition, a promising research direction can be to include automated vehicles in the traffic mix. Furthermore, the lane-changing controller can be integrated into other local control strategies such as ramp metering.

### **III: Operational driving behavior around freeway bottlenecks**





## 6 Impacts of a truck platooning application

---

Previous chapters presented new behavioral insights and a novel control method to improve on-trip behavior of road freight. This chapter focuses on the lowest layer of the driving behavior hierarchy, i.e. operational behavior and presents the impacts of a truck platooning application. State-of-the-art has largely focused only on traffic impacts of truck platoons around freeway bottlenecks. A key gap results from a lack of understanding about how truck platoons affect safety, a key performance criterion, around such bottlenecks. Add to this, these studies do not fully capture the uncertainty associated with the traffic and safety impacts caused by varying truck platooning characteristics (e.g., market penetration, length of the platoon, intra-platoon gap spacing, and desired speed) around freeway bottlenecks. To address this gap, this chapter aims at evaluating the effects of varying several truck platoon characteristics on traffic efficiency and safety at merging sections and contributes to answering the fifth research question of this dissertation. This chapter presents a comprehensive sensitivity analysis to identify the impact of truck platoon characteristics around a merging section using microscopic simulation. My personal contributions to this chapter are enriching a local level sensitivity analysis with qualitative trajectory plots and conducting a global level sensitivity analysis to identify and rank the impact of truck platooning characteristics on traffic efficiency and safety.

This chapter is based on the following journal and conference papers:

Faber, T., Sharma, S., Snelder, M., Klunder, G., Tavasszy, L. and van Lint, H. 2020. Evaluating traffic efficiency and safety by varying truck platoon characteristics in a critical traffic situation. *Transportation Research Record*, 2674(10), pp. 525-547.

Faber, T., Sharma, S., Snelder, M., Klunder, G., Tavasszy, L. and van Lint, H. 2020. Evaluating traffic efficiency and safety by varying truck platoon characteristics in a critical traffic situation. Paper presented in *99<sup>th</sup> Annual Meeting of the Transportation Research Board*.

---

## 6.1 Introduction

Cooperative adaptive cruise control (CACC) is an emerging technology with automated speed controls by using vehicle-to-vehicle (V2V) and/or infrastructure-to-vehicle (I2V) communication (Shladover et al., 2012). CACC is shown to be beneficial for road capacity improvement (Shladover et al., 2012, Tientrakool et al., 2011), traffic flow stability (Schakel et al., 2010, Van Arem et al., 2006), and traffic safety (Li et al., 2017a, Li et al., 2017b). CACC can be utilized to improve the efficiency and safety of road transport operations. The application of CACC to freight transport is known as truck platooning. In this system, trucks move together in tight platoons using V2V communication (Bhoopalam et al., 2018). Recent practical trials report significant fuel savings and emission reductions by introducing truck platoons (Eckhardt et al., 2016, Lammert et al., 2014), whereas simulation-based studies report mixed effects on traffic efficiency (Calvert et al., 2019, Mueller, 2012, Wang et al., 2019, Ramezani et al., 2018, Deng, 2016, Mesa-Arango and Fabregas, 2017). We use platoons and truck platoons interchangeably throughout this chapter.

The efficient transport of containers to the hinterland is an important part of the global supply chain. Grouping trucks together in a convoy might be an interesting proposal for port authorities and carriers to move containers out of the port area because of fuel savings, efficient use of labor, and safer operations. Yet, little research has been done so far to assess the impacts of truck platoons in critical traffic situations which are particularly interesting for road transport authorities. One of these situations lies around merging sections. The interactions of truck platoons with the surrounding vehicles in the vicinity of merging sections are not fully understood, and neither are the effects on safety and efficiency. Port terminals might generate a platoon demand through on-ramps in the future, and to the best of our knowledge, this chapter is the first to consider this probable scenario. Besides, the uncertainties associated with the potential traffic and safety impacts, when considering variable platoon characteristics (number of trucks in a platoon, intra-platoon headway, desired speed of platoon, market penetration of platoon vehicles, and lane-changing policy), call for a detailed sensitivity analysis.

Consequently, the main objective of this chapter is to evaluate the effects of varying several platoon characteristics on traffic efficiency and safety at merging sections. The contributions of this chapter are twofold. First, we develop a novel lateral controller in combination with an existing longitudinal controller for truck platoons. These controllers ensure collision-free, string-stable, and smooth driving behavior of platoon vehicles. Moreover, vehicles in a platoon can follow their respective leaders by following a desired time-gap policy. Traffic and safety impacts are subjected to the assumptions behind longitudinal and lateral controllers. Second, we perform a comprehensive sensitivity analysis, both at the local and global levels, to identify the impact of platoon's characteristics on traffic efficiency and safety around merging sections. We consider both low and high traffic intensity to identify platoon characteristics that might lead to positive or negative impacts on traffic efficiency and safety.

This chapter is structured as follows. First, section 6.2 presents a literature review on the modeling of truck platoons within the microscopic simulation and their effects on traffic and safety. Afterward, sections 6.3 and 6.4 present longitudinal and lateral controllers for truck platoons, respectively, which we have implemented in the microscopic simulation software OpenTrafficSim. Next, section 6.5 presents a case study of a merging section. Subsequent sections 6.6 shows the impact of introducing a reference truck platoon configuration. Then sections 6.7 and 6.8 discuss the impact of platoon characteristics on

traffic efficiency and safety by conducting local and global sensitivity analyses, respectively. Section 6.9 discusses the findings and section 6.10 concludes this chapter.

## 6.2 Literature review

This section presents a literature review on the modeling of truck platoons and evaluating their impact on traffic efficiency and safety.

### 6.2.1 Modeling of truck platoons

The longitudinal behavior of trucks in a platoon is controlled using CACC. Most of CACC controllers use a constant time-gap (CTG) policy in which the distance between vehicles is proportional to the speed (Milanés and Shladover, 2014, Van Arem et al., 2006, Montanaro et al., 2014, Ramezani et al., 2018, Deng, 2016). Other approaches mimic truck platooning field trials which use a constant distance gap policy (Lu et al., 2002, Shladover et al., 2006). Typically, a single leader is used for communicating information to CACC-equipped followers (Milanés and Shladover, 2014, Van Arem et al., 2006, Ramezani et al., 2018, Lu et al., 2002, Shladover et al., 2006). Other CACC variants report communications with multiple leaders (Montanaro et al., 2014, Santini et al., 2016). Previous research has shown that CACC controllers based on CTG policy can achieve string stability and collision-free performance in most situations. The car-following model such as IDM + has also been used to develop the CACC controller for truck platoon (Calvert et al., 2019); however, the IDM + model results in a variable time-gap policy in contrast to constant time or distance gap policy used in the standard CACC controllers.

Hsu and Liu (2004) specify lane-changing strategies for platoons. In one case, the leader of a platoon signals the followers and all the vehicles change lanes simultaneously. In the other case, vehicles become free agents and change lanes individually after the leader. Simultaneous lane changing of the truck platoon is also reported in the European truck platooning challenge (Eckhardt et al., 2016). However, previous research and practical trials are focused on platooning operation on mainline carriageways, and there exists a gap regarding the merging strategies of truck platoons.

### 6.2.2 Impact of truck platoons on traffic efficiency and safety

There are limited studies to assess the impacts of truck platoons, and most of them focus on traffic impacts. Mueller (2012) reports a 5.5% increase in road capacity with CACC-equipped trucks over a hypothetical 5 km-long three-lane carriageway using simulations. However, the test site does not include any discontinuities. Deng (2016) performs simulations over a 3.5 km-long two-lane carriageway without any discontinuities, and shows that average traffic flow significantly increases whereas space mean speed decreases with an increase in the market penetration of platoons. Ramezani et al. (2018) show that CACC-equipped trucks can reduce congestion propagation and improve traffic speed on a 15 mile-long I-170 corridor with 21 on-ramps and 20 off-ramps.

Wang et al. (2019) study the impact of truck platoons on the traffic operations near a merge section using simulation. Their results suggest that truck platooning may increase maximum outflow by 19% in congested conditions but has no substantial impact in free-flow conditions. However, the authors note that this increase may be attributed to the fact that some vehicles are deleted from the simulation if they are unable to merge in time. Mesa-Arango and Fabregas (2017) evaluate the impact of truck platoons on travel time and its reliability using VISSIM simulation around a motorway exit. Calvert et al. (2019) report negative effects on traffic flow under congested conditions when platoons are introduced on a 56.6 km trans-European corridor

in the Netherlands. Yang et al. (2019) use microscopic simulations near a merging and a diverging area to analyze the impact of truck platooning on traffic efficiency and safety. Their findings indicate that truck platooning increases traffic flow even in high traffic intensity. However, truck platooning negatively affects merging and diverging of vehicles along with traffic safety. To the best of our knowledge, only one study has attempted to investigate the safety impacts of truck platooning. This indicates a need to comprehensively study the safety impacts of truck platoons. In particular, scenarios involving truck platoons merging onto a mainline carriageway from an on-ramp have not been considered in the literature.

### 6.3 Longitudinal controller for truck platoons

This section presents a longitudinal controller that governs the car-following behavior of trucks in a platoon. We assume that there is no latency in V2V communication at the controller level and platoon vehicles do not communicate with the infrastructure. Moreover, vehicles in a platoon have homogeneous characteristics. We use a CTG policy and three different controllers or modes to simulate longitudinal movement trucks in platoons.

1. **Cooperative Adaptive Cruise Control (CACC):** In this case, the leader of a CACC-equipped truck is also a CACC-equipped vehicle, which means the vehicles can communicate all relevant dynamic information (headway, speed, acceleration, etc.) with each other.
2. **Adaptive Cruise Control (ACC):** In this case, the leader of a CACC-equipped truck is a non-CACC equipped vehicle. Only headway and speed-related information can be exchanged.
3. **Cruise Control (CC):** In this case, a CACC-equipped truck has no leader within sight.

#### 6.3.1 Preliminaries

An ego truck is a CACC-equipped truck. Let  $v_{\text{des}}$ ,  $r$ ,  $v$  and  $r_{\text{standstill}}$  be its desired speed, its current headway spacing from its leader, its current speed and minimum spacing at standstill (3 m), respectively. Let  $v_p$  and  $a_p$  be speed and acceleration of the leader of the ego truck, respectively.  $r_{\text{mode}}^{\text{safe}}$  is the safe following distance required for the ego mode truck (Equation 1). It is controller-specific, as it depends on the target time-gap setting,  $t_{\text{mode}}^{\text{system}}$ , in a particular mode. We use 0.5 s and 1.5 s for CACC and ACC, respectively.

$$r_{\text{mode}}^{\text{safe}} = t_{\text{mode}}^{\text{system}} \cdot v + r_{\text{standstill}} \quad \forall \text{mode} \in \{\text{CACC}, \text{ACC}\} \quad (6.1)$$

All three controllers are derived from the works of van Arem et al. (2006) and VanderWerf et al. (2001). As the original models were not designed to work in a dynamic traffic situation, we have adapted them for platoons by incorporating the following two characteristics.

1. **Gap-Closing:** The ego truck should be able to maintain the desired headway from its leader. If the current headway exceeds the desired headway, an ego truck should accelerate to reduce the excess headway.
2. **Acceleration-Following:** The ego truck should follow its accelerating leader in a string-stable manner.

The three controllers have the same structure, that is, the control variable ( $a_{\text{mode}}$ ) is bounded by the ego truck's minimum ( $a_{\text{min}}$ ) and maximum acceleration ( $a_{\text{max}}$ ) capabilities. The three controllers differ in terms of the information they use to compute  $a_{\text{mode}}$  which is based on  $a_{\text{mode}}^{\text{ego}}$  and  $a_{\text{mode}}^{\text{lead}}$ . Here,  $a_{\text{mode}}^{\text{ego}}$  is the maximum acceleration based on the desired speed and headway setting of controllers and  $a_{\text{mode}}^{\text{lead}}$  is the maximum acceleration based on the interaction with its leader.

### 6.3.2 Cooperative adaptive cruise control

The ego truck responds to the acceleration of the predecessor, deviations between its current speed and the speed of the predecessor, and the deviation between the current distance headway and the desired headway. The acceleration of the ego truck ( $a_{\text{CACC}}$ ) can then be computed using Equations 6.2-6.4.

$$a_{\text{CACC}}^{\text{ego}} = k \cdot (v_{\text{des}} - v) + k_d \cdot (r - r_{\text{CACC}}^{\text{safe}}) \quad (6.2)$$

$$a_{\text{CACC}}^{\text{lead}} = k_a \cdot a_p + k_v \cdot (v_p - v) + k_d \cdot (r - r_{\text{CACC}}^{\text{safe}}) \quad (6.3)$$

$$a_{\text{CACC}} = \min(a_{\text{max}}, \max(\min(a_{\text{CACC}}^{\text{ego}}, a_{\text{CACC}}^{\text{lead}}), a_{\text{min}})) \quad (6.4)$$

By considering the distance headway from its leader, the ego truck can close the gap if it is more than the desired headway, as shown in Equation 6.2. In this way, the ego truck can move within a platoon configuration by maintaining the desired spacing from its leader. Equation 6.4 ensures that the ego truck follows its accelerating leader in a string-stable manner.

### 6.3.3 Adaptive cruise control

The ego truck responds to the deviations between its current speed and the speed of the predecessor, and the deviation between the current distance headway and the desired headway. The acceleration of the ego truck ( $a_{\text{ACC}}$ ) can then be computed using Equations 6.5-6.7.

$$a_{\text{ACC}}^{\text{ego}} = k \cdot (v_{\text{des}} - v) + k_d \cdot (r - r_{\text{ACC}}^{\text{safe}}) \quad (6.5)$$

$$a_{\text{ACC}}^{\text{lead}} = k_v \cdot (v_p - v) + k_d \cdot (r - r_{\text{ACC}}^{\text{safe}}) \quad (6.6)$$

$$a_{\text{ACC}} = \min(a_{\text{max}}, \max(\min(a_{\text{ACC}}^{\text{ego}}, a_{\text{ACC}}^{\text{lead}}), a_{\text{min}})) \quad (6.7)$$

### 6.3.4 Cruise control

The ego truck responds to its deviations between its desired and current speed. The acceleration of the ego truck ( $a_{\text{CC}}$ ) can then be computed using Equations 6.8-6.9.

$$a_{\text{CC}}^{\text{ego}} = k \cdot (v_{\text{des}} - v) \quad (6.8)$$

$$a_{\text{CC}} = \min(a_{\text{max}}, \max(a_{\text{CC}}^{\text{ego}}, a_{\text{min}})) \quad (6.9)$$

The values of the controller parameters should be calibrated by considering acceleration-following, gap-closing, collision-free, and string-stable properties. We use the values of these

parameters from the work of van Arem et al. (2006). Here,  $k$ ,  $k_a$ ,  $k_d$ , and  $k_v$  are controller parameters whose values are chosen as 0.3, 1.0, 0.1, and 0.58, respectively. Besides, the parameter values should provide a smooth acceleration response by minimizing overshoot and oscillations. The values of  $a_{\max}$  and  $a_{\min}$  are chosen as  $1.25 \text{ m/s}^2$  and  $-5.0 \text{ m/s}^2$ , respectively. The acceleration capabilities of a truck that can be used in a platoon configuration should be chosen in consultation with truck manufacturers.

### 6.3.5 Verification tests for cooperative adaptive cruise control

We consider a platoon of five vehicles to conduct performance verification tests for our CACC controller. Figure 6.1 shows performance of CACC controller under three scenarios. First, we consider a stop-and-go scenario where the leader of a platoon first decelerates for 2 s and then accelerates again for 2 s. The CACC controller can respond to the changes in the state of its

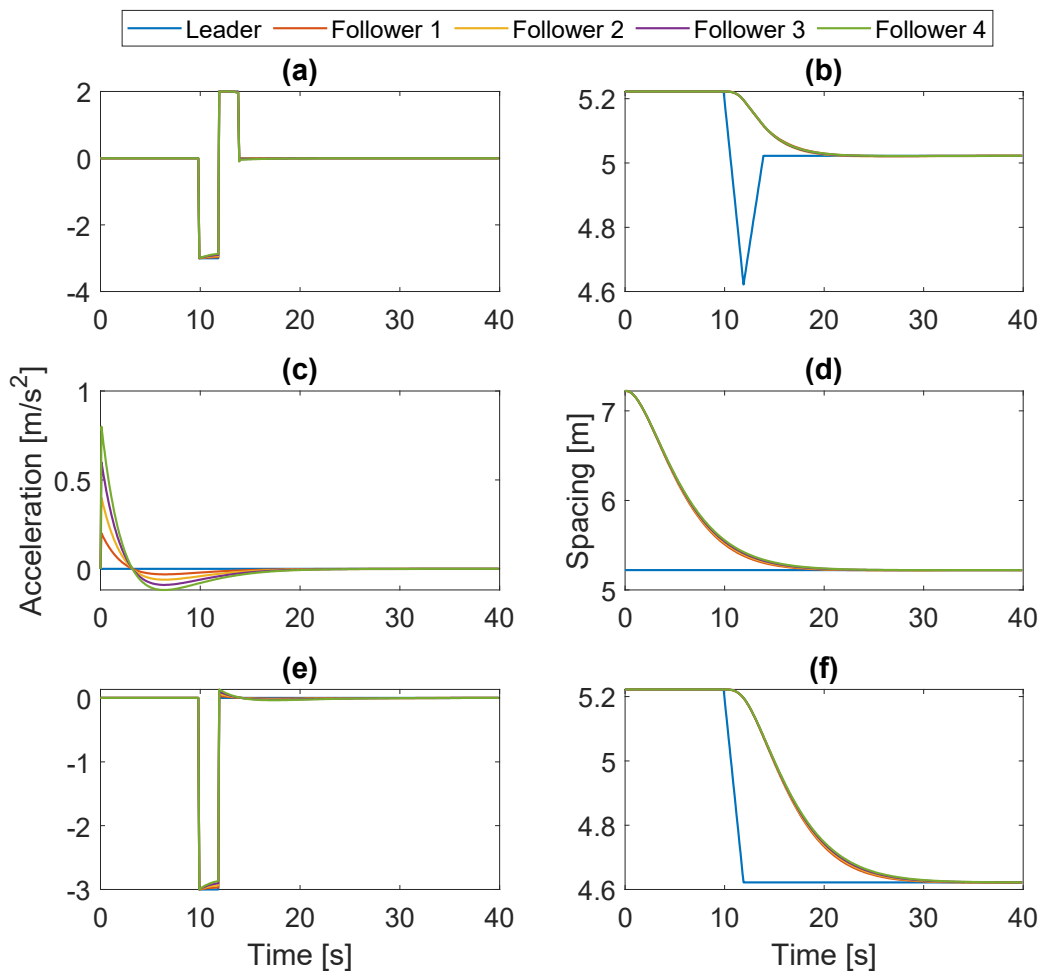


**Figure 6.1. Verification test for CACC controller's performance: (a) platoon acceleration under stop-and-go scenario, (b) gap spacing under stop-and-go scenario (blue line refers to the desired gap spacing), (c) platoon acceleration to keep gap spacing close to desired spacing, (d) variation in gap spacing as automatic gap closing triggers when current spacing exceeds desired spacing, (e) platoon acceleration under emergency braking scenario, and (f) gap spacing under emergency braking scenario.**

Note: CACC = cooperative adaptive cruise control.

leader and produces a smooth (i.e., oscillation-free) and collision-free behavior. Second, we consider a scenario where vehicles in a platoon have a gap spacing more than the desired gap spacing at the initial condition when a leading vehicle instantaneously brakes for 2 s. Our controller can bring vehicles in that platoon at a safe gap spacing, thus resulting in a string-stable behavior. Third, we consider an emergency braking scenario where the leader of a platoon decelerates for 2 s. Four following vehicles, equipped with the CACC controller, result in a safe (or collision-free) driving behavior as the spacing between the vehicles stabilizes after some time at around the desired safe following distance ( $r_{\text{safe}}$ ). We observe that the braking action decreases speed of all the vehicles, which in turn reduces the desired safe following distance ( $r_{\text{safe}}$ ) in a CTG policy. The controller's CACC response to emergency braking also produces a stable behavior in which the acceleration of four followers stabilizes at 30 s.

## 6.4 Lateral controller for truck platoons

The lateral controller for truck platoons governs the lane-changing process of the entire platoon. The lane-changing process of truck platoons comprises several logical steps (see Figure 6.2). The first step is to check if there exists a desire for a truck platoon to change lanes. The second step checks if this value of desire exceeds the fixed threshold of 0.1. A value of 0.1 ensures that only necessary and mandatory lane changes are performed. The lane-changing desire is

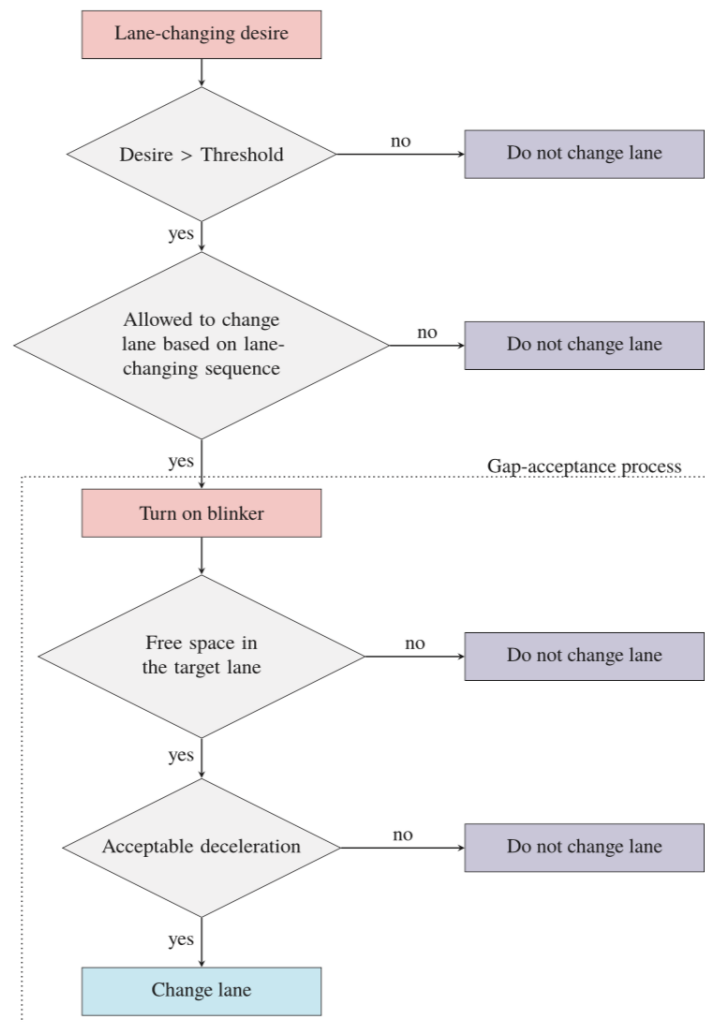


Figure 6.2. Lateral controller governing lane-changing of truck platoons.



explained in the following subsection. If a truck platoon has a desire more than the threshold, lane-change sequence step is activated that ensures that all trucks in that platoon can change lanes. Trucks in a platoon follow a last-vehicle-first principle to change lanes. Finally, a gap is accepted or rejected based on the resulting safe deceleration that follows from the car-following model and available space in the target lane. Here, the logic checks if space for a platoon to change lanes is free, which depends on the number of vehicles in that platoon desiring to change lanes. Besides, the deceleration for both the lane-changing platoon vehicle and the new follower in the target lane should be larger than some safe deceleration threshold (Schakel et al., 2012). The key concepts of the lateral behavioral model of truck platoons are described as follows.

### 6.4.1 Lane-changing desire

In this chapter, platoons only perform mandatory lane changes, and it is integrated into the lane-change model with relaxation and synchronization (LMRS) (Schakel et al., 2012). The LMRS is based on the desire to change lanes which is described as a combination of both mandatory and voluntary (discretionary) incentives. The desire to change lanes for platoons builds only upon the *route incentive* of the LMRS. Note that a strict keep-right policy is integrated into the LMRS, which ensures that platoons move on the rightmost lane of a mainline carriageway.

The desire to leave any lane  $k$  is denoted as  $d_r^k$ . The desire to change from lane  $i$  to lane  $j$  is denoted as  $d_r^{ij}$ , where  $i$  denotes the current lane and  $j$  denotes the target lane. The desire to leave lane  $k$  based on the route  $r$  is  $d_r^k$ , which is either based on the remaining distance to change lanes  $x^k$  or on the remaining time to change lanes  $t^k$ . If the speed is (relatively) low, the remaining distance on lane  $k$  is the dominant factor in determining the desire. Conversely, if the speed of the vehicle is (relatively) high, the time remaining on lane  $k$  becomes dominant in determining the desire to leave the lane. The following equation shows how the desire to leave lane  $k$  is determined:

$$d_r^k = \max\left(1 - \frac{x^k}{n^k \cdot x_0}, 1 - \frac{t^k}{n^k \cdot t_0}, 0\right) \quad (6.10)$$

The first term in Equation 6.10 refers to the desire based on the remaining distance to perform one (or multiple) lane change(s) ( $n^k$ ) within the available look-ahead distance ( $x_0$ ). The second term refers to the remaining time needed to perform one (or multiple) lane change(s) ( $t^k$ ), calculated as  $t^k = x^k / v$  ( $v$ , the current speed of the vehicle), within fixed remaining time before the lane ends.

Now that the desire for any lane ( $k$ ) can be determined, it is necessary to determine from the current lane ( $i$ ) to the target whether changing lane ( $j$ ) is desirable (denoted as  $d_r^{ij}$ ) using

$$d_r^{ij} = \begin{cases} d_r^i, & \Delta^j = 1 \quad \text{and} \quad d_r^i > d_r^j \\ 0, & \Delta^j = 1 \quad \text{and} \quad d_r^i = d_r^j \\ -d_r^j, & \Delta^j = 1 \quad \text{and} \quad d_r^i < d_r^j \\ -\infty, & \Delta^j = 0 \quad \text{and} \end{cases} \quad (6.11)$$

All cases in Equation 6.11 include a check on whether a route can still be followed on the target lane. We use a binary variable ( $\Delta_j$ ) which takes the value 1 if the route can be followed on the lane  $j$ . To derive the desire to perform the mandatory lane change, the desire to leave the current lane and the desire to leave the target lane are compared. If the desire to leave the target lane is smaller than the desire to leave the current lane, we use the desire to leave the current lane. If they are equal, we assume that there is no desire for a vehicle to perform the mandatory lane

change. If the desire to change from the current lane is smaller than the desire to leave the target lane, we use the negative value of the desire to leave the target lane to represent an undesirable mandatory lane change for a vehicle. In case the route cannot be followed on the target lane, a negative infinity desire is used to ensure that a vehicle does not change to the target lane.

### 6.4.2 Lane-changing sequence

We use the last-vehicle-first principle for trucks in a platoon configuration to perform mandatory lane changes or merging maneuvers. This sequence ensures a safe and smooth lane-changing maneuver as conflicts between vehicles in a platoon and the surrounding vehicles are minimized. The ability of a platoon to change lanes depends on the desire of the last vehicle. The first step for the lane-change logic is to assess the desire of the last vehicle in a platoon and compare it with a threshold. In the case in which the desire to change lane exceeds the threshold, the last vehicle turns on the blinker and looks for a gap in the target lane. The gap-acceptance process for the last vehicle in a platoon is similar to LMRS (Schakel et al., 2012) as it depends on both spatial availability and acceptable deceleration. Once the last vehicle accepts the gap, the rest of the vehicles in that platoon change lanes together once a suitable gap is available for them. When there is enough space (or gap) in the target lane, the rest of the vehicles in a platoon complete their lane-change maneuver. However, this gap-creation process for the rest of the vehicles in a platoon can be made faster by enabling a gap-creation algorithm. An illustration of a platoon's lane-changing sequence is shown in Figure 6.3.

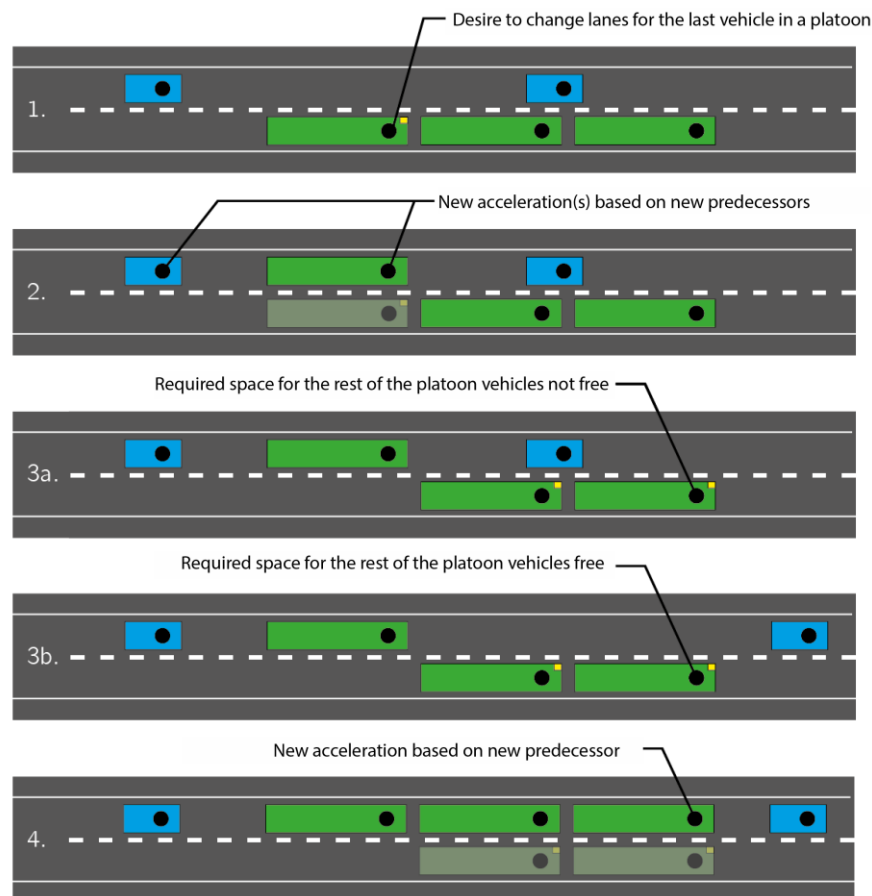
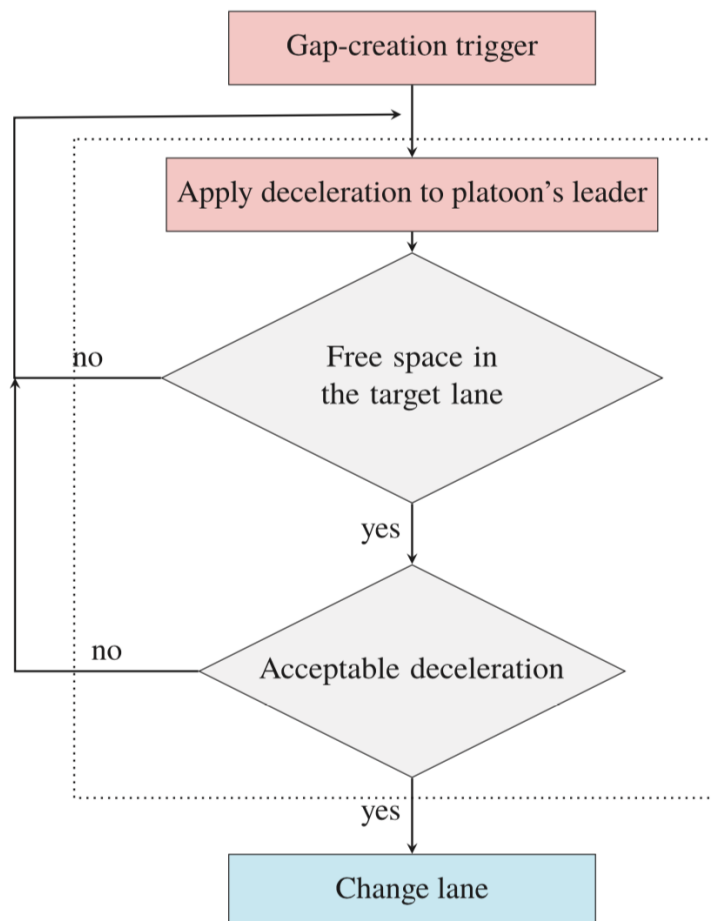


Figure 6.3. Lane-changing sequence of a truck platoon.

### 6.4.3 Gap-creation ability of truck platoons

The gap creation is considered here as the ability for a platoon to create a gap so that vehicles that are part of the platoon can change lanes. This is done by decreasing the platoon's speed in the case there is a desire to change lanes but one- or multiple vehicles in the platoon are not able to merge. For example, this situation may occur when the last vehicle in the platoon has changed lanes but the remaining vehicles in that platoon are unable to change lanes because of the presence of a vehicle obstructing space in the target lane. Then, the gap-creation algorithm is triggered when a platoon vehicle turns on its blinker (see process 3 in Figure 6.2). Depending on the gap-creation deceleration, the speed of the entire platoon is reduced by applying a deceleration to the leading vehicle in the platoon. As every vehicle in the platoon follows the speed of their predecessor, every vehicle essentially follows the speed of the leading vehicle of the platoon and the overall speed of the platoon is reduced. As the overall speed of the platoon is reduced, a gap is created more rapidly than when no gap-creation deceleration is applied. This process of gap creation is repeated until the platoon can merge. The gap-creation trigger is outlined in Figure 6.4. A verification test of the gap-creation ability of truck platoons is provided in Figure 6.5, where we observe that trucks in a platoon apply a deceleration during their lane-change maneuver.



**Figure 6.4. Logical steps in applying the gap-creation deceleration.**

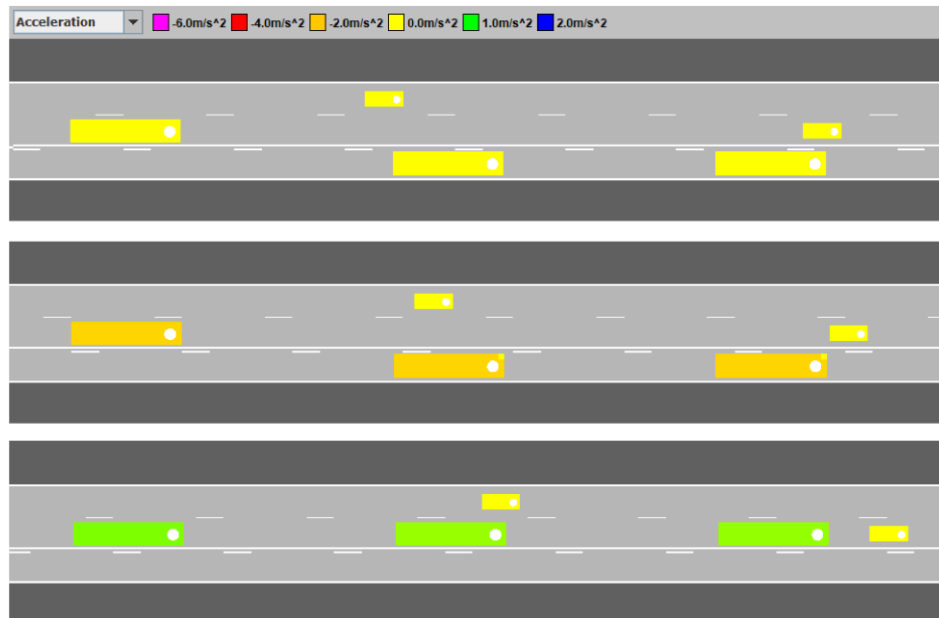


**Figure 6.5. Verification test for the gap-creation deceleration during lane changing of a truck platoon where colors represent deceleration(orange), constant speed (yellow), and acceleration (green).**

## 6.5 Experimental design

In this section, we describe the network used for simulation, demand profile, scenarios considered, and the performance indicators to assess the impacts of truck platoons.

### 6.5.1 Network modeling and demand data

The network used in the simulation represents an on-ramp to the A15 motorway near interchange Benelux in the Netherlands. The A15 motorway provides access to the port of Rotterdam from the hinterland, and it is one of the significant freight corridors. The simulated network is a two-lane mainline carriageway with an on-ramp. The length of the acceleration lane is 330 m. The total length of the simulated network is 3300 m. The loop detectors are installed just after the merging section. We consider two traffic situations, one with the low traffic intensity (LTI) and the other with high traffic intensity (HTI). The on-ramp to mainline demand ratio is fixed at 25%, and the percentage of trucks in the traffic is taken as 15%. Every simulation run has a total duration of 1 h, with a 15 min warm-up period to allow the network to be filled. Figure 6.6 shows network and demand profile.

### 6.5.2 Truck platoon configuration

We assume that truck platoons are formed before entering the network and they have the following variable characteristics.

1. Market penetration rate (MPR): 25%, 50%, 75%, and 100%
2. Platoon length: 2 trucks, 3 trucks, 4 trucks, and 5 trucks
3. Headway in a platoon: 0.3 s, 0.9 s, and 1.5 s
4. Platoon speed: 80 km/h and 100 km/h

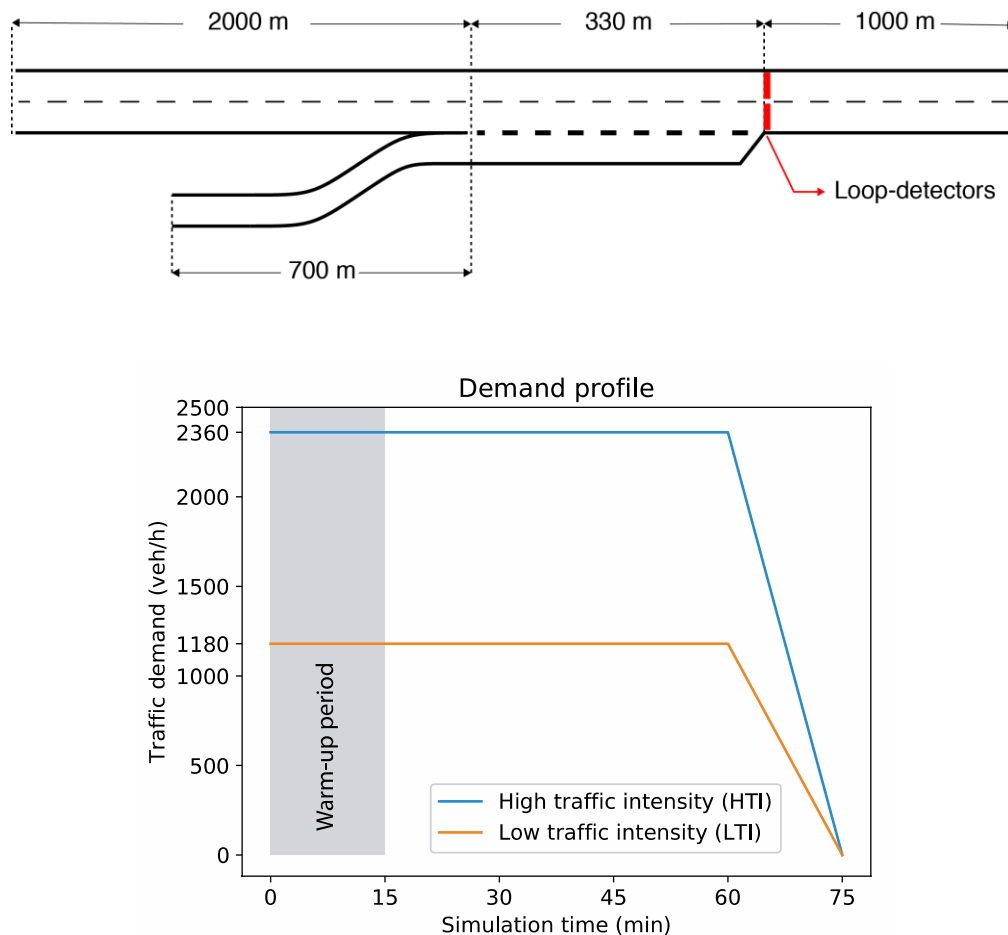


**Figure 6.6. Network (top) and demand profile (bottom).**

5. Gap-creation deceleration: 0 m/s<sup>2</sup> (off), 1.5 m/s<sup>2</sup> (low), and 3.0 m/s<sup>2</sup> (high)
6. Lane changing: only mandatory lane changing is allowed
7. Cut-ins: only if intra-platoon headway allows for that

A reference platoon configuration is chosen to represent a situation that, without further analysis, would neither result in the “worst” combination of characteristics nor the “best” combination of characteristics in terms of performance and safety. In the reference platoon configuration, we consider 50% of market penetration, 3 trucks, 0.9 s of headway, a maximum speed of 80 km/h for the platoon, and no gap-creation deceleration.

### 6.5.3 Scenarios

We consider the following three scenarios. Each scenario is simulated for both the LTI and HTI.

- **Base-Case Scenario:** Platoons are not present in traffic.
- **Traffic Scenario 1:** Platoons originate from the mainline carriageway and are a part of through traffic.
- **Traffic Scenario 2:** Platoons originate from the on-ramp and merge onto the mainline carriageway.

We use OpenTrafficSim (van Lint et al., 2016) to simulate above scenarios. OpenTrafficSim combines IDM+ car-following model (Schakel et al., 2010) with the LMRS (Schakel et al., 2012). For non-CACC equipped cars and trucks, we use default parameter settings. The model parameters are tabulated in Table 6.1. All the simulations are run 16 times with different random seeds, and the results are then averaged.

**Table 6.1 Simulation model parameters**

Symbol	Value	Description
<b>Car-following parameters</b>		
$a_{\text{car}}$	1.25	Maximum (desired) car-following acceleration for cars ( $\text{m/s}^2$ )
$a_{\text{truck}}$	0.40	Maximum (desired) car-following acceleration for trucks ( $\text{m/s}^2$ )
$b$	2.09	Maximum comfortable car-following deceleration ( $\text{m/s}^2$ )
$b_0$	0.50	Maximum adjustment deceleration ( $\text{m/s}^2$ )
$b_{\text{crit}}$	3.50	Maximum critical deceleration ( $\text{m/s}^2$ )
$f_{\text{speed}}$	1.00	The speed limit adherence factor for cars and trucks
$s_0$	3.00	Car-following stopping distance (m)
$T_{\text{max}}$	1.20	Maximum car-following headway (s)
$T_r$	0.50	Reaction time (s)
$v_{\text{des, car}}$	$N(123.7,12)$	Desired (maximum) speed for cars (km/h)
$v_{\text{des, truck}}$	$N(85.00,2.50)$	Desired (maximum) speed for trucks (km/h)
$l_{\text{car}}$	4.00	Length of cars (m)
$l_{\text{truck}}$	12.00	Length of trucks (m)
<b>Lane-changing parameters</b>		
$d_{\text{free}}$	0.365	Free lane change desire threshold
$d_{\text{sync}}$	0.577	Synchronized lane change desire threshold
$d_{\text{coop}}$	0.788	Cooperative lane change desire threshold
$T_{\text{min}}$	0.56	Minimum car-following headway (s)
$\tau$	25	Headway relaxation time (s)
$v_{\text{cong}}$	60	Speed threshold below which traffic is considered congested (km/h)
$v_{\text{gain}}$	69.60	Anticipation speed difference at full lane change desired (km/h)
$x_0$	295	Look-ahead distance (m)
$t_0$	43	Look-ahead time for mandatory lane changes (s)

### 6.5.4 Performance indicators

We consider average travel time and maximum flow to evaluate traffic efficiency. Time to collision and required braking rate are used as surrogate measures to evaluate traffic safety.

#### Average Travel Time

Since the total time spent ( $TTS$ ) in the network increases with traffic intensity, we use a normalized value of  $TTS$ , that is,  $TT_{av}$  which is computed by dividing  $TTS$  by the total number of vehicles generated in the simulation ( $N$ ):

$$TT_{av} = \frac{TTS}{N} \quad (6.12)$$

#### Maximum Flow

The maximum flow is only of interest in the HTI because of the presence of congestion and is considered as a proxy for merging capacity. The maximum flow,  $q_{max}$ , is calculated by continuously extracting a 5 min moving average of the flow,  $q_t$ , observed at the loop detectors to account for temporary variability, also because of the presence of truck platoons. For every minute instance,  $t$ , the following equation 6.13 can be used to compute  $q_t$ :

$$q_{av,t} = \frac{1}{5} \sum_{t-4}^t q_t \quad \forall t \in \{0, \dots, T\} \quad (6.13)$$

$$q_{max} = \max(q_{av,t}) \quad \forall t \in \{0, \dots, T\} \quad (6.14)$$

#### Time to Collision

The time-to-collision ( $TTC$ ) measures the time between two vehicles if there is a possibility of them colliding on a given trajectory. With vehicle  $i$  and its predecessor  $i - 1$ , vehicle's length  $l_i$ , their positions  $x_i$  and  $x_{i-1}$ , and their speeds  $v_i$  and  $v_{i-1}$ , we compute  $TTC_{i,t}$  in

$$TTC_{i,t} = \frac{x_i(t) - x_{i-1}(t) - l_i}{v_i(t) - v_{i-1}(t)} \quad \forall v_i(t) > v_{i-1}(t) \quad (6.15)$$

for every simulation time-step  $t$ . We only consider critical observations,  $TTC_{obs}$ , which are below the threshold value of 4 s (Horst, 1991) as shown in

$$TTC_{obs} = \sum_{i \in N} \sum_t TTC_{i,t} \quad \forall TTC_{i,t} < 4 \text{ s} \quad (6.16)$$

#### Required Braking Rate

To account for the inability of  $TTC$  to differentiate between severity in speed differences, the required braking rate ( $RBR$ ) is also considered which accounts for all the decelerations  $a_i(t)$  a vehicle  $i$  has undergone

$$RBR_{i,t} = a_i(t) \quad \forall t \in \{0, \dots, T\} \quad (6.17)$$

for every simulation time-step  $t$ . We only consider critical observations,  $RBR_{obs}$ , that exceed the threshold of  $-2.1 \text{ m/s}^2$  (Archer, 2005):

$$RBR_{obs} = \sum_{i \in N} \sum_t RBR_{i,t} \quad \forall RBR_{i,t} < -2.1 \text{ m/s}^2 \quad (6.18)$$

## 6.6 Impact of a reference platoon configuration

First, we introduce platoons as a part of the traffic demand with reference platoon characteristics. We assess the impacts on traffic flow and traffic safety in the LTI and HTI scenarios. In the following two subsections, we present the results for two traffic scenarios when platoons are introduced on the mainline carriageway (traffic scenario 1) and from an on-ramp (traffic scenario 2).

### 6.6.1 Traffic scenario 1: Truck platoons on mainline carriageway

The first traffic scenario is the one in which truck platoons traverse on the mainline carriageway. In this case, other vehicles merging onto the main road could be hindered by the presence of truck platoons. Compared with the base-case scenario, truck platoons increase the travel time of the system under both LTI and HTI at a significance level of 5% (see Table 6.2). The maximum flow rate decreases at a significance level of 10%. The number of critical TTC observations increases at a significance level of 5%, whereas the number of RBR observations increases under LTI and HTI at a significance level of 5% and 10%, respectively. The more time vehicles spend in the network, the higher are the chances that they incur safety-critical situations. Overall, it can be inferred that the presence of truck platoons on the mainline carriageway is detrimental to both traffic performance and safety. Figure 6.7 presents deteriorating effects of platoon on traffic flow.

**Table 6.2. Traffic and Safety Impacts of Introducing the Reference Platoon Configuration**

Scenario	TT <sub>av</sub> (s)	Flow (veh/h/lane)	TTC <sub>obs</sub> (n/veh/h)	RBR <sub>obs</sub> (n/veh/h)
<b>Low traffic intensity</b>				
Base-case scenario	117.12	-	0.00	0.76
Reference platoon configuration on mainline carriageway (traffic scenario 1)	119.65**	-	0.68**	4.25**
Reference platoon configuration merging onto mainline carriageway (traffic scenario 2)	117.51	-	0.02*	0.60**
<b>High traffic intensity</b>				
Base-case scenario	127.93	1884	27.95	18.44
Reference platoon configuration on mainline carriageway (traffic scenario 1)	149.04**	1682*	65.40**	49.01*
Reference platoon configuration merging onto mainline carriageway (traffic scenario 2)	132.16	1854	26.72	22.17

Note: TT<sub>av</sub> = average travel time spent in the network; veh/h/lane = vehicles per hour per lane; TTC<sub>obs</sub> = critical time-to-collision observations (TTC < 4s); n/veh/h = number of critical observations per vehicle per hour; RBR<sub>obs</sub> = critical braking rate observations (RBR < -2.1 m/s<sup>2</sup>).

\*\* and \*5% and 10% of significance level compared to the base-case scenario,



## 6.6.2 Traffic scenario 2: Truck platoons merging from an on-ramp

The second traffic scenario is the one in which platoons are merging onto mainline carriageway from an on-ramp. In this case, truck platoons may experience the difficulty of merging onto mainline carriageway but also affect the other traffic when doing so. Introducing truck platoons with reference characteristics does not affect the travel time of the system under both LTI and HTI at a significance level of 10% (see Table 6.2). Maximum traffic flow also is not different than the base-case scenario at a significance level of 10%. In terms of traffic safety, truck platoons merging from an on-ramp do not alter the number of critical RBR observations at a significance level of 10% for both low and high traffic intensity situation. Only in HTI, the presence of truck platoons lowers the critical TTR observations at a significance level of 5%. Overall, it can be inferred that platoons merging from an on-ramp do not affect traffic performance and safety. It should be noted that only 25% of platoons are generated in traffic scenario 2 compared with traffic scenario 1 because of the fixed on-ramp to mainline demand ratio.

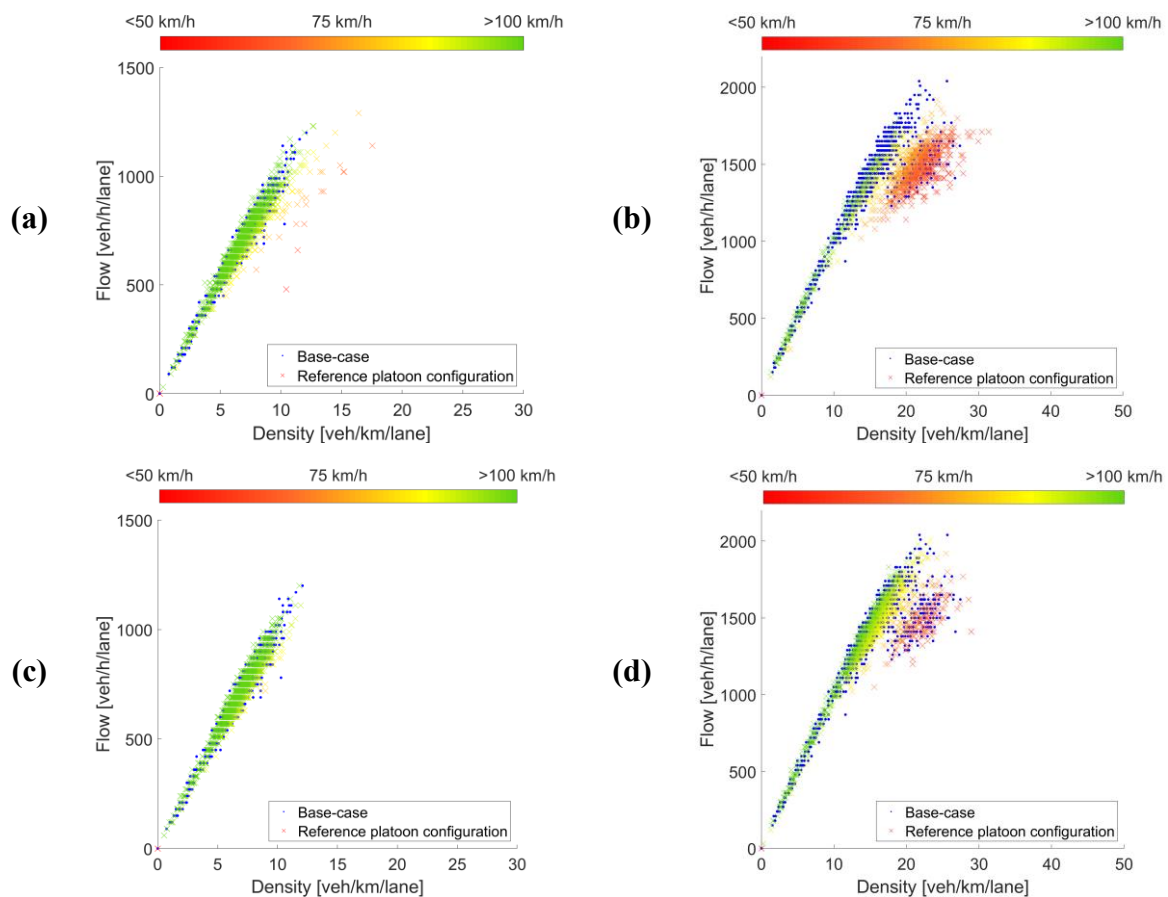


**Figure 6.7. Fundamental diagrams showing macroscopic impacts of the reference platoon configuration: (a) traffic scenario 1 – low traffic intensity, (b) traffic scenario 1 – high traffic intensity, (c) traffic scenario 2 – low traffic intensity, and (d) traffic scenario 2 – high traffic intensity.**

## 6.7 Impact of truck platoon's characteristics

In this section, we analyze the impact of a platoon's characteristics on traffic efficiency and safety at the local and global levels. First, we discuss one-at-a-time sensitivity analysis (OAT-SA) which measures the impact of varying a single variable on the outcome (Hamby, 1994). For our purpose, we change one characteristic of the platoon at a time by keeping others fixed at reference configuration and observe its effect on the output. For OAT-SA, we use a significance level of 5% to assess the results compared with the base-case scenario. Second, we present a global sensitivity analysis. In addition, we also look at vehicle trajectories at the merging section. These trajectory plots illustrate the impact of platoon configuration on traffic efficiency and safety. For each scenario, one simulation run that is close to the average of 16 simulation runs is selected for the purpose of illustration.

### 6.7.1 Traffic scenario 1: Truck platoons on mainline carriageway

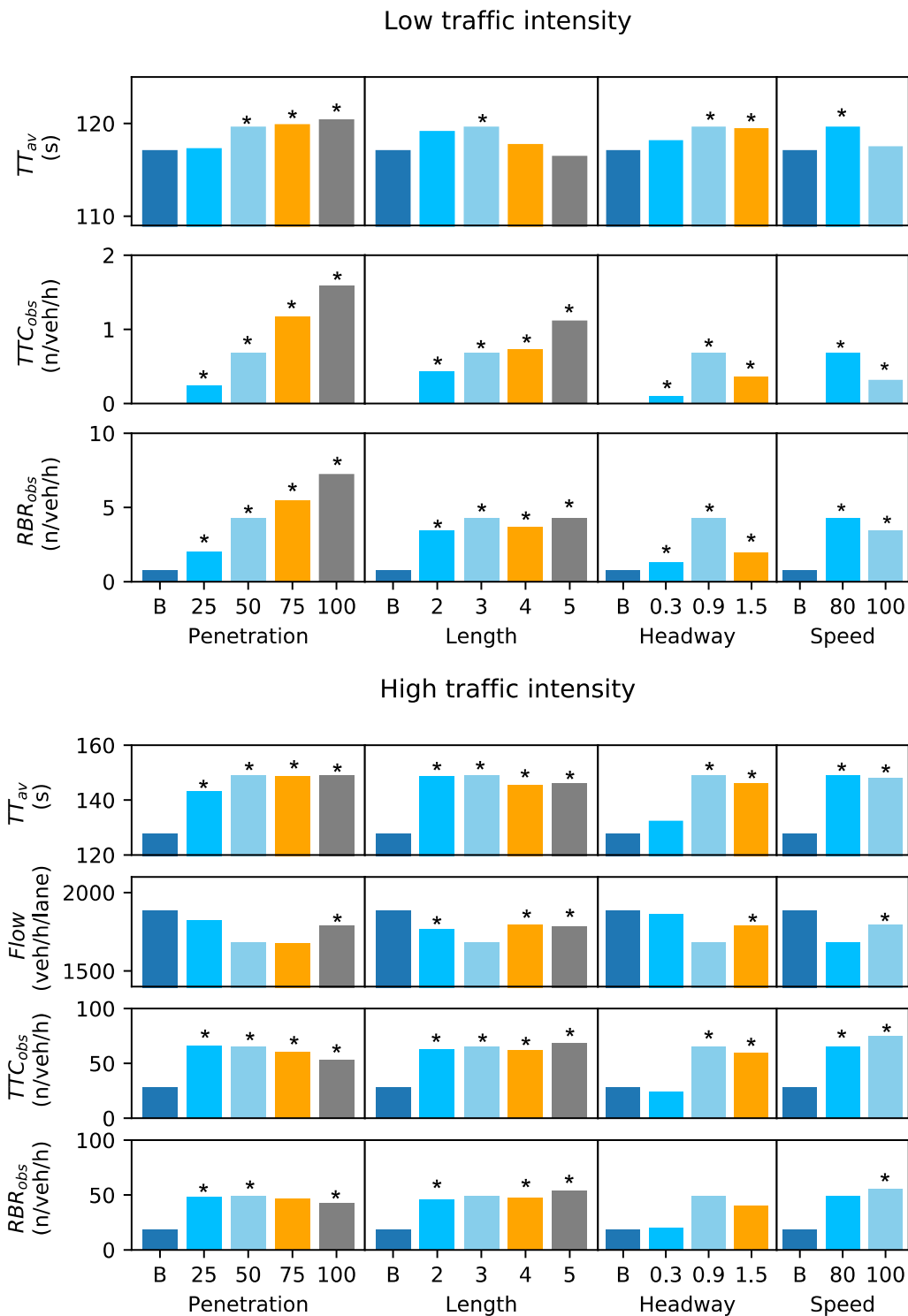
Figure 6.8 shows the results of OAT-SA for traffic scenario 1. In the subsequent subsections, we explain the results.

#### Market penetration rate

An increase in the MPR of truck platoons replaces non-CACC equipped trucks with CACC-equipped trucks. Conflicts among merging and mainline vehicles increase with an increase in the MPR of truck platoons. Therefore, shockwaves are generated at both the mainline carriageway and the acceleration lane. This effect is illustrated in Figure 6.9, where we present trajectories of both mainline and ramp vehicles. In HTI, ramp vehicles have the most difficulty merging onto the mainline carriageway at 100% MPR, whereas in LTI, ramp vehicles have limited difficulty as they can find a suitable gap to merge onto the mainline carriageway. As a result, we observe an increase in travel time with increasing MPR. Travel time can increase up to 2.8% and 16.5% in LTI and HTI, respectively. Maximum flow or merging capacity is only significantly affected at 100% MPR: we observe a 5% decrease in capacity compared with the base-case scenario. Similar to the impacts on traffic efficiency, an increase in MPR deteriorates safety as non-CACC vehicles often find themselves in risky and safety-critical situations as captured by TTC and RBR values. For all MPR scenarios, we observe that truck platoons have a negative impact on traffic safety compared with the base-case scenario under both LTI and HTI. Critical TTC and RBR observations in HTI can increase by a factor of 2.37 and 2.65, respectively.

#### Platoon length

As the platoon length increases, the total number of platoons decreases but the potential for a critical interaction with merging vehicles increases. It should be noted that the linear increase in the platoon length does not result in a linear decrease in the number of platoons. An interplay between the platoon length and the number of platoons governs the availability of potential gaps for merging traffic, which in turn affects traffic efficiency and safety. As a consequence of this interplay, we observe a non-monotonic relationship between the platoon length and performance indicators in both LTI and HTI. In HTI, this interplay results in more or less similar values of traffic efficiency and safety indicators, as trajectories of ramp vehicles are similar (see Figure 6.10). We observe a significant degradation of traffic efficiency and safety compared with the base-case. In LTI, changes in platoon length do not significantly affect travel time compared with the base-case but only for reference configuration with 3 trucks in a platoon.



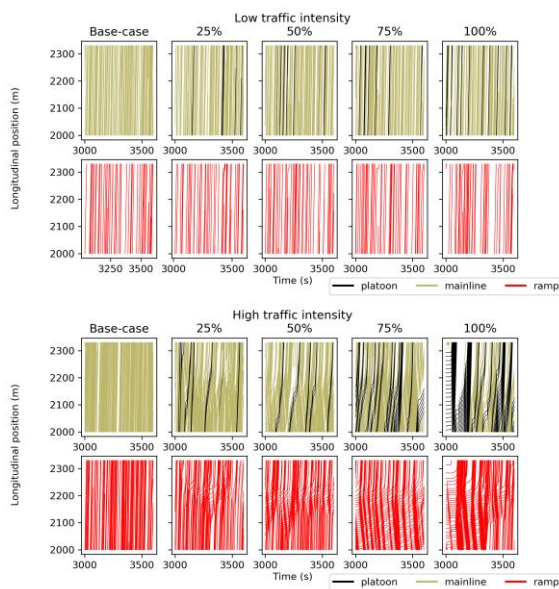


**Figure 6.9. Impact of the market penetration of truck platoon on vehicle trajectories for the traffic scenario 1.**

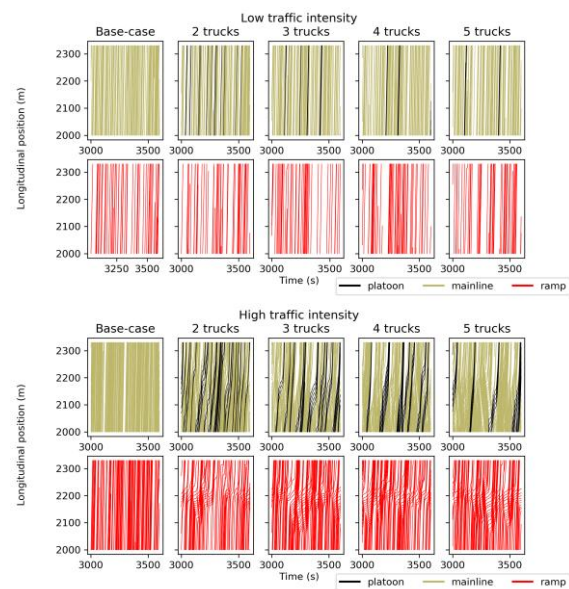


**Figure 6.10. Impact of the length of truck platoon on vehicle trajectories for the traffic scenario 1.**

However, the presence of longer platoons results in more braking actions and an increased intensity for merging interactions, which is reflected in significantly worse TTC and RBR compared with the base-case.

### Headway in a platoon

By increasing the intra-platoon headway, we increase the effective length of the platoon. Longer platoons on mainline carriageway thus present more obstacles to merging vehicles. Therefore, both efficiency and safety decrease. When we increase the intra-platoon headway to 1.5 s, we allow enough spacing for cut-ins between two trucks in platoon (see Figure 6.11). In this case, the situation results in an improvement to both traffic efficiency and safety compared with the platoon configuration with 0.9 s of intra-platoon headway. At very small inter-platoon headways of 0.3 s, we do not observe significantly different vehicle trajectories compared with the base-case scenario. A platoon configuration with 0.3 s of headway can be allowed in HTI.

### Platoon speed

Increasing the desired speed of platoon vehicles reduces the speed differences between platoons and surrounding traffic. Therefore, an increase in the speed of platoons to 100 km/h improves travel time in LTI compared with a platoon configuration with the desired speed of 80 km/h. At the high speed of a platoon configuration, we also observe low numbers of safety-critical situations. Overall, we observe a limited impact on travel time and safety in LTI. In HTI, vehicle trajectory plots (see Figure 6.12) show that conflicts among merging and mainline vehicles are present in both cases: 80 km/h and 100 km/h. As a result, we observe a deterioration of traffic efficiency and safety in both cases compared with the base-case scenario.

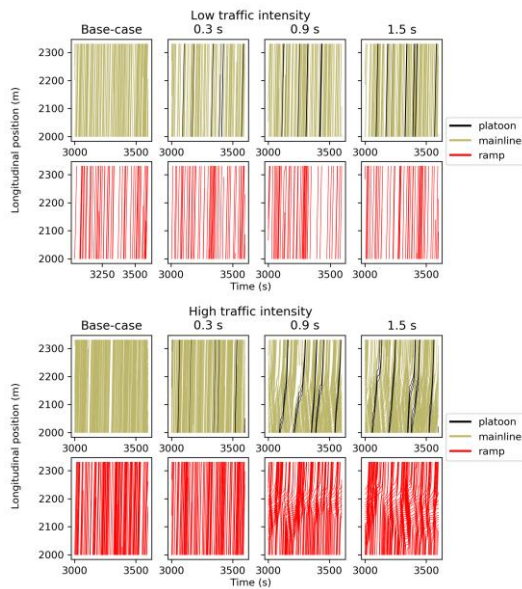


**Figure 6.11. Impact of intra-platoon headway on vehicle trajectories for the traffic scenario 1.**

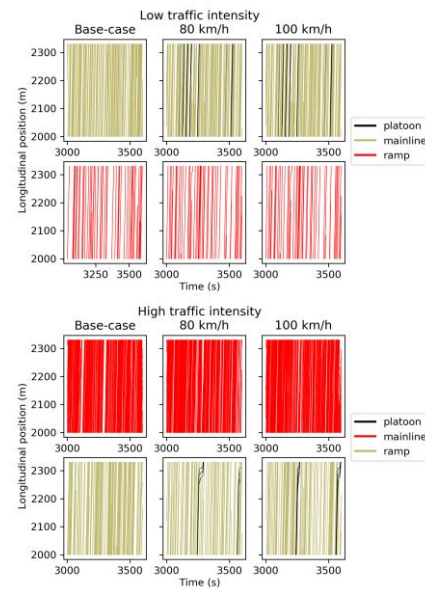


**Figure 6.12. Impact of speed of truck platoons on vehicle trajectories for the traffic scenario 1.**

## 6.7.2 Traffic scenario 2: Truck platoons merging from an on-ramp

Figure 6.13 shows the results of OAT-SA for traffic scenario 2. We explain the results in the following subsections.

### Market penetration rate

An increase in MPR of truck platoons groups individual trucks in several platoons, thus reducing the number of individual trucks originating from the ramp. On one hand, trucks in a platoon will have to seek one suitable gap to merge onto the mainline. On the other hand, they require a longer gap than the normal trucks; they might have to wait for a while on the acceleration lane. By looking at vehicle trajectories in Figure 6.14, we observe that truck platoons from ramp do not greatly affect traffic conditions either for the ramp or mainline vehicles. Irrespective of the merging process of truck platoons, vehicles following a truck platoon can merge onto the mainline carriageway if they can find sufficient gaps. As a result, the traffic and safety impacts are not significantly different than the base-case scenario in HTI, whereas in LTI, we observe the slight deterioration of travel time at 75% MPR than the base-case scenario. Similar degradation of safety is observed at 100% MPR than the base-case scenario. Still, the impacts on both traffic efficiency and safety are limited.

### Platoon length

As explained in the previous section, an increase in the number of trucks in a platoon configuration results in a decrease in the total number of platoons in the system. Longer platoons, although small in numbers, present more critical interactions with the surrounding vehicles and require a longer time to merge on the mainline carriageway. Therefore, this interplay between platoon length and the number of platoons governs traffic efficiency and safety. As a result, we observe non-monotonic relationships between performance indicators and the length of a platoon. Travel time in both LTI and HTI is not significantly different than the base-case scenario.

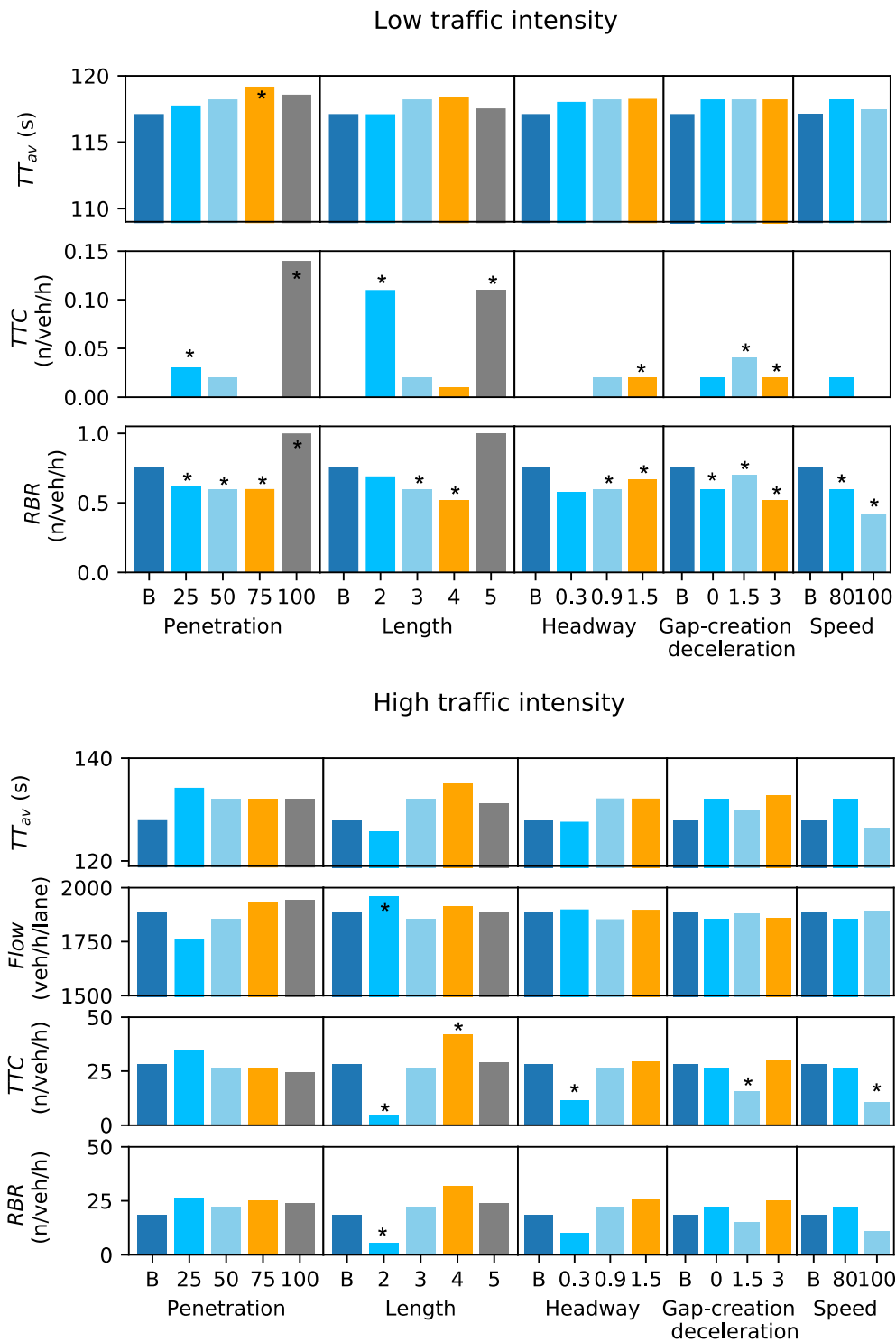


**Figure 6.13. One-at-a-time sensitivity analysis for traffic scenario 2.**

Note: B = base-case; TT<sub>av</sub> = average travel time spent in the network; veh/h/lane = vehicles per hour per lane; TTC<sub>obs</sub> = critical time-to-collision observations (TTC < 4s); n/veh/h = number of critical observations per vehicle per hour; RBR<sub>obs</sub> = critical braking rate observations (RBR < -2.1 m/s<sup>2</sup>).

\*Significance at 5%.

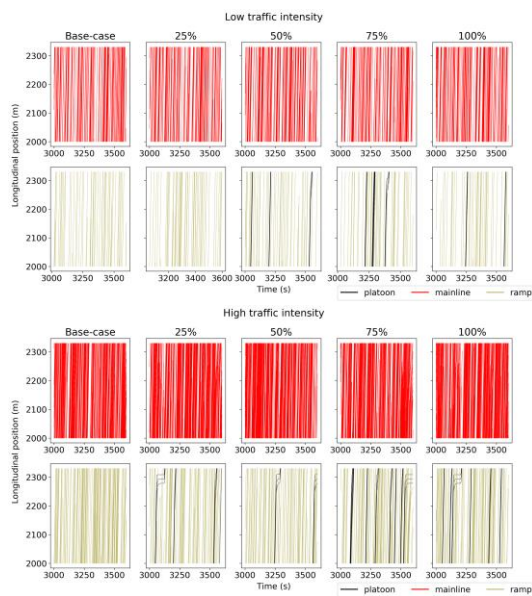


**Figure 6.14. Impact of the market penetration of truck platoon on vehicle trajectories for the traffic scenario 2.**

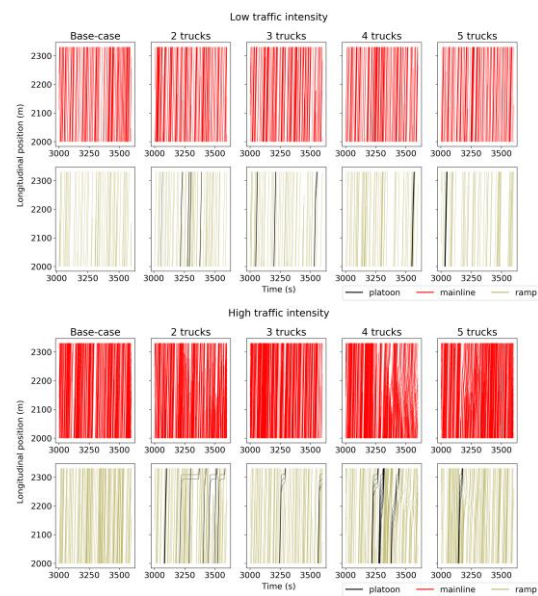


**Figure 6.15. Impact of the length of truck platoon on vehicle trajectories for the traffic scenario 2.**

A platoon configuration with 2 trucks in HTI is shown to increase maximum flow and decrease safety-critical interactions. As we increase the number of trucks in a platoon, we observe deterioration of traffic efficiency and safety in HTI (see Figure 6.15). Compared with a 4-truck configuration, the traffic and safety situation are improved in a 5-truck configuration because of the reduction of the number of platoons in the system. In contrast to HTI, longer truck platoon configurations (i.e., 5 trucks) slightly deteriorate traffic safety in LTI.

### Headway in a platoon

An increase in the intra-platoon headway increases the effective length of a platoon. Longer platoons will have to seek a larger gap to merge onto the mainline carriageway; therefore, there are higher chances for increased conflicts between a platoon and the surrounding vehicles (see Figure 6.16). Therefore, shorter intra-platoon headways (i.e., 0.3 s) result in fewer TTC observations in HTI. Travel time and maximum flow do not differ significantly by changing intra-platoon headways compared with the base-case scenario. However, in LTI intra-platoon headways have a limited impact on both traffic efficiency and safety.

### Gap-creation deceleration

The gap-creation policy is varied among no gap-creation, low gap-creation deceleration ( $1.5 \text{ m/s}^2$ ), and high gap-creation deceleration ( $3.0 \text{ m/s}^2$ ). With higher gap-creation deceleration, the time needed by platoons to merge will be shorter (see Figure 6.17). Consequently, a shorter lane-change duration minimizes conflicts with the surrounding vehicles and thus improves traffic efficiency and safety compared with the base-case. At least, the situation is no worse than the base-case when tested at a significance of 5%. Especially in HTI,  $1.5 \text{ m/s}^2$  of gap-creation deceleration significantly reduces safety-critical TTC observation by 43.5%. Similarly in LTI, mid and high gap-creation deceleration result in fewer RBR critical observations. The impact of applying a gap-creation deceleration on travel time and maximum flow is not significantly different than the base-case scenario.

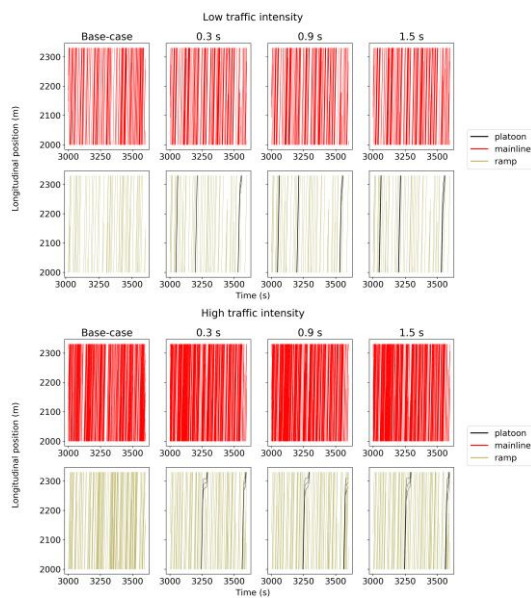


**Figure 6.16.** Impact of intra-platoon headway on vehicle trajectories for the traffic scenario 2.

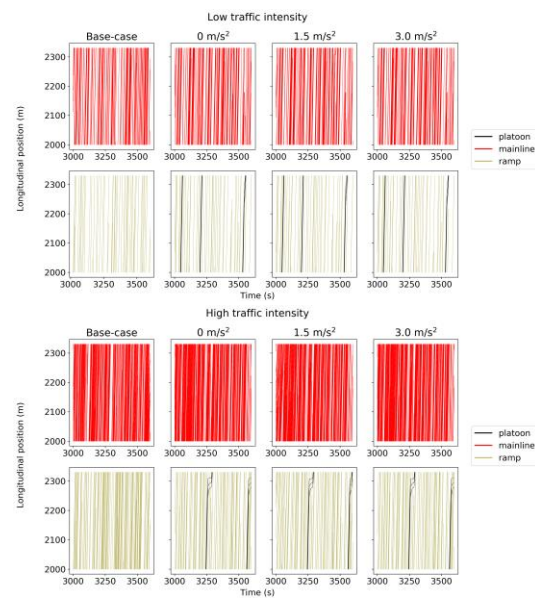


**Figure 6.17.** Impact of the gap-creation deceleration of truck platoons on vehicle trajectories for the traffic scenario 2.

### Platoon speed

With an increased desired speed, the platoon is effectively able to synchronize with the target lane (see Figure 6.18). This synchronization helps not only in the gap-searching process but also in easing conflict with the surrounding vehicles. Therefore, we observe an improvement in traffic efficiency and safety under both LTI and HTI.

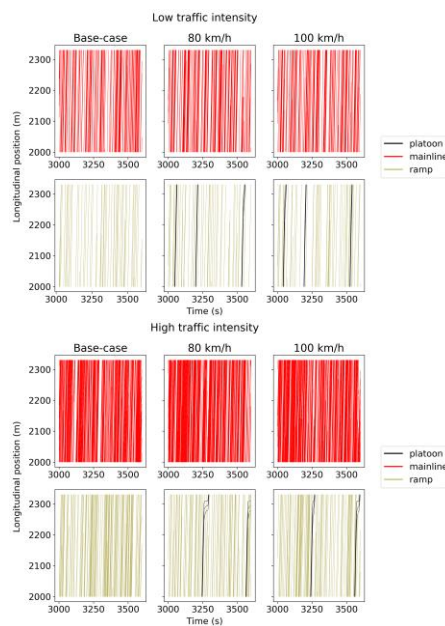


**Figure 6.18.** Impact of speed of truck platoons on vehicle trajectories for the traffic scenario 2.



## 6.8 Global sensitivity analysis

In the previous OAT-SA, we observe non-monotonic relationships as well as the presence of local optima. Furthermore, OAT-SA does not consider the entire input space, as it ignores the simultaneous variation of input parameters. We hypothesize that the interactions among platoon characteristics mostly affect the output or performance indicators. Therefore, we apply a global sensitivity analysis technique, moment-independent measure, as it also accounts for the correlations between input variables. Borgonovo's importance measure,  $\delta_i$ , analyzes the impact of input,  $X_i$ , uncertainty in the output distribution without any reliance on a specific moment of the output (Borgonovo, 2007). The higher the value of  $\delta_i$ , the higher will be the effect of input  $X_i$  on output. Moreover, the joint importance of all parameters equals unity,  $\delta_{1,2,\dots,n} = 1$ . We can use this property to obtain the contribution of model inputs or main effects ( $\sum_i \delta_i$ ) and interactions among model inputs ( $\delta_{1,2,\dots,n} - \sum_i \delta_i$ ) on the output uncertainty.

Let's say the model input be  $X = (X_1, X_2, \dots, X_n)$  and output be  $Y$ .  $f_Y(y)$  and  $f_{Y|X_i}(y)$  denote the unconditional and conditional probability density functions of the model output, respectively. Then, the shift between  $f_Y(y)$  and  $f_{Y|X_i}(y)$  can be computed by the area  $s(X_i)$

$$s(X_i) = \int |f_Y(y) - f_{Y|X_i}(y)| dy \quad (6.19)$$

The average effect of input  $X_i$  on the whole distribution of the output  $Y$  is given by

$$E_{X_i}[s(X_i)] = \int f_{X_i}(X_i) [\int |f_Y(y) - f_{Y|X_i}(y)|] dX_i \quad (6.20)$$

In the following equation, we define moment-independent sensitivity index  $\delta_i$

$$\delta_i = \frac{1}{2} E_{X_i}[s(X_i)] \quad (6.21)$$

For our analysis, we use Latin hypercube sampling to generate a sample of input parameters. The range of input parameters is as follows.

1. Market penetration rate (MPR): 0–100%
2. Platoon length: 2–5 trucks
3. Headway in a platoon: 0.3–1.5 s
4. Platoon speed: 80–100 km/h
5. Gap-creation deceleration: 0–3.0 m/s<sup>2</sup> (only used in traffic scenario 2)

For every simulation run, we use a fixed random seed to ensure that the output does not change as a result of seeds. We generate 100 samples which are later used for assessing the parameter's importance; 400 simulations are run to account for traffic scenarios and traffic intensities. Sensitivity analysis is performed for four scenarios using the SALib package (Herman and Usher, 2017) in Python 3.7, and the results are shown in Figure 6.19. Based on the values of  $\delta$ , important platoon characteristics can be identified for a given traffic scenario and a traffic intensity.

### 6.8.1 Traffic scenario 1: Truck platoons on mainline carriageway

In LTI, the platoon's speed is mostly relevant for TTS. For safety, MPR and length are the two most important input parameters, whereas in HTI, MPR, length, and headway affect TTS. Flow

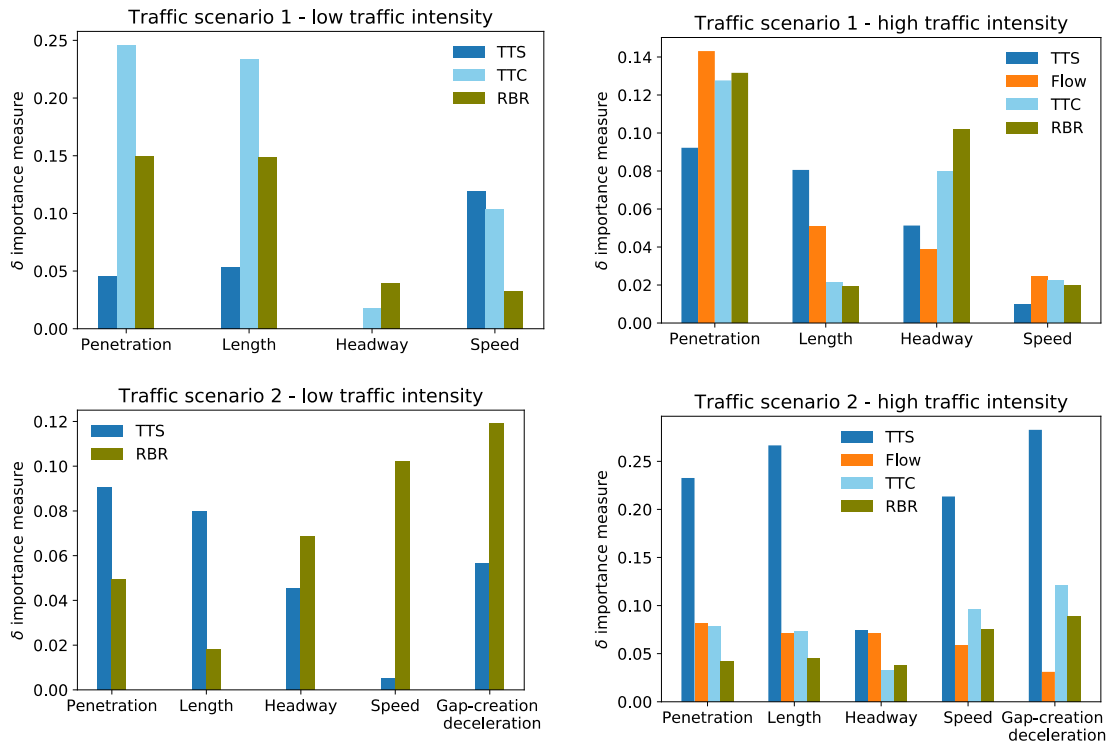


**Figure 6.19. Global sensitivity analysis for evaluating the impact of truck platoon characteristics on traffic efficiency and safety.**

Note: RBR = required braking rate; TTC = time-to-collision; TTS = total time spent.

is mostly affected by MPR. For safety, MPR and intra-platoon headway are the most important input parameters. In LTI, the contribution of model inputs ( $\sum_i \delta_i$ ) on uncertainty in TTS, TTC, and RBR is 0.20, 0.58, and 0.38, respectively. Similarly in HTI, the contribution of model inputs ( $\sum_i \delta_i$ ) on uncertainty in TTS, Flow, TTC, and RBR is 0.23, 0.25, 0.25, and 0.27, respectively. The low values of  $\sum_i \delta_i$  signal that a significant portion of the output uncertainty is explained by interaction terms in both LTI and HTI.

### 6.8.2 Traffic scenario 2: Truck platoons merging from an on-ramp

In LTI, MPR, length, and gap-creation deceleration are the three most relevant input variables for TTS. For RBR, Gap-creation deceleration and speed are the two most important input parameters. In HTI, MPR, length, speed, and gap-creation deceleration are relevant for TTS. In LTI, we do not perform sensitivity analysis for TTC as it is not affected by platoon characteristics and most of the values are zeros. Further the contribution of model inputs ( $\sum_i \delta_i$ ) on uncertainty in TTS and RBR is 0.22 and 0.36, respectively. In HTI, the model inputs can alone explain changes in TTS since  $\sum_i \delta_i = 0.99$ . In contrast, the contribution of model inputs ( $\sum_i \delta_i$ ) on uncertainty in the maximum flow, TTC, and RBR is 0.31, 0.40, and 0.29, respectively. The low values of  $\sum_i \delta_i$  show that interactions play a major role in output uncertainty.

## 6.9 Discussion

Our main finding is that truck platooning can be detrimental to traffic efficiency and safety. When truck platoons are part of the mainline traffic, traffic efficiency and safety are deteriorated in HTI around the merging section. By introducing truck platoons on the mainline carriageway,

especially in HTI, we limit the opportunities for the merging traffic and in turn increase the complexity of their merging maneuvers, as also reported in previous studies (Calvert et al., 2019, Wang et al., 2019). However, truck platoons, being a part of merging traffic, have a limited effect on traffic efficiency and safety.

The sensitivity analysis conducted in this chapter has allowed us to design a platoon configuration that can have limited negative impacts on traffic efficiency and safety. Allowing truck platooning at short headways around merging sections seems to be beneficial. An increase in headways may allow merging vehicles to cut-in but it is not better than the short-headway policy. Increasing the desired speed of truck platoons on the mainline carriageway is shown to increase conflicts with the merging traffic. However, when truck platoons are a part of merging traffic and also have a higher desired speed, they are shown to merge smoothly as they can better synchronize themselves with the target lane. The length of platoons is shown to have a non-linear relationship with traffic efficiency and safety indicators as we observe local optima. It shows that the number of platoons in the traffic system is also a significant parameter. Gap-creation deceleration is an important parameter that governs the lane changing of truck platoons. Reducing the merging duration of platoons is shown to have a positive impact on traffic efficiency and safety.

Recall that we have used the OAT-SA to capture the effect of individual platoon characteristics on efficiency and safety. It falls short of capturing the interactions among platoon characteristics. For this, we have used global sensitivity analysis which shows that we cannot separate the effects of individual platoon characteristics and analyze them, as interactions among platoon characteristics predominantly affect traffic efficiency and safety. These interactions also help us to explain non-monotonic relations between the length of a platoon and performance indicators governing traffic efficiency and safety. Therefore, several platoon configurations, resulting from a combination of platoon characteristics, should be evaluated for a comprehensive traffic and safety assessment in critical traffic situations. These situations may also include evaluations around off-ramps and weaving sections.

We have considered TTC and RBR as surrogate measures to identify safety-critical interactions. The TTC values depend only on relative spacing ( $ds$ ) and relative speed ( $dv$ ), whereas RBR values, being the control output of the IDM + car-following model, also depend on the current speed of vehicles. Figure 6.20 shows how TTC and RBR measures can capture critical interactions on  $ds - dv$  plane; the chances of critical interactions are high in the yellow region. Even for the blue region that is marked safe by the TTC indicator, there exists a probability of observing critical decelerations. If the current speed of a vehicle is high, that vehicle may be involved in critical interactions even at larger  $ds$  and smaller  $dv$  combinations as shown by the

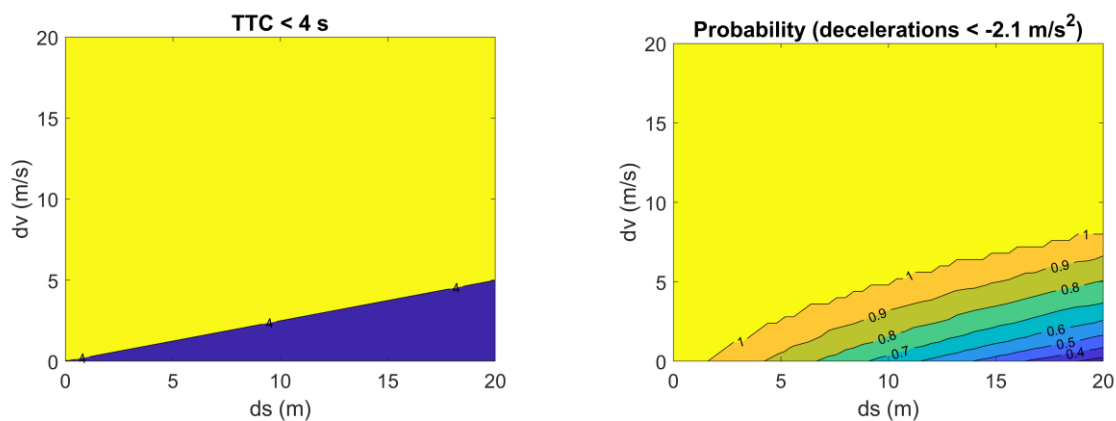


**Figure 6.20. Comparison of traffic safety indicators over relative spacing ( $ds$ ) and relative speed ( $dv$ ) plane (left) time to collision (TTC) (right) probability of occurring critical decelerations.**

RBR indicator. Furthermore, larger decelerations (or RBR values) can also be related to traffic instability which could lead to unsafe situations (Treiber et al., 2006).

## 6.10 Conclusions

This chapter presents a comprehensive evaluation of traffic efficiency and safety in a critical traffic situation, that is, a merging section, with the introduction of truck platoons in the traffic system. We propose a novel lateral behavior controller for truck platoons. We implement longitudinal and lateral controllers in microscopic simulation software OpenTrafficSim. The case study around a merging section near the port of Rotterdam shows that the introduction of the reference truck platoon configuration on mainline carriageway deteriorates traffic efficiency and safety in both low and high traffic intensity. However, truck platoons, being a part of the merging traffic from an on-ramp, do not significantly affect traffic efficiency and safety. We use local and global sensitivity analyses to study the impact of platoon characteristics on traffic efficiency and safety. The global sensitivity analysis emphasizes that the interactions among platoon characteristics contribute more to uncertainty in the performance indicators than the individual effects. In general, the results show that the interaction between truck platoons and surrounding traffic depends on the combination of platoon characteristics, traffic demand, and traffic scenarios.

Future research should look into improving the modeling of human-driven vehicles by incorporating human factors (van Lint and Calvert, 2018). Besides, the control parameters for truck platoons should be calibrated with field tests. In the coming years, autonomous vehicles (AVs) are likely to be part of the traffic mix. A promising research direction will be to analyze the impact of truck platooning in such a traffic mix of human-driven vehicles and AVs. AVs are likely to improve the traffic safety and utilization of available road space. However, merging conflicts between truck platoons and autonomous ramp vehicles might still cause problems for traffic efficiency. Cooperation between vehicles might further improve traffic stability and efficiency in critical situations.

Measures to prevent merging conflicts between truck platoons and merging vehicles can also be explored. One solution is to enable truck platoons with discretionary lane changing so that they can change lanes in anticipation of possible conflicts with the merging traffic. Future research should develop a discretionary lane-change controller for truck platoons which may also include other incentives such as gain in speed. This strategy might be effective in HTI to improve both traffic efficiency and safety. The other solution may come from highway management agencies. They may consider extending the length of the acceleration lane. However, such a solution might not be effective, as merging conflicts can still occur if arrival times of truck platoons and ramp traffic are synchronous.

Our findings suggest that truck platooning on mainline carriageways seems to be detrimental to traffic efficiency and safety in HTI. On the A15 motorway in the Netherlands with successive discontinuities, transporting containers out of the port area in tight platoons seems to be feasible in LTI or night hours. Disengagement of platoons near motorway discontinuous might be a possibility in HTI. Future research can also leverage the potential of communication and technological innovations to alleviate merging conflicts. Besides, a promising research direction can be to develop advanced and integrated traffic control measures. For instance, a lane-reservation scheme for truck platoons can be designed. It would, however, require a detailed analysis to quantify the impacts of reduced capacity and compare those with the gains. Another direction can be to utilize an integrated control measure by combining ramp metering with mainline traffic controls such as variable speed limits.



## 7 Conclusions

The final chapter first summarizes the main findings in section 7.1 and presents overall conclusions in section 7.2. Next, section 7.3 provides directions for future research. Finally, section 7.4 presents recommendations for practical use.

### 7.1 Main findings

This section first summarizes the main findings and then presents overall conclusions.

*How can characteristics of on-trip route choice behavior of trucks be estimated from sparse datasets? (Chapter 2)*

To address this research question, we propose a novel approach based on data fusion and bi-objective optimization. The estimation approach is framed as a bi-objective optimization problem where a (truck) driver is hypothesized to choose a most likely route that will (1) maximize his/her perceived utility and (2) minimize the deviation his/her experienced (computed from Bluetooth time stamps) and estimated (derived from loop detector data) travel times. This approach enables us to jointly estimate route choice characteristics for trucks and infer their actual route choices. After applying this approach to the Bluetooth dataset obtained from the port of Rotterdam in the Netherlands, we find that truck drivers can be segmented into four groups to better capture their route choices regarding their preferences to travel distance, expected travel time to destination, the unreliability of travel times at the time of departure, and route overlaps. Having captured the time-of-day effects, our findings indicate that not all truck drivers are risk-averse as a majority (around 85%) of truck drivers, who belong to the three segments, tends to trade-off travel times with its unreliability during off-peak hours. However, their route choice decisions improve during peak hours as nearly three-fourths of them, who belong to two segments, prefer routes with reliable travel times. Another significant aspect of our findings is that around two-thirds of truck drivers prefer routes with a high degree of overlaps, which indicates that they value the availability of a large number of alternatives to minimize uncertainty during their trips.

*How can merging and diverging strategies of truck drivers be identified? (Chapter 3)*

This research question is addressed by analyzing a trajectory dataset, collected for the Netherlands, that contains a sufficient number of merging and diverging maneuvers of truck drivers at ramps and weaving sections. The finite mixture modeling technique is applied to cluster truck drivers into distinct homogeneous subgroups with respect to their merging and diverging maneuvers on a feature set that includes their spatial, temporal, kinematic, and gap acceptance attributes. The clustering analysis reveals that truck drivers can be segmented into two and three subgroups based on their merging and diverging strategies, respectively. Furthermore, the number of subgroups with respect to merging or diverging is identical over different topologies such as ramps and weaving sections. Concerning merging strategies, a majority of truck drivers (60-70%) show an affinity to initiate merging maneuvers as early as possible by accepting the largest gaps available to them. The minority subgroup, on the other hand, comprises truck drivers who either could not find suitable gaps earlier or intentionally accept smaller gaps later on. Turning now to diverging strategies, truck drivers belonging to the first subgroup start exiting the mainline carriageway before the beginning of a bottleneck. Those belonging to the second subgroup initiate diverging just after reaching a bottleneck. These two subgroups comprise nearly 80% of truck drivers. In contrast, the remaining 20% of them exit at a later stage even though the gap acceptance is not found to be a primary factor in this process. Our findings also indicate that merging or diverging at the earliest opportunity is the dominant strategy for truck drivers. At least 75% of merging or diverging maneuvers occur, in most of the analyzed sites, within the initial 25% of the ramp or weaving segment lengths; these actions lead to turbulence at the beginning of a freeway bottleneck.

*What attributes affect the gap selection process of truck drivers within their discretionary lane changing, in comparison with other vehicle classes? (Chapter 4)*

To answer this research question, we investigate and compare the gap selection (acceptance/rejection) process of multiple vehicle classes (passenger cars, delivery vans, and trucks) to identify key attributes that impact their selection of gaps within their discretionary lane changing activity. For this purpose, we use a comprehensive trajectory dataset that contains thousands of driving trajectories of multiple vehicle classes around on-ramps, off-ramps, and weaving sections. Further, the feature set is built around three dimensions that include the characteristics of a gap-seeking vehicle, its interactions with surrounding vehicles, and its perception of the road topology. Having accounted for historical driving experience (long-term temporal interdependencies) and class imbalance, gated recurrent unit neural network models are respectively trained for each vehicle class. These models can predict their gap selections with geometric mean accuracies of 84% or higher. By unraveling the latent gap selection mechanism of each vehicle class through explainable artificial intelligence techniques, we learn that significant differences exist between vehicle classes in terms of the saliency of historical driving experience and the importance of feature dimensions. We find that trucks value a longer duration (nearly up to 6 seconds) of recent driving experience, in contrast to passenger cars and delivery vans which mostly use up to 3 seconds of their recent driving experiences. By computing the feature importance, we find that trucks consider the proposed three-dimensional attributes space that includes their kinematics (speed), their interactions with the surroundings (gap spacing with the current leading vehicle), and their perception of topology during their gap selection process. In contrast, passenger cars focus on their kinematic features (speed, acceleration) and their interactions with surrounding vehicles (the speed difference with the lag vehicle in the target lane). Whereas delivery vans value their interactions (gap spacing with current and future leading vehicles) and the type of topology to select gaps.

*To what extent can a lane changing advisory system for multiple vehicle classes improve traffic efficiency? (Chapter 5)*

To answer this research question, we propose a lane changing advisory system which aims at balancing traffic flow distribution over available lanes by individually controlling lane changing behavior of multiple vehicle classes (passenger cars and truck drivers) to improve traffic efficiency in the vicinity of a merging section. The lane changing controller uses a multi-class multi-lane macroscopic traffic flow model and is designed as a feedback-feedforward control law based on a linear quadratic regulator. We use a response surface method to fine-tune the weights of the linear quadratic regulator. This enables us to develop a novel multi-class cooperative ITS application that generalizes traffic management and control schemes using vehicle-to-everything communication technology. After evaluating the performance of this application using a microscopic traffic simulator on a test merging section, our results indicate that this application significantly improves the travel time of the system by 21% by suppressing shockwaves and reducing the variance of travel times in the system. Furthermore, we find that this application generates significant travel time benefits for both mainline and ramp vehicles nearly up to 20% and 42%, respectively.

*What is the impact of truck platoons with different characteristics on traffic efficiency and safety around a freeway bottleneck? (Chapter 6)*

To address this research question, we propose and implement new controllers that govern the car following behavior of truck platoons in a microscopic simulation model. Our proposed controllers for truck platoons ensure their collision-free, string-stable, and smooth driving behavior. Using the simulation model, we evaluate the impact of truck platooning characteristics (namely market penetration rate, number of trucks in a platoon, intra-platoon headway, and platoon speed) on traffic efficiency and safety in the vicinity of a merging section using detailed sensitivity analyses at both local and global levels. Our findings indicate that truck platooning, being a part of the mainline traffic, generally deteriorates traffic efficiency and safety under high traffic intensity around a merging section. Truck platoons deteriorate the travel time of the system and merging capacity by nearly up to 16.50% and 5%, respectively. Further, safety-critical events in the presence of truck platoons get increased by around 130%. Simulation experiments also suggest that interactions among truck platooning characteristics contribute more (around 75%) to the uncertainty in the overall traffic efficiency and safety than the individual characteristic effects (around 25%) under high traffic intensity. Having analyzed individual contributions, we find that the market penetration of truck platoons in the system produces the largest impact on traffic and safety followed by intra-platoon headway and the number of trucks in a platoon. In light traffic intensity such as off-peak or night hours, however, truck platoons can be promising to deploy as they do not significantly affect traffic efficiency and safety around a freeway bottleneck.

## 7.2 Overall conclusions

The overall conclusion is that drivers show different on-trip behaviors. These differences not only occur between drivers of multiple vehicle classes (e.g., passenger cars, delivery vans, and truck drivers) but also within drivers belonging to a single vehicle class. In this respect, inter-driver heterogeneity is observed in the strategic and tactical behavior of truck drivers and this heterogeneity can be useful to explain inefficiencies in their on-trip behavioral decisions. The existing traffic models can benefit by acknowledging and modeling vehicle-class specific driving behavior as well as incorporating different driver types within one vehicle class. By harnessing driver heterogeneity, a multi-class control strategy for the tactical level has been shown to improve traffic efficiency in terms of travel times of both mainline and ramp vehicles



around a freeway bottleneck. The tactical control method is promising to mitigate bottleneck congestion by reducing the variance of travel times. In turn, it will improve the reliability of routes that would lead to positively influencing strategic choices of truck drivers. Further, operational control in the form of deploying optimal truck platooning configurations can also boost traffic efficiency and safety.

## 7.3 Recommendations for further research

This section outlines recommendations for further research. In line with the research in this dissertation, we subdivide these recommendations in terms of strategical, tactical and operational behaviors of truck drivers, and close with a few recommendations pertaining to integrated modeling of these.

### 7.3.1 Strategic driving behavior

- *Estimation of advanced commodity-specific on-trip route choice models:* This dissertation proposes a novel approach that can be useful to estimate route choice characteristics from sparse datasets. This approach has enabled us to understand the route choice behavior of trucks where we do not differentiate between commodities. This approach can also be used to develop advanced commodity-specific route choice models by utilizing (sparse) travel diaries of freight commodities. These advanced models would make it possible to unravel how road freight moves on freeways in more detail.
- *Comparison of on-trip route choice characteristics of passenger car and truck drivers:* The Bluetooth dataset used in this dissertation can also be useful to develop on-trip route choice models for passenger car drivers. This may enable a comparison of route choice characteristics of truck drivers with those of passenger car drivers. This would be an important step in developing advanced on-trip route choice models to support multi-class traffic assignment to capture realistic traffic dynamics on freeway networks.
- *Improvement of the proposed approach that uses sparse datasets to estimate on-trip route choice models by incorporating panel effects:* The bi-objective optimization program could be improved to account for panel effects since they can capture heterogeneity within the route choice behavior of an individual truck driver. This would also allow us to compare the results of the latent class route choice model with that of a random-effects mixed logit model accounting for panel effects.
- *Development of segment-specific route guidance strategies:* Chapter 1 showed that truck drivers can be segmented into four groups with respect to their on-trip route choice characteristics. A promising research direction would be to develop segment-specific route guidance strategies to improve operations of road freight on freeways.

### 7.3.2 Tactical driving behavior

- *Comparison of heterogeneity between multiple vehicle classes with respect to their merging and diverging maneuvers:* The trajectory dataset used in this dissertation can also be useful to investigate heterogeneity with respect to the merging and diverging process of other vehicle classes such as passenger cars and delivery vans. This would allow us to develop multi-class driving behavior models to accurately perform traffic and safety assessments around freeway bottlenecks.
- *Development of a merge/diverge assistance system for truck drivers:* Chapter 3 showed that truck drivers tend to merge or diverge at the earliest available opportunity. This might cause turbulence at the beginning of freeway bottlenecks. A merge and diverge

assistance system could be developed aimed at reducing turbulence by optimizing the spatial distribution of merge and diverge maneuvers.

- *Comparison of merging and diverging process of truck drivers with other countries:* Chapter 3 studies the merging and diverging process of truck drivers operating within the Netherlands. A similar study could be performed on data collected for other countries with different driving behavior regulations. Such comparison across international truck drivers would allow us to design tools to improve current traffic models and also to improve traffic and safety assessments.
- *Development of an integrated discretionary lane changing model for truck drivers:* Truck drivers, in general, follow a structured hierarchy to perform their discretionary lane changing from selecting a target lane to executing the required maneuver. Since elements of the hierarchy are interconnected, an integrated discretionary lane changing model could be developed to realistically capture lane changing phenomenon.
- *Development of autonomous lane changing assistance systems for multiple vehicle classes:* Chapter 4 develops three gated recurrent unit neural network models to study the gap selection processes of multiple vehicle classes. These models can be further improved to develop autonomous lane changing assistance systems that are aimed to improve traffic safety.
- *Expansion of the case study on lane changing advisory system:* The case study of Chapter 5 includes two vehicle classes, namely passenger cars and trucks. The performance of the lane changing advisory system could be evaluated by incorporating other vehicle classes such as delivery vans, automated passenger cars or truck platoons. This system could also be useful to mitigate the negative aspects arising from the introduction of truck platoons at merging sections as explored in Chapter 6.
- *Analysis of the effects of varying compliance on the performance of the lane changing advisory system:* The case study of Chapter 5 assumes perfect compliance for road users. Analysis of the acceptance of the road users towards multi-class lane changing advisory system and therefore the partial compliance of them would lead to more realistic results. The study on varying compliance could also be used to reflect on the required penetration of connected vehicles to achieve desired performance from the lane changing advisory system.
- *Generalization of the lane changing advisory system to other freeway bottlenecks:* The lane changing advisory system is formulated for the merging section in Chapter 5. The formulation could be generalized to account for exiting traffic in order to apply it to other freeway bottlenecks such as off-ramps and weaving sections.
- *Development of an integrated lane changing controller:* Controls for freeway traffic are usually operated independently. A promising extension of Chapter 5 would be to integrate the multi-class lane changing advisory system with other control strategies such as a multi-class ramp metering system (Schreiter, 2013). Coordination of these two multi-class systems could improve traffic situations around merging sections.

### 7.3.3 Operational driving behavior

- *Expansion of the case study on truck platooning:* The case study presented in Chapter 6 is focused on a merging section. A similar case study could be performed around off-ramps and weaving sections to evaluate the traffic and safety impacts of the truck platooning application. In addition, truck platooning is likely to be deployed alongside automated vehicles. The case study could also take into account automated vehicles in the traffic mix to realistically capture traffic and safety impacts.

- *Evaluation of truck platooning impacts in realistic communication environments:* Chapter 6 assumes perfect and robust vehicle-to-vehicle communication that enables truck platooning application. The case study of chapter 6 would lead to realistic results in communication environments that are prone to uncertainties or vulnerabilities. Vehicular ad-hoc network simulators such as OTS-Artery (Sharma et al., 2021) could be useful to conduct these types of evaluations.

### 7.3.4 Integrated traffic models

- *Development of a multi-class traffic assignment model:* A promising idea for future research can be to integrate strategic, tactical and operational behavior models and control strategies proposed in this dissertation to develop a multi-class traffic assignment model. This model can be useful to accurately reproduce traffic dynamics on freeways with a high share of trucks.
- *Integration of a multi-class traffic assignment model with a port terminal model:* A multi-class traffic model can be integrated with a port terminal model to replicate the truck appointment system (or slot-allocation) and evaluate its impacts on congestion.

## 7.4 Recommendations for practical use

This dissertation provides tools to support the decision-making of traffic management agencies, trucking companies, and port authorities in order to achieve improved operations of road freight on freeways and also to mitigate congestion. Several behavioral models and control strategies have been developed in this dissertation; this section provides recommendations for their practical use.

- *Estimation of route choice models from automatic vehicle identification (AVI) data*  
The novel approach proposed in this dissertation to estimate route choice models from sparse datasets might open new possibilities to conduct behavioral investigations from readily available automatic vehicle identification data (camera, Bluetooth, or travel diaries), that too in a cost-effective manner.
- *Opportunity to revisit freeway design guidelines*  
Freeway bottlenecks are the main source of congestion. This dissertation showed that a majority of truck drivers and also drivers belonging to other vehicle classes merge or diverge at the beginning of freeway bottlenecks. The required lengths, prescribed in the freeway design guidelines, are seldom used by drivers to change lanes. Creating longer weaving sections might not bring any additional benefits. Therefore, guidelines should give due attention to the multi-class nature of traffic and it would be worthwhile to revisit the required distance for freeway bottlenecks.
- *Development of advanced driver assistance systems*  
Lane changing largely influences traffic dynamics and safety around freeway bottlenecks. Chapter 4 has presented multi-class gap selection models; Our findings could also be of significant interest to technology providers to design advanced driver assistance or safety systems to assist lane changing of drivers.
- *Application to simulation packages, real-time traffic management, and strategic planning systems*

Our findings can be implemented in current simulation packages to realistically capture traffic phenomena in order to support accurate and realistic traffic and safety assessments. In addition, these models could be useful for next-generation real-time dynamic traffic assignment systems that support traffic management. Furthermore, the route choice model of truck drivers can also be used for strategic planning through its implementation in the national model system (LMS) of the Netherlands and a hybrid simulation-based model used by the port of Rotterdam.

- *Significant improvement of traffic efficiency around a freeway bottleneck*

To mitigate congestion around a merging section, this dissertation showed that the multi-class lane changing advisory system based on cooperative ITS is found to be beneficial for both mainline and ramp vehicles. These generalized control schemes would be worthwhile to implement on significant freight corridors that witness a high share of trucks in the traffic mix. This type of cooperative ITS application requires vehicle-to-everything infrastructure to be installed. Once installed, this could also be used by numerous other traffic and safety-critical cooperative ITS applications.

- *Criteria necessary for successful market deployment of truck platoons*

We provide criteria such as traffic conditions and optimal truck platooning characteristics necessary for the successful market deployment of truck platoons. Concerning traffic conditions, this dissertation suggests that truck platooning on mainline carriageways is detrimental to traffic efficiency and safety in high traffic intensity. On major freight corridors such as A15 in the Netherlands, where successive bottlenecks are located, transporting containers out of the port area in tight platoons seems to be feasible in light traffic intensity or night hours. Regrading optimal characteristics, the results from sensitivity analysis could also be useful to create optimal truck platooning configurations by considering their traffic and safety impacts.



## Bibliography

- AGHABAYK, K., MORIDPOUR, S., YOUNG, W., SARVI, M. & WANG, Y.-B. 2011. Comparing heavy vehicle and passenger car lane-changing maneuvers on arterial roads and freeways. *Transportation Research Record: Journal of the Transportation Research Board*, 94-101.
- AGHAEI, J., AMJADY, N. & SHAYANFAR, H. A. 2011. Multi-objective electricity market clearing considering dynamic security by lexicographic optimization and augmented epsilon constraint method. *Applied Soft Computing*, 11, 3846-3858.
- AHMED, K. I. 1999. *Modeling drivers' acceleration and lane changing behavior*. Massachusetts Institute of Technology.
- AHN, S., VADLAMANI, S. & LAVAL, J. 2013. A method to account for non-steady state conditions in measuring traffic hysteresis. *Transportation Research Part C: Emerging Technologies*, 34, 138-147.
- AMIN, M. R. & BANKS, J. H. 2005. Variation in Freeway Lane Use Patterns with Volume, Time of Day, and Location. *Transportation Research Record*, 1934, 132-139.
- AMPL. 2019. *Streamlined Modeling for Real Optimization* [Online]. Available: <https://ampl.com/> [Accessed].
- ANDERSON, M. K., NIELSEN, O. A. & PRATO, C. G. 2017. Multimodal route choice models of public transport passengers in the Greater Copenhagen Area. *EURO Journal on Transportation and Logistics*, 6, 221-245.
- ARCHER, J. 2005. Indicators for traffic safety assessment and prediction and their application in micro-simulation modelling: A study of urban and suburban intersections.
- ARENTZE, T., FENG, T., TIMMERMANS, H. & ROBROEKS, J. 2012. Context-dependent influence of road attributes and pricing policies on route choice behavior of truck drivers: Results of a conjoint choice experiment. *Transportation*, 39, 1173-1188.
- ATRI 2021. *Critical Issues in the Trucking Industry - 2021*. Arlington, VA: American Transportation Research Institute.

- BALAL, E., CHEU, R. L. & SARKODIE-GYAN, T. 2016. A binary decision model for discretionary lane changing move based on fuzzy inference system. *Transportation Research Part C: Emerging Technologies*, 67, 47-61.
- BAŞ, D. & BOYACI, İ. H. 2007. Modeling and optimization I: Usability of response surface methodology. *Journal of Food Engineering*, 78, 836-845.
- BEKIARIS-LIBERIS, N., RONCOLI, C. & PAPAGEORGIOU, M. 2017. Highway traffic state estimation per lane in the presence of connected vehicles. *Transportation Research Part B: Methodological*, 106, 1-28.
- BEN-AKIVA, M. & BIERLAIRE, M. 1999. Discrete choice methods and their applications to short term travel decisions. *Handbook of transportation science*. Springer.
- BEN-AKIVA, M. & BIERLAIRE, M. 2003. Discrete Choice Models with Applications to Departure Time and Route Choice. In: HALL, R. W. (ed.) *Handbook of Transportation Science*. Boston, MA: Springer US.
- BEN-AKIVA, M. E., TOLEDO, T., SANTOS, J., COX, N., ZHAO, F., LEE, Y. J. & MARZANO, V. 2016. Freight data collection using GPS and web-based surveys: Insights from US truck drivers' survey and perspectives for urban freight. *Case Studies on Transport Policy*, 4, 38-44.
- BHOOPALAM, A. K., AGATZ, N. & ZUIDWIJK, R. 2018. Planning of truck platoons: A literature review and directions for future research. *Transportation Research Part B: Methodological*, 107, 212-228.
- BIERLAIRE, M. 2020. A short introduction to pandasbiogeme. *Technical report TRANSP-OR 200605*.
- BIERLAIRE, M. & FREJINGER, E. 2008. Route choice modeling with network-free data. *Transportation Research Part C: Emerging Technologies*, 16, 187-198.
- BOGERS, E. A. I. & VAN ZUYLEN, H. J. The importance of reliability in route choices in freight transport for various actors on various levels. European Transport Conference, 2004. 149-161.
- BONMIN. 2019. *Bonmin (Basic Open-source Nonlinear Mixed INteger programming) - COIN-OR project* [Online]. Available: <https://projects.coin-or.org/Bonmin> [Accessed].
- BORGONOVO, E. 2007. A new uncertainty importance measure. *Reliability Engineering & System Safety*, 92, 771-784.
- BURNHAM, K. P. & ANDERSON, D. R. 2004. Multimodel inference: understanding AIC and BIC in model selection. *Sociological Methods & Research*, 33, 261-304.
- CALVERT, S. C., SCHAKEL, W. J. & VAN AREM, B. 2019. Evaluation and modelling of the traffic flow effects of truck platooning. *Transportation Research Part C: Emerging Technologies*, 105, 1-22.
- CAO, Q., REN, G., LI, D., MA, J. & LI, H. 2020. Semi-supervised route choice modeling with sparse Automatic vehicle identification data. *Transportation Research Part C: Emerging Technologies*, 121, 102857.
- CASSIDY, M. J. & BERTINI, R. L. 1999. Some traffic features at freeway bottlenecks. *Transportation Research Part B: Methodological*, 33, 25-42.
- CASSIDY, M. J. & RUDJANAKANOKNAD, J. 2005. Increasing the capacity of an isolated merge by metering its on-ramp. *Transportation Research Part B: Methodological*, 39, 896-913.
- CHEN, D. & AHN, S. 2018. Capacity-drop at extended bottlenecks: Merge, diverge, and weave. *Transportation Research Part B: Methodological*, 108, 1-20.
- CHO, K., VAN MERRIENBOER, B., GULCEHRE, C., BOUGARES, F., SCHWENK, H. & BENGIO, Y. Learning phrase representations using RNN encoder-decoder for statistical machine translation. Conference on Empirical Methods in Natural Language Processing (EMNLP 2014), 2014.

- CHOUHDARY, R. & SHUKLA, S. 2021. A clustering based ensemble of weighted kernelized extreme learning machine for class imbalance learning. *Expert Systems with Applications*, 164, 114041.
- CLEVELAND, W. S. & DEVLIN, S. J. 1988. Locally Weighted Regression: An Approach to Regression Analysis by Local Fitting. *Journal of the American Statistical Association*, 83, 596-610.
- COIFMAN, B. & LI, L. 2017. A critical evaluation of the Next Generation Simulation (NGSIM) vehicle trajectory dataset. *Transportation Research Part B: Methodological*, 105, 362-377.
- DAGANZO, C. F. 2011. On the macroscopic stability of freeway traffic. *Transportation Research Part B: Methodological*, 45, 782-788.
- DAS, S., PAN, I., HALDER, K., DAS, S. & GUPTA, A. 2013. LQR based improved discrete PID controller design via optimum selection of weighting matrices using fractional order integral performance index. *Applied Mathematical Modelling*, 37, 4253-4268.
- DENG, Q. 2016. A general simulation framework for modeling and analysis of heavy-duty vehicle platooning. *IEEE Transactions on Intelligent Transportation Systems*, 17, 3252--3262.
- ECKHARDT, J., AARTS, L., VAN VLIET, A. & ALKIM, T. 2016. European truck platooning challenge 2016. *The Hague, Delta3*.
- ELAMRANI ABOU ELASSAD, Z., MOUSANNIF, H. & AL MOATASSIME, H. 2020. A proactive decision support system for predicting traffic crash events: A critical analysis of imbalanced class distribution. *Knowledge-Based Systems*, 205, 106314.
- EUROSTAT. 2021. *Freight transport statistics - modal split* [Online]. Available: [https://ec.europa.eu/eurostat/statistics-explained/index.php?title=Freight transport statistics - modal split](https://ec.europa.eu/eurostat/statistics-explained/index.php?title=Freight_transport_statistics_-_modal_split) [Accessed 09/06/2021 2021].
- FABER, T., SHARMA, S., SNELDER, M., KLUNDER, G., TAVASSZY, L. & VAN LINT, H. 2020. Evaluating Traffic Efficiency and Safety by Varying Truck Platoon Characteristics in a Critical Traffic Situation. *Transportation Research Record*, 2674, 525-547.
- FENG, T., ARENTZE, T. & TIMMERMANS, H. 2013. Capturing preference heterogeneity of truck drivers' route choice behavior with context effects using a latent class model. *European Journal of Transport and Infrastructure Research*, 13, 259-273.
- FUKUSHIMA, M. 2011. The latest trend of v2x driver assistance systems in Japan. *Computer Networks*, 55, 3134-3141.
- GIPPS, P. G. 1986. A model for the structure of lane-changing decisions. *Transportation Research Part B: Methodological*, 20, 403-414.
- GOLOB, T. F., RECKER, W. W. & ALVAREZ, V. M. 2004. Freeway safety as a function of traffic flow. *Accident Analysis & Prevention*, 36, 933-946.
- HABIB, M., KHOUCHA, F. & HARRAG, A. 2017. GA-based robust LQR controller for interleaved boost DC–DC converter improving fuel cell voltage regulation. *Electric Power Systems Research*, 152, 438-456.
- HAMBY, D. M. 1994. A review of techniques for parameter sensitivity analysis of environmental models. *Environmental monitoring and assessment*, 32, 135--154.
- HASSANI, K. & LEE, W.-S. 2016. Multi-objective design of state feedback controllers using reinforced quantum-behaved particle swarm optimization. *Applied Soft Computing*, 41, 66-76.
- HERMAN, J. & USHER, W. 2017. SALib: an open-source Python library for sensitivity analysis. *Journal of Open Source Software*, 2, 97.



- HERRERA, J. C. & BAYEN, A. M. 2010. Incorporation of Lagrangian measurements in freeway traffic state estimation. *Transportation Research Part B: Methodological*, 44, 460-481.
- HESS, S., QUDDUS, M., RIESER-SCHÜSSLER, N. & DALY, A. 2015. Developing advanced route choice models for heavy goods vehicles using GPS data. *Transportation Research Part E: Logistics and Transportation Review*, 77, 29-44.
- HOCHREITER, S. & SCHMIDHUBER, J. 1997. Long Short-Term Memory. *Neural Computation*, 9, 1735-1780.
- HOOOPER, A. 2018. *Cost of Congestion to the Trucking Industry: 2018 Update*, American Transportation Research Institute (ATRI).
- HORST, R. 1991. Time-to-collision as a cue for decision-making in braking. *Vision in Vehicles--III*.
- HSU, H. C. H. A. L. A. 2004. Platoon lane change maneuvers for automated highway systems.
- HUANG, X., SUN, J. & SUN, J. 2018. A car-following model considering asymmetric driving behavior based on long short-term memory neural networks. *Transportation Research Part C: Emerging Technologies*, 95, 346-362.
- JOHNSON, M. A. & GRIMBLE, M. J. 1987. Recent trends in linear optimal quadratic multivariable control system design. *IEE Proceedings D - Control Theory and Applications*, 134, 53-71.
- KAMALI, M., ERMAGUN, A., VISWANATHAN, K. & PINJARI, A. R. 2016. Deriving Truck Route Choice from Large GPS Data Streams. *Transportation Research Record: Journal of the Transportation Research Board*, 62-70.
- KANAZAWA, F., KANOSHIMA, H., SAKAI, K. & SUZUKI, K. 2010. Field operational tests of Smartway in Japan. *IATSS Research*, 34, 31-34.
- KEYVAN-EKBATANI, M., KNOOP, V. L. & DAAMEN, W. 2016. Categorization of the lane change decision process on freeways. *Transportation Research Part C: Emerging Technologies*, 69, 515-526.
- KINGMA, D. P. & BA, J. Adam: A Method for Stochastic Optimization. ICLR, 2015.
- KNOOP, V. L., DURET, A., BUISSON, C. & VAN AREM, B. Lane distribution of traffic near merging zones influence of variable speed limits. 2010 13th IEEE International Conference on Intelligent Transportation Systems (ITSC), 19-22 Sept. 2010. IEEE, 485-490.
- KNORRING, J. H., HE, R. & KORNHAUSER, A. L. 2005. Analysis of route choice decisions by long-haul truck drivers. *Transportation Research Record*, 46-60.
- KONDYLI, A. & ELEFTERIADOU, L. 2012. Driver behavior at freeway-ramp merging areas based on instrumented vehicle observations. *Transportation Letters*, 4, 129-142.
- KRAJEWSKI, R., BOCK, J., KLOEKER, L. & ECKSTEIN, L. The highD Dataset: A Drone Dataset of Naturalistic Vehicle Trajectories on German Highways for Validation of Highly Automated Driving Systems. 2018 21st International Conference on Intelligent Transportation Systems (ITSC), 4-7 Nov. 2018. 2118-2125.
- LAMMERT, M. P., DURAN, A., DIEZ, J., BURTON, K. & NICHOLSON, A. 2014. Effect of platooning on fuel consumption of class 8 vehicles over a range of speeds, following distances, and mass. National Renewable Energy Lab.(NREL), Golden, CO (United States).
- LAVAL, J. A. & DAGANZO, C. F. 2006. Lane-changing in traffic streams. *Transportation Research Part B: Methodological*, 40, 251-264.
- LEE, C., HELLINGA, B. & SACCOMANNO, F. 2003a. Proactive freeway crash prevention using real-time traffic control. 30, 1034-1041.

- LEE, C., HELLINGA, B. & SACCOMANNO, F. 2003b. Real-Time Crash Prediction Model for Application to Crash Prevention in Freeway Traffic. 1840, 67-77.
- LEE, J. & CASSIDY, M. J. 2008. An Empirical and Theoretical Study of Freeway Weave Bottlenecks. University of California Transportation Center.
- LI, G. 2018. Application of Finite Mixture of Logistic Regression for Heterogeneous Merging Behavior Analysis. *Journal of Advanced Transportation*, 2018, 1436521.
- LI, G. & SUN, L. 2018. Characterizing Heterogeneity in Drivers' Merging Maneuvers Using Two-Step Cluster Analysis. *Journal of Advanced Transportation*, 2018, 5604375.
- LI, X. & SUN, J.-Q. 2017. Studies of vehicle lane-changing dynamics and its effect on traffic efficiency, safety and environmental impact. *Physica A: Statistical Mechanics and its Applications*, 467, 41-58.
- LI, Y., XING, L., WANG, W., WANG, H., DONG, C. & LIU, S. 2017a. Evaluating impacts of different longitudinal driver assistance systems on reducing multi-vehicle rear-end crashes during small-scale inclement weather. *Accident Analysis & Prevention*, 107, 63-76.
- LI, Y., XU, C., XING, L. & WANG, W. 2017b. Integrated Cooperative Adaptive Cruise and Variable Speed Limit Controls for Reducing Rear-End Collision Risks Near Freeway Bottlenecks Based on Micro-Simulations. *IEEE Transactions on Intelligent Transportation Systems*, 18, 3157-3167.
- LI, Z., AHN, S., CHUNG, K., RAGLAND, D. R., WANG, W. & YU, J. W. 2014. Surrogate safety measure for evaluating rear-end collision risk related to kinematic waves near freeway recurrent bottlenecks. *Accident Analysis & Prevention*, 64, 52-61.
- LIANG, L., YUAN, J., ZHANG, S. & ZHAO, P. 2018. Design a software real-time operation platform for wave piercing catamarans motion control using linear quadratic regulator based genetic algorithm. *PLOS ONE*, 13, e0196107.
- LITTLE, T. D. 2013. *The Oxford handbook of quantitative methods in psychology: Vol. 2: statistical analysis*, Oxford University Press.
- LU, X.-Y., HEDRICK, J. K. & DREW, M. ACC/CACC-control design, stability and robust performance. Proceedings of the 2002 American Control Conference (IEEE Cat. No. CH37301), 2002. IEEE, 4327-4332.
- LUONG, T. D., TAHLYAN, D. & PINJARI, A. R. 2018. Comprehensive Exploratory Analysis of Truck Route Choice Diversity in Florida. *Transportation Research Record*.
- MARKANTONAKIS, V., SKOUFOULAS, D. I., PAPAMICHAIL, I. & PAPAGEORGIOU, M. 2019. Integrated Traffic Control for Freeways using Variable Speed Limits and Lane Change Control Actions. *Transportation Research Record: Journal of the Transportation Research Board*, 2673, 602-613.
- MCKAY, M. D., BECKMAN, R. J. & CONOVER, W. J. 1979. A Comparison of Three Methods for Selecting Values of Input Variables in the Analysis of Output from a Computer Code. *Technometrics*, 21, 239-245.
- MENENDEZ, M. & HE, H. 2017. Final report on project WEAVE-Capacity and level of service for freeway weaving areas. *Technical Report VSS*, 2011.
- MESA-ARANGO, R. & FABREGAS, A. 2017. Traffic impact of automated truck platoons in highway exits. *Transport Infrastructure and Systems*. CRC Press.
- MICHON, J. A. 1985. A Critical View of Driver Behavior Models: What Do We Know, What Should We Do? In: EVANS, L. & SCHWING, R. C. (eds.) *Human Behavior and Traffic Safety*. Boston, MA: Springer US.
- MILANÉS, V. & SHLADOVER, S. E. 2014. Modeling cooperative and autonomous adaptive cruise control dynamic responses using experimental data. *Transportation Research Part C: Emerging Technologies*, 48, 285-300.

- MONTANARO, U., TUFO, M., FIENGO, G., DI BERNARDO, M., SALVI, A. & SANTINI, S. Extended cooperative adaptive cruise control. 2014 IEEE Intelligent Vehicles Symposium Proceedings, 2014. IEEE, 605-610.
- MORIDPOUR, S. 2017. *Modelling heavy vehicle lane changing*.
- MORIDPOUR, S., MAZLOUMI, E. & MESBAH, M. 2015. Impact of heavy vehicles on surrounding traffic characteristics. *Journal of advanced transportation*, 49, 535-552.
- MORIDPOUR, S., SARVI, M., ROSE, G. & MAZLOUMI, E. 2012. Lane-changing decision model for heavy vehicle drivers. *Journal of Intelligent Transportation Systems*, 16, 24-35.
- MUELLER, S. 2012. The Impact of Electronic Coupled Heavy Trucks on Traffic Flow.
- MURRAY-TUITE, P. 2008. Evaluation of strategies to increase transportation system resilience to congestion caused by incidents. *Mid-Atlantic University Transportation Center*.
- MYERS, R. H., KIM, Y. & GRIFFITHS, K. L. 1997. Response Surface Methods and the Use of Noise Variables. *Journal of Quality Technology*, 29, 429-440.
- NADI, A. 2022. *Data Driven Modelling of Routing and Scheduling in Freight Transport*. PhD, Delft University of Technology.
- NAMAKI ARAGHI, B., KRISHNAN, R. & LAHRMANN, H. 2016. Mode-Specific Travel Time Estimation Using Bluetooth Technology. *Journal of Intelligent Transportation Systems*, 20, 219-228.
- NG, C., SUSILAWATI, S., KAMAL, M. A. S. & CHEW, I. M. L. 2020. Development of a binary logistic lane change model and its validation using empirical freeway data. *Transportmetrica B: Transport Dynamics*, 8, 49-71.
- OKA, H., HAGINO, Y., KENMOCHI, T., TANI, R., NISHI, R., ENDO, K. & FUKUDA, D. 2019. Predicting travel pattern changes of freight trucks in the Tokyo Metropolitan area based on the latest large-scale urban freight survey and route choice modeling. *Transportation Research Part E: Logistics and Transportation Review*.
- OSSEN, S., HOOGENDOORN, S. P. & GORTE, B. G. H. 2006. Interdriver Differences in Car-Following: A Vehicle Trajectory-Based Study. *Transportation Research Record*, 1965, 121-129.
- PAN, T., LAM, W. H., SUMALEE, A. & ZHONG, R. 2016. Modeling the impacts of mandatory and discretionary lane-changing maneuvers. *Transportation research part C: emerging technologies*, 68, 403-424.
- PANG, M.-Y., JIA, B., XIE, D.-F. & LI, X.-G. 2020. A probability lane-changing model considering memory effect and driver heterogeneity. *Transportmetrica B: Transport Dynamics*, 8, 72-89.
- PAPADOPOULOU, S., RONCOLI, C., BEKIARIS-LIBERIS, N., PAPAMICHAIL, I. & PAPAGEORGIOU, M. 2018. Microscopic simulation-based validation of a per-lane traffic state estimation scheme for highways with connected vehicles. *Transportation Research Part C: Emerging Technologies*, 86, 441-452.
- PEETA, S., RAMOS, J. L. & PASUPATHY, R. 2000. Content of variable message signs and on-line driver behavior. *Freight Travel Behavior, Route Choice Behavior, And Advanced Traveler Information Systems: Planning And Administration*. 500 FIFTH ST, NW, WASHINGTON, DC 20001 USA: Transportation Research Board Natl Research Council.
- PENG, Y., LI, C., WANG, K., GAO, Z. & YU, R. 2020. Examining imbalanced classification algorithms in predicting real-time traffic crash risk. *Accident Analysis & Prevention*, 144, 105610.
- PUNZO, V., BORZACCHIELLO, M. T. & CIUFFO, B. 2011. On the assessment of vehicle trajectory data accuracy and application to the Next Generation SIMulation (NGSIM)

- program data. *Transportation Research Part C: Emerging Technologies*, 19, 1243-1262.
- RAHMAN, M., CHOWDHURY, M., XIE, Y. & HE, Y. 2013. Review of Microscopic Lane-Changing Models and Future Research Opportunities. *IEEE Transactions on Intelligent Transportation Systems*, 14, 1942-1956.
- RAMEZANI, H., SHLADOVER, S. E., LU, X.-Y. & ALTAN, O. D. 2018. Micro-Simulation of Truck Platooning with Cooperative Adaptive Cruise Control: Model Development and a Case Study. *Transportation Research Record*, 2672, 55-65.
- RAMEZANI, M. & YE, E. 2019. Lane density optimisation of automated vehicles for highway congestion control. *Transportmetrica B: Transport Dynamics*, 7, 1096–1116.
- REGIOLAB-DELFT. 2019. *Regiolab-Delft: A DiTTLab project* [Online]. Available: <http://www.regiolab-delft.nl/> [Accessed].
- REYNOLDS, D. 2009. *Gaussian Mixture Models*, Boston, MA, Springer US.
- RIESER-SCHÜSSLER, N., BALMER, M. & AXHAUSEN, K. W. 2013. Route choice sets for very high-resolution data. *Transportmetrica A: Transport Science*, 9, 825-845.
- RONCOLI, C., BEKIARIS-LIBERIS, N. & PAPAGEORGIOU, M. 2016. Optimal lane-changing control at motorway bottlenecks. *IEEE*, 1785–1791-1785–1791.
- RONCOLI, C., BEKIARIS-LIBERIS, N. & PAPAGEORGIOU, M. Optimal lane-changing control at motorway bottlenecks. 2016 19th IEEE International Conference on Intelligent Transportation Systems (ITSC), 1-4 Nov. 2016 2016. *IEEE*, 1785-1791.
- RONCOLI, C., BEKIARIS-LIBERIS, N. & PAPAGEORGIOU, M. 2017. Lane-Changing Feedback Control for Efficient Lane Assignment at Motorway Bottlenecks. *Transportation Research Record: Journal of the Transportation Research Board*, 2625.
- ROWELL, M., GAGLIANO, A. & GOODCHILD, A. 2014. Identifying truck route choice priorities: The implications for travel models. *Transportation Letters*, 6, 98-106.
- SAEEDNIA, M. & MENENDEZ, M. 2017. A Consensus-Based Algorithm for Truck Platooning. *IEEE Transactions on Intelligent Transportation Systems*, 18, 404-415.
- SAIF, M. 1989. Optimal linear regulator pole-placement by weight selection. *International Journal of Control*, 50, 399-414.
- SANTINI, S., SALVI, A., VALENTE, A. S., PESCAPE, A., SEGATA, M. & CIGNO, R. L. 2016. A consensus-based approach for platooning with intervehicular communications and its validation in realistic scenarios. *IEEE Transactions on Vehicular Technology*, 66, 1985-1999.
- SARVI, M. & KUWAHARA, M. 2008. Using ITS to Improve the Capacity of Freeway Merging Sections by Transferring Freight Vehicles. *IEEE Transactions on Intelligent Transportation Systems*, 9, 580-588.
- SCHAKEL, W. J., KNOOP, V. L. & VAN AREM, B. 2012. Integrated Lane Change Model with Relaxation and Synchronization. *Transportation Research Record: Journal of the Transportation Research Board*, 2316, 47-57.
- SCHAKEL, W. J. & VAN AREM, B. 2014. Improving Traffic Flow Efficiency by In-Car Advice on Lane, Speed, and Headway. *IEEE Transactions on Intelligent Transportation Systems*, 15, 1597-1606.
- SCHAKEL, W. J., VAN AREM, B. & NETTEN, B. D. 2010. Effects of cooperative adaptive cruise control on traffic flow stability.
- SCHREITER, T. 2013. *Vehicle-class Specific Control of Freeway Traffic*. Doctoral dissertation, Delft University of Technology.
- SCHWARZ, G. 1978. Estimating the dimension of a model. *The annals of statistics*, 6, 461-464.

- SEO, T., KUSAKABE, T. & ASAKURA, Y. 2015. Estimation of flow and density using probe vehicles with spacing measurement equipment. *Transportation Research Part C: Emerging Technologies*, 53, 134-150.
- SHARMA, S., AL-KHANAK, E. N., RIEBL, R., SCHAKEL, W., KNOPPERS, P., VERBRAECK, A. & VAN LINT, J. Impact of radio channel characteristics on the longitudinal behaviour of truck platoons in critical car-following situations. Conference on Networked Systems 2021 (NetSys 2021), 2021. European Association of Software Science and Technology (EASST).
- SHARMA, S., SNELDER, M., TAVASSZY, L. & VAN LINT, H. 2020. Categorizing Merging and Diverging Strategies of Truck Drivers at Motorway Ramps and Weaving Sections using a Trajectory Dataset. *Transportation Research Record*, 2674, 855-866.
- SHARMA, S., SNELDER, M. & VAN LINT, H. Deriving on-trip route choices of truck drivers by utilizing Bluetooth data, loop detector data and variable message sign data. 6th International Conference on Models and Technologies for Intelligent Transportation Systems (MT-ITS), 5-7 June 2019 2019. 1-8.
- SHLADOVER, S. E., LU, X.-Y., SONG, B., DICKEY, S., NOWAKOWSKI, C., HOWELL, A., BU, F., MARCO, D., TAN, H.-S. & NELSON, D. 2006. Demonstration of automated heavy-duty vehicles.
- SHLADOVER, S. E., SU, D. & LU, X.-Y. 2012. Impacts of Cooperative Adaptive Cruise Control on Freeway Traffic Flow. *Transportation Research Record*, 2324, 63-70.
- SIMONYAN, K., VEDALDI, A. & ZISSERMAN, A. Deep inside convolutional networks: Visualising image classification models and saliency maps. In Workshop at International Conference on Learning Representations, 2014. Citeseer.
- SIUHI, S. & KASEKO, M. Parametric study of stimulus-response behavior for car-following models. Paper 10-1179. The 89th Annual Meeting of the Transportation Research Board Compendium of Papers, 2010.
- SJOBERG, K., ANDRES, P., BUBURUZAN, T. & BRAKEMEIER, A. 2017. Cooperative Intelligent Transport Systems in Europe: Current Deployment Status and Outlook. *IEEE Vehicular Technology Magazine*, 12, 89-97.
- SNELDER, M. 2016. *ToGRIP: GRIP on freight TRIPS*, Big Data: real time ICT for logistics – Compartment 2.
- SUBRAVETI, H. H. S. N., KNOOP, V. L. & VAN AREM, B. 2020. Improving Traffic Flow Efficiency at Motorway Lane Drops by Influencing Lateral Flows. *Transportation Research Record: Journal of the Transportation Research Board*, doi: 10.1177/0361198120948055.
- SULEJIC, D., JIANG, R., SABAR, N. R. & CHUNG, E. 2017. Optimization of lane-changing distribution for a motorway weaving segment. *Transportation Research Procedia*, 21, 227-239.
- SUN, D. J. & ELEFTERIADOU, L. 2011. Lane-changing behavior on urban streets: A focus group-based study. *Applied ergonomics*, 42, 682-691.
- SUN, D. J. & ELEFTERIADOU, L. 2012. Lane-Changing Behavior on Urban Streets: An “In-Vehicle” Field Experiment-Based Study. *Computer-Aided Civil and Infrastructure Engineering*, 27, 525-542.
- SUN, Y., TOLEDO, T., ROSA, K., BEN-AKIVA, M. E., FLANAGAN, K., SANCHEZ, R. & SPISSU, E. 2013. Route choice characteristics for truckers. *Transportation Research Record*, 115-121.
- TAALE, H. & WILMINK, I. 2016. Traffic in The Netherlands 2016 *TrafficQuest*.
- TAJDARI, F., RONCOLI, C., BEKIARIS-LIBERIS, N. & PAPAGEORGIOU, M. Integrated ramp metering and lane-changing feedback control at motorway bottlenecks. 2019 18th European Control Conference (ECC), 2019/06 2019. IEEE, 3179-3184.

- TAJDARI, F., RONCOLI, C. & PAPAGEORGIOU, M. 2020. Feedback-Based Ramp Metering and Lane-Changing Control With Connected and Automated Vehicles. *IEEE Transactions on Intelligent Transportation Systems*, doi: 10.1109/TITS.2020.3018873.
- TANG, L., WANG, H., ZHANG, W., MEI, Z. & LI, L. 2020. Driver Lane Change Intention Recognition of Intelligent Vehicle Based on Long Short-Term Memory Network. *IEEE Access*, 8, 136898-136905.
- TIENTRAKOOL, P., HO, Y.-C. & MAXEMCHUK, N. F. Highway capacity benefits from using vehicle-to-vehicle communication and sensors for collision avoidance. 2011 IEEE Vehicular Technology Conference (VTC Fall), 2011. IEEE, 1-5.
- TILG, G., YANG, K. & MENENDEZ, M. 2018. Evaluating the effects of automated vehicle technology on the capacity of freeway weaving sections. *Transportation Research Part C: Emerging Technologies*, 96, 3-21.
- TLN. 2020. *Economische Wegwijzer 2020* [Online]. Available: [https://www.tln.nl/app/uploads/2020/11/TLN\\_EcoWegwijzer\\_2020\\_A4\\_2P\\_DEF\\_RGB\\_HR.pdf](https://www.tln.nl/app/uploads/2020/11/TLN_EcoWegwijzer_2020_A4_2P_DEF_RGB_HR.pdf) [Accessed 07/01/2021 2021].
- TOLEDO, T., ATASOY, B., JING, P., DING-MASTERA, J., SANTOS, J. O. & BEN-AKIVA, M. 2020. Intercity truck route choices incorporating toll road alternatives using enhanced GPS data. *Transportmetrica A: Transport Science*, 16, 654-675.
- TOLEDO, T. & KATZ, R. 2009. State Dependence in Lane-Changing Models. *Transportation Research Record*, 2124, 81-88.
- TOLEDO, T., KOUTSOPOULOS, H. N. & BEN-AKIVA, M. E. 2003. Modeling Integrated Lane-Changing Behavior. *Transportation Research Record*, 1857, 30-38.
- TOLEDO, T., SUN, Y., ROSA, K., BEN-AKIVA, M., FLANAGAN, K., SANCHEZ, R. & SPISSU, E. 2013. Decision-Making Process and Factors Affecting Truck Routing. In: BEN-AKIVA, M., MEERSMAN, H. & VAN DE VOORDE, E. (eds.) *Freight Transport Modelling*.
- TREIBER, M., KESTING, A. & HELBING, D. 2006. Delays, inaccuracies and anticipation in microscopic traffic models. *Physica A: Statistical Mechanics and its Applications*, 360, 71-88.
- TSUGAWA, S., JESCHKE, S. & SHLADOVER, S. E. 2016. A Review of Truck Platooning Projects for Energy Savings. *IEEE Transactions on Intelligent Vehicles*, 1, 68-77.
- TUKEY, J. W. 1993. Exploratory data analysis. *Addison-Wesley series in behavioral science : quantitative methods*.
- UTGOFF, P. E. & STRACUZZI, D. J. 2002. Many-layered learning. *Neural computation*, 14, 2497-2529.
- VAN AREM, B., VAN DRIEL, C. J. G. & VISSER, R. 2006. The impact of cooperative adaptive cruise control on traffic-flow characteristics. *IEEE Transactions on intelligent transportation systems*, 7, 429--436.
- VAN BEINUM, A. 2018. Motorway Turbulence - Empirical Trajectory Data. 4TU centre for research data.
- VAN BEINUM, A., FARAH, H., WEGMAN, F. & HOOGENDOORN, S. 2018. Driving behaviour at motorway ramps and weaving segments based on empirical trajectory data. *Transportation Research Part C: Emerging Technologies*, 92, 426-441.
- VAN LINT, H. 2004. *Reliable travel time prediction for freeways: Bridging artificial neural networks and traffic flow theory*. PhD, Delft University of Technology.
- VAN LINT, H., SCHAKEL, W., TAMMINGA, G., KNOPPERS, P. & VERBRAECK, A. 2016. Getting the Human Factor into Traffic Flow Models: New Open-Source Design to Simulate Next Generation of Traffic Operations. *Transportation Research Record: Journal of the Transportation Research Board*, 2561, 25-33.

- VAN LINT, J. W. C. 2010. Empirical Evaluation of New Robust Travel Time Estimation Algorithms. *Transportation Research Record*, 2160, 50-59.
- VAN LINT, J. W. C. & CALVERT, S. C. 2018. A generic multi-level framework for microscopic traffic simulation—Theory and an example case in modelling driver distraction. *Transportation Research Part B: Methodological*, 117, 63-86.
- VAN LINT, J. W. C., HOOGENDOORN, S. P. & SCHREUDER, M. 2008a. Fastlane: New Multiclass First-Order Traffic Flow Model. *Transportation Research Record*, 2088, 177-187.
- VAN LINT, J. W. C., VAN ZUYLEN, H. J. & TU, H. 2008b. Travel time unreliability on freeways: Why measures based on variance tell only half the story. *Transportation Research Part A: Policy and Practice*, 42, 258-277.
- VANDERWERF, J., SHLADOVER, S., KOURJANSKAIA, N., MILLER, M. & KRISHNAN, H. 2001. Modeling Effects of Driver Control Assistance Systems on Traffic. *Transportation Research Record*, 1748, 167-174.
- VISSER, I. & SPEEKENBRINK, M. 2010. depmixS4: an R package for hidden Markov models. *Journal of statistical Software*, 36, 1-21.
- VITI, F., RINALDI, M., CORMAN, F. & TAMPE'RE, C. M. J. 2014. Assessing partial observability in network sensor location problems. *Transportation Research Part B: Methodological*, 70, 65-89.
- WANG, M., VAN MAARSEVEEN, S., HAPPEE, R., TOOL, O. & VAN AREM, B. 2019. Benefits and Risks of Truck Platooning on Freeway Operations Near Entrance Ramp. *Transportation Research Record*, 2673, 588-602.
- WU, N. 2006. Equilibrium of Lane Flow Distribution on Motorways. *Transportation Research Record: Journal of the Transportation Research Board*, 1965, 48-59.
- XIE, D.-F., FANG, Z.-Z., JIA, B. & HE, Z. 2019. A data-driven lane-changing model based on deep learning. *Transportation Research Part C: Emerging Technologies*, 106, 41-60.
- YANG, D., KUIJPERS, A., DANE, G. & VAN DER SANDE, T. 2019. Impacts of large-scale truck platooning on Dutch highways. *Transportation research procedia*, 37, 425-432.
- YUAN, Y., LINT, J. W. C. V., WILSON, R. E., WAGENINGEN-KESSELS, F. V. & HOOGENDOORN, S. P. 2012. Real-Time Lagrangian Traffic State Estimator for Freeways. *IEEE Transactions on Intelligent Transportation Systems*, 13, 59-70.
- YUAN, Y., VAN LINT, H., VAN WAGENINGEN-KESSELS, F. & HOOGENDOORN, S. 2014. Network-Wide Traffic State Estimation Using Loop Detector and Floating Car Data. *Journal of Intelligent Transportation Systems*, 18, 41-50.
- ZHANG, C., SABAR, N. R., CHUNG, E., BHASKAR, A. & GUO, X. 2019. Optimisation of lane-changing advisory at the motorway lane drop bottleneck. *Transportation Research Part C: Emerging Technologies*, 106, 303-316.
- ZHANG, S., ABDEL-ATY, M., WU, Y. & ZHENG, O. 2020. Modeling pedestrians' near-accident events at signalized intersections using gated recurrent unit (GRU). *Accident Analysis & Prevention*, 148, 105844.
- ZHANG, Y. & IOANNOU, P. A. 2017. Combined Variable Speed Limit and Lane Change Control for Highway Traffic. *IEEE Transactions on Intelligent Transportation Systems*, 18, 1812-1823.
- ZHENG, A. & CASARI, A. 2018. *Feature engineering for machine learning: principles and techniques for data scientists*, " O'Reilly Media, Inc."
- ZHENG, J., SUZUKI, K. & FUJITA, M. 2014. Predicting driver's lane-changing decisions using a neural network model. *Simulation Modelling Practice and Theory*, 42, 73-83.

- 
- ZHENG, Z. 2014. Recent developments and research needs in modeling lane changing. *Transportation Research Part B: Methodological*, 60, 16-32.
- ZIEGEL, E. R. 1997. Response Surfaces: Designs and Analyses. *Technometrics*, 39, 342-342.





## Summary

Congestion, a frequent problem on freeways, is often considered a major challenge for the operations of road freight transport. Trucks, the main choice for road freight, not only suffer from congestion but they also contribute to it. Consequently, billions of dollars are lost worldwide in trucking operations, which also impedes economic growth and prosperity. Understanding driving behavior and on-trip decision-making of truck drivers are critically important to design measures that mitigate the impacts of congestion on truck traffic, and vice versa, to design measures that mitigate the impacts of truck traffic on congestion. In this respect, the on-trip behavior of truck drivers can be decomposed—like driving behavior in general—into strategical, tactical, and operational behavior, depicting route choice, short-term path-planning (e.g. merging, lane changing), and the steering & accelerating of the vehicle, respectively. Whereas these on-trip behaviors have been studied in-depth for drivers of passenger cars, there are larger gaps in our knowledge when it comes to strategical, tactical and operational behavior of trucks. Furthermore, our limited insight into the driving behavior of truck drivers inhibits the design of appropriate traffic control and management measures.

To improve freight and traffic operations on freeways, this dissertation focuses on obtaining insights into the on-trip behavior of truck drivers and influencing this behavior for congestion relief. To this end, this dissertation develops new mathematical models and control methods for the strategical, tactical and operational behavior of truck drivers by analyzing emerging datasets and designing novel cooperative intelligent transportation system (C-ITS) applications.

Firstly, this dissertation focuses on the strategical behavior of truck drivers. We develop a novel approach to estimate characteristics of route choice behavior using automatic vehicle identification datasets that are sparse and lacks actual route choices of drivers (unlabeled). This proposed approach, which is based on data fusion and bi-objective optimization, can simultaneously infer actual route choices of drivers (labels) and estimate their characteristics. This approach is applied to study the on-trip route choice behavior of truck drivers through sparse Bluetooth and loop-detector datasets by accounting for inter-driver heterogeneity (i.e. taste variations) and time-of-day effects. We conclude that the proposed approach can be used to estimate route choice models from readily available sparse datasets.

Secondly, this dissertation investigates the tactical behavior of truck drivers by focusing on three elements. The first element is mandatory lane changing (i.e., merging and diverging) of truck drivers, a phenomenon observed around freeway bottlenecks and occurs due to a driver's necessity to follow a path leading to his/her destination. By applying finite mixture models on a large trajectory dataset, we conclude that inter-driver heterogeneity is observed in the merging and diverging behavior of truck drivers. The second element focuses on discretionary lane changing where we analyze the gap selection process of truck drivers, which is an important part of the lane changing process where a driver explicitly seeks a suitable and safe opportunity in order to initiate lane changing maneuver. By using gated recurrent unit neural network models, we conclude that truck drivers consider a three-dimensional feature set, which includes their kinematic characteristics, their interactions with surrounding vehicles and their perception of a road topology, along with recent driving experience during their gap selection. The neural network models, when opened up using explainable artificial intelligence techniques, reveal the differences in gap selection between vehicle classes in terms of the saliency of recent driving experience and the importance of features. Since lane changing has a significant influence on traffic flow, the third element focuses on influencing the lane changing behavior around freeway bottlenecks in order to improve traffic efficiency. For this purpose, we propose a multi-class lane changing advisory system using the linear quadratic regulator (LQR) framework. The LQR controller issues personalized lane changing advice to drivers based on their vehicle classes using C-ITS technology in order to balance traffic flow distribution over available lanes of a freeway. Based on simulation results, we conclude that the proposed advisory system improves the travel time of the system by 21% by suppressing shockwaves. This system is beneficial to both mainline and ramp vehicles as it improves their travel times by 20% and 42%, respectively.

Thirdly, this dissertation investigates the operational behavioral level of truck drivers by analyzing the effects of C-ITS based truck platooning application. By using cooperative adaptive cruise control (CACC), this application influences the operational behavior of trucks so that multiple trucks can organize themselves into a group of close-following vehicles. We conduct a simulation-based sensitivity analysis to identify the effect of characteristics of a truck platoon (namely market penetration rate, number of trucks in a platoon, intra-platoon headway, and platoon speed) on the uncertainty of traffic and safety impacts around a merging section. Based on the results of a sensitivity analysis, we conclude that truck platooning does not deteriorate traffic efficiency and safety in low traffic intensity; however, truck platooning negatively affects traffic efficiency and safety in high traffic intensity. This effect is mainly caused by the following three characteristics: the market penetration of truck platoons in the system, intra-platoon headway and the number of trucks in a platoon. These individual effects have a minimal contribution (around 25%) to the uncertainty in traffic and safety impacts, as indicated by the Borgonovo importance measure. The uncertainty is mainly caused by prevailing interactions among truck platooning characteristics.

In summary, this dissertation provides new insights into the strategical and tactical behavior of truck drivers by developing novel behavioral models through analyzing new truck activity datasets. In addition, this dissertation creates novel control methods to influence the tactical and operational behavior of truck drivers in order to improve traffic efficiency and safety on freeways. To conclude, these behavioral investigations and C-ITS applications are useful to identify design inefficiencies, develop accurate driving behavior models, and improve system-wide traffic operations including those of road freight. These tools provide support to a wide range of stakeholders and decision-makers, including trucking companies, technology providers, road management agencies, and port authorities.

## Samenvattig

Congestie wordt vaak beschouwd als een grote uitdaging voor de activiteiten van het goederenvervoer over de weg. Vrachtwagens, de belangrijkste keuze voor het goederenvervoer over de weg, hebben niet alleen last van files, maar dragen daar ook aan bij. Bijgevolg gaan er wereldwijd miljarden dollars verloren aan vrachtvervoer. Het begrijpen van het rijgedrag en de besluitvorming van vrachtwagenchauffeurs tijdens de rit zijn van cruciaal belang voor het ontwerpen van maatregelen die de impact van congestie op het vrachtverkeer verzachten, en omgekeerd, voor het ontwerpen van maatregelen die de impact van het vrachtverkeer op de congestie verzachten. In dit opzicht kan het rijgedrag van vrachtwagenchauffeurs – net als het rijgedrag in het algemeen – worden ontleed in strategisch, tactisch en operationeel gedrag, waarbij routekeuze, routeplanning op korte termijn (bijvoorbeeld invoegen, wisselen van rijstrook) en respectievelijk het sturen en accelereren van het voertuig. Hoewel dit rijgedrag diepgaand is bestudeerd bij bestuurders van personenauto's, zijn er grotere hiaten in onze kennis als het om vrachtwagens gaat.

Om de vracht- en verkeersactiviteiten op snelwegen te verbeteren, richt dit proefschrift zich op het verkrijgen van inzicht in het reisgedrag van vrachtwagenchauffeurs en het beïnvloeden van dit gedrag om files te verminderen. Daartoe ontwikkelt dit proefschrift nieuwe wiskundige modellen en controlemethoden voor het strategische, tactische en operationele gedrag van vrachtwagenchauffeurs door opkomende datasets te analyseren en nieuwe toepassingen voor coöperatieve intelligente transportsystemen (C-ITS) te ontwerpen.

In de eerste plaats richt dit proefschrift zich op het strategische gedrag van vrachtwagenchauffeurs. We ontwikkelen een nieuwe aanpak om kenmerken van routekeuzegedrag te schatten met behulp van automatische voertuigidentificatiedatasets die schaars zijn en feitelijke routekeuzes van bestuurders missen (niet-gelabeld). Deze aanpak, die gebaseerd is op datafusie en bi-objectieve optimalisatie, kan tegelijkertijd de daadwerkelijke routekeuzes van chauffeurs (labels) afleiden en hun kenmerken inschatten. Deze aanpak wordt toegepast om het routekeuzegedrag van vrachtwagenchauffeurs tijdens de rit te bestuderen via schaarse Bluetooth- en lusedetectordatasets, door rekening te houden met heterogeniteit tussen chauffeurs (dat wil zeggen smaakvariaties) en tijd-van-dag-effecten. We concluderen dat de

voorgestelde aanpak kan worden gebruikt om routekeuzemodellen te schatten op basis van direct beschikbare schaarse datasets.

Ten tweede onderzoekt dit proefschrift het tactische gedrag van vrachtwagenchauffeurs door zich te concentreren op drie elementen. Het eerste element is het verplicht wisselen van rijstrook (d.w.z. invoegen en uitwijken) voor vrachtwagenchauffeurs. Door eindige mengselmodellen toe te passen op een grote dataset met trajecten, concluderen we dat heterogeniteit tussen chauffeurs wordt waargenomen in het samenvoeg- en divergerende gedrag van vrachtwagenchauffeurs. Het tweede element richt zich op het discretionair wisselen van rijstrook, waarbij we het selectieproces van vrachtwagenchauffeurs analyseren, wat een belangrijk onderdeel is van het rijstrookwisselproces waarbij een bestuurder expliciet een geschikte en veilige mogelijkheid zoekt om een rijstrookwisselmanoeuvre te initiëren. Door gebruik te maken van gated recurrent unit neurale netwerkmodellen concluderen we dat vrachtwagenchauffeurs rekening houden met een driedimensionale kenmerkenset, die hun kinematische kenmerken, hun interacties met omringende voertuigen en hun perceptie van een wegtopologie omvat, samen met recente rijervaring tijdens hun selectie van gaten. De verklaarbare kunstmatige-intelligentietechnieken brengen ook de verschillen in gap-selectie tussen voertuigklassen aan het licht. Omdat het wisselen van rijstrook een aanzienlijke invloed heeft op de verkeersdoorstroming, richt het derde element zich op het beïnvloeden van het rijstrookwisselgedrag rond knelpunten op snelwegen om de verkeersefficiëntie te verbeteren. Voor dit doel stellen we een adviessysteem voor het wisselen van rijstrook met meerdere klassen voor, waarbij gebruik wordt gemaakt van het lineaire kwadratische regulator (LQR) raamwerk. De LQR-controller geeft bestuurders gepersonaliseerd rijstrookadvies op basis van hun voertuigklassen met behulp van C-ITS-technologie om de verkeersstroomverdeling over de beschikbare rijstroken op een snelweg in evenwicht te brengen. Op basis van simulatieresultaten concluderen we dat het voorgestelde adviessysteem de reistijd van het systeem met 21% verbetert door schokgolven te onderdrukken.

Ten derde onderzoekt dit proefschrift het operationele gedragsniveau van vrachtwagenchauffeurs door de effecten van op C-ITS gebaseerde vrachtwagenplatooning-applicaties te analyseren. We voeren een op simulatie gebaseerde gevoeligheidsanalyse uit om het effect van de kenmerken van een vrachtwagenpeloton (namelijk marktpenetratiegraad, aantal vrachtwagens in een peloton, volgtijd binnen het peloton en pelotonsnelheid) op de onzekerheid van het verkeer en de veiligheidseffecten rond een peloton te identificeren. samenvoegende sectie. Op basis van de resultaten van een gevoeligheidsanalyse concluderen we dat platooning van vrachtwagens een negatieve invloed heeft op de verkeersefficiëntie en veiligheid bij hoge verkeersintensiteit. Dit effect wordt voornamelijk veroorzaakt door de volgende drie kenmerken: de marktpenetratie van vrachtwagenpelotons in het systeem, de volgtijd binnen het peloton en het aantal vrachtwagens in een peloton. Zoals aangegeven door de Borgonovo-belangmaatstaf, wordt de onzekerheid voornamelijk veroorzaakt door de heersende interacties tussen de kenmerken van vrachtwagenpelotoning.

Samenvattend biedt dit proefschrift nieuwe inzichten in het strategische en tactische gedrag van vrachtwagenchauffeurs door nieuwe gedragsmodellen te ontwikkelen door nieuwe datasets voor vrachtwagenactiviteiten te analyseren. Daarnaast creëert dit proefschrift nieuwe controlemethoden om het tactische en operationele gedrag van vrachtwagenchauffeurs te beïnvloeden om zo de verkeersefficiëntie en veiligheid op snelwegen te verbeteren. Concluderend kunnen deze gedragsonderzoeken en C-ITS-toepassingen nuttig zijn om inefficiënties in het ontwerp te identificeren, nauwkeurige modellen voor rijgedrag te ontwikkelen en de verkeersactiviteiten in het hele systeem te verbeteren, inclusief die van het goederenvervoer over de weg. Deze tools bieden ondersteuning aan een breed scala aan belanghebbenden en besluitvormers, waaronder transportbedrijven, technologieleveranciers, wegbeheerbureaus en havenautoriteiten.

## About the author



Salil Sharma was born in Jalaun, India, on January 31, 1988. He received the bachelor (B. Tech.) degree in Civil Engineering from the Indian Institute of Technology (IIT) Guwahati, India in 2010 and the masters (M. Sc.) degree in Transportation Systems from the Technical University of Munich (TUM), Germany in 2016. In between 2010 and 2013, he worked as an Assistant Executive Engineer for Oil and Natural Gas Corporation (ONGC) Limited on the construction of a Green Building. After completing his masters degree, he spent a year in the Purdue University where he collaborated with Indiana Department of Transportation (INDOT) to help them create a road map towards the connected and automated vehicle future.

In March 2018, Salil started the PhD program at the department of Transport & Planning of Delft University of Technology (TU Delft), the Netherlands. His PhD research was a part of the ToGRIP project which aimed at developing a data-driven integrated traffic and logistics model. He applied his multidisciplinary knowledge from the traffic flow theory, artificial intelligence, control theory, optimization, and simulation to develop new approaches in order to understand and improve on-trip behavior of truck drivers. He received the best paper award by the Traffic Flow Theory and Characteristics Committee of the Transportation Research Board in 2021. During his PhD project, Salil participated in three business use cases for the ToGRIP project and engaged with stakeholders to develop proof-of-concepts towards improving port-to-hinterland trucking operations. Besides, his interest in vehicle connectivity and automation led him to collaborate internationally on developing a novel and open-source vehicle ad-hoc network simulator. Other activities included supervising master's students.

Salil is currently a Data scientist at Vanderlande, continuing his passion to generate value from data. He is supporting Vanderlande's vision to create digital (data-driven) services platform aimed at improving processes and operations of material handling systems.

## Author's publications

### Journal articles

- Sharma, S.**, Lüßmann, J., & So, J. (2018). Controller independent software-in-the-loop approach to evaluate rule-based traffic signal retiming strategy by utilizing floating car data. *IEEE Transactions on Intelligent Transportation Systems*, 20(9), 3585-3594.
- Sharma, S.**, Snelder, M., Tavasszy, L., & van Lint, H. (2020). Categorizing merging and diverging strategies of truck drivers at motorway ramps and weaving sections using a trajectory dataset. *Transportation research record*, 2674(9), 855-866. (**Young First Author Best Paper Award**)
- Faber, T., **Sharma, S.**, Snelder, M., Klunder, G., Tavasszy, L., & van Lint, H. (2020). Evaluating traffic efficiency and safety by varying truck platoon characteristics in a critical traffic situation. *Transportation research record*, 2674(10), 525-547.
- Nadi, A., **Sharma, S.**, Snelder, M., Bakri, T., van Lint, H., & Tavasszy, L. (2021). Short-term prediction of outbound truck traffic from the exchange of information in logistics hubs: A case study for the port of Rotterdam. *Transportation Research Part C: Emerging Technologies*, 127, 103111.
- Sharma, S.**, Papamichail, I., Nadi, A., van Lint, H., Tavasszy, L., & Snelder, M. (2021). A Multi-Class Lane-Changing Advisory System for Freeway Merging Sections Using Cooperative ITS. *IEEE Transactions on Intelligent Transportation Systems*, 23(9), 15121-15132.
- Sharma, S.**, Van Lint, H., Tavasszy, L., & Snelder, M. (2022). Unraveling Gap Selection Process During Discretionary Lane Changing by Vehicle Class. *IEEE Access*, 10, 30643-30654.
- Nadi, A., **Sharma, S.**, van Lint, J. W. C., Tavasszy, L., & Snelder, M. (2022). A data-driven traffic modeling for analyzing the impacts of a freight departure time shift policy. *Transportation Research Part A: Policy and Practice*, 161, 130-150.
- Sharma, S.**, van Lint, H., Tavasszy, L., & Snelder, M. (2022). Estimating Route Choice Characteristics of Truck Drivers from Sparse Automated Vehicle Identification Data through Data Fusion and Bi-Objective Optimization. *Transportation Research Record*, 2676(12), 280-292.

### Conference papers

- Nadi, A., Snelder, M., Tavasszy, L., **Sharma, S.**, & Van Lint, H. (2019, May). Truck identification on freeways using Bluetooth data analysis [Paper presentation]. 15th World Conference on Transport Research, Mumbai, India.
- Sharma, S.**, Snelder, M., & Van Lint, H. (2019, June). Deriving on-Trip route choices of truck drivers by utilizing Bluetooth data, loop detector data and variable message sign data. In *2019 6th International Conference on Models and Technologies for Intelligent Transportation Systems (MT-ITS)* (pp. 1-8). IEEE.
- Faber, T., **Sharma, S.**, Snelder, M., Klunder, G., Tavasszy, L. and van Lint, H. (2020, January). Evaluating traffic efficiency and safety by varying truck platoon characteristics in a critical

traffic situation [Poster presentation]. 99<sup>th</sup> Annual Meeting of the Transportation Research Board, Washington D.C, USA.

**Sharma, S.**, Snelder, M., Tavasszy, L. and van Lint, H. (2020, January). Categorizing merging and diverging strategies of truck drivers at motorway ramps and weaving sections using a trajectory dataset [Paper presentation]. 99<sup>th</sup> Annual Meeting of the Transportation Research Board, Washington D.C, USA. **(Young First Author Best Paper Award)**

**Sharma, S.**, Papamichail, I., Nadi, A., Van Lint, H., Tavasszy, L. and Snelder, M. (2021, June). A Multi-class Lane-changing Advisory System for Freeway Merging Sections. In *16<sup>th</sup> IFAC Symposium on Control in Transportation Systems*, 54(2), 93-98. IFAC-PapersOnLine.

**Sharma, S.**, Al-Khannaq, E., Riebl, R., Schakel, W., Knoppers, P., Verbraeck, A., & van Lint, H. (2021, September). Impact of radio channel characteristics on the longitudinal behaviour of truck platoons in critical car-following situations. In *Conference on Networked Systems 2021 (NetSys 2021)*, 80. Electronic Communications of the EASST.

**Sharma, S.**, van Lint, H., Tavasszy, L. and Snelder, M. (2022, January). Estimating Route Choice Characteristics of Truck Drivers from Sparse Bluetooth Data through Data Fusion and Bi-objective Optimization [Poster presentation]. 101<sup>st</sup> Annual Meeting of the Transportation Research Board, Washington D.C, USA.

**Sharma, S.**, van Lint, H., Tavasszy, L. and Snelder, M. (2022, January). Unraveling the Gap Selection Process of Truck Drivers within Their Discretionary Lane-changing through Gated Recurrent Unit Neural Networks [Poster presentation]. 101<sup>st</sup> Annual Meeting of the Transportation Research Board, Washington D.C, USA.

**Sharma, S.**, Schakel, W., Riebl, R., Knoppers, P., Verbraeck, A., & van Lint, H. (2022, January). Evaluating the Impact of Imperfect Radio Channels on the Longitudinal Behavior of Truck Platoons in Critical Car-following Situations [Poster presentation]. 101<sup>st</sup> Annual Meeting of the Transportation Research Board, Washington D.C, USA.

## Extended abstract

Najafabadi, A. N., **Sharma, S.**, Snelder, M., Tavasszy, L., & van Lint, H. (2019). Analyzing the role of seaport operations in generating inbound/outbound truck traffic demand and its implications on traffic system. In *TRAIL PhD Congress 2019* (p. 13).

## Technical report

Ukkusuri, S. V., Sagir, F., Mahajan, N., Bowman, B., & **Sharma, S.** (2019). *Strategic and tactical guidance for the connected and autonomous vehicle future* (No. FHWA/IN/JTRP-2019/02). Purdue University. Joint Transportation Research Program.

## Working paper

**Sharma, S.**, & Axhausen, K. W. (2009). Design diagrams for road infrastructure elements: High capacity roads. *Arbeitsberichte Verkehrs-und Raumplanung*, 559.





## TRAIL Thesis Series

The following list contains the most recent dissertations in the TRAIL Thesis Series. For a complete overview of more than 275 titles see the TRAIL website: [www.rsTRAIL.nl](http://www.rsTRAIL.nl).

The TRAIL Thesis Series is a series of the Netherlands TRAIL Research School on transport, infrastructure and logistics.

Sharma, S., *On-trip Behavior of Truck Drivers on Freeways: New mathematical models and control methods*, T2023/18, October 2023, TRAIL Thesis Series, the Netherlands

Ashkrof, P., *Supply-side Behavioural Dynamics and Operations of Ride-sourcing Platforms*, T2023/17, October 2023, TRAIL Thesis Series, the Netherlands

Sun, D., *Multi-level and Learning-based Model Predictive Control for Traffic Management*, T2023/16, October 2023, TRAIL Thesis Series, the Netherlands

Brederode, L.J.N., *Incorporating Congestion Phenomena into Large Scale Strategic Transport Model Systems*, T2023/15, October 2023, TRAIL Thesis Series, the Netherlands

Hernandez, J.I., *Data-driven Methods to study Individual Choice Behaviour: with applications to discrete choice experiments and Participatory Value Evaluation experiments*, T2023/14, October 2023, TRAIL Thesis Series, the Netherlands

Aoun, J., *Impact Assessment of Train-Centric Rail Signaling Technologies*, T2023/13, October 2023, TRAIL Thesis Series, the Netherlands

Pot, F.J., *The Extra Mile: Perceived accessibility in rural areas*, T2023/12, September 2023, TRAIL Thesis Series, the Netherlands

- Nikghadam, S., *Cooperation between Vessel Service Providers for Port Call Performance Improvement*, T2023/11, July 2023, TRAIL Thesis Series, the Netherlands
- Li, M., *Towards Closed-loop Maintenance Logistics for Offshore Wind Farms: Approaches for strategic and tactical decision-making*, T2023/10, July 2023, TRAIL Thesis Series, the Netherlands
- Berg, T. van den, *Moral Values, Behaviour, and the Self: An empirical and conceptual analysis*, T2023/9, May 2023, TRAIL Thesis Series, the Netherlands
- Shelat, S., *Route Choice Behaviour under Uncertainty in Public Transport Networks: Stated and revealed preference analyses*, T2023/8, June 2023, TRAIL Thesis Series, the Netherlands
- Zhang, Y., *Flexible, Dynamic, and Collaborative Synchromodal Transport Planning Considering Preferences*, T2023/7, June 2023, TRAIL Thesis Series, the Netherlands
- Kapetanović, M., *Improving Environmental Sustainability of Regional Railway Services*, T2023/6, June 2023, TRAIL Thesis Series, the Netherlands
- Li, G., *Uncertainty Quantification and Predictability Analysis for Traffic Forecasting at Multiple Scales*, T2023/5, April 2023, TRAIL Thesis Series, the Netherlands
- Harter, C., *Vulnerability through Vertical Collaboration in Transportation: A complex networks approach*, T2023/4, March 2023, TRAIL Thesis Series, the Netherlands
- Razmi Rad, S., *Design and Evaluation of Dedicated Lanes for Connected and Automated Vehicles*, T2023/3, March 2023, TRAIL Thesis Series, the Netherlands
- Eikenbroek, O., *Variations in Urban Traffic*, T2023/2, February 2023, TRAIL Thesis Series, the Netherlands
- Wang, S., *Modeling Urban Automated Mobility on-Demand Systems: an Agent-Based Approach*, T2023/1, January 2023, TRAIL Thesis Series, the Netherlands
- Szép, T., *Identifying Moral Antecedents of Decision-Making in Discrete Choice Models*, T2022/18, December 2022, TRAIL Thesis Series, the Netherlands
- Zhou, Y., *Ship Behavior in Ports and Waterways: An empirical perspective*, T2022/17, December 2022, TRAIL Thesis Series, the Netherlands
- Yan, Y., *Wear Behaviour of A Convex Pattern Surface for Bulk Handling Equipment*, T2022/16, December 2022, TRAIL Thesis Series, the Netherlands
- Giudici, A., *Cooperation, Reliability, and Matching in Inland Freight Transport*, T2022/15, December 2022, TRAIL Thesis Series, the Netherlands
- Nadi Najafabadi, A., *Data-Driven Modelling of Routing and Scheduling in Freight Transport*, T2022/14, October 2022, TRAIL Thesis Series, the Netherlands

Heuvel, J. van den, *Mind Your Passenger! The passenger capacity of platforms at railway stations in the Netherlands*, T2022/13, October 2022, TRAIL Thesis Series, the Netherlands

Haas, M. de, *Longitudinal Studies in Travel Behaviour Research*, T2022/12, October 2022, TRAIL Thesis Series, the Netherlands

Dixit, M., *Transit Performance Assessment and Route Choice Modelling Using Smart Card Data*, T2022/11, October 2022, TRAIL Thesis Series, the Netherlands

Du, Z., *Cooperative Control of Autonomous Multi-Vessel Systems for Floating Object Manipulation*, T2022/10, September 2022, TRAIL Thesis Series, the Netherlands

Larsen, R.B., *Real-time Co-planning in Synchromodal Transport Networks using Model Predictive Control*, T2022/9, September 2022, TRAIL Thesis Series, the Netherlands

Zeinaly, Y., *Model-based Control of Large-scale Baggage Handling Systems: Leveraging the theory of linear positive systems for robust scalable control design*, T2022/8, June 2022, TRAIL Thesis Series, the Netherlands